LATVIJAS UNIVERSITĀTE

Olesja Koleda

ELECTROCHEMICAL SYNTHESIS OF BIOLOGICALLY RELEVANT HETEROCYCLES

Doctoral Thesis

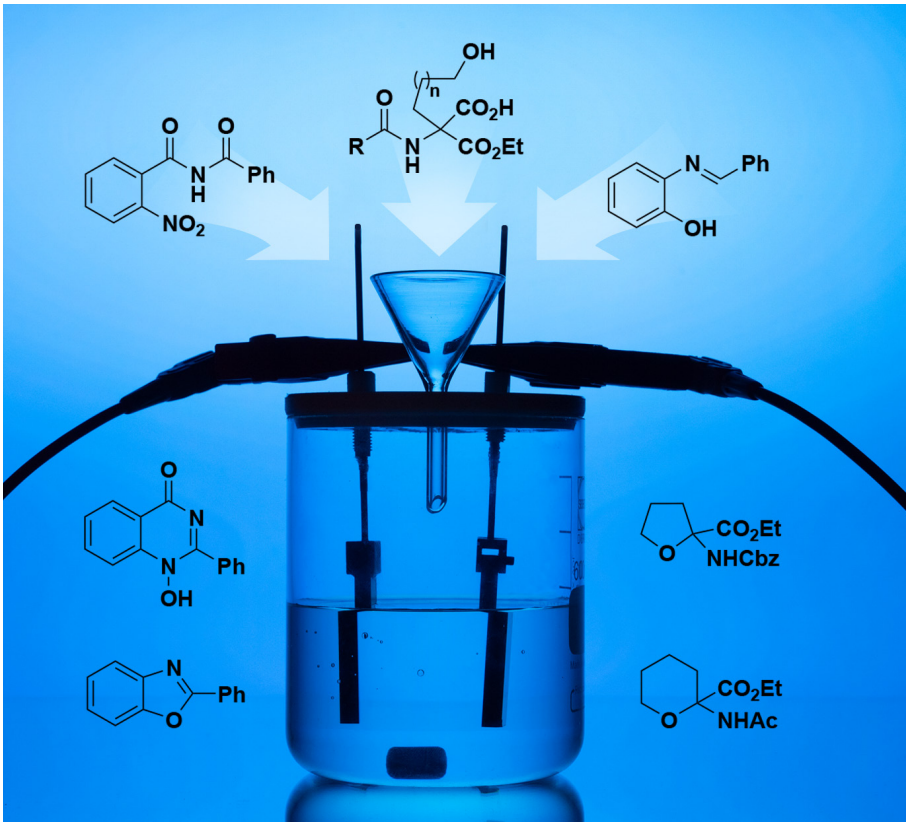

Riga 2023

UNIVERSITY
OF LATVIA

FACULTY OF CHEMISTRY

Olesja Koleda

ELECTROCHEMICAL SYNTHESIS OF BIOLOGICALLY RELEVANT HETEROCYCLES

Doctoral Thesis

Submitted for the PhD degree in the Natural Science
Subfield of organic chemistry

Supervisors:
Prof. Dr. chem. Edgars Suna
Prof. PhD Siegfried R. Waldvogel

RIGA 2023

The development of the doctoral thesis was carried out at the Latvian Institute of Organic Synthesis from 2015 to 2023.

UNIVERSITY OF LATVIA

The thesis comprises the following sections: Introduction, 3 Chapters, Conclusions and 4 Appendices. Form of the thesis: dissertation in chemistry, organic chemistry.

Supervisors: Prof., Dr. chem. Edgars Suna, Prof., PhD Siegfried R. Waldvogel

Reviewers:

1) Dr. chem. Janis Veliks (reviewer of the doctoral committee)
2) Prof., Dr. Thomas Wirth (Cardiff University, United Kingdom)
3) PhD Maksim Ošeka (Tallinn University of Technology, Estonia)

The thesis will be defended at the public session of the Doctoral Committee of chemistry, University of Latvia, at 10:00 on January 23, 2024 at the Academic Center of Natural Science of the University of Latvia, Riga, Jelgavas street 1.

The thesis is available at the Library of the University of Latvia, Raiņa blvd. 19.

Chairman of the Doctoral Committee_____/*Edgars Suna*/

Secretary of the Doctoral Committee_____/*Vita Rudoviča*/

ISBN 978-9934-36-147-0
ISBN 978-9934-36-148-7 (PDF)

ABSTRACT

Electrochemical synthesis of biologically relevant heterocycles. Olesja Koleda, supervisors: Prof., Dr. Chem. Edgars Suna, Prof., PhD Siegfried R. Waldvogel. Doctoral thesis, 94 pages, 6 tables, 76 figures, 170 references, 4 appendices. In English.

Electrochemical syntheses of various pharmaceutically relevant heterocycles have been developed. First, the electrochemically generated hypervalent iodine(III) mediator was employed in the *ex-cell* synthesis of benzoxazoles from iminophenols. The approach was compatible with a range of redox-sensitive functional groups. Moreover, an unprecedented concerted reductive elimination mechanism for benzoxazole formation was proposed based on the control experiments and DFT calculations. Next, the direct anodic decarboxylation of *N*-substituted amino malonic acid derivatives and a subsequent intramolecular etherification provided an access to THF and THP-containing unnatural amino acids. A successful bioisosteric replacement of 1-aminocyclohexane-1-carboxylic acid subunit by the THP-containing amino acid fragment in cathepsin K inhibitor balicatib has helped to reduce lipophilicity while retaining low nanomolar enzyme inhibitory activity. Finally, sustainable and scalable synthesis of 1-hydroxy- and 1-oxy-quinazolin-4-ones has been developed based on cathodic reduction of nitrobenzamides as the key step. The broad applicability of this protocol was demonstrated by the high yield synthesis of 27 differently substituted heterocycles.

Keywords: HETEROCYCLES, ORGANIC ELECTROSYNTHESIS, ANODIC OXIDATION, CATHODIC REDUCTION, REDOX-ACTIVE MEDIATOR.

CONTENTS

ABBREVIATIONS 6
INTRODUCTION 8

1. SYNTHESIS OF BENZOXAZOLES USING ELECTROCHEMICALLY GENERATED HYPERVALENT IODINE(III) COMPOUNDS 12
1.1. Electrochemically generated iodine(III) compounds in heterocycle synthesis 12
1.1.1. *Ex-cell* approach in iodine(III)–mediated heterocycle synthesis 14
1.1.2. Electrochemical *in-cell* approach in iodine(III) mediated synthesis of heterocycles 19
1.2. Electrochemical synthesis of benzoxazoles 26
1.3. Results and discussion 29
1.3.1. Mediator properties 29
1.3.2. Benzoxazole synthesis 31
1.3.3. Mechanistic studies 33
1.3.4. Computational studies 36
1.3.5. Summary 38
REFERENCES 40

2. ELECTROCHEMICAL SYNTHESIS OF THF AND THP DERIVATIVES BY INTRAMOLECULAR HOFER-MOEST REACTION 45
2.1. Direct electrochemical decarboxylation of carboxylic acids in Hofer-Moest reaction 45
2.1.1. Electrolysis conditions: Kolbe vs Hofer-Moest reactions 45
2.1.2. Hofer-Moest reaction 47
2.2. Results and discussion 60
2.2.1. Optimization of the reaction conditions 61
2.2.2. Scope of the developed electrochemical reaction 63
2.2.3. Elucidation of the reaction mechanism 65
2.2.4. Synthetic modifications of THF-AA and THP-AA 66
2.2.5. Summary 68
REFERENCES 69

3. DIRECT ELECTROREDUCTIVE SYNTHESIS OF *N*-HYDROXY QUINAZOLIN-4-ONES 73
3.1. Electrochemical nitro group reduction in the synthesis of heterocycles 73
3.1.1. Synthesis of 5-membered heterocycles by cathodic nitro reduction 74
3.1.2. 6-Membered heterocycles via the cathodic reduction of a nitro group 79

3.2. Results and discussion 82
3.2.1. Optimization of the reaction conditions 83
3.2.2. Scope of the reductive cyclization 85
3.2.3. Mechanistic studies 88
3.2.4. Summary 89
REFERENCES 90

CONCLUSIONS 93
APPENDICES 95

Appendix I – "Synthesis of Benzoxazoles Using Electrochemically Generated Hypervalent Iodine" 96

Appendix II – "Electrochemical Synthesis of Unnatural Amino Acids via Anodic Decarboxylation of *N*-Acetylamino Malonic Acid Derivatives" 110

Appendix III – "Simple and Scalable Electrosynthesis of 1 *H* -1-Hydroxy-Quinazolin-4-Ones" 116

Appendix IV – Publications of abstracts 124

ABBREVIATIONS

Ac – acetyl
Ar – aryl
BDD – boron-doped diamond
BINAP – BINAP 2,2′-bis(diphenylphosphino)-1,1′-binaphthyl
Bn – benzyl
Boc – *tert*-butyloxycarbonyl
C – graphite
Cbz – carboxybenzyl
CCE – constant current electrolysis
CE – counter electrode
CPE – constant potential electrolysis
CSA – camphorsulfonic acid
CV – cyclic voltammetry
dba – dibenzylideneacetone
DDQ – 2,3-dichloro-5,6-dicyano-1,4-benzoquinone
DFT – density functional theory
DIPEA – *N*,*N*-diisopropylethylamine
DMA – *N*,*N*-dimethylacetamide
DMAP – 4-dimethylaminopyridine
DMF – dimethylformamide
DMSO – dimethylsulfoxide
dr – diastereomeric ratio
ee – enantiomeric excess
E_p – peak potential
$E_{pa/2}$ – anodic half-wave potential
equiv – equivalent
EWG – electron-withdrawing group
Fc – ferrocene
FDA – Food and Drug Administration
FE – Faradaic efficiency
GC – glassy carbon
HATU – hexafluorophosphate azabenzotriazole tetramethyl uronium
HFIP – hexafluoro-2-propanol
HPLC – high-performance liquid chromatography
IC_{50} – half maximal inhibitory concentration
j – current density
LC-MS – liquid chromatography-mass spectrometry
m-CPBA – *meta*-chloroperoxybenzoic acid
MOM – methoxymethyl
Ms – methanesulfonyl
MS – molecular sieves
NMR – nuclear magnetic resonance
Nu – nucleophile

Pht	– phtalimide
PIDA	– (diacetoxyiodo)benzene
PIFA	– (bis(trifluroacetoxy)iodo)-benzene
Pin	– pinacole
PPB	– plasma protein binding
Q	– quantity of electric charge
rt	– room temperature
RVC	– reticulated vitreous carbon
SCE	– saturated calomel electrode
SET	– single-electron transfer
SiO_2–Pip	– silica gel-supported piperidine
$t_{1/2}$	– metabolic stability
TEMPO	– 2,2,6,6-tetramethylpiperidine-1-oxyl
TFA	– trifluoroacetic acid
TFE	– 2,2,2-trifluoroethanol
THF	– tetrahydrofuran
THP	– tetrahydropyran
Tol	– toluene
Ts	– toluenesulfonyl group
UV	– ultraviolet
WE	– working electrode

INTRODUCTION

The synthesis of heterocyclic compounds holds a prominent position in organic chemistry. The importance of this field is attributed to the widespread appearance of functionalized heterocycles in biologically active natural products, organic materials, agrochemicals, and pharmaceuticals. For instance, nitrogen-containing heterocycles are common structural elements in pharmaceuticals, and around 59% of FDA approved small-molecule drugs contain a nitrogen heterocycle.[1] The most frequently encountered heterocycles in drug molecules are known as "privileged scaffolds". Such a privileged scaffold is quinazolinone that is incorporated in a variety of sedative drugs (etaqualone, mecloqualone, and nolatrexed).[2] Likewise, a range of marketed drugs contain a benzoxazole motif, namely, tafamidis, calcimycin, boxazomycin, chlorzoxazone, and others.[2] Notably, oxygen-containing heterocycles are the second most common type of heterocyclic components in the structure of small molecule pharmaceuticals. About 27% of FDA approved drugs contain an oxygen heterocycle.[3] Around 89% of these heterocycles are nonaromatic, including 13 THF- and 14 THP-containing derivatives. As a result, the synthesis and modification of heterocycles stand as core elements in organic chemistry. The development of synthetic approaches to obtain pharmaceutically relevant heterocyclic frameworks is important not only from an academic perspective but also because the industry requires practical and economical access to the heterocyclic structures.

There is a broad range of synthetic approaches that has been developed for the construction of heterocycles starting from the appropriate acyclic compounds. Typically, these methods require the use of expensive reagents, harsh reaction conditions, and produce substantial waste. Even though remarkable progress has been achieved in recent decades in the transition-metal-catalyzed heterocycle synthesis, high cost and toxicity of precious metal catalysts and their air and moisture sensitivity is an important drawback. Hence, the development of economical, scalable, and sustainable methods for heterocycle synthesis is an important task for organic chemists.

Organic electrosynthesis offers a scalable, economically efficient, and sustainable approach to heterocycles.[4,5] The electrochemical methods allow for the replacement of toxic and harmful reagents by electrical current, thus reducing energy consumption and amount of waste. Advantages of electroorganic synthesis include also the ability to control electron energy through auxiliary devices. Additionally, methods of organic electrosynthesis often demonstrate high and frequently predictable functional group tolerance. Hence, the development of the electrochemical methods for the synthesis of medicinally relevant heterocycles is the main focus of the doctoral thesis.

The doctoral thesis consists of three parts. **The first part** discloses the electrochemical generation of a hypervalent iodine(III) reagent and its application in the *ex-cell* synthesis of benzoxazoles. **The second part** describes the results of the anodic oxidation of substituted *N*-acetylamino malonic acid monoesters for the synthesis of THP and THF-containing derivatives. Finally, **the third part** focuses on the electroreductive synthesis of *N*-hydroxy-quinazolin-4-ones.

Aim of the doctoral thesis

The aim of the doctoral thesis is to demonstrate the suitability of electrochemical oxidative and reductive methods for the synthesis of pharmaceutically relevant heterocycles.

Objectives of the doctoral thesis:

1. Use the electrochemically generated hypervalent iodine(III) mediator for the *ex-cell* synthesis of benzoxazoles and explore the reaction mechanism.
2. Develop a method for the synthesis of tetrahydrofuran and tetrahydropyran-containing amino acid derivatives via electrochemical decarboxylation/etherification of acetylamino malonic acid monoesters.
3. Develop a method for the electroreductive synthesis of *N*-hydroxy-quinazolin-4-ones from nitrobenzamides.

The novelty and practical significance of the doctoral thesis

Within **the first part** of the thesis, a hypervalent iodine(III) electron transfer mediator was synthesized by anodic oxidation and utilized in the *ex-cell* synthesis of substituted benzoxazoles. Benzoxazole formation was proven to proceed via previously unreported concerted reductive elimination. The developed *ex-cell* method is compatible with redox-sensitive functional groups in benzoxazole, and allows for recovery and reuse of the reduced form of iodine-based mediator. Within **the second part** of the thesis, the developed direct anodic decarboxylation/etherification reaction of *N*-acetamidomalonates provided a variety of previously unreported THF and THP-containing amino acid derivatives. A successful bioisosteric replacement of cyclohexyl fragment in cathepsin K inhibitor balicatib with tetrahydropyran moiety was also demonstrated, showcasing an application potential in drug discovery. Finally, in **the third part** of the thesis, a method for the synthesis of *N*-hydroxy-quinazolin-4-ones by direct electrochemical reduction of nitrobenzamides was developed. In contrast to the known approaches, the newly developed method features improved scalability and utilizes sustainable carbon-based electrodes and an environmentally benign solvent mixture, which is advantageous in the manufacturing processes.

Research of the doctoral thesis has been published in the following articles

1. Koleda, O.; Broese, T.; Noetzel, J.; Roemelt, M.; Suna, E.; Francke, R. Synthesis of Benzoxazoles Using Electrochemically Generated Hypervalent Iodine. *J. Org. Chem.* **2017**, *82*, 11669–11681. DOI: 10.1021/acs.joc.7b01686.
2. Koleda, O.; Prane, K.; Suna, E. Electrochemical Synthesis of Unnatural Amino Acids via Anodic Decarboxylation of *N*-Acetylamino Malonic Acid Derivatives. *Org. Lett.* **2023**, *25*,7958–7962. DOI: 10.1021/acs.orglett.3c02687.
3. Koleda, O.; Prenzel, T.; Winter, J.; Hirohata, T.; De Jesús Gálvez-Vázquez, M.; Schollmeyer, D.; Inagi, S.; Suna, E.; Waldvogel, S. R. Simple and Scalable Electrosynthesis of 1*H*-1-Hydroxy-quinazolin-4-ones. *Chem. Sci.* **2023**, *14*, 2669–2675. DOI: 10.1039/D3SC00266G.

Poster presentations at conferences

1. Koleda, O.; Prane, K.; Suna, E. Electrochemical decarboxylation of *N*-substituted 2-aminomalonic acid monoesters in intramolecular Hofer-Moest reaction. *Program & Abstracts*, Balticum Organicum Syntheticum, Vilnius, Lithuania, July 3–6, 2022, PO057 p. 101 (**Best poster award**).
2. Koleda, O.; Prane, K.; Suna, E. Electrochemical decarboxylation of *N*-substituted 2-aminomalonic acid monoesters in intramolecular Hofer-Moest reaction. 23rdTetrahedron Symposium, Gothenburg, Sweden, June 27–30, 2023, P1.050.

ACKNOWLEDGMENTS

I want to express my deepest gratitude to Prof. Edgars Suna, my supervisor, for his invaluable guidance, support, motivation, and the opportunities he provided throughout these years. I am thankful to Prof. Siegfried R. Waldvogel for the possibility to join his group for three fruitful months and for affording me the opportunity to amass knowledge and experience at Johannes Gutenberg University Mainz. I am grateful to Prof. Robert Francke for introducing me to organic electrochemistry. I appreciate his guidance through this field and his responsiveness. I am grateful to the entire staff of the Latvian Institute of Organic Synthesis for their generous assistance and support in the technical and administrative aspects of my research. I deeply appreciate my colleagues from the Suna research group for their assistance, support encouragement, and scientific discussion. Thanks to my students Haralds Baunis and Katrina Prane for all their hard work and contributions to my thesis. Finally, I warmly thank my parents, my husband, and my daughter for their endless love, sacrifices, and encouragement.

Funding

Latvian Science Council (Grant 274/2012).
INNOVA-BALT project.
Latvian Science Council (LZP-2021/1-0595)

1. SYNTHESIS OF BENZOXAZOLES USING ELECTROCHEMICALLY GENERATED HYPERVALENT IODINE(III) COMPOUNDS

1.1. Electrochemically generated iodine(III) compounds in heterocycle synthesis

Electroorganic synthesis can be categorized into two types: direct and indirect electrolysis. In the direct electrolysis, an electron transfer occurs between a substrate and an electrode (Figure 1.1A). In the indirect electrolysis, an electron transfer first occurs between an electrode and a redox-active mediator (Figure 1.1B and C).[6] The redox-active mediator typically is a redox-active molecule that easily undergoes oxidation at low potentials (or high potentials for reduction) and is capable of selective oxidation or reduction of a substrate without side reactions. The indirect electrolysis can be further classified into two processes: *in-cell* and *ex-cell* regimes (Figure 1.1B and C, respectively). In the *in-cell* process, electrolysis is performed in the presence of both a substrate and an electron transfer mediator. Electron transfer between a mediator and a substrate generates inactive form of the mediator that can be regenerated under electrolysis conditions back to its redox-active form. Such an approach allows for the use of mediators in catalytic quantities. However, the *in-cell* process is only feasible if the oxidation potential of a mediator is lower than that of a substrate (for the anodic oxidation). If the opposite is true, then electrolysis is conducted as an *ex-cell* process (Figure 1.1C).[7] This means the substrate is introduced to the electrolyte solution after the generation of the redox-active form of a mediator and the discontinuation of the electrolysis.

An array of redox-active mediators such as TEMPO, DDQ, X^+/X^- (X = I, Br, Cl), Fe^{II}/Fe^{III}, and Cr^{VI}/Cr^{III} redox pairs have found their application in anodic oxidation reactions.[6] Recently, hypervalent iodine(III) species such as aryl-λ^3-iodanes have emerged as efficient mediators in electrochemical oxidation reactions.[8] Typically, aryl-λ^3-iodanes are synthesized by oxidation of aryl iodides

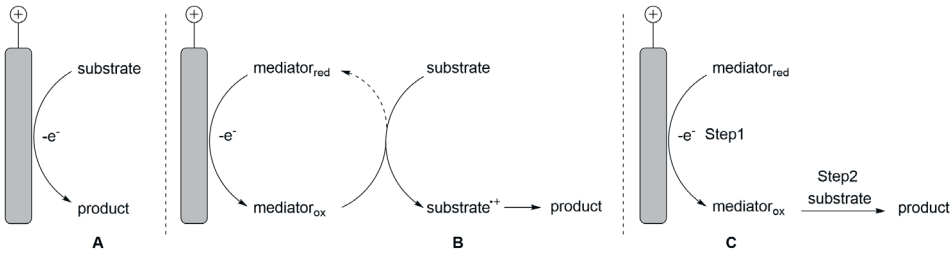

Figure 1.1. **Direct electrolysis (A); indirect *in-cell* electrolysis (B); indirect *ex-cell* electrolysis (C)**

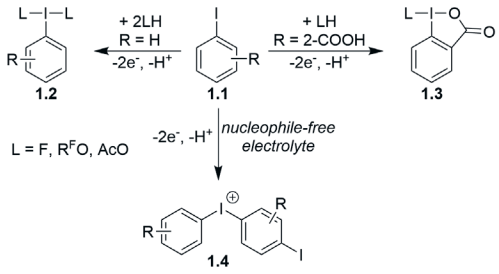

Figure 1.2. **Electrochemical generation of iodine(III) species from aryl iodide**

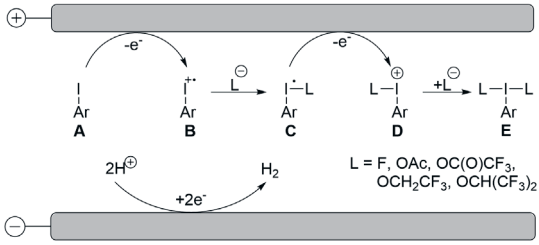

Figure 1.3. **General scheme for electrochemical generation of iodine(III) compounds**

with an excess or stoichiometric amounts of oxidizing reagents such as *m*-CPBA or oxone.[9–14] The reactions mediated by iodine(I)/iodine(III) pair offers advantage in terms of reduced environmental footprint, however, the terminal oxidants remain the source of stoichiometric waste. Electrochemical two-electron oxidation of aryl iodide **1.1** into aryl-λ^3-iodanes **1.2** and **1.3**[6,15–24] provides an attractive alternative to hazardous chemical oxidants because inexpensive electric current as the terminal oxidant offers considerable advantages in terms of waste reduction, increased atom economy, and cost-efficiency (Figure 1.2).

The outcome of the anodic oxidation of aryl iodide depends on the substitution in the aromatic ring and on the electrolyte (Figure 1.2). The electrolysis in the presence of stabilizing anionic species (fluoride, fluorinated alcohols, acetate) affords relatively stable aryl-λ^3-iodanes **1.2**.[20,25–27] The presence of a coordinating *ortho*-substituent in the aromatic ring (e.g., carboxyl group) leads to the formation of cyclic λ^3-iodanes (e.g. benziodoxolones **1.3**).[28] In contrast, anodic oxidation of an aryl iodide in a non-nucleophilic electrolyte ($AcOH/Ac_2O/H_2SO_4$) affords diaryl iodonium compounds **1.4** via electrophilic aromatic substitution.[29,30]

In terms of the mechanism,[31] iodine(III) electrosynthesis (Figure 1.3) typically follows ECEC manifold, where an initial one-electron oxidation of an aryl iodide **A** on the anode surface delivers radical cation **B** (electrochemical step, E) that reacts with an anionic ligand L present in the electrolyte to form iodine(II) species **C** (chemical step, C). Next, the iodonyl radical **C** undergoes another one-electron oxidation to iodine(III) intermediate **D** (electrochemical step, E) that undergoes addition of another anionic ligand (chemical step C) affording aryl-λ^3-iodane **E**. Typically, the cathodic half-reaction involves the reduction of protons and the generation of hydrogen.

Depending on the oxidation potentials of a redox-active iodine mediator **A** and a reaction substrate, the electrochemical generation of the hypervalent iodine reagent **E** may proceed by either the *in-cell* or the *ex-cell* approach (Figure 1.1). In the *in-cell* approach, the anodic oxidation of iodoarene into λ^3-iodane occurs in the presence of a substrate, and the *in-situ* generated λ^3-iodane mediates subsequent oxidation of a substrate within the same cell. On the contrary, in the *ex-cell* approach the anodic oxidation of iodoarene proceeds without the added substrate. After the electrochemical generation of the hypervalent iodine(III) reagent, the electrolysis is discontinued and a substrate is added to the *in-situ* generated λ^3-iodane. In the following sections, both approaches will be discussed with a focus on the application of electrochemically generated aryl-λ^3-iodanes in the synthesis of heterocycles.

1.1.1. *Ex-cell* approach in iodine(III)–mediated heterocycle synthesis

Iodobenzene difluoride **1.6** (Figure 1.4) is among the first electrochemically generated hypervalent iodine compounds. It was prepared by anodic oxidation of iodobenzene in the presence of $Et_3N{\times}3HF$ or $Et_3N{\times}5HF$.[32,33,21] Even though iodobenzene difluorides are not stable when isolated, they have found application in the synthesis of fluorinated heterocycles using *ex-cell* and *in-cell* (see section 1.1.2) approaches. For example, Lennox and co-workers utilized electrochemically generated difluoro-λ^3-tolyl iodane **1.6** as a mediator in the *ex-cell* electrochemical synthesis of fluorinated chromanes **1.10** from allyl phenol ethers **1.9** (Figure 1.4).[7] The *in-cell* approach was unsuitable due to the lower oxidation potential of allyl phenol ether **1.9a** ($E_{pa/2}$ = +1.4 V vs Fc/Fc^+) as compared to that iodotoluene **1.5a** ($E_{pa/2}$ = +1.7 V vs Fc/Fc^+). Therefore, iodotoluene was first oxidized to difluoro-λ^3 -iodane **1.6** in a divided cell in the presence of amine×HF under constant current conditions and employing platinum electrodes. Afterwards, one equivalent of phenol ether **1.9** was added to electrochemically generated iodane **1.6** leading to

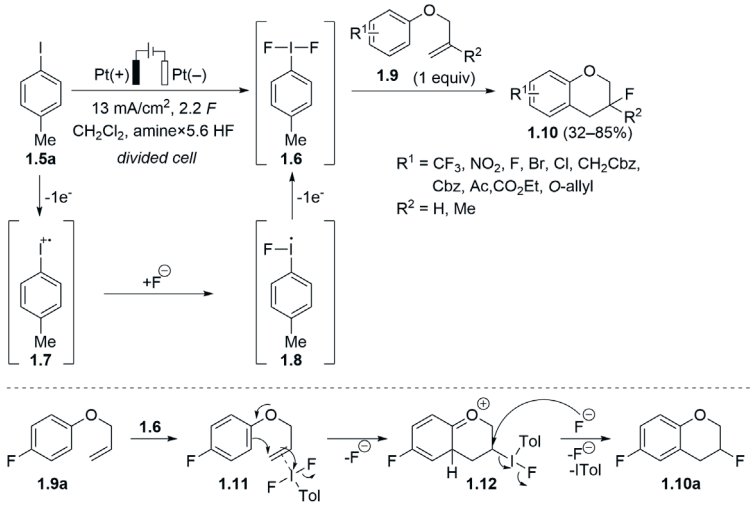

Figure 1.4. **Electrochemical *ex-cell* synthesis of fluorinated chromones**

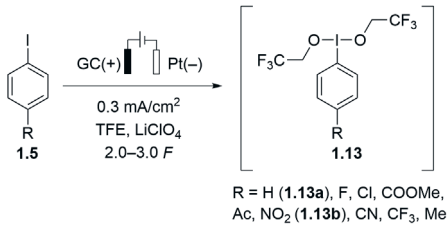

Figure 1.5. **Electrochemical generation of [bis(trifluoroethoxy)iodo]arenes 1.13**

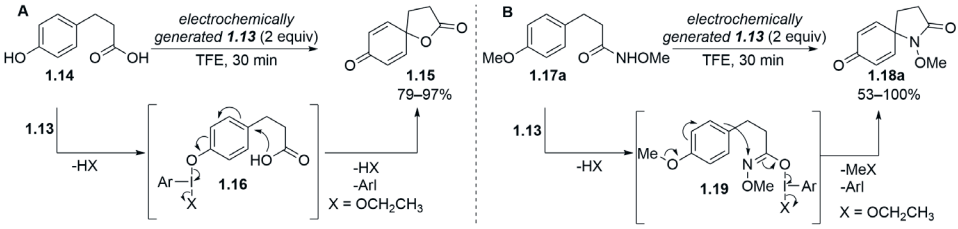

Figure 1.6. **Electrochemically generated [bis(trifluoroethoxy)iodo]arenes 1.13 in spirocyclization reactions**

the formation of transient complex **1.11** that underwent intramolecular cyclization to λ^3-iodane intermediate **1.12**, followed by fluoride substitution of iodanyl leaving group. This procedure yielded a variety of electron-poor chromones **1.10** in moderate to very good yields.[7]

Nishiyama and co-workers reported on the electrochemical synthesis of [bis(trifluoroethoxy)iodo]arenes **1.13** (Figure 1.5) by oxidation iodobenzenes **1.5** at glassy carbon (GC) anode at a constant current in an undivided cell, using 0.05 M $LiClO_4$ solution in trifluoroethanol (TFE).[26,34,35] Most of the electrochemically generated hypervalent iodine reagents **1.13** turned out to be stable only in the reaction solution. Only the anodic oxidation of 4-nitroiodobenzene allowed for the formation of a relatively stable iodane **1.13b** that could be isolated as a solid substance.[35]

The reactivity of λ^3-iodanes **1.13** was examined in the *ex-cell* dearomatization/spirocyclization of 4-hydroxyphenylpropionic acid (**1.14**) or methoxyamide **1.17a** (Figure 1.6A and B, respectively).[35] Interestingly, direct anodic oxidation of propionic acid **1.14** afforded the spirolactone **1.15** in poor 29% yield. In contrast, the oxidation by electrochemically generated λ^3-iodanes **1.13** (the *ex-cell* approach) afforded the spirocyclic products **1.15** and **1.18a** in considerably improved yields (79–97%; see Figure 1.6A). The spirocyclization likely proceeds through intermediates **1.16** and **1.19**, respectively. λ^3-Iodane reagent **1.13a** was the most reactive across the series, affording the highest yields of spirocyclization products **1.15** and **1.18a** (97% and 100%, respectively). It should be noted that the commercially available PIFA turned out to be less efficient as an oxidant, affording spirocycle **1.15** in lower 84% yield.[35]

The electrochemically generated iodane **1.13a** was further used in the oxidative cyclization of different methoxyamide derivatives (Figure 1.7).[26,34] Halogen-substituted methoxyamides **1.17b**,**c** afforded the corresponding spirocycles **1.18b**,**c** in high yields

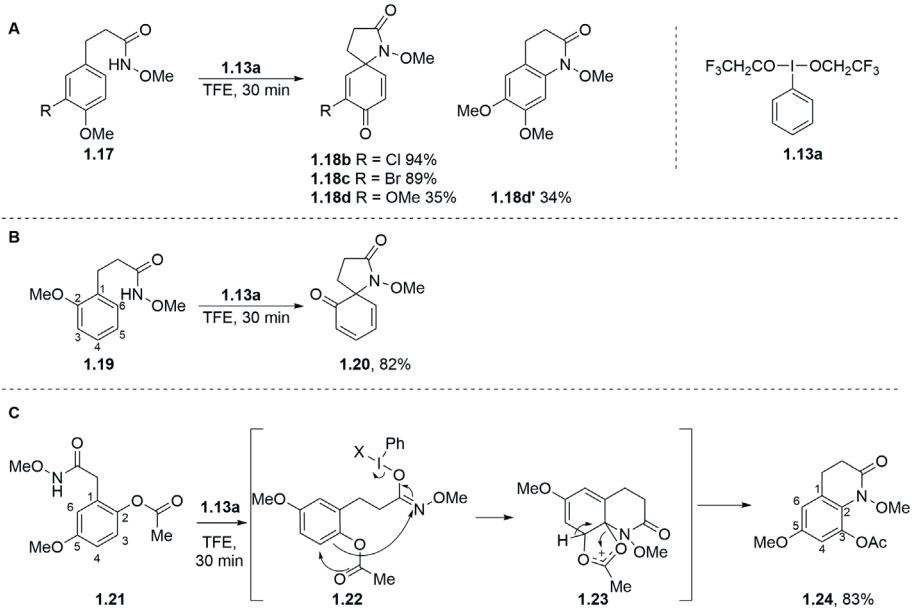

Figure 1.7. ***Ex-cell*** **cyclization of methoxyamide derivatives by electrochemically generated iodane 1.13a**

(89–99%). However, a mixture of two products (**1.18d** and **1.18d'**) was formed from dimethoxy-substituted amide **1.17d** (Figure 1.7A). Electrochemical oxidation of amide **1.19** with the electrochemically formed λ^3-iodane **1.13a** resulted in the spirocyclization product **1.20** with an 82% yield (Figure 1.7B).[26]

Unusual migration of acetate group was observed in the synthesis of quinoline derivative **1.24** (Figure 1.6C). Upon oxidation of amide **1.21** by the electrochemically generated λ^3-iodane **1.13a**, cyclization preferentially occurs at position C-2 of the aromatic ring. The formed cationic *ipso*-substitution intermediate **1.23** undergoes deprotonation/1,2-shift of the acetoxy substituent to afford quinolone **1.24** as the main reaction product.[34]

The *ex-cell* hypervalent λ^3-iodine-mediated approach was also utilized in the synthesis of a variety of natural compounds. For instance, electrochemically generated λ^3-iodane **1.13a** was successfully utilized in the synthesis of tetrahydropyrrolo iminoquinone alkaloids **1.27** and **1.28** (Figure 1.8A).[22] Furthermore, hypervalent iodine(III)–mediated oxidative cyclization of biaryl acetamide **1.29** afforded carbazole **1.30** that served as a scaffold for the synthesis of glycozoline **1.31** (Figure 1.8B).[23] The plausible carbazole **1.30** formation mechanism[36] involves an initial ligand exchange between λ^3-iodane **1.13a** and acetamide **1.29**, followed by oxidation of acetamide to nitrenium ion **1.33** (Figure 1.8C). The transient nitrenium ion **1.33** undergoes electrophilic aromatic substitution followed by aromatization to yield carbazole **1.30**.

Zhang and co-workers developed a methodology for the iodine(III)-promoted synthesis of fused cyclopropane **1.37** using the *ex-cell* approach (Figure 1.9).[37] Accordingly, anodic oxidation of iodobenzene (**1.5b**) in an HFIP

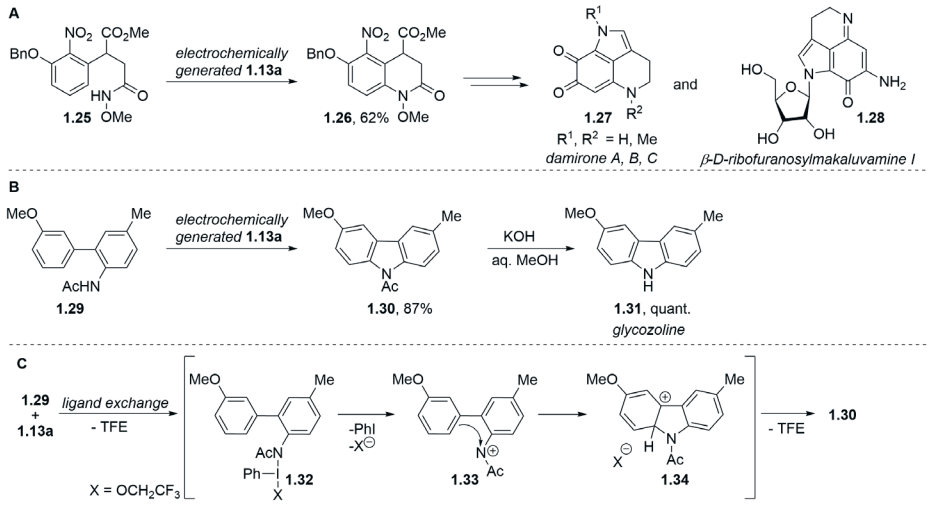

Figure 1.8. **Examples of natural compounds synthesized by using electrochemically generated iodine(III) compound 1.13a**

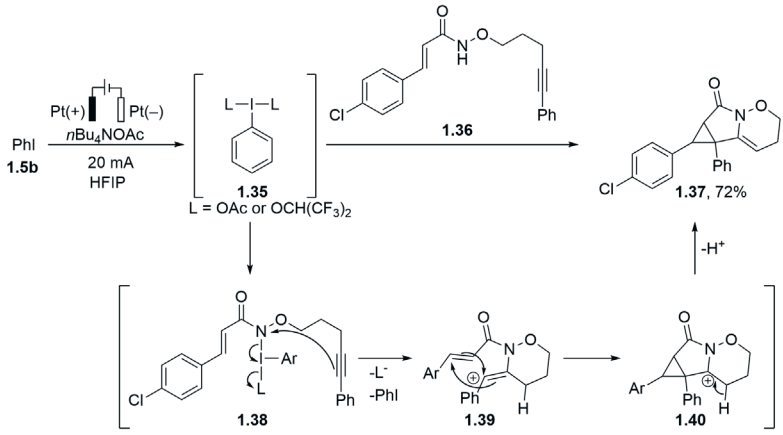

Figure 1.9. **Annulation reaction mediated by electrochemically generated iodane 1.35**

solution in the presence of nBu$_4$NOAc generated aryl-λ^3-iodane **1.35**. Subsequent post-electrolysis addition of alkyne **1.36** resulted in the generation of transient iodane **1.38** via ligand exchange. Then, iodane **1.38** could be trapped by the internal alkyne, generating alkenyl cation **1.39**, which undergoes cation-induced cyclization to afford cation **1.40**. After the proton loss, heterocycle **1.37** is formed in 72% yield.

A different type of a redox mediator for the *ex-cell* approach was developed by Francke and Broese (Figure 1.10).[38] By merging the redox-active iodoarene subunit with a tetraalkyl ammonium moiety, they designed ionically–tagged phenyl iodide **1.41** that served both as a redox mediator and supporting electrolyte. Such a design not only allowed for the electrochemical generation of I(III) reagent **1.42** without

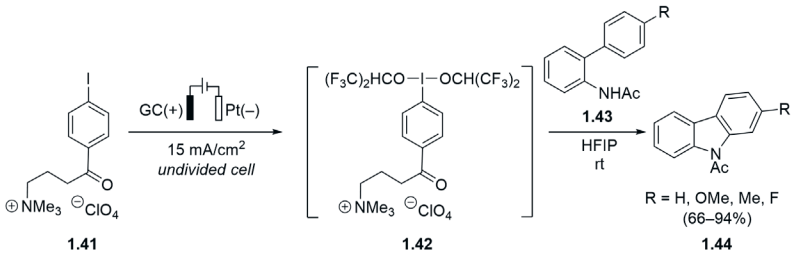

Figure 1.10. **Electrochemically generated λ^3-iodane 1.42 in carbazole synthesis**

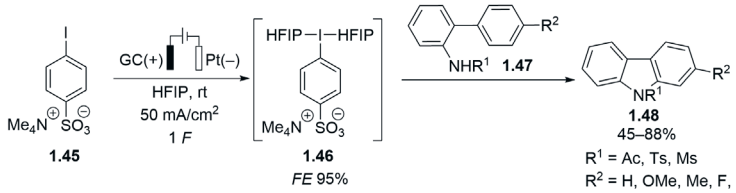

Figure 1.11. **Electrochemically generated λ^3-iodane 1.46 in carbazole synthesis**

added external supporting electrolyte, but also facilitated efficient separation and reuse of the iodoarene mediator **1.41**.[38] The ionically-tagged mediator **1.42** was obtained in an undivided cell at a current density of 15 mA/cm^2 in HFIP solution. Employment of HFIP as the solvent was found to be critical for the successful generation of a hypervalent iodine reagent **1.42**. The key role of HFIP was attributed to its great anodic stability, high conductivity and easy proton reduction due to its low pKa value. Additionally, HFIP is known to stabilize intermediate radicals such as iodanyl radicals and also iodine(III) species. Notwithstanding the stabilizing effect of HFIP, attempted isolation of λ^3-iodane **1.42** led to decomposition. Since λ^3-iodane **1.42** is stable only in the reaction medium, the authors were unable to confirm its structure.

Since aryl iodide **1.41** is irreversibly oxidized to λ^3-iodane **1.42** at +2.16 V potential (vs Ag/$AgNO_3$), substrates possessing oxidation potential below that of **1.41** have to be added to the generated λ^3-iodane **1.42** after the completion of electrolysis (*ex-cell*). Thus, the addition of acetamides **1.43** to the electrochemically generated λ^3-iodane **1.42** afforded carbazoles **1.44**. (Figure 1.10).[38]

Based on these findings, the authors further explored other ionic moiety-containing iodoarenes such as iodoarene sulfonates and iodobenzoates both as mediators and electrolytes for *ex-cell* electrosynthesis.[39] In terms of Faradaic efficiency, conductivity, and reactivity, 4-iodobenzenesulfonate **1.45** appeared to be the most suitable redox-active supporting electrolyte (Figure 1.11). Electrolysis of iodobenzene **1.45** in HFIP solution using glassy carbon anode and Pt cathode resulted in generation of hypervalent iodine(III) reagent **1.46** with very high Faradaic efficiency (95% *FE*). After the electrolysis, 2-substituted amidobiphenyls **1.47** were added to the solution of λ^3-iodane **1.46** in HFIP leading to the formation of carbazoles **1.48**.[39]

The *ex-cell* approach in the electrochemical generation of λ^3-iodanes and their application in the synthesis of heterocycles can be expanded from the batch electrolysis to the electrolysis in a flow cell.[40] Thus in 2019, Wirth and co-workers developed

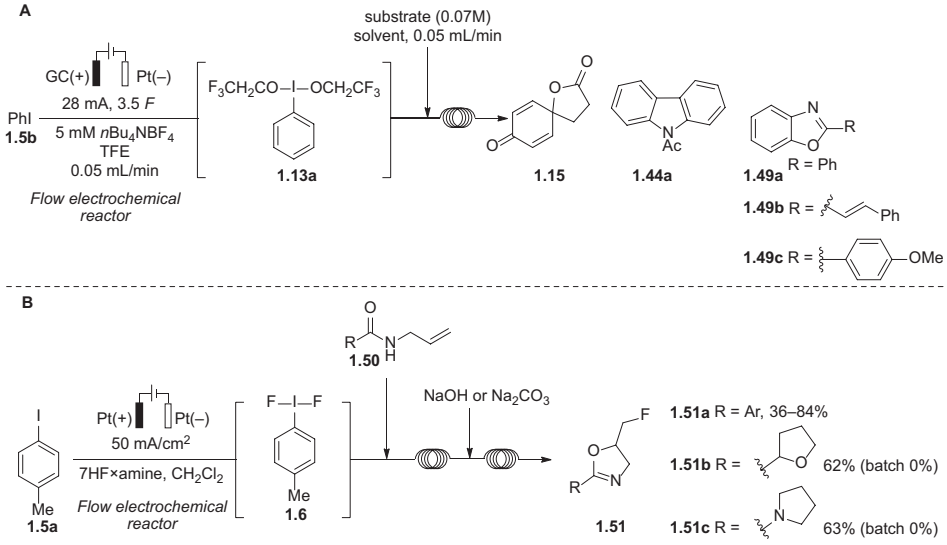

Figure 1.12. **Electrochemical generation of iodine(III) reagents 1.13a and 1.6 in a flow cell and their application in the synthesis of heterocycles**

anodic oxidation of iodoarenes under flow conditions (Figure 1.12A).[41] The anodic oxidation of iodobenzene (**1.5b**) proceeded in TFE and afforded the unstable hypervalent iodine(III) reagent **1.13a**. A variety of oxidative transformations was achieved under flow conditions using the pre-formed λ^3-iodane **1.13a**. Following this approach, a variety of heterocycles such as benzoxazoles **1.49**, carbazole **1.44a** and spiro heterocycle**1.15** were successfully synthesized (Figure 1.12A).

Two years later, the same group reported the electrochemical generation of iodine(III)difluoride **1.6** under flow conditions (Figure 1.12B).[42] Since $ArIF_2$ compounds are not bench-stable and decompose if the reaction solvent is removed, their continuous generation and immediate application is desirable. The electrochemically generated $ArIF_2$ was successfully employed in the oxidative fluorocyclization of substituted *N*-allylbenzamides **1.50** under flow conditions. Importantly, the flow methodology enabled formation of such substituted dihydrooxazoles as compounds **1.51b** and **1.51c**, which could not be obtained in a batch *ex-cell* approach (Figure 1.12B).

1.1.2. Electrochemical *in-cell* approach in iodine(III) mediated synthesis of heterocycles

The synthesis of fluoromethyl-substituted 2-oxazolines from *N*-allylcarboxamides has been accomplished using hypervalent I(III) species as catalysts.[43] The Waldvogel research group employed electrochemically generated iodobenzene difluoride **1.6** to effect fluorocyclization of *N*-allylcarboxamides **1.50** and *N*-propargylamides **1.52** (Figure 1.13). Notably, fluorinated oxazolines[25] and oxazoles[44] were prepared using *in-cell* approach, where λ^3-iodane **1.6** was generated *in the presence* of substrates **1.50** and **1.52**. The electrolysis was performed in an undivided cell equipped with

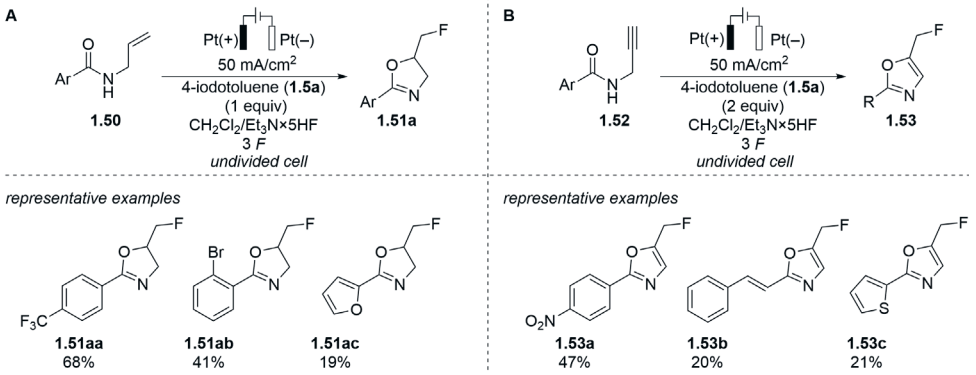

Figure 1.13. **Electrochemical *in-cell* synthesis of fluorinated oxazolines 1.51a (A) and oxazoles 1.53 (B)**

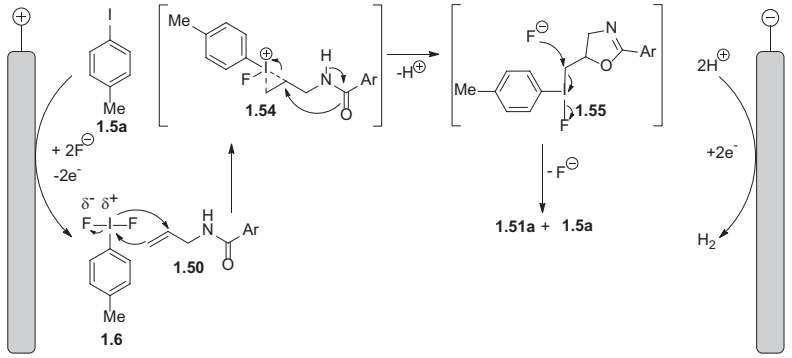

Figure 1.14. **Mechanism for electrochemical synthesis of fluorinated oxazolines 1.51a**

platinum electrodes, using constant current electrolysis, in the presence of $Et_3N{\times}5HF$ and a stoichiometric amount of iodotoluene (**1.5a**). The ionic liquid $Et_3N{\times}5HF$ was employed both as the electrolyte and as fluoride source. Efficiency of the *in-cell* method was demonstrated by synthesis of 16 oxazolines **1.51a** and 15 oxazoles **1.53** that possessed electron-donating and electron-withdrawing substituents as well as heterocycles such as furan and thiophene (Figure 1.13).

The authors also proposed a working mechanism,[25] where the anodic oxidation of iodotoluene to λ^3-iodane **1.6** was followed by the formation of iodonium species **1.54** (Figure 1.14). Subsequent intramolecular ring opening/cyclization delivered λ^3-iodane **1.55** that underwent S_N2-type substitution of iodanyl leaving group by fluoride to furnish heterocycle **1.51a**.

Another example of the *in-cell* heterocycle synthesis was reported by Wirth and co-workers. They have showcased enantioselective synthesis of spirocyclic lactones **1.56** by the electrochemical generation of a chiral lactate-based iodane **1.58** and its subsequent *in-cell* reaction with diketone **1.55** (Figure 1.15).[45] The spirocyclic lactone formation was conducted using 2,2,2-trifluoroethanol (TFE) as the solvent, and the presence of trifluoroacetic acid was found to improve both yield and enantioselectivity. The authors

proposed that the electrochemically generated iodane **1.58** reacts with diketone **1.55**-derived enolate to form the hypervalent intermediate **1.59** that undergoes enantioselective spirolactonization to afford products **1.56** in moderate to very good yields with enantiomeric excess levels reaching up to 71% (Figure 1.15).

The above mentioned *in-cell* examples rely on stoichiometric amounts of iodine mediators, and only a handful of reports on electrocatalytic applications of iodoarenes are known to date. One of the earliest examples of an iodine(III)-mediated electrocatalytic reaction was reported by Fuchigami and co-workers.[20] They disclosed the anodic gem-difluorination of dithioketals **1.60** under constant potential in the presence of 20 mol% of 4-iodoanisole (**1.5c**) catalyst using 0.67 M $Et_3N{\times}3HF$ solution in MeCN as the electrolyte (Figure 1.16).

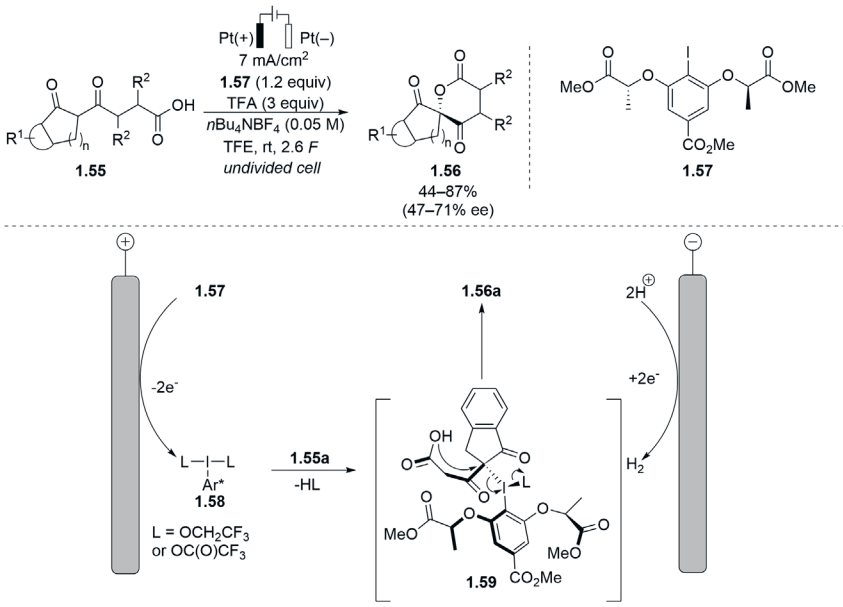

Figure 1.15. ***In-cell*** **enantioselective spirolactonization by chiral iodane mediator 1.57**

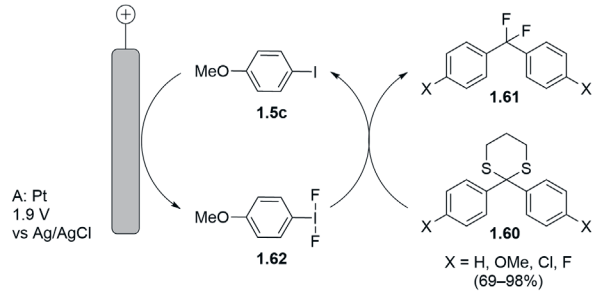

Figure 1.16. **Electrocatalytic fluorination of dithioketals 1.60**

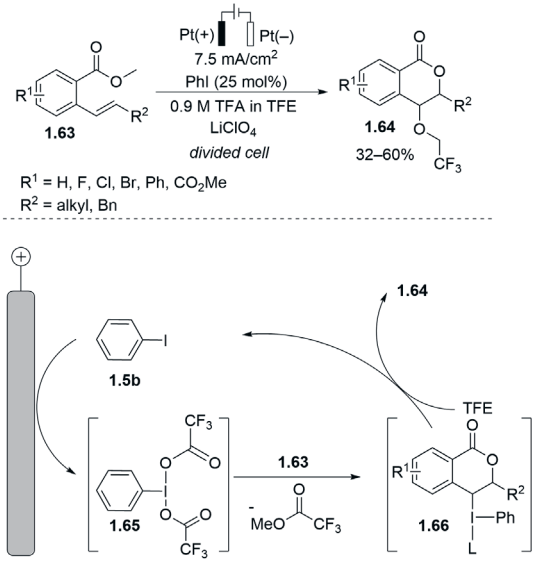

Figure 1.17. **I(III)–mediated electrocatalytic trifluoroethoxy lactonization**

Only recently, a series of reports on the electrocatalytic synthesis of heterocycles using I(III) mediators has appeared in the literature. In 2018, Gerhard and co-workers disclosed iodine(III)-mediated electrocatalytic trifluoroethoxy lactonization to obtain substituted trifluororethoxy isochromanones **1.64** in moderate to good yields (Figure 1.17).[46] The electrolysis was conducted in a divided cell at constant current using 0.9 M TFA solution in TFE. The authors suggested that anodic oxidation of phenyl iodide (**1.5b**) results in the generation of λ^3-iodane catalyst **1.65** that activates the double bond in alkene **1.63** for intramolecular cyclization to intermediate **1.66**. Subsequent nucleophilic substitution of iodanyl hypernucleophuge leaving group by trifluoroethanol afforded isochromanones **1.64**. Electron-neutral and electron-deficient substrates were compatible with the method. However, electron-rich substrates (R^1 = OMe, Figure 1.17) underwent decomposition under electrolysis conditions, yielding only traces of the desired heterocycle **1.64**.

In 2020, Powers and colleagues showcased the first example of metal-free C–H functionalization using hypervalent iodine(III) electrocatalysis (Figure 1.18A).[47] Initially, the authors surveyed the onset oxidation potential of a variety of substituted iodoarenes by cyclic voltammetry (CV). They determined that 4-iodoanisole (**1.5c**) is the most suitable for electrocatalysis due to its relatively low onset oxidation potential (+1.4 V vs Ag^+/Ag). Next, the authors optimized the electrocatalytic oxidative conditions for the C–H activation in amidobyphenyls by aryl iodide **1.5c** catalyst in HFIP under constant potential electrolysis. They found out that the addition of 2 equivalents of nBu$_4$NOAc was crucial for a successful C–H activation and the formation of *N*-acetyl carbazole **1.44**. The role of the additive was attributed to the stabilization of anodically generated iodanyl radicals **1.5c-A** by forming acetoxy iodine(II) species **1.5c-B** (Figure 1.18B). The formation of

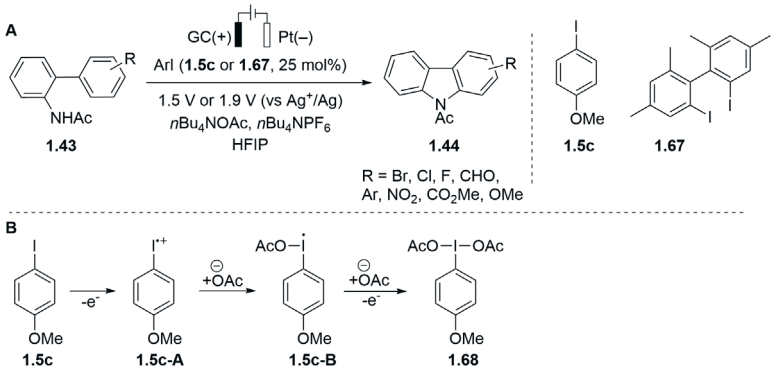

Figure 1.18. **Electrocatalytic synthesis of carbazoles 1.44 using aryl iodide catalyst 1.5c or 1.67**

previously unreported iodanyl radicals **1.5c-A** was supported by CV analysis.[47] It was shown that oxidation of aryl iodide **1.5c** is irreversible in HFIP at low scan rates (< 100 mV/s), while reversibility appeared at higher scan rates (> 250 mV/s). Addition of nBu$_4$NOAc to the solution of aryl iodide **1.5c** in HFIP in the CV experiment resulted in the loss of reversibility and the increase in the anodic current, which indicates that electrochemically generated radical cation **1.5c-A** was captured by the added acetate. The iodine(II) intermediate **1.5c-B** undergoes one-electron oxidation to furnish iodane **1.68**. Finally, scope of the potentiostatic *in-cell* electrolysis of biphenylacetamides **1.43** was evaluated by employing 25 mol% of the catalyst **1.5c**. Carbazoles **1.44** bearing halogen, formyl, phenyl, and methoxy substituents were obtained in good yield. Oxidation of biaryls possessing electron-withdrawing groups such as NO_2 or CO_2Me required stronger oxidant than 4-iodoanisole (**1.5c**). The authors found that diiodo biaryl **1.67** (onset potential for oxidation is +1.68 V vs Ag/Ag$^+$) is the most suitable for the synthesis of nitro- and ester-containing carbazoles **1.44** (Figure 1.18).

In a follow-up study, Powers elaborated on the structure of aryl iodide catalyst and demonstrated that as low as 0.5 mol% of 1,2-diiodo-4,5-dimethoxybenzene (**1.71**) is sufficient for the electrocatalytic synthesis of carbazole **1.44a** in excellent yield (Figure 1.19A).[48] Notably, electrocatalyst **1.71** operated at lower potential than 4-iodoanisole (**1.5c**) (+1.22 V vs Ag./Ag$^+$ and +1.50 V vs Ag/Ag$^+$, respectively) and it was also efficient in the synthesis of various heterocycles such as spirocycle **1.18a** and benzo[*c*]chromen-6-one **1.70** (Figure 1.19B and C, respectively). The in-depth mechanistic studies evidenced that diiodide **1.71** underwent one-electron electrochemical oxidation leading to the formation of iodanyl radical **1.72** that is stabilized by three-electron I–I bonding with adjacent *ortho*-iodine moiety (Figure 1.19D). Notably, the authors were able to isolate and properly characterize iodanyl radical **1.72**.

In 2021, Xu and colleagues demonstrated that 4-iodoanisole (**1.5c**) can also serve as an efficient electrocatalyst in the synthesis of dibenzothiazines **1.74** (Figure 1.20).[49] First, sulfide **1.73** is oxidized in the presence of electrochemically generated hypervalent iodine(III) catalyst **1.68** and ammonia, generating NH-sulfoximine **1.75**. Oxidation

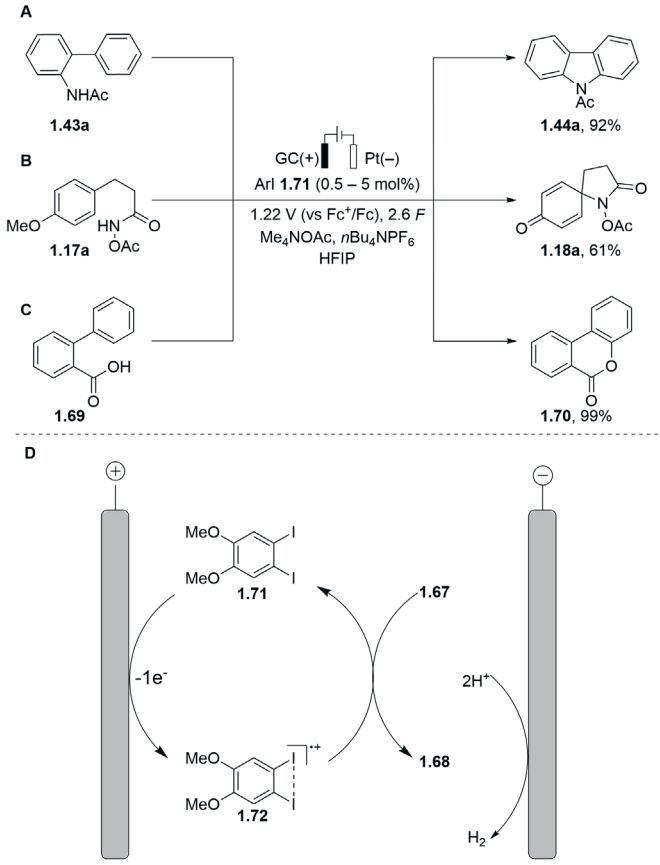

Figure 1.19. **Electrochemical formation of a stable iodanyl radical 1.72 and its application in electrocatalytic reactions**

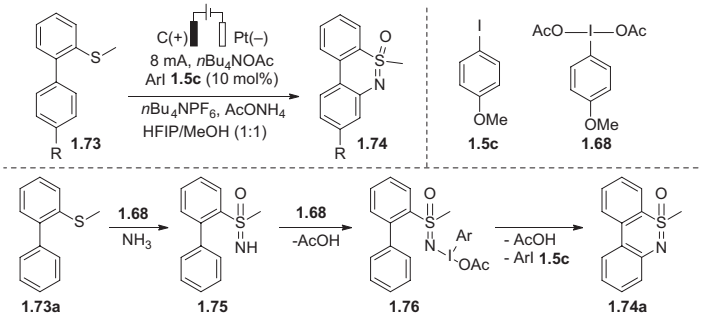

Figure 1.20. **Electrocatalytic synthesis of dibenzothiazines 1.74**

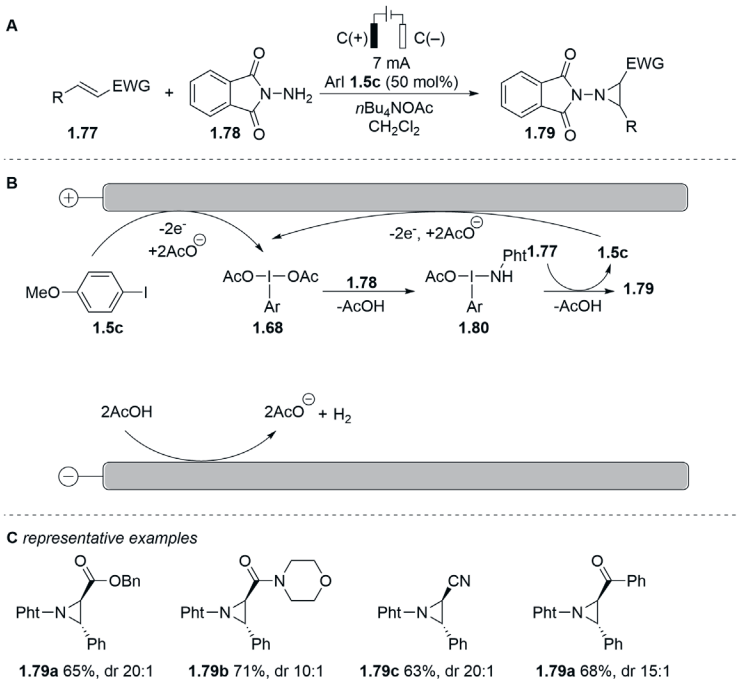

Figure 1.21. **Electrocatalytic aziridination of alkenes 1.77**

of sulfoximine **1.75** by iodane **1.68** generates a transient hypervalent intermediate **1.76** that upon cyclization affords dibenzothiazine **1.74a**.[50]

4-Iodoanisole (**1.5c**) can also catalyze electrochemical aziridination of electron-deficient alkenes **1.77** with *N*-aminophtalimide (**1.78**) in an undivided cell (Figure 1.21).[51] Catalytic amounts of electrochemically generated aryl-λ^3-iodane **1.68** undergoes ligand exchange with phtalimide **1.78** to form intermediate **1.80** that directly reacts with alkene **1.77** yielding aziridine **1.79** (Figure 1.21B).[52] This protocol is suitable for aziridination of cinnamate, cinnamide, α,β-unsaturated nitrile, and α,β-unsaturated ketones **1.77** (Figure 1.21C).[51]

In 2023, Moran and Elsherbini presented electrochemical generation of Koser salt **1.85** and its electrocatalytic application in the oxidative cyclization of *N*-allylic and *N*-homoallylic amides **1.81** into the corresponding heterocycles **1.82** and **1.83** (Figure 1.22).[53] In their approach, iodobenzene (**1.5b**) was anodically oxidized into unstable HFIP-containing hypervalent iodine(III) reagent **1.84** that underwent ligand exchange with TsOH to form a more stable Koser's reagent **1.85**. The *in situ* formed iodine(III) reagent **1.85** activates the double bond of allyl amide **1.81a** for intramolecular cyclization into intermediate **1.87**. The latter undergoes S_N2 type substitution of iodanyl leaving group by tosylate to form heterocycle **1.82a** and iodobenzene (**1.5b**) that is regenerated.[53]

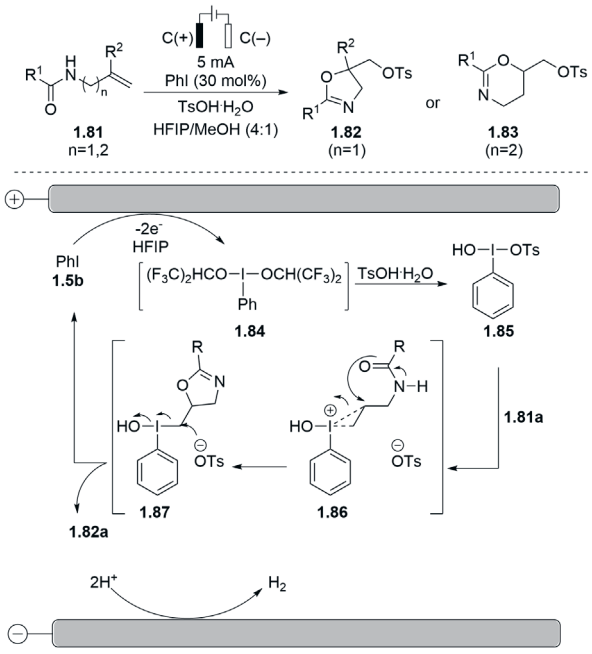

Figure 1.22. **Electrocatalytic synthesis of dihydrooxazoles 1.82 and dihydro-1,3-oxazines 1.83**

To sum up, electrochemically generated hypervalent iodine(III) species are suitable as reagents in the synthesis of heterocyclic compounds. Anodic formation of an iodine(III) compound occurs via two-electron oxidation of iodoarenes in the presence of stabilizing solvents (TFE, HFIP) or other anionic additives in the electrolysis solution (fluorides, acetates, tosylates). The electrochemically generated iodine(III) mediators typically are unstable and should be either generated in the presence of a substrate (*in-cell* approach) or obtained *in situ* prior to the addition of a substrate (*ex-cell* approach). Iodine(III) mediated electrochemical synthesis of heterocycles is also possible by using catalytic amounts of aryl iodide. Moreover, one recent example depicts an emerging concept of I(I)/I(II) based electrocatalysis, which includes the electrochemical generation of an isolable iodanyl radical and its participation in the C–H functionalization reaction.

1.2. Electrochemical synthesis of benzoxazoles

Benzoxazole is frequently encountered structural motif in biologically active natural products[12] and pharmaceuticals.[54] Several marketed drugs such as benoxaprofen, caboxamycin, flunoxaprofen, tafamidis, and pseudopteroxazole possess the benzoxazole subunit (Figure 1.23).

Among a plethora of the methods for the synthesis of benzoxazoles,[55] electrochemical synthesis is one of the most appealing as it provides excellent atom economy

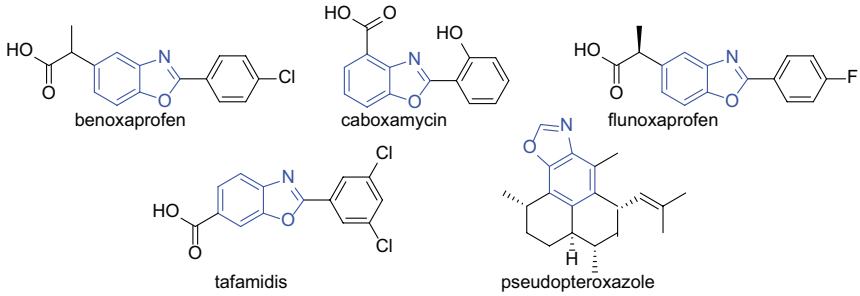

Figure 1.23. **Examples of benzoxazole moiety-containing marketed drugs.**

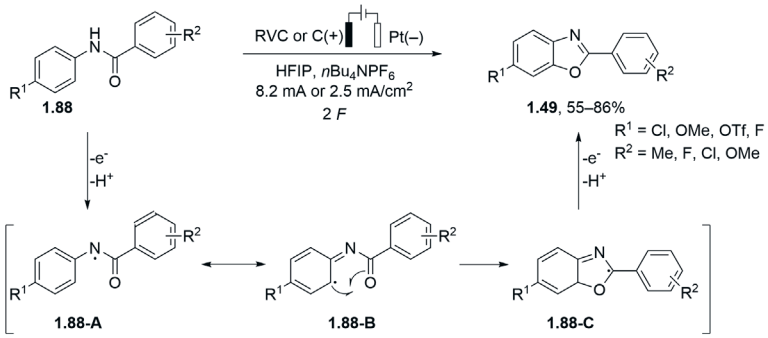

Figure 1.24. **Direct electrochemical synthesis of benzoxazoles 1.49 from anilides 1.88**

and sustainability. For instance, benzoxazoles **1.49** have been prepared by direct electrochemical oxidation of anilides **1.88** under galvanostatic mode in HFIP (Figure 1.24).[56] Accordingly, one-electron oxidation of anilide **1.88** to resonance-stabilized amidyl radical **1.88-A** was followed by the cyclization and the second one-electron oxidation to afford benzoxazoles **1.49** in good yields. The developed approach is operationally simple. However, the method has only been demonstrated for substrates possessing specific substituents (F, Cl, or MeO) *para* to aniline nitrogen in benzamide **1.88**.

Yoshida and coworkers developed anodic oxidation of 2-phenoxypirimidines **1.89** followed by a chemical reaction of cyclized cationic intermediate **1.90** with piperidine, which provided access to 2-aminobenzoxazoles **1.91** (Figure 1.25).[57] Thus, one-electron oxidation of phenol derivative **1.89a** in a divided cell under constant current conditions and subsequent intramolecular cyclization reaction generated radical cation **1.89-B**. Another one-electron oxidation and deprotonation resulted in the formation of heterocyclic cation **1.90a**. After completion of the electrolysis, piperidine was added to the electrochemically generated cation **1.90a**, which resulted in the formation of aminal **1.90-A**. Subsequent ring opening in Zincke-type reaction led to the formation of the 2-aminobenzoxazole **1.91a**. Benzoxazoles **1.91** were obtained in good yields and many electron-withdrawing groups, such as CF_3, CN, CO_2R, were tolerated under these conditions (Figure 1.25). However, this approach features decreased atom economy due to the need for a post-electrochemical functionalization step.

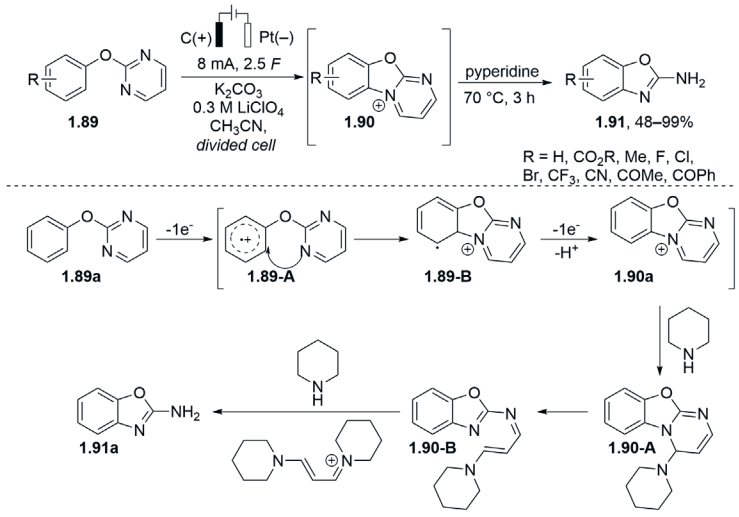

Figure 1.25. **Electrochemical synthesis of 2-aminobenzoxazoles 1.91**

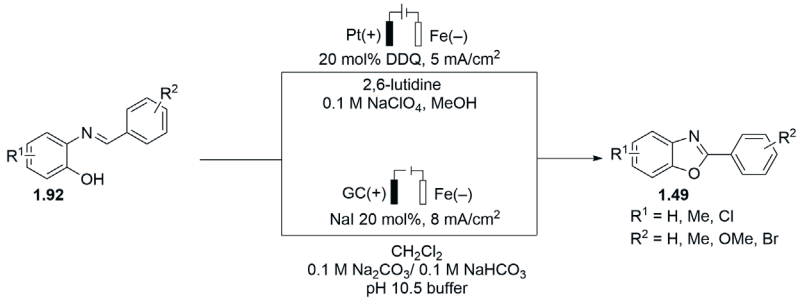

Figure 1.26. **Indirect electrochemical syntheses of benzoxazoles 1.49 from iminophenols 1.92**

Direct electrochemical synthesis of benzoxazoles from iminophenols is also possible. However, it requires the addition of LiOMe to facilitate the formation of benzoxazoles.[58] The presence of the strongly basic methoxide decreases the functional group compatibility. Little and coworkers have showcased that indirect electrocatalytic reaction using redox mediators such as DDQ[59] or sodium iodide[60] allows for the formation of benzoxazoles **1.49** from iminophenols **1.92** under considerably milder conditions (Figure 1.26). Both approaches were conducted in an undivided cell under constant current using 20 mol% of the redox mediator. However, stoichiometric additives such as carbonate buffer (in NaI mediated reaction) or 2,6-lutidine and supporting electrolyte (in DDQ mediated process) were necessary to accomplish the indirect electrosynthesis. Furthermore, relatively electron-rich imines were only used in oxidative cyclization (R = Me, Cl), and nitro-substituted imines were unreactive.

To sum up, there are several electrochemical approaches to synthesize benzoxazoles, including direct and mediated electrolysis. Although these methods provide

benzoxazoles in good yields, they are applicable mainly to the substrates bearing electron-donating groups. The single approach that allows for the employment of electron-withdrawing groups-containing substrates in Zincke-type reaction features the decreased atom economy. We envisioned that the electrochemical indirect *ex-cell* approach would be beneficial for the synthesis of functionalized benzoxazoles.

1.3. Results and discussion

This section is based on the published article (*J. Org. Chem.* 2017, *82*, 11669–11681).[61]

Based on the advantageous use of a recyclable redox-active iodine mediator **1.41** reported by Francke and Broese[38] (Figure 1.10) and our interest in the electrochemical synthesis of heterocycles, we envisioned developing an approach to synthesize benzoxazoles from iminophenols using the *ex-cell* approach. This would include the electrochemical generation of iodine(III) mediator **1.42** before the addition of the starting imine.

1.3.1. Mediator properties

The electrochemical generation of hypervalent iodine compound **1.42** from iodoarene **1.41** was conducted using previously established optimized electrolysis conditions using glassy carbon anode and Pt cathode (j = 15 mA/cm^2, Q = 1 F, [**1.41**] = 0.2 M, rt) (Figure 1.27).[38] The key factor for the successful oxidation of iodoarene **1.41** to iodane **1.42** was the selection of HFIP as the electrolysis solvent. Unfortunately, the exact structure of the electrochemically prepared iodine(III) reagent **1.42** could not be determined due to its immediate decomposition upon removal of HFIP. All attempts to isolate iodane **1.42** in a pure form were unsuccessful. The ^{1}H-NMR spectrum of the HFIP solution of iodane **1.42** (acquired immediately after electrolysis with added 50 vol% CH_2Cl_2–d_2) displayed signals corresponding to parent aryl iodide **1. 41** (δ 7.95 and 7.67 ppm), along with a downfield-shifted *para*-substituted aromatic spin system (δ 8.28 and 8.13 ppm; see Figure 1.27). The downfield signals were attributed to the aromatic subunit of iodine(III) reagent **1.42** based on the similarity between ^{1}H and ^{13}C chemical shift values to those of the hypervalent iodonium species **1.93** and **1.94**, prepared by the chemical methods (Figure 1.27). Further indirect evidence supporting the electrochemical formation of the iodine(III) reagent was obtained in a control experiment where the HFIP solution of electrochemically generated iodine(III) reagent **1.42** effectively oxidized hydroquinone to 1,4-benzoquinone within 15 minutes at room temperature.

Notably, iodine(III) reagent **1.42**, derived from the anodic oxidation of iodide **1.41**, exhibited stability in HFIP solution at room temperature for several days (entry 1, Table 1.1). The observed stability of iodane **1.42** is remarkable, as hypervalent iodine(III) species have been previously reported to oxidize secondary alcohols to the corresponding ketones.[62–64] In fact, a relatively rapid reduction of iodine(III) reagent **1.93** to aryl iodide **1.95** (ca. 40% after 15 minutes and ca. 65% after 20 hours) occurred at room temperature, accompanied by the oxidation of HFIP to hexafluoroacetone (as evidenced by the appearance of a signal at -82.9 ppm in

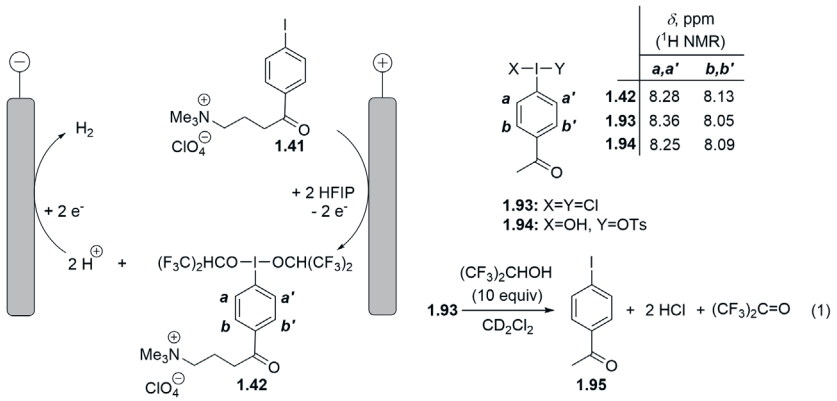

Figure 1.27. **Anodic oxidation of aryl iodide 1.41to iodane 1.42 in HFIP** (WE – GC; CE – Pt)

the ^{19}F spectrum) (eq 1, Figure 1.27). Several control experiments were conducted to shed light on the unusual stability of the electrochemically generated iodine(III) species **1.42** and the observed rapid decomposition of structurally related λ^3-iodane **1.93** in HFIP solution (eq 1, Figure 1.27). It was hypothesized that the formation of HCl during the ligand exchange between iodane **1.93** and HFIP might facilitate the reductive elimination of iodane **1.93** to yield iodoarene **1.95** and hexafluoroacetone (Figure 1.27, eq 1). Indeed, the addition of anhydrous HCl to the electrochemically generated iodine **1.42** led to the rapid formation of aryl iodide **1.41** (entry 2, Table 1.1). The nature of the anion in the acid played a more pivotal role than the acidity of the proton, as demonstrated by a significantly slower conversion of iodane **1.42** to iodide **1.41** in the presence of sulfuric acid (entry 3). Furthermore, the introduction of excess nBu$_4$NCl (10 equiv) as a chloride source triggered the reductive elimination of iodane **1.42** to iodide **1.41** under essentially neutral conditions (entry 4). Notably, other halide anions proved to be much more effective (entries 5–7), with iodide having the most pronounced effect on the rapid decomposition of iodane **1.42** (entry 7).[a]

The addition of a stoichiometric amount of TEMPO did not impact the iodide-mediated conversion of iodane **1.42** to idodoarene **1.41** (entry 8), ruling out the reductive decomposition of iodane **1.42** via a radical chain process. Finally, the stability of the electrochemically generated iodane **1.42** in the presence of an added tertiary amine base (entry 10), as well as in the presence of a non-nucleophilic hydrogen sulfate additive (entry 9), led us to suggest that the nucleophilic reactivity of added halides is responsible for the conversion of iodane **1.42** to aryl iodide **1.41**. Therefore, we propose a plausible mechanism for the halide anion-facilitated reductive decomposition of iodane **1.42**, which involves the addition of halide anion X to iodane **1.42**, resulting in the formation of equilibrating isomers of tetra-coordinated [12-I-4] iodate **1.96** (scheme in Table 1.1).[65] Subsequent intramolecular β-elimination leads to the oxidation of HFIP and simultaneous reduction of the iodine(III) species

[a] The published oxidation of sec-alcohols to ketones by I(III) reagents required the use of KBr as an additive.[62–64]

Table 1.1. **Stability of electrochemically generated iodine(III) species 1.42**

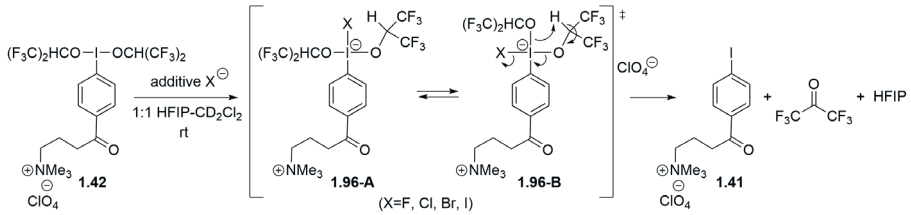

Entry	Additive (equiv)	Time	1.41, %[a]	conv. 1.42, %[a]
1	none	10 days	12[b]	12
2	anhydrous HCl (1.4)	5 min	20[c]	76[c,d]
3	H_2SO_4 (1.4)	60 min	12[c]	12[c]
4	nBu$_4$NCl (10)	10 min	15	36[d]
5	nBu$_4$NF (10)	10 min	61	61
6	nBu$_4$NBr (10)	10 min	76	76
7	nBu$_4$NI (10)	10 min	86	86
8	1:1 nBu$_4$NI/TEMPO (1)	10 min	44	44
9	nBu$_4$NHSO$_4$ (10)	24 h	12	12
10	DIPEA (1)	24 h	6	6

[a] Determined by ^{1}H NMR using 1-methyl-1*H*-pyrrole-2,5-dione as an internal standard. [b] Electrochemically generated solution of **1.42** was stored at +4 °C. [c] CH_2Cl_2 was employed as the internal standard. [d] Inseparable mixture of unidentified side-products was also formed.

to iodoarene **1.41**. Intermolecular β-elimination is considered a less likely mechanistic scenario, as it necessitates the dissociation of the highly basic HFIP-derived alkoxide from the tetracoordinated iodate **1.96**. The stability of the electrochemically generated iodonium species **1.42** is attributed to the absence of nucleophilic ligands in the electrolyte. Attempts to prepare iodane **1.42** using various oxidizing agents were unsuccessful. Treating aryl iodide **1.41** with excess of sodium peroxysulfate or excess of H_2O_2 (30% aqueous solution) in HFIP did not result in any conversion, whereas the use of *m*-CPBA (2 equiv.) yielded iodane **1.42** along with substantial amounts of an unidentified side-product. Therefore, electrosynthesis offers a pathway for the preparation of hypervalent iodine(III) species that are challenging to access through chemical methods like oxidation or ligand exchange.

1.3.2. Benzoxazole synthesis

Next, the electrochemically generated iodine(III) reagent **1.42** was utilized for the oxidative cyclization of 2-(benzylideneamino)phenol **1.92**[b] to yield benzoxazole **1.49**. The redox pair **1.41**/**1.42** exhibits a higher oxidation potential (E_P(**1.41**) = +2.2 V vs. Ag/AgNO$_3$) compared to that of imine **1.92**

[b] See J. Org. Chem. featured article published in 2017[61] for the synthesis of imines **1.92**.

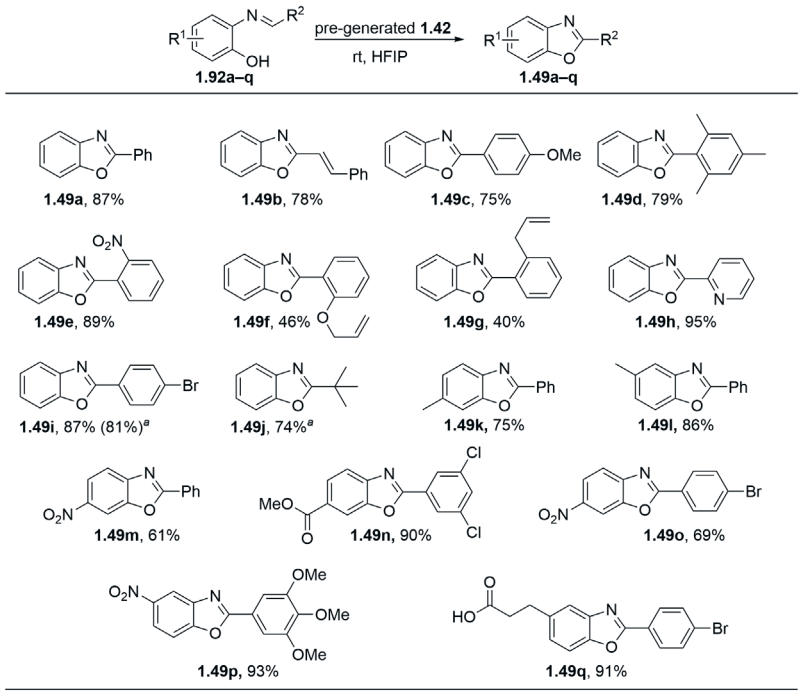

[a] Yield of sequential one-pot two-step synthesis.

Figure 1.28. **Scope of the synthesized benzoxazoles 1.49a–q**

(E_P(**1.92b**) = +0.8 V vs. Ag/$AgNO_3$).[c] Therefore, the electrochemical generation of the redox mediator **1.42** in the presence of imine **1.92** (an *in-cell* process) is not feasible, as in this scenario, the phenolic substrate **1.92** would undergo oxidation prior to iodoarene **1.41**. Consequently, imine **1.92** must be introduced to the electrolyte after the completion of the anodic conversion of iodide **1.41** to iodane **1.42** (an *ex-cell* process). Indeed, the addition of imine **1.92a** to the stoichiometric amount of electrochemically generated iodine(III) mediator **1.42** resulted in the formation of 2-phenyl benzoxazole **1.49a** (Figure 1.28) in 87% yield (3.3 *F* of passed charge with regard to the substrate **1.92a**). The iodine(III)-mediated *ex-cell* electrochemical cyclization is compatible with a wide range of functional groups in substrates, such as alkene moieties (**1.92b**,**f**,**g**), bromine (**1.92i**,**o**,**q**), nitro groups (**1.92e**,**m**,**o**,**p**),[d] ether moieties (**1.92c**,**f**,**p**), ester (**1.92n**), and even carboxylic acid (**1.92q**). Various imines derived from non-enolizable aldehydes, including electron-rich (**1.92c**,**d**,**f**,**g**,**p**) and electron-deficient (**1.92e**) aromatic aldehydes, pyridyl-2-aldehyde (**1.92h**), cinnamaldehyde (**1.92b**), and pivalic aldehyde (**1.92j**), are suitable for the iodine(III)-mediated cyclization (Figure 1.28). The formation of benzoxazoles **1.49a–q** is not sensitive to steric hindrance in the imine moiety, as evidenced by the facile oxidative

[c] Since both species are oxidized irreversibly, peak potentials E_P are reported instead of the equilibrium potentials E_0.

[d] Nitro-substituted imines were not suitable as substrates in DDQ and NaI-mediated electrocyclizations.[59, 60]

cyclization of *ortho*-substituted imines (**1.92d**,**e**,**f**,**g**) (Figure 1.28). It is worth noting that simple ester hydrolysis in benzoxazole **1.49n** leads to the formation of the FDA-approved drug tafamidis.[66]

Benzoxazoles **1.49** can also be synthesized in a one-pot sequential two-step process from *ortho*-aminophenol and non-enolizable aldehyde without the isolation of intermediate imine **1.92**. In this manner, the addition of iodine(III) mediator **1.42** to the *in situ* formed imine **1.92i,j** furnished the corresponding benzoxazoles **1.49i,j** in high yields (Figure 1.28). Finally, both HFIP and aryl iodide **1.41** can be recovered after the completion of the cyclization. Following the removal of HFIP by distillation, the redox-active iodoarene **1.41**, bearing the tetraalkylammonium moiety, can be recovered and purified by dissolving the solid residue in acetone followed by precipitation upon the addition of diethyl ether (typical recovery yield is 90–95%).

1.3.3. Mechanistic studies

A series of control experiments were conducted to elucidate the mechanism of benzoxazole **1.49** formation. Initially, a potential mechanistic scenario involving single-electron transfer (SET) from the relatively electron-rich arene **1.92a-A** to λ^3-iodane **1.42** was considered (pathway A, Figure 1.29).[67,68] The resulting radical cation intermediate **IIa**,**b** would then undergo another SET, leading to the formation of the nitrenium-type species **IVb**, ultimately yielding benzoxazole **1.49a** through a proton loss (Figure 1.29). To investigate the possibility of benzoxazole **1.49a** formation via the SET pathway, a radical inhibition test was conducted. Accordingly, the reaction between imine **1.92a-A** and iodane **1.42** was performed in the presence

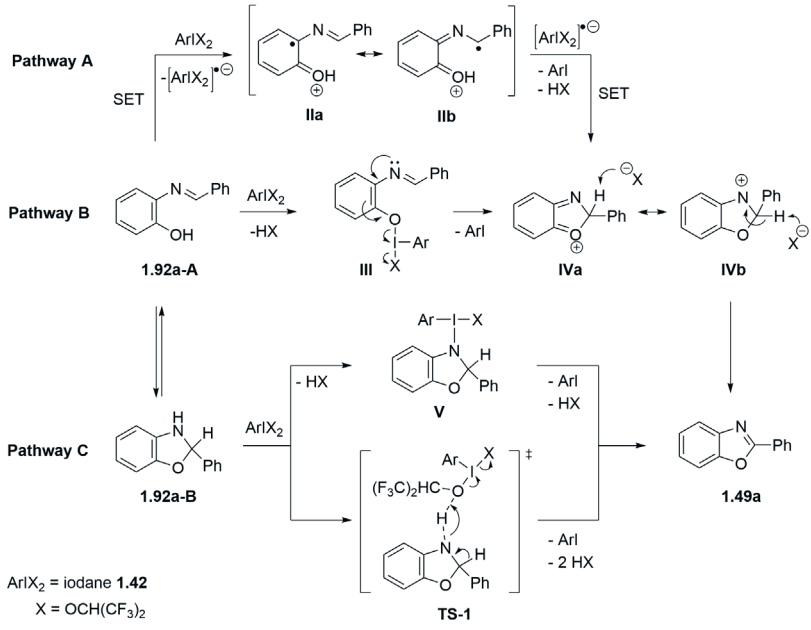

Figure 1.29. **Plausible pathways for the formation of benzoxazole 1.49a**

of added radical scavengers such as TEMPO[69] (1 equiv) or *N-tert*-butyl-α-phenyl nitrone[70] (1 equiv). However, neither of these additives had any influence on the yield of benzoxazole **1.49a** (87% yield in both cases; Figure 1.28).

Subsequently, imine **1.92g**, which contains an *ortho*-allyl moiety as a radical clock probe, was utilized to investigate the potential involvement of radical cation species like **II** in the benzoxazole synthesis (Figure 1.30). Based on the analogy with a previous study on the cyclization of 2-allylbenzyl radicals, where a rapid *5-exo-trig* cyclization was reported (rate constant $k = 3 \times 10^2$ s^{-1}),[71] one might anticipate the formation of 2-methyl-2,3-dihydro-1*H*-indene **VI** after hydrogen atom abstraction from the medium (eq 1, Figure 1.30). However, in our experiments, benzoxazole **1.49g** emerged as the major product, and no detectable amounts of the cyclization product **VI** were observed (eq 2, Figure 1.30). These findings offer evidence that the iodine(III)-mediated benzoxazole formation takes place without the involvement of benzyl radicals such as **IIb** (pathway A, Figure 1.29).

Alternatively, in pathway B, the nucleophilic phenolic oxygen can react with iodane **1.42** in a ligand-exchange process to give rise to aryloxy-λ^3-iodane **III**. The subsequent decomposition of the intermediate **III**, involving phenol oxidation followed by cyclization, would lead to the formation of intermediate **IV**, which then transforms into benzoxazole **1.49a** through a proton loss (Figure 1.29). To verify the potential intermediacy of aryloxy-λ^3-iodane **III** in benzoxazole formation,

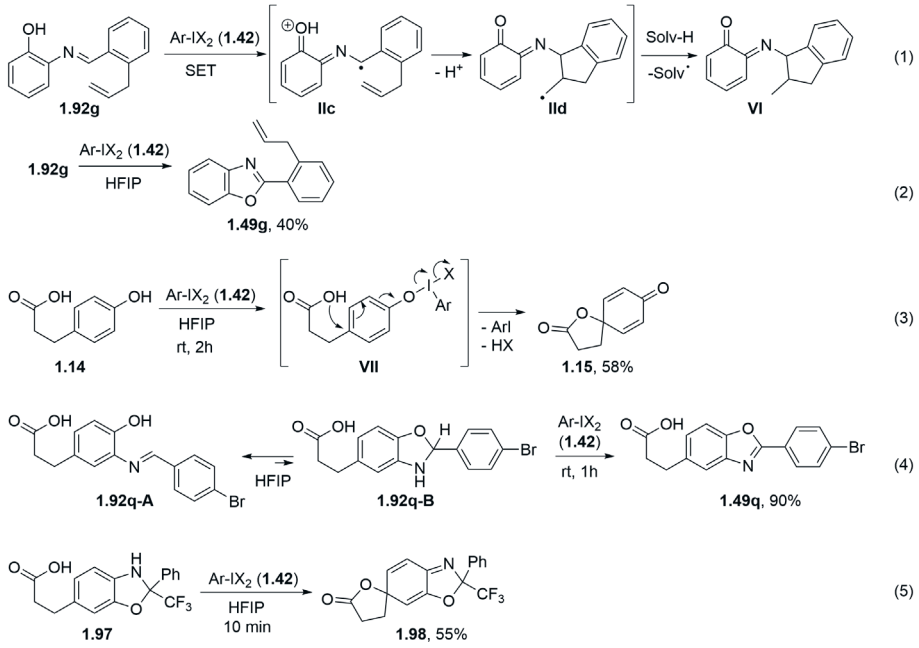

Figure 1.30. **Control experiments for elucidation of the mechanism for the benzoxazole 1.49 formation**

substrates **1.92q** and **1.14**, featuring a *para*-propionic acid moiety in proximity to the phenolic oxygen, were synthesized (eq 3 and 4, Figure 1.30). It is well-established that the tethered carboxylic acid is suitable as a nucleophile for the intramolecular trapping of phenol oxidation products, arising from the fragmentation of transient aryloxy-λ^3-iodanes.[72] Indeed, the electrochemically generated iodine(III) reagent **1.42** reacted with phenol **1.14** to form spirocycle **1.15** within 2 hours at room temperature (eq 3, Figure 1.30). In sharp contrast, structurally related imine **1.92q** was converted to benzoxazole **1.49q** under similar conditions (2 hours, room temperature, 90% yield), and none of the spirocyclization products were observed in the reaction mixture (eq 4, Figure 1.30). Thus, the potential involvement of aryloxy-λ^3-iodane **III** in the formation of benzoxazoles may be called into question.

As a third option, the pathway C involves the formation of cyclic hemiaminal **1.92a-B** from imine **1.92a-A**, followed by its reaction with iodine(III) species **1.42** to generate a new hypervalent iodine(III) intermediate **V**. These species undergo reductive elimination of aryl iodide **1.42** to yield **1.49a**. It is worth noting that the formation of **V** can also occur directly from imine **1.92a-A** and iodane **1.42** without the involvement of cyclic tautomer **1.92a-B**. In this scenario, the interaction between the Lewis basic imine nitrogen in **1.92a-A** and the Lewis acidic iodine(III) center in iodane **1.42** promotes the cyclization to form **V**, along with the concurrent production of HFIP.[73] Additionally, benzoxazole **1.49a** can be formed directly from cyclic hemiaminal **1.92a-B** through a concerted reductive elimination process via transition state **TS-1** (Figure 1.29). Although cyclic hemiaminal **1.92a-B** has not been observed by NMR methods in a 1:1 HFIP/CD_2Cl_2 solution of imine **1.92a-B** (only signals at δ = 8.67 (^{1}H–C=N) and δ = 159.1 (^{13}C=N) were detected), the potential formation of its equilibrium cannot be ruled out. Moreover, it is possible that the cyclic tautomer **1.92a-B** may react with iodine(III) reagent **1.42** significantly faster than imine **1.92a-A** (Curtin-Hammett conditions). In fact, such a scenario aligns with the observed distinct reactivity of phenols **1.92q-A** and **1.14** with iodine(III) reagent **1.42** (eq 3 and 4, Figure 1.30). To confirm the involvement of cyclic tautomer **1.92a–B** in benzoxazole formation, a structurally related ketimine **1.97** with a tethered carboxylic acid was synthesized. As anticipated, NMR spectra of ketimine **1.97** in a 1:1 HFIP/CD_2Cl_2 solution only displayed the presence of the cyclic hemiaminal tautomer (indicated by the ^{13}C signal at δ = 98.7, J = 32.2 Hz). Notably, the clean transformation of ketimine **1.97** to spirocycle **1.98** (as a 1:1 mixture of diastereomers) was observed upon addition of iodine(III) reagent **1.42** under standard conditions (HFIP, room temperature, 10 minutes, 55% yield; see eq 5, Figure 1.30). The facile formation of spirocycle **1.98** from the cyclic ketimine **1.97** and the absence of spirocyclization products for the non-cyclic aldimine **1.92q-A** support pathway C (Figure 1.29) as the most likely mechanism for benzoxazole formation. Further computational investigations provide additional support for pathway C as the most probable mechanistic scenario, and suggest that the concerted reductive elimination via transition state **TS-1** is favored over the involvement of intermediate **V** in pathway C.

1.3.4. Computational studies[e]

The proposed reaction pathways B and C (Figure 1.29) were examined by quantum chemical computations on a model comprising substrate **1.92a**, iodine reagent **1.99**,[f] and an additional solvent molecule (Figure 1.31).[g] In the computed reaction pathway B, a phenolic proton transfer occurs from **92a-A** to the HFIP ligand of mediator **1.99**, initiating a ligand substitution at the I(III) center and leading to the formation of intermediate **III** (Figure 1.32). This substitution is calculated to be exothermic by 5.6 kcal mol^{-1}. Additionally, the corresponding transition state **TS-2** has been identified. It is associated with a reaction barrier of 7.2 kcal mol^{-1}, and its reaction coordinate is dominated by the proton transfer from the substrate to the HFIP ligand. Following the binding of the substrate to the I(III) center, a reductive elimination from the iodine center triggers the ring closure to yield intermediate **IVa**,**b**. The total reaction enthalpy for this step is ΔG = -7.4 kcal mol^{-1}, indicating thermodynamic feasibility. Unfortunately, despite intense efforts, the optimization of the corresponding transition state did not meet the convergence criteria. Nevertheless, our comprehensive search of the potential energy surface yielded a configuration with a single imaginary harmonic frequency, associated with a symmetric mode of the iodine–oxygen bonds. Since such a motion eventually leads to the desired minima (as confirmed by separate relaxed surface scans), we have strong confidence that the obtained structure closely resembles the actual transition state. Consequently, the obtained value of $\Delta G^{‡}$ = 18.0 kcal mol^{-1} corresponding to **TS-3** provides a reasonable approximation for the reaction barrier.

It is crucial to explicitly include an additional solvent molecule (Figure 1.31) to obtain realistic reaction enthalpies for the reductive elimination. This solvent molecule stabilizes the generated HFIP anion by forming a strong hydrogen bond. Additionally, the explicit inclusion of an HFIP molecule is indispensable as a structural facilitator during the ring closure process. In the absence of any solvent molecule near the imine group, no ring closure is observed. Following the solvent-induced ring annulation, the formed nitrenium cation **IV** is stabilized by the neighboring alkoxide ion (X^-).

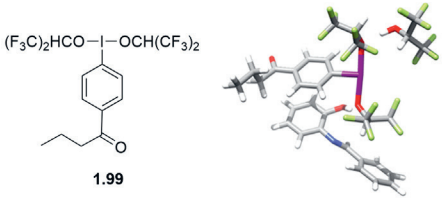

Figure 1.31. **The model system containing iodine(III) species 1.99, imine 1.92a and an additional HFIP molecule**

[e] Computational studies were performed by Dr. J. Noetzel and Dr. M. Roemelt.

[f] It was assumed that the presence of ammonium group and its ClO_4^- counterion in the aliphatic chain of the mediator **1.42** have no influence on the cyclization reaction. Therefore, the charged moiety has been omitted in the model to reduce the computational costs (see structure **1.99**, Figure 1.31).

[g] Detailed technical information, as well as the chosen theoretical approach, can be found in the Experimental Section and the Supporting Information of the featured article published in J. Org. Chem. in 2017.[61]

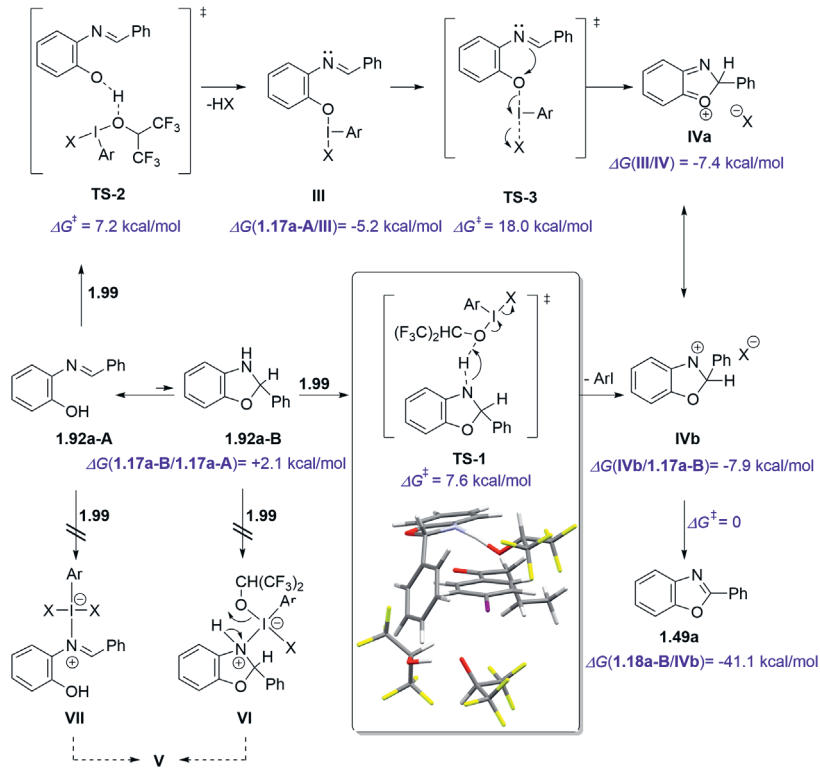

(cf. Figure 1.29). The structure of transition state **TS-1** is inserted as sticks model (with iodine displayed violet, hydrogen white, carbon grey, oxygen red, nitrogen blue and fluorine green). The black arrows indicate the corresponding reaction coordinate which is dominated by the proton transfer from the substrate to its adjacent HFIP anion.

Figure 1.32. **Summary of the computational results on the proposed pathways B and C**

However, this ion pair **IVa**,**b** is metastable. By manually introducing the HFIP anion in close proximity to the proton in α-position to the nitrenium ion, the proton is abstracted without a barrier, leading to the formation of the final product and a gain of ΔG = -41.1 kcal mol^{-1}. This manual procedure simulates a solvent-mediated motion of the HFIP anion, an event we expect to readily occur at room temperature.[h] Alternatively, under the condition of sufficiently high concentrations of mediator and substrate, an HFIP anion from an adjacent reaction center could act as the necessary base. In both scenarios, the final product is generated with a notable release of heat.

[h] Of course, the applied computational model is unfit to yield any reasonable estimates of the rates at which such a movement occurs or its associated barriers. An adequate description of this event would require a full molecular dynamics simulation that explicitly includes many shells of solvent molecules. Such a molecular dynamics simulation is out of scope of this work and from our perspective not worthwhile regarding the limited relevance of this step for the overall reaction mechanism. We believe it is safe to assume that, at room temperature, the anion itself or at least its negative charge is sufficiently mobile in the HFIP solution to readily undergo the required motion at sufficiently high rates.

Next, we conducted theoretical investigations to explore two alternative reaction coordinates (**TS-1** vs intermediate **V**) in pathway C (Figure 1.29). Intermediate **V** could be potentially formed from imine **1.92a-A** and **1.99** through tetracoordinated [12-I-4] iodate **VII**. However, we were unable to find stationary points on the potential energy surface corresponding to intermediate **VII** (Figure 1.32). Alternatively, iodine(III) reagent **1.99** might react with cyclic hemiaminal **1.92a-B** to generate iodate **VI**, which subsequently releases an HFIP molecule to yield intermediate **V** (refer to Figure 1.29). The latter pathway involves cyclic hemiaminal **1.92a-B**, which we have not observed by using ^{1}H-NMR methods. Interestingly, our calculations suggest that the tautomerization of imine **1.92a-A** to hemiaminal **1.92a-B**, in the presence of iodine(III) species **1.99**, is energetically favored by 5.7 kcal mol^{-1} (Figure 1.32). It is worth noting that this relative stability is reversed when the free Gibbs enthalpies of imine **1.92a-A** and hemiaminal **1.92a-B** are calculated without iodane **1.99** and an additional HFIP molecule (ΔG(**1.92a-A**/**1.92a-B**) = 2.1 kcal mol^{-1}), suggesting a potential stabilization of the cyclic hemiaminal tautomer by iodine(III) species **1.99**. However, our calculations did not lead to stationary points on the potential energy surface corresponding to intermediate **VI**.

Furthermore, intermediate **V** spontaneously undergoes reductive elimination when optimized with a solvent molecule in the vicinity of its hemiaminal part. This raises doubts about the involvement of the key intermediate **V** in pathway **C** for benzoxazole formation. Instead, we found that pre-coordination, facilitated by hydrogen bonding of N–H in hemiaminal **1.92a-B** with the Lewis basic oxygen of the HFIP ligand in iodane **1.99**, initiates a concerted reductive elimination via **TS-1** to form iodoarene and an ion pair comprising nitrenium cation **IVa**,**b** and an HFIP anion. This concerted reaction is exergonic with ΔG = –7.9 kcal mol^{-1} and exhibits a relatively low reaction barrier of $\Delta G^{\ddagger}$ = 7.6 kcal mol^{-1} (**TS-1**). Transition state **TS-1** displays elongated I–O bonds (2.69 Å and 2.72 Å), while the N–H and O–H bond lengths are 1.18 Å and 1.31 Å, respectively. This suggests that at this point the reductive elimination is nearly completed while the hydride transfer has yet to occur. Accordingly, the corresponding reaction coordinate is primarily composed of the hydride transfer movement, accompanied by only a minor stretching of the I–O bonds (refer to the stick model for transition state **TS-1** in Figure 1.32). The computed reaction barrier corresponding to transition state **TS-1** ($\Delta G^{\ddagger}$ = 7.6 kcal mol^{-1}, pathway C) is significantly lower in energy compared to that for **TS-3** ($\Delta G^{\ddagger}$ = 18.0 kcal mol^{-1}, pathway B). Consequently, our computational findings strongly support pathway C (Figure 1.29) as the most likely mechanism for the observed oxidative cyclization. This pathway involves low kinetic barriers for each step and is thermodynamically favorable. Among the two possible scenarios within pathway C, our results strongly favor the concerted reductive elimination via transition state **TS-1** as the most probable mechanism for benzoxazole formation.

1.3.5. Summary

Anodic oxidation of iodoarenes in HFIP as a solvent allows for convenient preparation of iodine(III) species under essentially neutral conditions and at room temperature. The electrochemically generated dialkoxy-λ^3-iodane is stable as a solution in HFIP for more than a week at +4 °C (12% decomposition after 10 days). In the presence of nucleophilic anions such as halides, facile reductive elimination of

iodine(III) species to the corresponding aryl iodide, hexafluoroacetone, and HFIP takes place. Poor compatibility of dialkoxy-λ^3-iodanes with nucleophiles renders anodic oxidation a convenient alternative to the traditional approaches such as chemical oxidation or ligands exchange reaction for generation of HFIP-containing I(III) species. Addition of electrochemically generated iodine(III) species to *ortho*-imino phenols results in clean formation of benzoxazoles. The *ex-cell* electrochemical synthesis of benzoxazoles is compatible with a broad range of redox-sensitive functional groups, including alkene, bromine and carboxylic acid. Benzoxazoles can be also synthesized in a one-pot sequential two-step process by addition of electrochemically generated iodine(III) oxidant to the *in situ* formed imines. Our combined experimental and theoretical approach suggests that oxidative cyclization of *ortho*-imino phenols to benzoxazoles proceeds through 2,3-dihydrobenzoxazole as the key intermediate. DFT studies of several conceivable pathways indicate that a sequence via a concerted reductive elimination represents the most plausible mechanistic scenario for the formation of benzoxazoles.

REFERENCES

(1) Vitaku, E.; Smith, D. T.; Njardarson, J. T. Analysis of the Structural Diversity, Substitution Patterns, and Frequency of Nitrogen Heterocycles among U.S. FDA Approved Pharmaceuticals: Miniperspective. *J. Med. Chem.* **2014**, *57*, 10257–10274. DOI: 10.1021/jm501100b.

(2) Welsch, M. E.; Snyder, S. A.; Stockwell, B. R. Privileged Scaffolds for Library Design and Drug Discovery. *Curr. Opin. Chem. Biol.* **2010**, *14*, 347–361. DOI: 10.1016/j.cbpa.2010.02.018.

(3) Delost, M. D.; Smith, D. T.; Anderson, B. J.; Njardarson, J. T. From Oxiranes to Oligomers: Architectures of U.S. FDA Approved Pharmaceuticals Containing Oxygen Heterocycles. *J. Med. Chem.* **2018**, *61*, 10996–11020. DOI: 10.1021/acs.jmedchem.8b00876.

(4) Jiang, Y.; Xu, K.; Zeng, C. Use of Electrochemistry in the Synthesis of Heterocyclic Structures. *Chem. Rev.* **2018**, *118*, 4485–4540. DOI: 10.1021/acs.chemrev.7b00271.

(5) Francke, R. Recent Advances in the Electrochemical Construction of Heterocycles. *Beilstein J. Org. Chem.* **2014**, *10*, 2858–2873. DOI: 10.3762/bjoc.10.303.

(6) Francke, R.; Little, R. D. Redox Catalysis in Organic Electrosynthesis: Basic Principles and Recent Developments. *Chem. Soc. Rev.* **2014**, *43*, 2492–2521. DOI: 10.1039/c3cs60464k.

(7) Doobary, S.; Poole, D. L.; Lennox, A. J. J. Intramolecular Alkene Fluoroarylation of Phenolic Ethers Enabled by Electrochemically Generated Iodane. *J. Org. Chem.* **2021**, *86*, 16095–16103. DOI: 10.1021/acs.joc.1c01946.

(8) Chen, C.; Wang, X.; Yang, T. Recent Updates on Electrogenerated Hypervalent Iodine Derivatives and Their Applications as Mediators in Organic Electrosynthesis. *Front. Chem.* **2022**, *10*, 883474. DOI: 10.3389/fchem.2022.883474.

(9) Richardson, R. D.; Wirth, T. Hypervalent Iodine Goes Catalytic. *Angew. Chem., Int. Ed.* **2006**, *45*, 4402–4404. DOI: 10.1002/anie.200601817.

(10) Ochiai, M.; Miyamoto, K. Catalytic Version of and Reuse in Hypervalent Organo-λ^3- and λ^5-Iodane Oxidation. *Eur. J. Org. Chem.* **2008**, *2008*, 4229–4239. DOI: 10.1002/ejoc.200800416.

(11) Dohi, T.; Kita, Y. Hypervalent Iodine Reagents as a New Entrance to Organocatalysts. *Chem. Commun.* **2009**, *2009*, 2073–2085. DOI: 10.1039/b821747e.

(12) Dohi, T. Recycling and Catalytic Approaches for the Development of a Rare-Metal-Free Synthetic Method Using Hypervalent Iodine Reagent. *Chem. Pharm. Bull.* **2010**, *58*, 135–142. DOI: 10.1248/cpb.58.135.

(13) Singh, F. V.; Wirth, T. Hypervalent Iodine-Catalyzed Oxidative Functionalizations Including Stereoselective Reactions. *Chem.-Asian J.* **2014**, *9*, 950–971. DOI: 10.1002/asia.201301582.

(14) Liu, D.; Lei, A. Iodine-Catalyzed Oxidative Coupling Reactions Utilizing C–H and X–H as Nucleophiles. *Chem.-Asian J.* **2015**, *10*, 806–823. DOI: 10.1002/asia.201403248.

(15) Qian, X.-Y.; Li, S.-Q.; Song, J.; Xu, H.-C. TEMPO-Catalyzed Electrochemical C–H Thiolation: Synthesis of Benzothiazoles and Thiazolopyridines from Thioamides. *ACS Catal.* **2017**, *7*, 2730–2734. DOI: 10.1021/acscatal.7b00426.

(16) Hou, Z.; Mao, Z.; Zhao, H.; Melcamu, Y. Y.; Lu, X.; Song, J.; Xu, H. Electrochemical C–H/N–H Functionalization for the Synthesis of Highly Functionalized (Aza)Indoles. *Angew. Chem., Int. Ed.* **2016**, *55*, 9168–9172. DOI: 10.1002/anie.201602616.

(17) Röse, P.; Emge, S.; König, C. A.; Hilt, G. Efficient Oxidative Coupling of Arenes *via* Electrochemical Regeneration of 2,3-Dichloro-5,6-Dicyano-1,4-Benzoquinone (DDQ) under Mild Reaction Conditions. *Adv. Synth. Catal.* **2017**, *359*, 1359–1372. DOI: 10.1002/adsc.201601331.

(18) Jiang, Y.; Wang, Q.-Q.; Liang, S.; Hu, L.-M.; Little, R. D.; Zeng, C.-C. Electrochemical Oxidative Amination of Sodium Sulfinates: Synthesis of Sulfonamides Mediated by NH_4I as a Redox Catalyst. *J. Org. Chem.* **2016**, *81*, 4713–4719. DOI: 10.1021/acs.joc.6b00615.

(19) Kang, L.-S.; Luo, M.-H.; Lam, C. M.; Hu, L.-M.; Little, R. D.; Zeng, C.-C. Electrochemical C–H Functionalization and Subsequent C–S and C–N Bond Formation: Paired Electrosynthesis of 3-Amino-2-thiocyanato-α,β-unsaturated Carbonyl Derivatives Mediated by Bromide Ions. *Green Chem.* **2016**, *18*, 3767–3774. DOI: 10.1039/C6GC00666C.

(20) Fuchigami, T.; Fujita, T. Electrolytic Partial Fluorination of Organic Compounds. 14. The First Electrosynthesis of Hypervalent Iodobenzene Difluoride Derivatives and Its Application to Indirect Anodic Gem-Difluorination. *J. Org. Chem.* **1994**, *59*, 7190–7192. DOI: 10.1021/jo00103a003.

(21) Fujita, T.; Fuchigami, T. Electrolytic Partial Fluorination of Organic Compounds. 20. Electrosynthesis of Novel Hypervalent Iodobenzene Chlorofluoride Derivatives and Its Application to Indirect Anodic Gem-Difluorination. *Tetrahedron Lett.* **1996**, *37*, 4725–4728. DOI: 10.1016/0040-4039(96)00951-3.

(22) Inoue, K.; Ishikawa, Y.; Nishiyama, S. Synthesis of Tetrahydropyrroloiminoquinone Alkaloids Based on Electrochemically Generated Hypervalent Iodine Oxidative Cyclization. *Org. Lett.* **2010**, *12*, 436–439. DOI: 10.1021/ol902566p.

(23) Kajiyama, D.; Inoue, K.; Ishikawa, Y.; Nishiyama, S. A Synthetic Approach to Carbazoles Using Electrochemically Generated Hypervalent Iodine Oxidant. *Tetrahedron* **2010**, *66*, 9779–9784. DOI: 10.1016/j.tet.2010.11.015.

(24) Watts, K.; Gattrell, W.; Wirth, T. A Practical Microreactor for Electrochemistry in Flow. *Beilstein J. Org. Chem.* **2011**, *7*, 1108–1114. DOI: 10.3762/bjoc.7.127.

(25) Haupt, J. D.; Berger, M.; Waldvogel, S. R. Electrochemical Fluorocyclization of *N*-Allylcarboxamides to 2-Oxazolines by Hypervalent Iodine Mediator. *Org. Lett.* **2019**, *21*, 242–245. DOI: 10.1021/acs.orglett.8b03682.

(26) Amano, Y.; Nishiyama, S. Oxidative Synthesis of Azacyclic Derivatives through the Nitrenium Ion: Application of a Hypervalent Iodine Species Electrochemically Generated from Iodobenzene. *Tetrahedron Lett.* **2006**, *47*, 6505–6507. DOI: 10.1016/j.tetlet.2006.07.050.

(27) Massignan, L.; Tan, X.; Meyer, T. H.; Kuniyil, R.; Messinis, A. M.; Ackermann, L. C–H Oxygenation Reactions Enabled by Dual Catalysis with Electrogenerated Hypervalent Iodine Species and Ruthenium Complexes. *Angew. Chem., Int. Ed.* **2020**, *59*, 3184–3189. DOI: 10.1002/anie.201914226.

(28) Zu, B.; Ke, J.; Guo, Y.; He, C. Synthesis of Diverse Aryliodine(III) Reagents by Anodic Oxidation. *Chin. J. Chem.* **2021**, *39*, 627–632. DOI: 10.1002/cjoc.202000501.

(29) Peacock, M. J.; Pletcher, D. The Electrosynthesis of Diaryliodonium Salts. *Tetrahedron Lett.* **2000**, *41*, 8995–8998. DOI: 10.1016/S0040-4039(00)01620-8.

(30) Peacock, M. J.; Pletcher, D. The Synthesis of Diaryliodonium Salts by the Anodic Oxidation of Aryl Iodide/Arene Mixtures. *J. Electrochem. Soc.* **2001**, *148*, D37. DOI: 10.1149/1.1353574.

(31) Winterson, B.; Bhattacherjee, D.; Wirth, T. Hypervalent Halogen Compounds in Electrochemical Reactions: Advantages and Prospects. *Adv. Synth. Catal.* **2023**, *365*, 2676–2689. DOI: 10.1002/adsc.202300412.

(32) Schmidt, H.; Meinert, H. Zum Mechanismus Der Elektrochemischen Fluo- Rierung Und Iiber Die Bildung von Jod-Monofluorid. *Angew. Chem.* **1960**, *72*, 109–110. DOI: 10.1002/ange.19600720305.

(33) Rozhkov, I. N. Radical-Cation Mechanism of the Anodic Fluorination of Organic Compounds. *Russ. Chem. Rev.* **1976**, *45*, 615–629. DOI: 10.1070/RC1976v045n07ABEH002697.

(34) Amano, Y.; Inoue, K.; Nishiyama, S. Oxidative Access to Quinolinone Derivatives with Simultaneous Rearrangement of Functional Groups. *Synlett* **2008**, *2008*, 134–136. DOI: 10.1055/s-2007-1000829.

(35) Nishiyama, S.; Amano, Y. Effects of Aromatic Substituents of Electrochemically Generated Hypervalent Iodine Oxidant on Oxidation Reactions. *Heterocycles* **2008**, *75*, 1997–2003. DOI: 10.3987/COM-08-11331.

(36) Samanta, R.; Kulikov, K.; Strohmann, C.; Antonchick, A. Metal-Free Electrocyclization at Ambient Temperature: Synthesis of 1-Arylcarbazoles. *Synthesis* **2012**, *44*, 2325–2332. DOI: 10.1055/s-0032-1316743.

(37) Yuan, D.-F.; Wang, Z.-C.; Geng, R.-S.; Ren, G.-Y.; Wright, J. S.; Ni, S.-F.; Li, M.; Wen, L.-R.; Zhang, L.-B. Hypervalent Iodine Promoted the Synthesis of Cycloheptatrienes and Cyclopropanes. *Chem. Sci.* **2022**, *13*, 478–485. DOI: 10.1039/D1SC05429E.

(38) Broese, T.; Francke, R. Electrosynthesis Using a Recyclable Mediator–Electrolyte System Based on Ionically Tagged Phenyl Iodide and 1,1,1,3,3,3-Hexafluoroisopropanol. *Org. Lett.* **2016**, *18*, 5896–5899. DOI: 10.1021/acs.orglett.6b02979.

(39) Roesel, A. F.; Broese, T.; Májek, M.; Francke, R. Iodophenylsulfonates and Iodobenzoates as Redox-Active Supporting Electrolytes for Electrosynthesis. *ChemElectroChem* **2019**, *6*, 4229–4237. DOI: 10.1002/celc.201900540.

(40) Elsherbini, M.; Wirth, T. Electroorganic Synthesis under Flow Conditions. *Acc. Chem. Res.* **2019**, *52*, 3287–3296. DOI: 10.1021/acs.accounts.9b00497.

(41) Elsherbini, M.; Winterson, B.; Alharbi, H.; Folgueiras-Amador, A. A.; Génot, C.; Wirth, T. Continuous-Flow Electrochemical Generator of Hypervalent Iodine Reagents: Synthetic Applications. *Angew. Chem., Int. Ed.* **2019**, *58*, 9811–9815. DOI: 10.1002/anie.201904379.

(42) Winterson, B.; Rennigholtz, T.; Wirth, T. Flow Electrochemistry: A Safe Tool for Fluorine Chemistry. *Chem. Sci.* **2021**, *12*, 9053–9059. DOI: 10.1039/D1SC02123K.

(43) Scheidt, F.; Thiehoff, C.; Yilmaz, G.; Meyer, S.; Daniliuc, C. G.; Kehr, G.; Gilmour, R. Fluorocyclisation via I(I)/I(III) Catalysis: a Concise Route to Fluorinated Oxazolines. *Beilstein J. Org. Chem*. **2018**, *14*, 1021–1027. DOI: 10.3762/bjoc.14.88.

(44) Herszman, J. D.; Berger, M.; Waldvogel, S. R. Fluorocyclization of *N*-Propargylamides to Oxazoles by Electrochemically Generated $ArIF_2$. *Org. Lett.* **2019**, *21*, 7893–7896. DOI: 10.1021/acs.orglett.9b02884.

(45) Gao, W.-C.; Xiong, Z.-Y.; Pirhaghani, S.; Wirth, T. Enantioselective Electrochemical Lactonization Using Chiral Iodoarenes as Mediators. *Synthesis* **2019**, *51*, 276–284. DOI: 10.1055/s-0037-1610373.

(46) Möckel, R.; Babaoglu, E.; Hilt, G. Iodine(III)-Mediated Electrochemical Trifluoroethoxy-lactonisation: Rational Reaction Optimisation and Prediction of Mediator Activity. *Chem.-Eur. J.* **2018**, *24*, 15781–15785. DOI: 10.1002/chem.201804152.

(47) Maity, A.; Frey, B. L.; Hoskinson, N. D.; Powers, D. C. Electrocatalytic C–N Coupling via Anodically Generated Hypervalent Iodine Intermediates. *J. Am. Chem. Soc.* **2020**, *142*, 4990–4995. DOI: 10.1021/jacs.9b13918.

(48) Frey, B. L.; Figgins, M. T.; Van Trieste, G. P.; Carmieli, R.; Powers, D. C. Iodine–Iodine Cooperation Enables Metal-Free C–N Bond-Forming Electrocatalysis via Isolable Iodanyl Radicals. *J. Am. Chem. Soc.* **2022**, *144*, 13913–13919. DOI: 10.1021/jacs.2c05562.

(49) Kong, X.; Lin, L.; Chen, X.; Chen, Y.; Wang, W.; Xu, B. Electrochemical Oxidative Syntheses of NH-Sulfoximines, NH-Sulfonimidamides and Dibenzothiazines via Anodically Generated Hypervalent Iodine Intermediates. *ChemSusChem* **2021**, *14*, 3277–3282. DOI: 10.1002/cssc.202101002.

(50) Hui, C.; Antonchick, A. P. *Org. Chem. Front.* **2022**, *9*, 3897–3907. DOI: 10.1039/D2QO00739H.

(51) Liu, F.; Dai, J.; Cheng, X. Aryl-Iodide-Mediated Electrochemical Aziridination of Electron-Deficient Alkenes. *Chin. J. Org. Chem.* **2021**, *41*, 4014–4020. DOI: 10.6023/cjoc202105046.

(52) Richardson, R. D.; Desaize, M.; Wirth, T. Hypervalent Iodine-Mediated Aziridination of Alkenes: Mechanistic Insights and Requirements for Catalysis. *Chem.-Eur. J.* **2007**, *13*, 6745–6754. DOI: 10.1002/chem.200700306.

(53) Elsherbini, M.; Moran, W. J. Toward a General Protocol for Catalytic Oxidative Transformations Using Electrochemically Generated Hypervalent Iodine Species. *J. Org. Chem.* **2023**, *88*, 1424–1433. DOI: 10.1021/acs.joc.2c02309.

(54) Demmer, C. S.; Bunch, L. Benzoxazoles and Oxazolopyridines in Medicinal Chemistry Studies. *Eur. J. Med. Chem.* **2015**, *97*, 778–785. DOI: 10.1016/j.ejmech.2014.11.064.

(55) Rajasekhar, S.; Maiti, B.; Chanda, K. A Decade Update on Benzoxazoles, a Privileged Scaffold in Synthetic Organic Chemistry. *Synlett* **2017**, *28*, 521–541. DOI: 10.1055/s-0036-1588671.

(56) Gieshoff, T.; Kehl, A.; Schollmeyer, D.; Moeller, K. D.; Waldvogel, S. R. Electrochemical Synthesis of Benzoxazoles from Anilides – a New Approach to Employ Amidyl Radical Intermediates. *Chem. Commun.* **2017**, *53*, 2974–2977. DOI: 10.1039/C7CC00927E.

(57) Morofuji, T.; Shimizu, A.; Yoshida, J. Electrochemical Intramolecular C–H Amination: Synthesis of Benzoxazoles and Benzothiazoles. *Chem.-Eur. J.* **2015**, *21*, 3211–3214. DOI: 10.1002/chem.201406398.

(58) Shih, Y.; Ke, C.; Pan, C.; Huang, Y. Transition-Metal Catalyst Free C–N Coupling with Phenol/Phenoxide: A Green Synthesis of a Benzoxazole Scaffold by an Anodic Oxidation Reaction. *RSC Adv.* **2013**, *3*, 7330–7336. DOI: 10.1039/c3ra00128h.

(59) Kang, L.-S.; Xiao, H.; Zeng, C.-C.; Hu, L.-M.; Little, R. D. Electrochemical Synthesis of Benzoxazoles Mediated by 2,3-Dichloro-5,6-Dicyano-p-Hydroquinone (DDH) as a Redox Catalyst. *J. Electroanal. Chem.* **2016**, *767*, 13–17. DOI: 10.1016/j.jelechem.2015.12.051.

(60) Li, W.-C.; Zeng, C.-C.; Hu, L.-M.; Tian, H.-Y.; Little, R. D. Efficient Indirect Electrochemical Synthesis of 2-Substituted Benzoxazoles Using Sodium Iodide as Mediator. *Adv. Synth. Catal.* **2013**, *355*, 2884–2890. DOI: 10.1002/adsc.201300502.

(61) Koleda, O.; Broese, T.; Noetzel, J.; Roemelt, M.; Suna, E.; Francke, R. Synthesis of Benzoxazoles Using Electrochemically Generated Hypervalent Iodine. *J. Org. Chem.* **2017**, *82*, 11669–11681. DOI: 10.1021/acs.joc.7b01686.

(62) Tohma, H.; Maegawa, T.; Takizawa, S.; Kita, Y. Facile and Clean Oxidation of Alcohols in Water Using Hypervalent Iodine(III) Reagents. *Adv. Synth. Catalyis* **2002**, *344*, 328–337. DOI: 10.1002/1615-4169(200206)344:3/4<328::AID-ADSC328>3.0.CO;2-S.

(63) Tohma, H.; Takizawa, S.; Maegawa, T.; Kita, Y. Facile and Clean Oxidation of Alcohols in Water Using Hypervalent Iodine(III) Reagents. *Angew. Chem., Int. Ed.* **2000**, *39*, 1306–1308. DOI: 10.1002/(SICI)1521-3773(20000403)39:7<1306::AID-ANIE1306>3.0.CO;2-J.

(64) Dohi, T.; Maruyama, A.; Yoshimura, M.; Morimoto, K.; Tohma, H.; Shiro, M.; Kita, Y. A Unique Site-Selective Reaction of Ketones with New Recyclable Hypervalent Iodine(III) Reagents Based on a Tetraphenylmethane Structure. *Chem. Commun.* **2005**, *2005*, 2205–2207. DOI: https://doi.org/10.1039/b501475a.

(65) Ochiai, M. Reactivities, Properties and Structures. In *Hypervalent Iodine Chemistry*; Wirth, T., Ed.; de Meijere, A., Kessler, H., Ley, S. V., Thiem, J., Vögtle, F., Houk, K. N., Lehn, J.-M., Schreiber, S. L., Trost, B. M., Yamamoto, H., Series Eds.; Springer Berlin Heidelberg: Berlin, Heidelberg, 2003; Vol. 224, pp 5–68. DOI: 10.1007/3-540-46114-0_2.

(66) Said, G.; Grippon, S.; Kirkpatrick, P. Tafamidis. *Nat. Rev. Drug Discov.* **2012**, *11*, 185–186. DOI: 10.1038/nrd3675.

(67) Dohi, T.; Yamaoka, N.; Kita, Y. Fluoroalcohols: Versatile Solvents in Hypervalent Iodine Chemistry and Syntheses of Diaryliodonium(III) Salts. *Tetrahedron* **2010**, *66*, 5775–5785. DOI: 10.1016/j.tet.2010.04.116.

(68) Dohi, T.; Ito, M.; Yamaoka, N.; Morimoto, K.; Fujioka, H.; Kita, Y. Unusual Ipso Substitution of Diaryliodonium Bromides Initiated by a Single-Electron-Transfer Oxidizing Process. *Angew. Chem., Int. Ed.* **2010**, *49*, 3334–3337. DOI: 10.1002/anie.200907281.

(69) Sokolovs, I.; Lubriks, D.; Suna, E. Copper-Catalyzed Intermolecular C–H Amination of (Hetero)Arenes via Transient Unsymmetrical λ^3-Iodanes. *J. Am. Chem. Soc.* **2014**, *136*, 6920–6928. DOI: 10.1021/ja502174d.

(70) Antonchick, A. P.; Samanta, R.; Kulikov, K.; Lategahn, J. Organocatalytic, Oxidative, Intramolecular C–H Bond Amination and Metal-Free Cross-Amination of Unactivated Arenes at Ambient Temperature. *Angew. Chem., Int. Ed.* **2011**, *50*, 8605–8608. DOI: 10.1002/anie.201102984.

(71) Franz, J. A.; Barrows, R. D.; Camaioni, D. M. Arrhenius Parameters for Rearrangements of the Neophyl, 1-Indanylmethyl, 2-Allylbenzyl, and 2-(2-Vinylphenyl)Ethyl Radicals Relative to Hydrogen Abstraction from Tributylstannane. *J. Am. Chem. Soc.* **1984**, *106*, 3964–3967. DOI: 10.1021/ja00326a013.

(72) Dohi, T.; Uchiyama, T.; Yamashita, D.; Washimi, N.; Kita, Y. Efficient Phenolic Oxidations Using μ-Oxo-Bridged Phenyliodine Trifluoroacetate. *Tetrahedron Lett.* **2011**, *52*, 2212–2215. DOI: 10.1016/j.tetlet.2010.12.037.

(73) Varma, R. S.; Saini, R. K.; Prakash, O. Hypervalent Iodine Oxidation of Phenolic Schiff's Bases: Synthesis of 2-Arylbenzoxazoles. *Tetrahedron Lett.* **1997**, *38*, 2621–2622. DOI: 10.1016/S0040-4039(97)00444-9.

2. ELECTROCHEMICAL SYNTHESIS OF THF AND THP DERIVATIVES BY INTRAMOLECULAR HOFER-MOEST REACTION

2.1. Direct electrochemical decarboxylation of carboxylic acids in Hofer-Moest reaction

One of the oldest organic electrochemical reactions is Kolbe electrolysis.[1,2] In the Kolbe decarboxylation, a carboxylate undergoes anodic one-electron oxidation to produce acyloxy radicals. These radicals are rather unstable and a spontaneous decarboxylation occurs to give a corresponding alkyl radical (Figure 2.1). Depending on the structure of the carboxylate and on the electrolysis conditions, the formed alkyl radical can undergo either coupling reaction (Kolbe reaction) or further oxidation to carbenium ion. The later can react with a nucleophile and give a non-Kolbe product (Hofer-Moest reaction).[3]

2.1.1. Electrolysis conditions: Kolbe vs Hofer-Moest reactions

The experimental parameters that influence the outcome of the anodic decarboxylation reaction (Kolbe vs Hofer-Moest) are current density, anode material, the pH of the reaction media, additives and the solvent (Table 2.1).[4,5] Both reactions are usually performed in an undivided cell at constant current density. One-electron oxidation/decarboxylation results in a formation of an alkyl radical. This radical pathway is favored by employment of high current density (> 250 mA/cm^2) that favors absorption of the carboxylate on the anode and ensures high concentration of radicals and their homocoupling at the anode surface.[6,7] In contrast, low current densities facilitate the second one-electron oxidation of the alkyl radical and generation of a carbocation. It is beneficial to use a smooth Pt anode for a successful radical coupling reaction (Kolbe reaction), whereas the Hofer-Moest reaction is favored by the employment of a rough anode surface (soft graphite). However, if a nonporous carbon anode such as glassy carbon is employed, then Kolbe dimers are produced. This implies that the actual surface areas on the different carbon-based electrodes

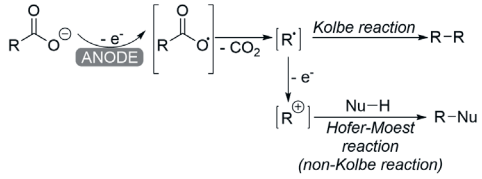

Figure 2.1. **General scheme for anodic decarboxylation reaction**

Table 2.1. **Comparison of reaction conditions for Kolbe coupling and Hofer-Moest reaction**

Kolbe decarboxylation	Hofer-Moest reaction
High current density (> 250 mA/cm^2)	Low current density
Anode material: Pt (smooth surface)	Anode material: graphite (rough surface)
Low pH	Basic media
Additives should be avoided	Additives are beneficial
Solvent: MeOH, aqueous MeOH	MeOH, aqueous MeOH, MeCN
–	Carbon cation stabilizing groups

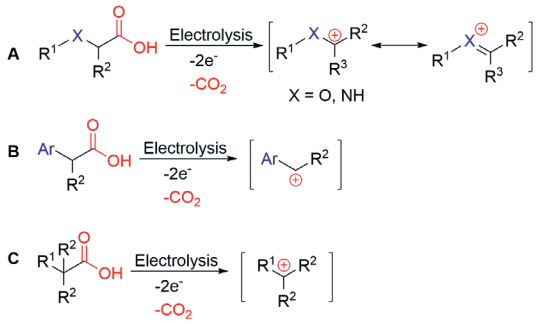

Figure 2.2. **General structures of carboxylic acid that favor the Hofer-Moest reaction**

vary, which results in different current densities. Different current densities lead to different concentrations of radicals at the electrode. The dense glassy graphite and smooth Pt anode provides high concentration of alkyl radicals and favors bimolecular dimerization, while soft graphite anode with lower concentration of alkyl radicals favors the second electron transfer and the generation of carbocation.[4] The nature of cathode material is not critical for both reactions since in most cases neither a starting carboxylate nor a product is reduced at the potential more positive than the one required for hydrogen evolution.

The pH of the reaction solution in Hofer-Moest electrolysis can be chosen rather freely. However, usually, basic media facilitates carboxylic acids to undergo two-electron oxidation. In contrast, low pH values are favorable for the Kolbe reaction, and only 2–10% of a base (alkali metal hydroxide or methoxide) are required to ensure carboxylate formation for one-electron-oxidation. Moreover, an alkali metal carboxylate can also serve as a supporting electrolyte. Thus, no other additives are required for a successful Kolbe reaction. Moreover, the addition of supporting electrolytes might have a negative impact on the outcome of the Kolbe reaction. Thus, foreign anions, such as ClO_4^-, BF_4^-, SO_4^-, $H_2PO_4^-$, HCO_3^-, and F^- should be avoided, because they inhibit the radical reactions and favor the formation of carbenium species (Hofer-Moest reaction). This effect is explained by the adsorption of foreign anions at the anode, which lowers radical concentration at the electrode. Finally,

MeOH and aqueous MeOH usually are the solvents of choice for Kolbe oxidation. DMF and wet MeCN also can be used, although the yields of Kolbe dimers are low in solvents that contain more than 4% water.[4,5,8] Finally, the structure of the carboxylate can also influence the outcome of the anodic decarboxylation reaction (Figure 2.2). Introduction of oxygen or nitrogen atom (Figure 2.2A), or aromatic ring (Figure 2.2B) to the α-position of a starting carboxylic acid favors the anodic generation of a carbon cation. Moreover, bulky substituents that hinder the adsorption of radicals also favor the Hofer-Moest reaction (Figure 2.2C).[4,5,9]

To summarize, the experimental conditions that promote the carbocation formation during anodic decarboxylation (Hofer-Moest reaction) include low current density, a porous graphite anode, the introduction of foreign anions (e.g. perchlorate), elevated pH levels, as well as carbon cation stabilizing groups in the corresponding carboxylic acid.

2.1.2. Hofer-Moest reaction

In 1902 Hofer and Moest reported the electrochemical decarboxylation reaction of fatty acid salts in water. The electrolysis afforded alcohol that resulted from water addition to the cationic intermediate generated during the electrochemical decarboxylation.[3] In general, electrochemical generation of carbocation by oxidative decarboxylation followed by a reaction with a nucleophile is known as non-Kolbe or Hofer-Moest reaction (Figure 1.1).

C_{sp3}–O bond formation in intermolecular Hofer-Moest reaction

A new C_{sp3}–O bond is formed during Hofer-Moest reaction when an alkyl carboxylic acid undergoes anodic decarboxylation in the presence of an *O*-nucleophile in the reaction solution (Figure 2.3). For example, oxidative decarboxylation in the presence of other carboxylic acid affords an ester. A Hofer-Moest reaction in aqueous media might results in formation of an alcohol. Finally, if the *O*-nucleophile is an alcohol, then the Hofer-Moest reaction can provide ethers, hemiaminals or ketals (Figure 2.3).[4]

Readily available amino acids are suitable substrates for the electrochemical two-electron oxidation/decarboxylation reaction, since the transient carbocation can be stabilized by the adjacent nitrogen atom. Thus, Linstead et al. in

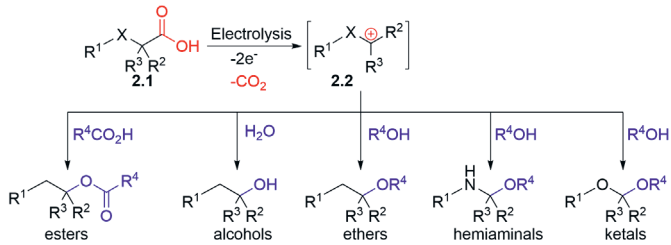

Figure 2.3. **C_{sp3}–O bond formation in the Hofer-Moest reaction**

1951 reported the synthesis of hemiaminals **2.4** by anodic decarboxylation of *N*-protected glycine or alanine **2.3** in alcoholic solvent (MeOH, EtOH, ^{i}PrOH) under galvanostatic control at a current of 100–200 mA/cm^2 using Pt electrodes (Figure 2.4A).[10] Later, similar approach was employed to conduct alkoxylation of proline derivatives **2.5** (Figure 2.4B). The electrolysis was performed also in alcoholic solvent, using graphite electrodes.[11] In 1989, Seebach et al. disclosed methoxylation and acetoxylation of peptides **2.7** (Figure 2.4C).[12] Tertiary amines (Et_3N or DIPEA) were used as a base and employment of Pt or GC electrodes provided a product **2.8**.

In the last decade, Mazurkiewicz et al. elaborated this approach to electrochemical decarboxylative α-methoxylation of *N*-acyl-α-amino acids **2.9** (Figure 2.4D).[13] The authors expanded the scope of the amino acids suitable for the electrochemical α-methoxylation to tyrosine, asparagine, glutamine, serine, threonine, aspartic acid, glutamic acid, histidine, lysine. However, electrolysis of *N*-acylated cysteine, methionine, tryptophan resulted in complex reaction mixtures without formation of the desired hemiaminal. Most likely it is attributed to the presence of redox-sensitive functional groups (e.g., sulfide, indole) in the side chain of these amino acids. NaOMe and silica gel-supported piperidine (SiO_2–Pip) were efficient bases for this reaction. The later usually provided higher yields and higher Faradaic efficiency. Moreover, SiO_2–Pip can be separated and reused.[13]

Other readily available and suitable substrates for electrochemical decarboxylation are malonates and their derivatives, e. g. *N*-acyl malonates. In 1970s, Iwasaki, Horikawa et al. reported electrochemical synthesis of 2-alkoxy-2-amino acid and 2-acetoxy-2-amino acid derivatives **2.12** from the corresponding *N*-acyl malonic acid derivatives **2.11** (Figure 2.5A).[14–16] All the reactions were performed in an undivided cell at constant current in the presence of NaOMe or sodium carboxylate. The authors showed that both Pt and graphite electrodes are suitable for this reaction. Interestingly, the presence of ClO_4^- or BF_4^- completely shut down the alkoxylation reaction and the starting material was completely recovered.[14] The authors assumed that oxidation of the solvent occurred instead of the desired anodic decarboxylation of malonates

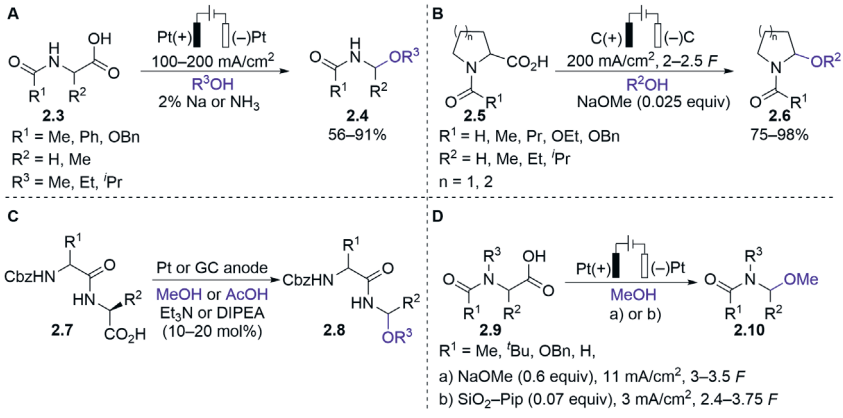

Figure 2.4. **Electrochemical α-akoxylation of amino acids**

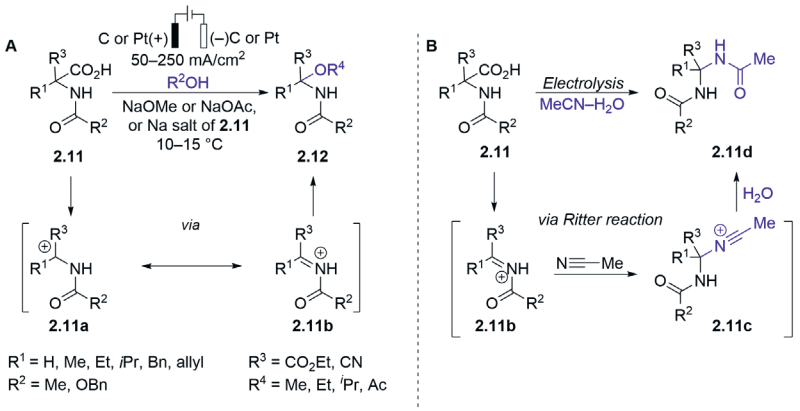

Figure 2.5. **Electrochemical α-alkoxylation and α-acetoxylation of *N*-acyl malonates 2.11 (A); electrochemical Ritter reaction (B)**

2.11, which was supported by the CV measurements in the presence of ClO_4^- or BF_4^- anions. In the most cases the products **2.12** were isolated in excellent yields, and no rearrangement products or Kolbe dimers were detected. Oxidation of a benzylic moiety was not observed as well.[14–16]

The high Faradaic efficiencies of the reported electrolysis also support the generation of a cation intermediate. A lower current efficiency would be observed if the reaction undergoes the radical pathway. Another strong support for the cation intermediate involvement is the formation of 2-acetamide **2.11d** (Ritter reaction product) when the electrolysis was performed in MeCN/H_2O media (Figure 2.5B).[14] The authors emphasized that electrochemical synthesis of α-alkoxy and α-acetoxy-2-amino acid derivatives **2.12** (Figure 2.5A) should be carried out at temperatures not higher than 25 °C due to their poor stability.[14,15] When acetoxyamino acids **2.12** were treated with AcOH at 50 °C, elimination of AcOH and formation of 2,3-dehydro-2-amino acid derivatives were observed. Likewise, the electrolysis of *N*-acyl-aspartic acid monoester **2.13** was conducted at 5 °C in AcOH/THF solution and resulted in the formation of hemiaminals **2.14** in 40–76% yield with alkene **2.15** as the major byproduct (Figure 2.6A). When the electrolysis was performed at the temperature higher than 20 °C, compound **2.15** was the major reaction product.[15]

Iwasaki and co-workers also attempted to synthesize α-hydroxy amino acid derivatives **2.19** (Figure 2.6B).[16] The electrolysis was carried out in H_2O/THF solvent in a presence of KOH. Even though the decarboxylation proceeded smoothly, the formed hemiaminal **2.19** was unstable under the electrolysis conditions, and cleavage of C–N led to the isolation of ethyl phenylpyruvate (**2.18a**) or phenylacetone (**2.18b**).[16]

Malonic acids have been widely used in organic synthesis and they are also suitable as substrates for electrochemical decarboxylation. Anodic oxidation of a malonate **2.21** produces an unstable radical intermediate **A** (Figure 2.7). The subsequent decarboxylation affords a carboxy-stabilized radical **B**. Next, the radical **B** might be further oxidized to zwiterionic species **C**. The intramolecular capture of the cation **C** by the carboxylate moiety leads to the α-lactone **D**. On the other hand, the lactone **D**

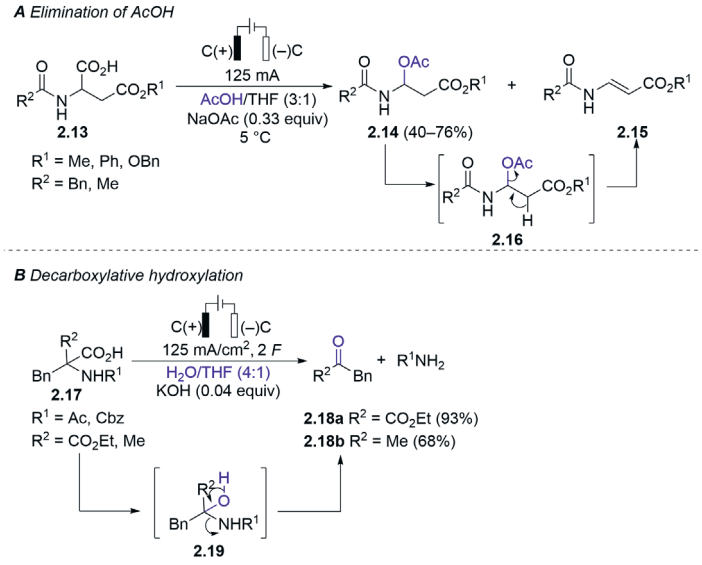

Figure 2.6. **Stability of α-hydroxylated and α-acetoxylated of amino acid derivatives 2.19 and 2.14**

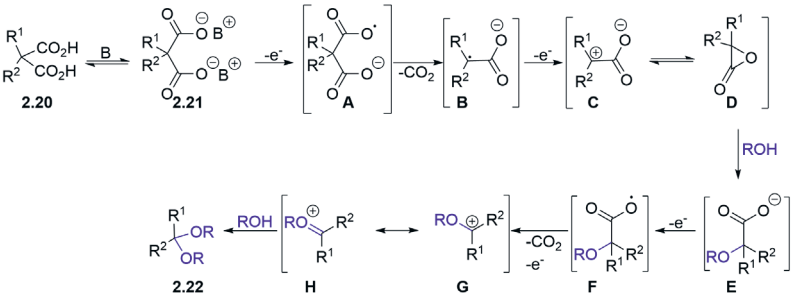

Figure 2.7. **Electrochemical decarboxylation of malonic acid derivative 2.20**

can be formed directly from the radical **B**. Being in equilibrium, the species **C**/**D** react with a nucleophile, which leads to formation of α-alkoxy carboxylate **E**, which is prone to undergo Hofer-Moest reaction.[17–19] After anodic decarboxylation, the oxonium ion **H** is formed. The intermolecular reaction of the cation **H** with alcohol produces a ketal **2.22** (Figure 2.7).

The Hofer-Moest reaction of malonic acids was the first time reported by Nokami et al.[20] under constant current conditions using Pt electrodes in the two-layer system (H_2O–Et_2O) in the presence of NaOH. The substrate scope for this reaction was not explored, and the anodic decarboxylation was applied for only three 2,2-dialkyl-malonic acids. Inspired by this work,[20] Markó and coworkers in 2015 developed an electrochemical synthesis of symmetrical and asymmetrical ketals **2.24** and

ketones **2.25** from the corresponding malonic acids **2.23** (Figure 2.8).[19] The electrolysis was performed in an undivided cell using graphite electrodes at constant current density of 20 mA/cm^2. The use of 2.1 equivalents of NH_3 afforded the desired ketals **2.24** in yields up to 85%. Variety of functional groups, such as esters, alkenes, vinylsilanes, alkynes, and aromatic groups were compatible with the anodic oxidation conditions (for representative examples, see Figure 2.8). Acidic treatment of the ketals **2.24** afforded ketones **2.25**. Recently this methodology was expanded to the electrochemical synthesis of diketones, ketoesters, and tetraketones.[21]

Double decarboxylation of substituted ammonium malonate **2.26** under Hofer-Moest conditions was utilized in the three-step synthesis of spiroketal **2.27**, which is a fragment of ocadaic acid (Figure 2.9).[22] In the first step, malonate **2.26** was electrolyzed under constant current in MeOH using graphite electrodes to afford a ketal **2.26-1**. Next, acetoxy groups of the ketal intermediate were hydrolyzed. Acidic treatment of the ketal **2.26-2** resulted in the intramolecular capture of the carbocation intermediate and spiroketal **2.27** formation in 61% yield over three steps.[22]

In 1982, Wuts and Sutherland reported electrochemical synthesis of monocyclic ketals **2.29** from 2-carboxy-2-allyl-tetrahydropyrans **2.28** (Figure 2.10).[23] The Hofer-Moest reaction was conducted in anhydrous MeOH using Et_4NClO_4 as a supporting

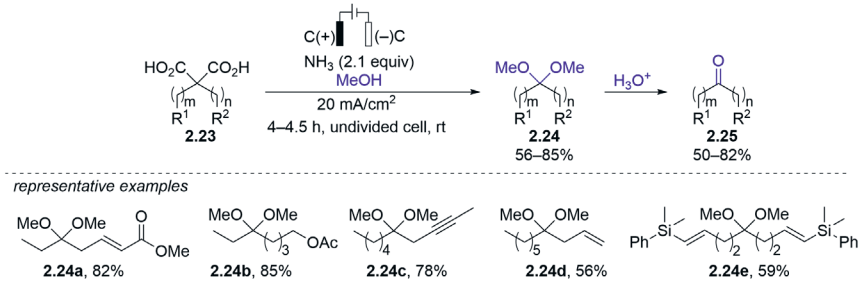

Figure 2.8. **Electrochemical synthesis of ketals and ketones from malonic acid derivatives**

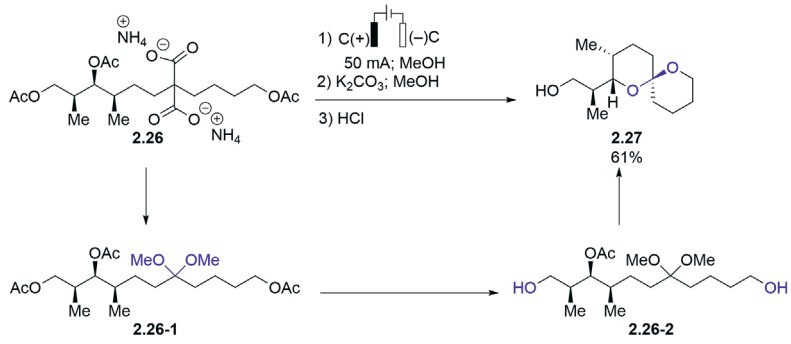

Figure 2.9. **Electrochemical synthesis of cyclic ketal 2.27**

electrolyte and K_2CO_3 as a base. Interestingly, for a successful synthesis of ketals **2.29** the electrolysis was performed in a divided cell to prevent hydrogenation of a double bond at the platinum cathode where the hydrogen evolution occurred.

The Hofer-Moest electrolysis was also employed for preparation of methoxymethyl (MOM) ethers. In 1993 Klocke et al. reported anodic synthesis of methoxymethyl alkyl ethers using high current density, undivided cell and Pt electrodes.[24] Recently, the synthesis of MOM alkyl ethers and acetals was elaborated by Lam group (Figure 2.11A).[25] The authors reported that MOM ethers **2.31** can be obtained from α-alkoxy carboxylic acids **2.30** in high yields (75–93%) by using graphite electrodes in MeOH as solvent. Despite good reaction yields, the Faradaic efficiency of this reaction was low (*FE* 0.15%) due to concurrent anodic oxidation of the solvent. A year later Waldvogel and coworkers reported electrochemical synthesis of aryl MOM ethers **2.34** from aryloxy acetic acids **2.33** using similar reaction conditions (Figure 2.11B).[26] By increasing amount of NaOMe and decreasing current density to 20 mA/cm^2, the authors not only prepared MOM ethers **2.34** in good yields, but they also were able significantly to increase the Faradaic efficiency (from 0.15% to 26% for the ether **2.32**).

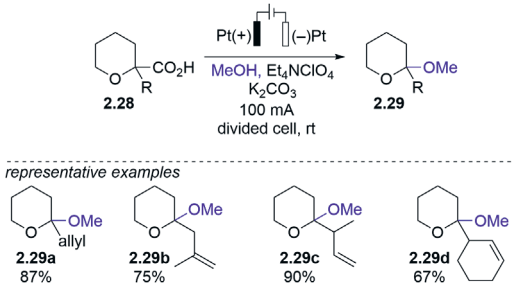

Figure 2.10. **Electrochemical synthesis of monocyclic ketals 2.29**

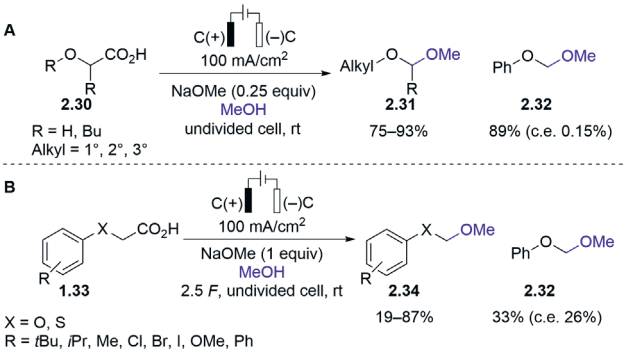

Figure 2.11. **Electrochemical synthesis of methoxymethyl ethers**

In all the examples above, the solvent not only served as a reaction media, but it also played a role of a nucleophile. In 2019, Baran and coworkers disclosed an electrochemical synthesis of hindered dialkyl ethers **2.37** (Figure 2.12A), which might be quite challenging by conventional organic synthesis.[27] In this case only 3 equivalents of an alcohol were required and the reaction was performed in an undivided cell at constant current of 10 mA. 0.1 M Solution of nBu$_4$NPF$_6$ was employed as electrolyte

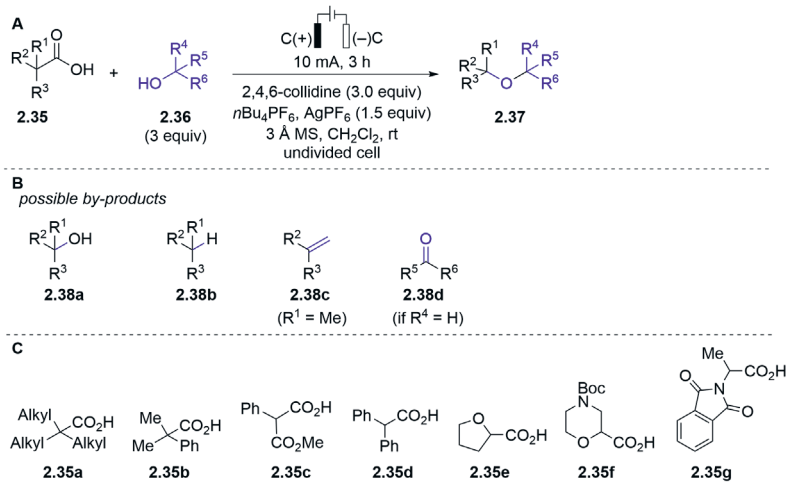

Figure 2.12. **Electrochemical synthesis of hindered ethers 2.37**

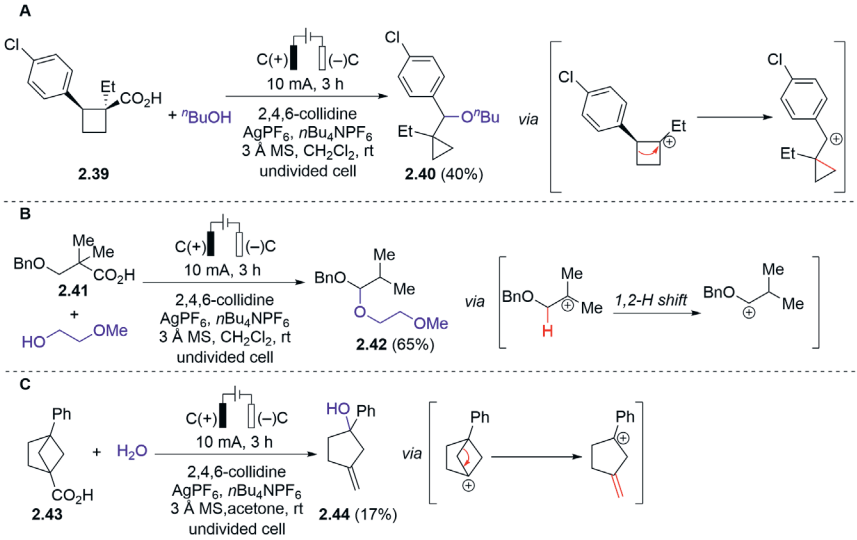

Figure 2.13. **Examples of control experiments**

in CH_2Cl_2. The addition of molecular sieves prevented water quench of transient carbocation to form **2.38a** (Figure 2.12B). The radical pathway and formation of H atom addition product **2.38b** or elimination product **2.38c** was suppressed by addition of 1.5 equivalent of silver salt as a sacrificial oxidant. 2,4,6-Collidine played a crucial role in this reaction, because the desired ether **2.37** was not observed in the absence of the base and the oxidation of alcohol **2.36** (if R^4 = H) took place, generating ketone **2.38d** (Figure 2.12B).[27] The method is applicable for such carboxylic acids **2.35** that allow for the generation of a stabilized carbocation after the anodic decarboxylation (for selected examples see figure 2.12C). For example, decarboxylation of carboxylic acid **2.35a** or **2.35b** afforded a tertiary carbocation. Carboxylic acids **2.35e–g** contain an oxygen or nitrogen atom at the α-position capable of stabilizing the electrochemically generated carbocation.

The formation of a cationic intermediate after decarboxylation was supported by control experiments using acid **2.39** (Figure 2.13). Anodic decarboxylation of **2.39** resulted in a ring contraction and the formation of a cyclopropane **2.40** (Figure 2.13A). Likewise, strain release favored the formation of cyclopentane **2.44** from bicyclic carboxylic acid **2.43** (Figure 2.13C). Interestingly, 1,2-hydride shift and the formation of more stable carbocation occurred after decarboxylation of carboxylic acid **2.41** (Figure 2.13B).[27]

C_{sp3}–N and C_{sp3}–F bond formation in the intermolecular Hofer-Moest reaction

The early examples of C–N bond formation during Hofer-Moest reaction were described for the electrolysis conducted in MeCN solvent (Figure 2.14). Carboxylic acids **2.45** were electrolyzed and the generated cations reacted with MeCN as a *N*-nucleophile toward acetamides **2.46** (analogue of the Ritter reaction, Figure 2.5).[4, 28]

Nitrogen heterocycles are also suitable nucleophiles for the trapping of the electrochemically generated carbocation (Figure 2.15).[29] Interestingly, when the electrolysis was performed under dialkyl ether formation conditions (see Figure 2.12),[27] the desired *N*-alkylated products **2.49** were isolated in poor yield. The main deviation from the etherification conditions occurred when the graphite cathode was substituted with nickel. Variables such as supporting electrolyte and silver salt additive did not have a big impact on the yield of the decarboxylative amination reaction. However, better results were achieved in the absence of the silver salt. The resulting electrochemical conditions (Figure 2.15) exhibited a broad substrate scope with respect to both carboxylic acids **2.47** and heterocycles **2.48** (for representative examples, see Figure 2.15). Thus, a variety of functional groups were tolerated, e.g., ester, BPin, trifluoromethyl, Boc-protected amines. A range of

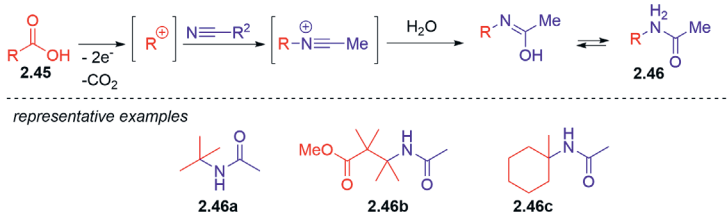

Figure 2.14. **Formation of acetamides 2.46 in Hofer-Moest reaction in MeCN**

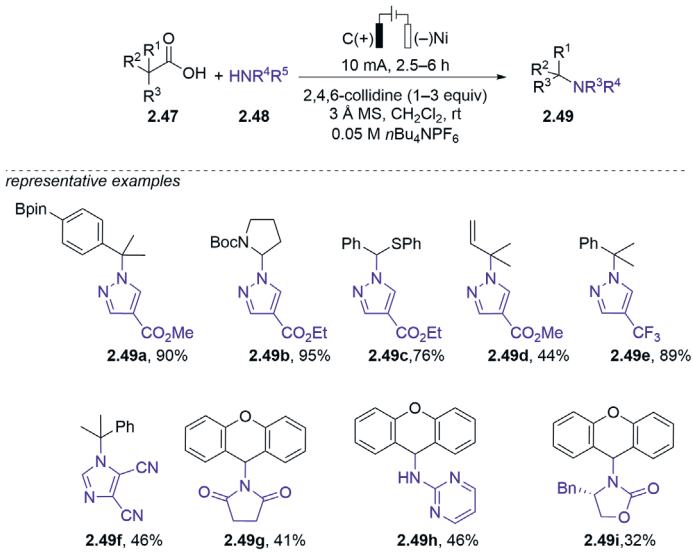

Figure 2.15. **Electrochemical *N*-alkylation of heterocycles 2.48**

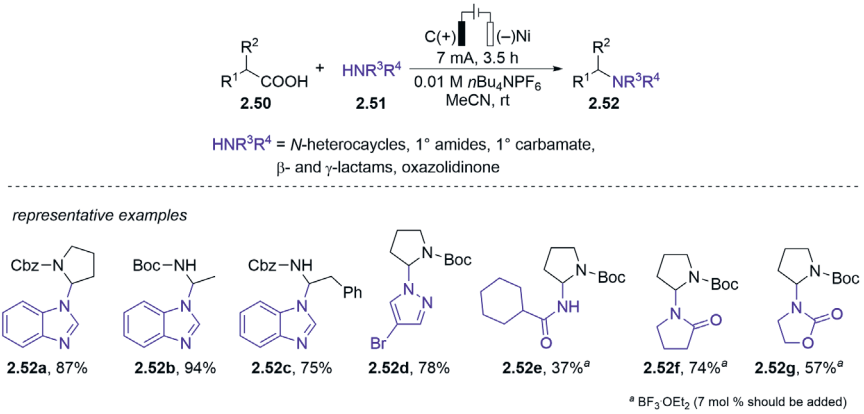

Figure 2.16. **Electrochemical decarboxylation of amino acids 2.50**

heterocycles **2.48** including pyrazoles, triazoles, tetrazoles, imidazoles, indazoles, succinimides, and pyrimidines could be alkylated by this method.

Echavarren et al. have also reported anodic decarboxylative C_{sp3}–N bond formation reaction (Figure 2.16).[30] In contrast to the previously described work of the group of Baran, in this approach, the electrolysis was performed in MeCN solution, and the addition of a base was not required for a successful transformation. Thus, acyclic amino acids **2.50a** and cyclic amino acids **2.50b** as well as phenylacetic acid derivatives **2.50e** were found to be suitable as substrates for decarboxylative C–N bond formation (for representative examples, see Figure 2.16). Primary amides **2.51a–c**, lactams **2.51d,e**, and carbamates **2.51f,g** turned out to be efficient *N*-nucleophiles in

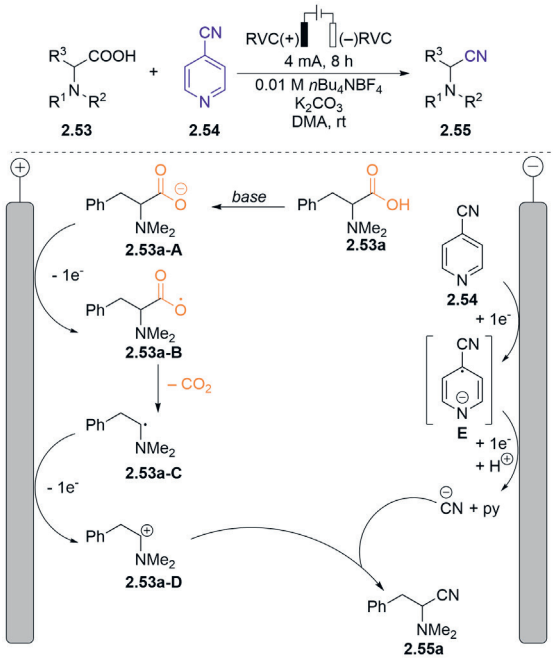

Figure 2.17. **A paired electrochemical decarboxylative cyanation of amino acids 2.53**

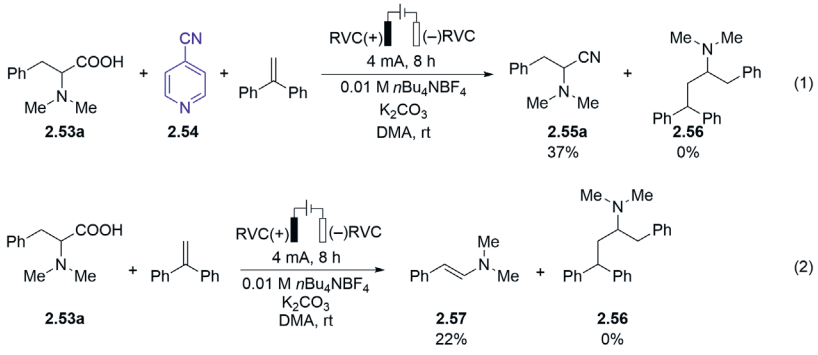

Figure 2.18. **Control experiments for paired decarboxylative cyanation of amino acid 2.53**

the intermolecular Hofer-Moest reaction.[30] In general, the electrolysis did not require the basic additive to deprotonate the carboxylic acid **2.50**. Probably, heterocyclic *N*-nucleophiles played a role of a base. However, a catalytic amount of Lewis acid ($BF_3 \times Et_2O$) was required to facilitate anodic decarboxylation when non-basic amides **2.51e** or lactams **2.52f,g** were electrochemically alkylated.

Rueping and coworkers developed a paired electrolysis for decarboxylative cyanation (Figure 2.17).[31] Thus, anodic decarboxylation of amino acid derivatives

2.53 generated a stabilized carbocation **2.53a-D**, whereas cathodic reduction of 4-CN pyridine **2.54** provided a cyanide anion that reacted with the cationic species to produce α-amino nitrile **2.55**.

The authors performed control experiments to prove that the reaction proceeded through a nucleophilic substitution rather than the radical pathway (Figure 2.18).[31] Electrolysis of the amino acid **2.53a** and 4-CN-pyridine (**2.54**) in the presence of 1,1-diphenylethylene as a radical acceptor afforded only nitrile **2.55a** without the formation of the radical addition product **2.56** (eq 1). The radical addition product **2.56** was not observed also in the absence of 4-CN-pyridine. Instead, the authors observed enamine **2.57** that obviously formed from iminium ion intermediate (eq 2).

Baran and coworkers have also employed the above mentioned electrochemical decarboxylative/etherification conditions (Figure 2.12) for fluorination of carboxylic acids **2.58**.[27] Electrochemical decarboxylative fluorination of carboxylic acid **2.58** in the presence of KF and crown ether afforded useful fluorinated substrates **2.59a–d**.

In 2020, the Waldvogel group also demonstrated that fluoride can serve as a nucleophile in the Hofer-Moest reaction (Figure 2.20).[32] The authors accomplished

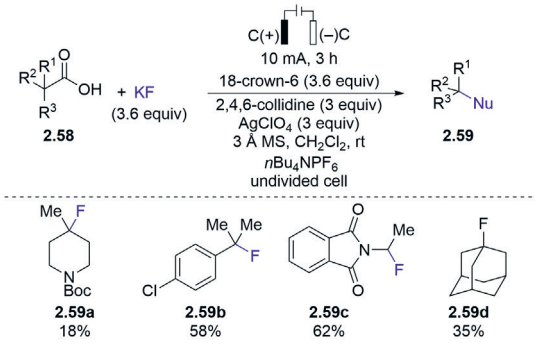

Figure 2.19. **Electrochemical fluorination of carboxylic acids 2.58**

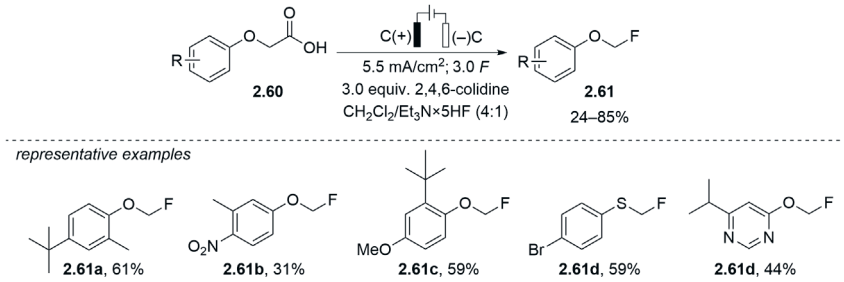

Figure 2.20. **Electrochemical synthesis of fluoromethyl aryl ethers 2.61**

oxidative decarboxylation of aryloxycetic acids **2.60** on graphite anode applying a current density of 5.5 mA/cm^2. The reaction was performed in CH_2Cl_2 in the presence of 2,4,6-collidine, and the oxocarbenium ion intermediate was converted into fluoromethyl aryl ethers **2.61** using $Et_3N{\times}5HF$ as the fluoride source.

Intramolecular Hofer-Moest reaction

The first intramolecular Hofer-Moest reaction was disclosed by Seebach and co-workers in 1989 (Figure 2.21).[12] The authors showed that anodic decarboxylation of dipeptides **2.62** and **2.64**, followed by intramolecular trap of the generated cation with *N*-nucleophile provided heterocycles **2.63** and **2.65**, respectively.

A single example of intramolecular C–O bond formation upon the electrolysis of carboxylic acid **2.67** was reported by Baran (Figure 2.22, eq 1).[27] The substituted tetrahydrofuran **2.68** was obtained in 44% yield. Echavarren and co-workers also reported a single example of the intramolecular Hofer-Moest reaction (Figure 2.22, eq 2), using their conditions for decarboxylative C_{sp3}–N bond formation reaction (see Figure 2.16).[30] Under these conditions, *N*-protected glutamine **2.69** underwent anodic decarboxylation/cyclization reaction, which afforded the cyclized product **2.70** in 60% yield (Figure 2.22, eq 2). [30]

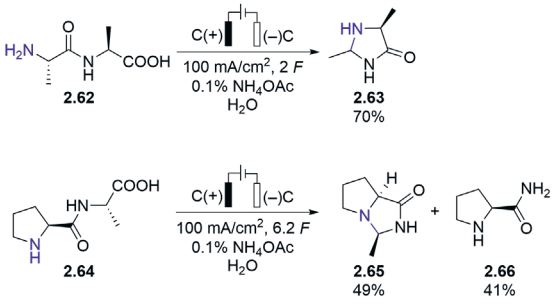

Figure 2.21. **Intramolecular C–N bond formation via Hofer-Moest reaction**

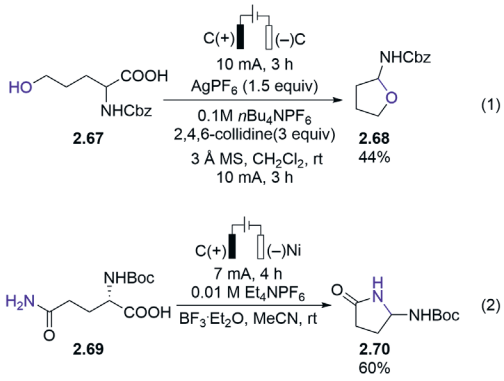

Figure 2.22. **Intramolecular anodic decarboxylative cyclization examples**

Yamada and co-workers reported an intramolecular Hofer-Moest synthesis of substituted morpholines.[33] Using electrolysis conditions reported by Baran group (see Figure 2.12),[27] the authors isolated morpholine **2.72a** in 75% yield. Improvement in yield of morpholine **2.72a** was achieved by replacing $AgPF_6$ and nBu_4NPF_6 with $AgClO_4$ and nBu_4NClO_4, respectively (Figure 2.23). Anodic decarboxylation of tertiary carboxylic acids **2.71** afforded corresponding morpholines **2.72a**,**b** in high yields. Interestingly, 2,2-benzylphenyl-substituted morpholine **2.72c** was obtained in only 36% yield. The authors assumed that due to the steric repulsion and the decomposition of the transient carbocation, the formation of morpholine **2.72c** was less efficient. The presence of α-phenyl substituent in the carboxylic acid **2.71** is crucial for the successful formation of morpholine **2.72**, as a phenyl ring stabilizes the electrochemically generated tertiary carbocation. Thus, electrolysis of α,α-dimethyl carboxylic acid **2.71d** provided the morpholine **2.72d** in only 15% yield. The intramolecular Hofer-Moest reaction worked well with both secondary and tertiary alcohols as nucleophiles. The authors also expanded the intramolecular Hofer-Moest reaction to the synthesis of seven- and 8-membered heterocycles **2.72g** and **2.72h**, respectively (Figure 2.23).[33]

In summary, employment of graphite anode is beneficial in most of the Hofer-Moest reactions described above. Cathode material usually is graphite or nickel. A majority of the intermolecular etherification reactions are performed in alcoholic media in the presence of a base that also plays the role of a supporting electrolyte. Anodic decarboxylative etherification, amination, and fluorination reactions in non-protic media (CH_2Cl_2, DMA) require not only an excess of a base but also an ammonium salt to ensure conductivity of the electrolyte. Although there are several examples of intramolecular Hofer-Moest reaction, the application of this approach is not broadly explored in the synthesis of heterocycles and, in some cases, is limited

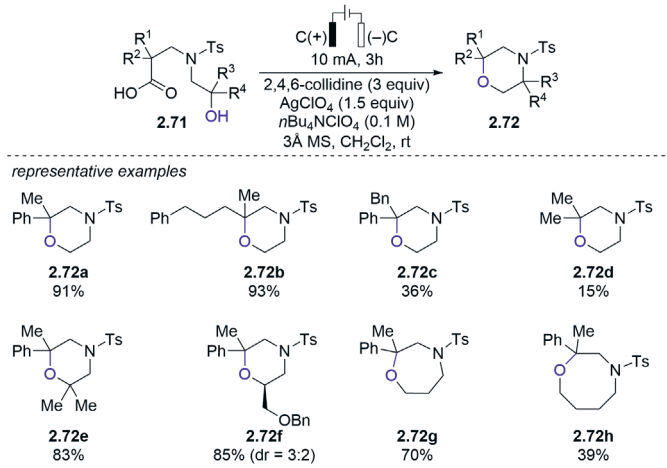

Figure 2.23. **Electrochemical synthesis of substituted morpholines 2.72 via intramolecular Hofer-Moest reaction**

to a few examples. Moreover, an excess of a base is required for intramolecular anodic decarboxylative etherification if the electrolysis is performed in non-protic media (CH_2Cl_2). We envisioned that the intramolecular Hofer-Moest reaction of functionalized *N*-acetylamino malonates could be accomplished in an aqueous environment without the need for an additional base, as the concurrent cathodic reduction of water would produce hydroxide anions. The development and the results of this approach in the synthesis of tetrahydrofuran (THF) and tetrahydropyran (THP) fragment-containing amino acids are described in the section below.

2.2. Results and discussion

This section is based on the published article (*Org. Lett.* 2023, *25*, 7958-7962).[34]

Unnatural (non-proteinogenic) amino acids are extensively utilized as structural components in the design of small molecule drugs and peptidomimetics.[35–37] Specifically, α,α-disubstituted cyclic amino acids have been integrated into clinically utilized anesthetics like carfentanil **2.73** and remifentanil **2.74**, as well as the anticancer drug candidate AZD5363 (**2.75**),[38] the FDA-approved antipruritic medication difelikefalin **2.76**, and an antipruritic drug candidate **2.77**,[39] as well as in the development of osteoporosis candidate balicatib **2.78**[40] and a cathepsin C inhibitor **2.79** for treating COPD[41] (Figure 2.24). α,α-Disubstituted cyclic amino acids are also frequently employed to introduce constraints into a peptide backbone, enhancing stability, permeability, and bioavailability of peptidomimetics.[42–45] The extensive use and valuable attributes of α,α-disubstituted cyclic amino acids underscore the necessity for designing new analogues and emphasize the need for efficient synthesis methods to access these medically relevant structural elements.

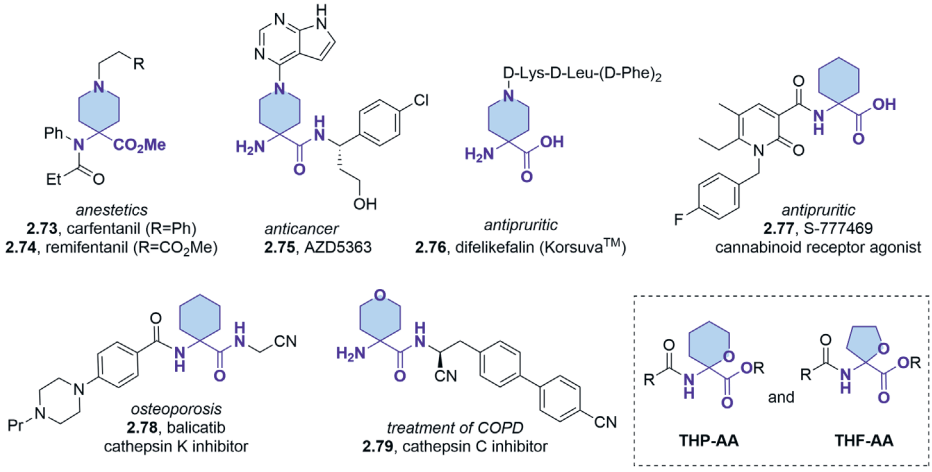

Figure 2.24. **α,α–Disubstituted unusual amino acids in drug design**

We envisioned that previously unreported THP-amino acid and THF-amino acid derivatives[i] could be accessed from readily available *N*-acetylamino malonic acid monoester in the Hofer-Moest reaction that includes electrochemical decarboxylation/oxidation to transient *N*-acyliminium intermediate, followed by etherification with a tethered *O*-nucleophile.

2.2.1. Optimization of the reaction conditions

We chose *N*-acetylamino malonate **2.80a** as the initial substrate to develop intramolecular etherification under Hofer-Moest conditions (Table 2.2). This acid **2.80a** was readily synthesized in two steps from the commercially available diethyl 2-acetamidomalonate by an alkylation/hydrolysis sequence.[47,j] The choice of initial conditions for the anodic decarboxylation of acid **2.80a** was guided by a review of existing literature. In this context, graphite emerges as the most commonly utilized anode material for the Hofer-Moest reaction,[4,48] while Pt is conventionally employed as a cathode to promote proton reduction.[13,14] Additionally, the Hofer-Moest reaction benefits from low current densities and polar aprotic solvents.[4] Consequently, the initial electrolysis of acid **2.80a** was conducted in an undivided cell under constant current conditions (j = 10 mA/cm^2) in an aqueous MeCN medium, without the inclusion of any added base or supporting electrolyte. Pleasingly, the desired heterocycle **2.81a** was formed in 44% yield after passing 1.3 *F* charge (Table 2.2, entry 1). Unfortunately, incomplete conversion of acid **2.80a** was noted, and the decarboxylation process stalled due to low conductivity (the electrolysis reached a potential of >30 V). The addition of Li_2CO_3 (0.5 equiv relative to acid **2.80**) as a supporting electrolyte helped to enhance conductivity, resulting in an increased yield of THF derivative **2.81a** to 55% (entry 2). A further increase in the yield of product **2.81a** to 62% was achieved by substituting Pt with the notably less expensive Ni as a cathode material (entry 3).

A screening of various salts (entries 4–6, 8–10) led to the identification of NaOAc, $LiClO_4$, and NaTFA as the preferred supporting electrolytes for the decarboxylative cyclization, yielding 74–77% of product **2.81a** (entries 4, 6, and 10, respectively). The similar efficiency of the non-basic $LiClO_4$ and the relatively basic NaOAc as supporting electrolytes indicated that an external base was not required for the anodic decarboxylation. A brief evaluation of anode materials using NaOAc as the supporting electrolyte confirmed the superiority of graphite over glassy carbon (GC), reticulated vitreous carbon (RVC), and boron-doped diamond (BDD) (entries 17–19). However, THF derivative **2.81a** was obtained in higher yield when graphite was used instead of Ni as the cathode material, both with NaOAc (76%, entry 12) and $LiClO_4$ as the supporting electrolytes (83%, entry 13). Consequently, graphite was selected as the material for both the anode and cathode, and $LiClO_4$ was chosen as the non-basic and non-nucleophilic supporting electrolyte for all subsequent experiments. An increase in current density from 10 mA/cm^2 to 12 mA/cm^2 did not impact the yield of product **2.81a** (82%, entry 15), although larger deviations led to less

[i] A single report exists on a photochemical synthesis of *N*-Ac-and *N*-Bz-substituted THF-AA methyl esters.[46]

[j] See Supporting information of featured article published in 2023[34] for the synthesis of carboxylic acid **2.80**.

favorable results (entries 14 and 16). Only a slight decrease in the reaction yield was observed when the concentration of the starting carboxylic **2.81a** was increased from 0.05 M to 0.1 M and 0.5 M (entries 21 and 22, respectively).

Table 2.2. **Optimization of anodic decarboxylative etherification**

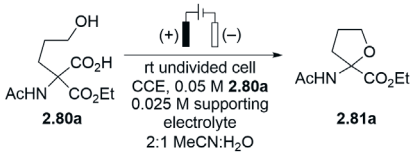

Entry	Anode	Cathode	Supporting electrolyte[a]	*j*, mA/cm^2	Yield, %[b]
1[c]	C	Pt	-	10	44
2[d]	C	Pt	Li_2CO_3	10	55
3[d]	C	Ni	Li_2CO_3	10	62
4[e]	C	Ni	NaOAc	10	74[g]
5[e]	C	Ni	LiOAc	10	69
6[f]	C	Ni	NaTFA	10	74
7[f]	C	Ni	Li_2CO_3	10	71
8[d]	C	Ni	NaO*t*Bu	10	60
9[e]	C	Ni	NH_4OAc	10	69
10[e]	C	Ni	$LiClO_4$	10	77
12[e]	C	C	NaOAc	10	76[g]
13[e]	C	C	$LiClO_4$	10	83
14[e]	C	C	$LiClO_4$	8	72
15[e]	**C**	**C**	**$LiClO_4$**	**12**	**82 (80[h])**
16[e]	C	C	$LiClO_4$	15	78
17[e]	RVC	Ni	NaOAc	10	56
18[e]	GC	Ni	NaOAc	10	63
19[e]	BDD	Ni	NaOAc	10	31
20[e]	Pt	Ni	NaOAc	10	22
21[e,i]	C	C	$LiClO_4$	12	75
22[e,j]	C	C	$LiClO_4$	12	79[h]

[a] 0.5 equiv. with respect to **2.80a**; [b] Yields were determined by ^{1}H NMR spectroscopy of the post-electrolysis solution using CH_2Br_2 as the internal standard. [c] 1.3 *F*; [d] 4 *F*; [e] 3 *F*; [f] 2 *F*; [g] Average yield of two runs; [h] Isolated yield in parenthesis. [i] 0.1 M of **2.80a**. [j] 0.5 M of **2.80a**.

2.2.2. Scope of the developed electrochemical reaction

With the optimized conditions in hand (entry 15, Table 2.2), we explored the scope of the developed method (Figure 2.25). *N*-Acetyl, *N*-Cbz, and *N*-Boc protected aminotetrahydrofuran-2-carboxylates **2.81a–c** were easily obtained in 51%–80% yield. The decarboxylative anodic oxidation demonstrated compatibility with relatively easy-to-oxidize 3-furanoyl and 4-anisoyl substituents (heterocycles **2.81e**, **2.81k**), as well as with the presence of cyano, mesyl, and trifluoromethyl groups in the aryl moiety of cyclic ethers **2.81j**,**h**,**l** (see Figure 2.25A). It is worth noting the compatibility with bromo substituents, which enables further transformations of compounds **2.81i**,**o**, such as in the Buchwald-Hartwig amination as illustrated below. The electrochemical decarboxylation of the substrate containing pyridine (**2.80f**) was sluggish, yielding only 7% of the desired product **2.81f** along with multiple side-products. Six-membered heterocycles **2.81m–o** (Figure 2.25B) can also be synthesized under the developed conditions, albeit with slightly lower yields (56–64%) compared to their corresponding five-membered analogs **2.81a**,**b**,**i** (68–80%). The diminished yield of tetrahydropyrans **2.81m–o** may be attributed to the slower formation of six-membered ring[49] from *N*-acyl iminium intermediates and the competing formation of an open-chain hemiaminal in reaction with water. Indeed, hemiaminal **2.82** was the predominant product in the attempted decarboxylative cyclization of malonate **2.80z** (Figure 2.25E) that yielded only trace amounts of the desired seven-membered heterocycle **2.81z**, as evidenced by LC-MS assay of the crude reaction mixture. The developed anodic decarboxylation/cyclization method is also applicable to amino acid derivatives, such as the protected 2,3-diamino propionic acid derivatives **2.80p**,**q**, as well as the aspartic acid ester **2.80r** (Figure 2.25C).

Given the widespread use of unnatural amino acids in the design of peptidomimetics, we sought to evaluate the suitability of the developed conditions for dipeptide synthesis. Encouragingly, the cyclization of amino acid-containing substrates **2.80s–y** afforded dipeptides **2.81s–y** in 50–86% yield. Notably, the decarboxylative cyclization is compatible with an alkene moiety and a cyclopropyl subunit, as evidenced by the formation of dipeptides **2.81y** and **2.81v**, respectively. All dipeptides **2.81s–y** were obtained as a 1:1 mixture of diastereomers, and the lack of diastereoselectivity in the cyclization was also observed for Mosher amide **2.81d**. The newly formed stereogenic center is configurationally stable as evidenced by the absence of epimerization for diastereomerically and enantiomerically pure THF derivative **(*S*,*S*)-2.81x** under the cyclization conditions. In contrast, moderate diastereoselectivity could be achieved in the cyclization of chiral secondary alcohols (Figure 2.25F), with the highest diastereomeric ratio of 73:27 observed for the formation of the product **2.81ad** from the parent (*R*)-benzyl alcohol. The configuration of the quaternary stereogenic center in the major diastereomer **(*S*,*R*)-2.81ad** was established through X-ray crystallography.[k] Finally, to demonstrate the practical synthetic utility and scalability of the developed method, the synthesis of the five-membered heterocycle **2.81b** was successfully scaled up from 0.9 mmol to 3.5 mmol, to afford 0.83 g of the heterocycle in a single electrolysis batch. A similar upscale from 0.9 mmol to 2.8 mmol was also accomplished for the six-membered products **2.81n**,**o**.

[k] X-Ray crystallographic analysis was performed by Dr. S. Belyakov (Latvian Institute of Organic Synthesis).

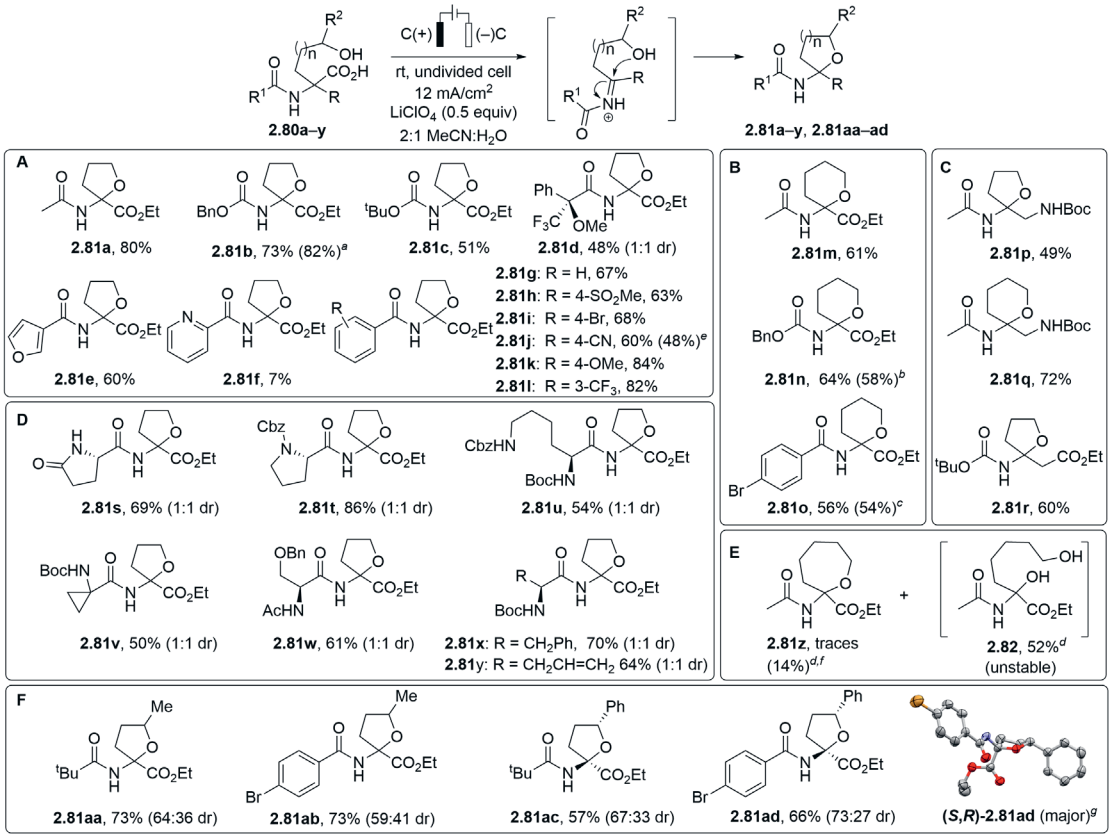

[a] Performed at 1.17 g scale. [b] At 1.00 g scale. [c] At 2.0 g scale. [d] NMR yield. [e] Obtained according to the procedure from ref.33.
[f] Obtained according to the procedure from ref.27. [g] Ellipsoids are shown at 50% probability with hydrogen atoms omitted for clarity.

Figure 2.25. **Scope of decarboxylation/cyclization reaction**

2.2.3. Elucidation of the reaction mechanism

A concise mechanistic investigation was conducted to provide experimental support for the two-electron anodic oxidation to *N*-acyliminium ion (Hofer-Moest reaction) versus the one-electron oxidation (Kolbe electrolysis). In this context, cyclic voltammetry (CV) studies of acid **2.80a** revealed a single irreversible feature at a scan rate of 100 mV/s (E_P = +1.77 V vs. Ag/Ag$^+$), corresponding to the oxidation of the carboxylate (Figure 2.26).[1] Interestingly, carboxylic acid **2.80a** exhibited two anodic peaks at a higher scan rate (600 mV/s), suggesting the formation of an unstable intermediate after the initial irreversible oxidation step (E_{P1} = +1.98 V vs. Ag/Ag$^+$), which then undergoes a chemical transformation, followed by a second oxidation step (E_{P2} = +2.24 V vs. Ag/Ag$^+$). Therefore, the CV data suggests an ECE pathway for the decarboxylative cyclization, involving the anodic oxidation of malonate **2.80a**, followed by decarboxylation, and subsequently, the second oxidation of the carbon-centered radical to form the *N*-acyliminium ion, a scenario characteristic of the Hofer-Moest reaction.

Further support for the ionic pathway in the cyclization process was garnered by subjecting unsaturated acid **2.83** to the established anodic decarboxylation conditions (Figure 2.27). It has been documented that 5-hexenyl acids, which share structural similarity with compound **2.83**, readily undergo radical *5-exo-trig* cyclization under Kolbe electrolysis conditions.[50] These radical cyclizations occur at remarkably high-rate constants (for instance, 1.6 × 10^8 s^{-1} for the 6-cyano-5-hexenyl radical),[51] making

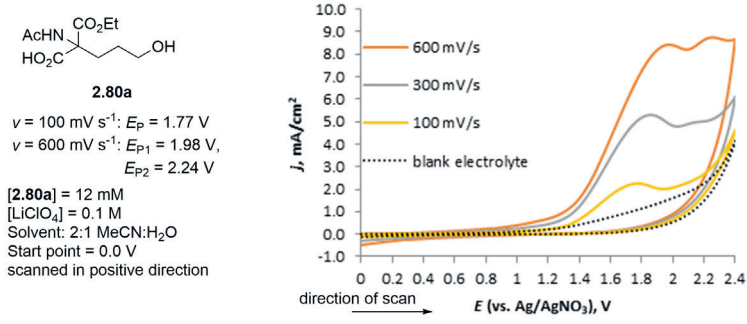

Figure 2.26. **CV analysis of carboxylic acid 2.80a**

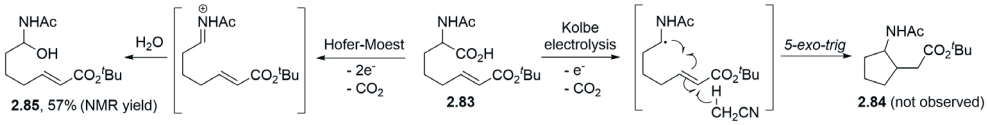

Figure 2.27. **Radical clock experiment**

[1] See Supporting information of featured article published in 2023[47] for the detailed description of CV measurements.

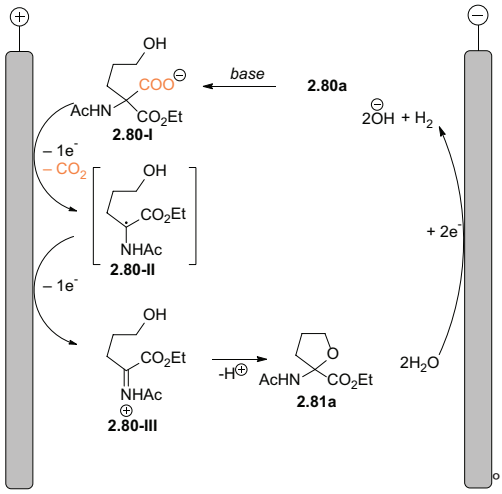

Figure 2.28. **Proposed mechanism for the intramolecular Hofer-Moest reaction**

them valuable tools in radical clock reactions. Notably, the formation of the *5-exo-trig* cyclization product **2.84** from carboxylic acid **2.83** was not observed (Figure 2.27). Instead, the major product formed was an unstable hemiaminal **2.85** (57% NMR yield), along with the unreacted acid **2.83** (18%). Taken together, these mechanistic studies offer compelling evidence in favor of the two-electron anodic decarboxylation of carboxylic acid **2.80a** and the generation of *N*-acyliminium ion **2.80-III** (Figure 2.28). Eventually cation **2.80-III** undergoes intramolecular etherification with tethered *O*-nucleophile, which affords THF and THP-containing amino acid derivatives **2.81**.

2.2.4. Synthetic modifications of THF-AA and THP-AA

We proceeded to briefly investigate the reactivity of THF- and THP-AA derivatives. It was observed that THF-amino acid remains stable under basic conditions, as demonstrated by the hydrolysis of ester **2.81b** to acid **2.86** in 78% yield using aqueous LiOH (Figure 2.29A). Acid **2.86** is also stable at pH4 (phosphate buffer) for at least 48 hours. Additional confirmation of the relative stability of THF-AA under basic conditions was obtained through the successful *N*-alkylation of ester **2.81n**, yielding amide **2.89** (40%). Pd-catalyzed hydrogenolysis of *N*-Cbz group in THF derivative **2.81b** resulted in the ring-opening product **2.88** (87%). This indicates the instability of the *N*-unprotected hemiaminal, which evidently undergoes reduction of the open-chain imine tautomer. In the meantime, the *N*-Cbz protection can be swapped with *N*-Boc in a two-step sequence involving the *N*-acylation of carbamate **2.81b** with Boc_2O, catalyzed by DMAP, followed by Pd-catalyzed hydrogenolysis (86% overall yield over two steps; Figure 2.29A).

Finally, we have synthesized THP-amino acid derivative **2.92** (Figure 2.29B) to investigate its bioisosteric relationship with balicatib **2.78** (Figure 2.24). This involved a sequence of reactions including Pd-catalyzed amination of compound **2.81n** with piperazine, followed by ester hydrolysis and amide bond formation, resulting

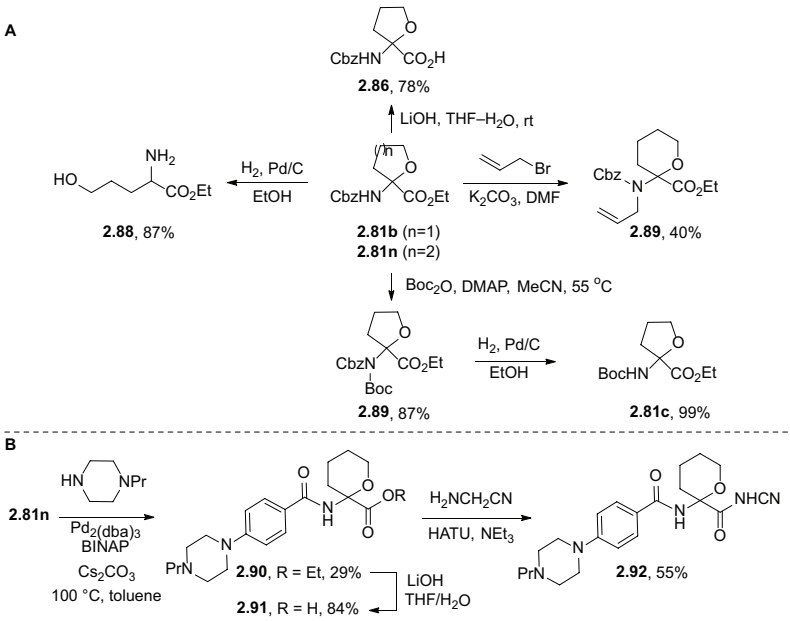

Figure 2.29. **Synthetic modifications of THF-AA and THP-AA**

Table 2.3. **Comparison of pharmacokinetic properties of balicatib (2.78) and its analogue 2.92**

Compound	**2.78**	**2.92**
Inhibition of Cathepsin K, IC_{50} (nM)	0.46 ±0.08	0.34 ±0.11
cLog *P*[a]	1.245	-0.015
Log *P*[b]	1.60	0.95
$t_{1/2}$ (min) (H)[c]	>120	>120
PPB (% free)[d]	45.6	55.2

[a] Calculated with ChemDraw 21.0. [b] Determined by HPLC-UV method. [c] Human liver microsomes.
[d] Determined in human plasma.

in the formation of balicatib analogue **2.92**. As expected, the THP-AA derivative **2.92** exhibits reduced lipophilicity (Log *P* = 0.95)[m] compared to balicatib **2.78** (Log *P* = 1.60) (Table 2.3). Additionally, it displays similar enzymatic activity[n] (0.34 nM vs. 0.46 nM, respectively), along with comparable metabolic stability and plasma protein binding[o] (Table 2.3). Hence, THF and THP-containing amino acids serve as suitable

[m] Log P was determined by Dr. H. Kazoka (Latvian Institute of Organic Synthesis).
[n] Inhibitory potency measurements were performed by Dr. I. Kanepe (Latvian Institute of Organic Synthesis).
[o] Plasma protein binding and metabolic stability measurements were performed by B. Gukalova (Latvian Institute of Organic Synthesis).

bioisosteres for the corresponding α,α-disubstituted carbocyclic amino acids, offering a reduction in lipophilicity (Log *P*).

2.2.5. Summary

The electrochemical oxidative decarboxylation-intramolecular etherification of inexpensive and readily available *N*-acetyl malonic acid monoesters under Hofer-Moest conditions offers a route to previously unreported THP and THF-containing amino acid derivatives. This decarboxylative cyclization, conducted under constant current conditions in an undivided cell, occurs in aqueous media without any added bases. It demonstrates compatibility with relatively easy-to-oxidize 3-furanoyl and 4-anisoyl moieties, as well as with cyano and bromo substituents within an aryl ring. The versatility of this electrochemical synthesis method was showcased by 29 examples, yielding products with up to 86% isolated yield. When incorporated into dipeptides and peptidomimetics, THP and THF-containing amino acids can serve as bioisosteres for α, α-disubstituted cyclic amino acids. We successfully replaced the 1-aminocyclohexane-1-carboxamide moiety in balicatib with a THP-amino acids fragment, resulting in reduced lipophilicity (Log *P*), while preserving low nanomolar cathepsin K inhibitory activity and comparable microsomal stability to that of the original balicatib. Given the broad utility of α,α-disubstituted cyclic amino acids in organic and medicinal chemistry, we believe that the oxygen-containing unnatural amino acid scaffolds presented in this study have great potential for application in drug discovery campaigns.

REFERENCES

(1) Faraday, M. Siebente Reihe von Experimental-Untersuchungen Über Elektricität. *Ann. Phys. Chem.* **1834**, *109*, 481–520. DOI: 10.1002/andp.18341093102.

(2) Kolbe, H. Zersetzung Der Valeriansäure Durch Den Elektrischen Strom. *Ann. Chem.* **1848**, *64*, 339–341. DOI: 10.1002/jlac.18480640346.

(3) Hofer, H.; Moest, M. Ueber Die Bildung von Alkoholen Bei Der Elektrolyse Fettsaurer Salze. *Justus Liebigs Ann. Chem.* **1902**, *323*, 284–323. DOI: 10.1002/jlac.19023230304.

(4) Schäfer, H.-J. Recent Contributions of Kolbe Electrolysis to Organic Synthesis. In *Electrochemistry IV*; Steckhan, E., Ed.; Topics in Current Chemistry; Springer-Verlag: Berlin/Heidelberg, **1990**, *152*, 91–151. DOI: 10.1007/BFb0034365.

(5) Tanaka, H.; Kuroboshi, M.; Torii, S. Oxidation of Carboxylic Acids and Derivatives. In *Organic Electrochemistry*; Taylor & Francis Group, **2016**.

(6) Leech, M. C.; Lam, K. Electrosynthesis Using Carboxylic Acid Derivatives: New Tricks for Old Reactions. *Acc. Chem. Res.* **2020**, *53*, 121–134. DOI: 10.1021/acs.accounts.9b00586.

(7) Dickinson, T.; Wynne-Jones, W. F. K. Mechanism of Kolbe's Electrosynthesis. Part 3. Theoretical Discussion. *Trans. Faraday Soc.* **1962**, *58*, 400–404. DOI: 10.1039/TF9625800400.

(8) Schäfer, H. J. Recent Synthetic Applications of the Kolbe Electrolysis. *Chem. Phys. Lipids* **1979**, *24*, 321–333. DOI: 10.1016/0009-3084(79)90117-8.

(9) Ramadoss, V.; Zheng, Y.; Shao, X.; Tian, L.; Wang, Y. Advances in Electrochemical Decarboxylative Transformation Reactions. *Chem.-Eur. J.* **2021**, *27*, 3213–3228. DOI: 10.1002/chem.202001764.

(10) Linstead, R. P.; Shephard, B. R.; Weedon, B. C. L. 634. Anodic Syntheses. Part V. Electrolysis of *N*-Acylamino-Acids. A Novel Alkoxylation Reaction. *J. Chem. Soc.* **1951**, 2854–2858. DOI: 10.1039/jr9510002854.

(11) Iwasaki, T.; Horikawa, H.; Matsumoto, K.; Miyoshi, M. Synthetic Electroorganic Chemistry. 11. Electrochemical Synthesis of Semicyclic and Cyclic *N*-Acyl *N*, *O*-Acetals. *J. Org. Chem.* **1979**, *44*, 1552–1554. DOI 10.1021/jo01323a038.

(12) Seebach, D.; Charczuk, R.; Gerber, C.; Renaud, P.; Berner, H.; Schneider, H. Elektrochemische Decarboxylierung von L-Threonin-und Oligopeptid-Derivaten unter Bildung von *N*-Acyl-*N*, *O*-acetalen: Herstellung von Oligopeptiden mit Carboxamid-oder Phosphonat-C-Terminus. *Helv. Chim. Acta* **1989**, *72*, 401–425. DOI: 10.1002/hlca.19890720302.

(13) Mazurkiewicz, R.; Adamek, J.; Październiok-Holewa, A.; Zielińska, K.; Simka, W.; Gajos, A.; Szymura, K. α-Amidoalkylating Agents from *N*-Acyl-α-amino Acids: 1-(*N*-Acylamino) alkyltriphenylphosphonium Salts. *J. Org. Chem.* **2012**, *77*, 1952–1960. DOI: 10.1021/jo202534u.

(14) Horikawa, H.; Iwasaki, T.; Matsumoto, K.; Miyoshi, M. A New Synthesis of 2-Alkoxy-and 2-Acetoxy-2-amino Acids by Anodic Oxidation. *Tetrahedron Lett.* **1976**, *17*, 191–194. DOI: 10.1016/0040-4039(76)80012-3.

(15) Iwasaki, T.; Horikawa, H.; Matsumoto, K.; Miyoshi, M. An Electrochemical Synthesis of 2-Acetoxy-2-amino Acid and 3-Acetoxy-3-amino Acid Derivatives. *J. Org. Chem.* **1977**, *42*, 2419–2423. DOI: 10.1021/jo00434a015.

(16) Iwasaki, T.; Horikawa, H.; Matsumoto, K.; Miyoshi, M. Electrochemical Synthesis and Reactivity of α-Alkoxy α-Amino Acid Derivatives. *Bull. Chem. Soc. Jpn.* **1979**, *52*, 826–830. DOI: 10.1246/bcsj.52.826.

(17) Adam, W.; Rucktaeschel, R. Cyclic Peroxides. V. α-Lactone Intermediate via Photodecarboxylation of a Monomeric Malonyl Peroxide. *J. Am. Chem. Soc.* **1971**, *93*, 557–559. DOI: 10.1021/ja00731a062.

(18) Crandall, J. K.; Sojka, S. A.; Komin, J. B. Reactions of Ketenes with Peracids and Ozone. *J. Org. Chem.* **1974**, *39*, 2172–2175. DOI: 10.1021/jo00929a007.

(19) Ma, X.; Luo, X.; Dochain, S.; Mathot, C.; Markò, I. E. Electrochemical Oxidative Decarboxylation of Malonic Acid Derivatives: A Method for the Synthesis of Ketals and Ketones. *Org. Lett.* **2015**, *17*, 4690–4693. DOI: 10.1021/acs.orglett.5b02084.

(20) Nokami, J.; Yamamoto, T.; Kawada, M.; Izumi, M.; Ochi, N.; Okawara, R. New Synthetic Reaction by Electrolysis Malonic Acid as a Ketone Synthon. *Tetrahedron Lett.* **1979**, *20*, 1047–1048. DOI: 10.1016/S0040-4039(01)87187-2.

(21) Ma, X.; Dewez, D. F.; Du, L.; Luo, X.; Markó, I. E.; Lam, K. Synthesis of Diketones, Ketoesters, and Tetraketones by Electrochemical Oxidative Decarboxylation of Malonic Acid Derivatives: Application to the Synthesis of *Cis*-Jasmone. *J. Org. Chem.* **2018**, *83*, 12044–12055. DOI: 10.1021/acs.joc.8b01994.

(22) Dochain, S.; Nshimyumuremyi, J.-B.; Dewez, D. F.; Body, J.-F.; Elias, B.; Singleton, M. L.; Markó, I. E. Electrochemical and Photochemical Approaches for the Synthesis of the C28–C38 Fragment of Okadaic Acid. *Tetrahedron* **2019**, *75*, 2280–2283. DOI: 10.1016/j.tet.2019.02.060.

(23) Wuts, P. G. M.; Sutherland, C. An Electrochemical Ketal Synthesis from 2-Carboxy-2-allyl-tetrahydropyrans. *Tetrahedron Lett.* **1982**, *23*, 3987–3990. DOI: 10.1016/S0040-4039(00)88676-1.

(24) Klocke, E.; Matzeit, A.; Gockeln, M.; Schäfer, H. J. Electroorganic Synthesis, 55[1]. Influences on the Selectivity of the Kolbe versus the Non-Kolbe Electrolysis in the Anodic Decarboxylation of Carboxylic Acids. *Chem. Ber.* **1993**, *126*, 1623–1630. DOI: 10.1002/cber.19931260720.

(25) Luo, X.; Ma, X.; Lebreux, F.; Markó, I. E.; Lam, K. Electrochemical Methoxymethylation of Alcohols – a New, Green and Safe Approach for the Preparation of MOM Ethers and Other Acetals. *Chem. Commun.* **2018**, *54*, 9969–9972. DOI: 10.1039/C8CC05843A.

(26) de Kruijff, G. H. M.; Waldvogel, S. R. Electrochemical Synthesis of Aryl Methoxymethyl Ethers. *ChemElectroChem* **2019**, *6*, 4180–4183. DOI: 10.1002/celc.201801880.

(27) Xiang, J.; Shang, M.; Kawamata, Y.; Lundberg, H.; Reisberg, S.; Chen, M.; Mykhailiuk, P.; Beutner, G.; Collins, M.; Davies, A.; Del Bel, M.; Gallego, G.; Spangler, J.; Starr, J. T.; Yang, S.; Blackmond, D.; Baran, P. Hindered Dialkyl Ether Synthesis via Electrogenerated Carbocations. *Nature*, **2019**, *573*, 398–402. DOI: 10.1038/s41586-019-1539-y.

(28) Eberson, L.; Nyberg, K.; Ekbom, K.; Borgström, B. Studies on the Kolbe Electrolytic Synthesis. V. An Electrochemical Analogue of the Ritter Reaction. *Acta Chem. Scand.* **1964**, *18*, 1567–1568. DOI: 10.3891/acta.chem.scand.18-1567.

(29) Sheng, T.; Zhang, H.-J.; Shang, M.; He, C.; Vantourout, Julien. C.; Baran, Phil. S. Electrochemical Decarboxylative *N*-Alkylation of Heterocycles. *Org. Lett.* **2020**, *22*, 7594–7598. DOI: 10.1021/acs.orglett.0c02799.

(30) Shao, X.; Zheng, Y.; Tian, L.; Martín-Torres, I.; Echavarren, A. M.; Wang, Y. Decarboxylative C_{sp3}–N Bond Formation by Electrochemical Oxidation of Amino Acids. *Org. Lett.* **2019**, *21*, 9262–9267. DOI: 10.1021/acs.orglett.9b03696.

(31) Kumar, G. S.; Shinde, P. S.; Chen, H.; Muralirajan, K.; Kancherla, R.; Rueping, M. Paired Electrolysis for Decarboxylative Cyanation: 4-CN-Pyridine, a Versatile Nitrile Source. *Org. Lett.* **2022**, *24*, 6357–6363. DOI: 10.1021/acs.orglett.2c01897.

(32) Berger, M.; Herszman, J. D.; Kurimoto, Y.; de Kruijff, G. H. M.; Schüll, A.; Ruf, S.; Waldvogel, S. R. Metal-Free Electrochemical Fluorodecarboxylation of Aryloxyacetic Acids to Fluoromethyl Aryl Ethers. *Chem. Sci.* **2020**, *11*, 6053–6057. DOI: 10.1039/D0SC02417A.

(33) Yamada, R.; Sakata, K.; Yamada, T. Electrochemical Synthesis of Substituted Morpholines via a Decarboxylative Intramolecular Etherification. *Org. Lett.* **2022**, *24*, 1837–1841. DOI: 10.1021/acs.orglett.2c00377.

(34) Koleda, O.; Prane, K.; Suna, E. Electrochemical Synthesis of Unnatural Amino Acids via Anodic Decarboxylation of *N*-Acetylamino Malonic Acid Derivatives. *Org. Lett.* **2023**, 25,7958–7962. DOI: 10.1021/acs.orglett.3c02687.

(35) Blaskovich, M. A. T. Unusual Amino Acids in Medicinal Chemistry. *J. Med. Chem.* **2016**, *59*, 10807–10836. DOI: 10.1021/acs.jmedchem.6b00319.

(36) Han, J.; Konno, H.; Sato, T.; Soloshonok, V. A.; Izawa, K. Tailor-Made Amino Acids in the Design of Small-Molecule Blockbuster Drugs. *Eur. J. Med. Chem.* **2021**, *220*, 113448. DOI: 10.1016/j.ejmech.2021.113448.

(37) Hickey, J. L.; Sindhikara, D.; Zultanski, S. L.; Schultz, D. M. Beyond 20 in the 21st Century: Prospects and Challenges of Non-Canonical Amino Acids in Peptide Drug Discovery. *ACS Med. Chem. Lett.* **2023**, *14*, 557–565. DOI: 10.1021/acsmedchemlett.3c00037.

(38) Addie, M.; Ballard, P.; Buttar, D.; Crafter, C.; Currie, G.; Davies, B. R.; Debreczeni, J.; Dry, H.; Dudley, P.; Greenwood, R.; Johnson, P. D.; Kettle, J. G.; Lane, C.; Lamont, G.; Leach, A.; Luke, R. W. A.; Morris, J.; Ogilvie, D.; Page, K.; Pass, M.; Pearson, S.; Ruston, L. Discovery of 4-Amino-*N*-[(1*S*)-1-(4-chlorophenyl)-3-hydroxypropyl]-1-(7*H*-pyrrolo[2,3-*d*]pyrimidin-4-yl)piperidine-4-carboxamide (AZD5363), an Orally Bioavailable, Potent Inhibitor of Akt Kinases. *J. Med. Chem.* **2013**, *56*, 2059–2073. DOI: 10.1021/jm301762v.

(39) Odan, M.; Ishizuka, N.; Hiramatsu, Y.; Inagaki, M.; Hashizume, H.; Fujii, Y.; Mitsumori, S.; Morioka, Y.; Soga, M.; Deguchi, M.; Yasui, K.; Arimura, A. Discovery of S-777469: An Orally Available CB2 Agonist as an Antipruritic Agent. *Bioorg. Med. Chem. Lett.* **2012**, *22*, 2803–2806. DOI: 10.1016/j.bmcl.2012.02.072.

(40) Falgueyret, J.-P.; Desmarais, S.; Oballa, R.; Black, W. C.; Cromlish, W.; Khougaz, K.; Lamontagne, S.; Massé, F.; Riendeau, D.; Toulmond, S.; Percival, M. D. Lysosomotropism of Basic Cathepsin K Inhibitors Contributes to Increased Cellular Potencies against Off-Target Cathepsins and Reduced Functional Selectivity. *J. Med. Chem.* **2005**, *48*, 7535–7543. DOI: 10.1021/jm0504961.

(41) Furber, M.; Tiden, A.-K.; Gardiner, P.; Mete, A.; Ford, R.; Millichip, I.; Stein, L.; Mather, A.; Kinchin, E.; Luckhurst, C.; Barber, S.; Cage, P.; Sanganee, H.; Austin, R.; Chohan, K.; Beri, R.; Thong, B.; Wallace, A.; Oreffo, V.; Hutchinson, R.; Harper, S.; Debreczeni, J.; Breed, J.; Wissler, L.; Edman, K. Cathepsin C Inhibitors: Property Optimization and Identification of a Clinical Candidate. *J. Med. Chem.* **2014**, *57*, 2357–2367. DOI: 10.1021/jm401705g.

(42) Ding, Y.; Ting, J. P.; Liu, J.; Al-Azzam, S.; Pandya, P.; Afshar, S. Impact of Non-Proteinogenic Amino Acids in the Discovery and Development of Peptide Therapeutics. *Amino Acids* **2020**, *52*, 1207–1226. DOI: 10.1007/s00726-020-02890-9.

(43) Grauer, A.; König, B. Peptidomimetics – A Versatile Route to Biologically Active Compounds. *Eur. J. Org. Chem.* **2009**, *2009*, 5099–5111. DOI: 10.1002/ejoc.200900599.

(44) Maity, P.; König, B. Enantio- and Diastereoselective Syntheses of Cyclic Cα-Tetrasubstituted α-Amino Acids and Their Use to Induce Stable Conformations in Short Peptides. *Biopolymers* **2008**, *90*, 8–27. DOI: 10.1002/bip.20902.

(45) Tanaka, M. Design and Synthesis of Chiral α,α-Disubstituted Amino Acids and Conformational Study of Their Oligopeptides. *Chem. Pharm. Bull.* **2007**, *55*, 349–358. DOI: 10.1248/cpb.55.349.

(46) Du, Y.; Wei, Z.; Wang, T. Visible-Light-Mediated Synthesis of Oxidized Amides via Organic Photoredox Catalysis. *Synthesis* **2018**, *50*, 3379–3386. DOI: /10.1055/s-0036-1591988.

(47) Prāne, K. Electrochemical Synthesis of Non-proteinogenic Amino Acids and Bromanes. Master thesis. **2023**. University of Latvia.

(48) Heard, D. M.; Lennox, A. J. J. Electrode Materials in Modern Organic Electrochemistry. *Angew. Chem., Int. Ed.* **2020**, *59*, 18866–18884. DOI: 10.1002/anie.202005745.

(49) Di Martino, A.; Galli, C.; Gargano, P.; Mandolini, L. Ring-Closure Reactions. Part 23. Kinetics of Formation of Three- to Seven-Membered-Ring N-Tosylazacycloalkanes.

The Role of Ring Strain in Small- and Common-Sized-Ring Formation. *J. Chem. Soc., Perkin Trans. 2* **1985**, 1345–1349. DOI: 10.1039/p29850001345.

(50) Lebreux, F.; Buzzo, F.; Markó, I. Synthesis of Five- and Six-Membered-Ring Compounds by Environmentally Friendly Radical Cyclizations Using Kolbe Electrolysis. *Synlett* **2008**, *2008*, 2815–2820. DOI: 10.1055/s-0028-1083547.

(51) Newcomb, M.; Varick, T. R.; Ha, C.; Manek, M. B.; Yue, X. Picosecond Radical Kinetics. Rate Constants for Reaction of Benzeneselenol with Primary Alkyl Radicals and Calibration of the 6-Cyano-5-hexenyl Radical Cyclization. *J. Am. Chem. Soc.* **1992**, *114*, 8158–8163. DOI: 10.1021/ja00047a026.

3. DIRECT ELECTROREDUCTIVE SYNTHESIS OF *N*-HYDROXY QUINAZOLIN-4-ONES

3.1. Electrochemical nitro group reduction in the synthesis of heterocycles

Electrochemical transformations that rely on anodic reactions have found significantly broader utilization as compared to those facilitated by cathodic reduction. Despite the conceptual appeal of both approaches,[1,2] cathodic reduction chemistry features several inherent challenges. For instance, many of the cathodic reductions have to be conducted under moisture-and oxygen-free conditions due to the competing proton and O_2 reduction at relatively low overpotentials. Moreover, it can be challenging to design a suitable counter oxidation reaction at the anode. Unlike proton-to-hydrogen reduction being the commonly used counter-reaction in anodic oxidation, the counter-reaction for cathodic reduction such as the oxidation of a sacrificial anode or an amine introduces undesired byproducts that may interfere with the desired transformation.[3] Despite that, recent years have witnessed a growing interest in reactions enabled by cathodic reduction.[4]

The cathodic reduction of the N–O bond is probably the most extensively studied electroreductive transformation.[5] One of the reasons for this is the widespread presence of N–O bond in e.g. nitro-substituted organic compounds. Electrochemical reduction of nitroaryls **3.1** can lead to the formation of nitroso compounds **3.2**, hydroxylamines **3.3**, and amines **3.4** (Figure 3.1).[5] It is noteworthy that the reduction of nitroso moiety is more facile than the reduction of a nitro group. Hence, two-electron reduction of nitro group is difficult to stop at nitroso stage, whereas four-electron reduction to hydroxylamines **3.3** is a facile process. Further two-electron reduction of hydroxylamines to anilines **3.4** is challenging due to the sensitivity of hydroxylamines **3.3** to oxidation. Of note, hydroxylamines **3.3** can react with a nitroso intermediate **3.2** to furnish diazene oxide **3.5** that upon reduction forms azobenzenes **3.6** or hydrazobenzenes **3.7**.[6,7] Under basic conditions, hydrazobenzene **3.7** can be electrochemically reduced to form aniline **3.4**.[8]

The electrochemical reduction of a nitro group in arenes provides an access to valuable nitrogen-containing heterocycles.[4,5] These compounds are prevalent in

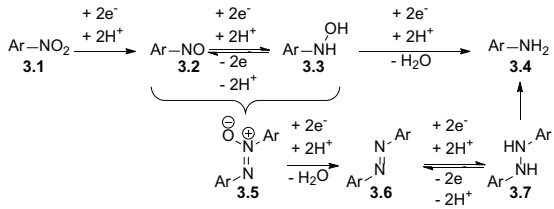

Figure 3.1. **Possible products of electrochemical reduction of nitroarenes**

pharmaceuticals[9] and serve as core motifs in various biomolecules.[10] The subsequent sections will focus on the literature survey of the electroreductive synthesis of nitrogen-containing 5- and 6-membered heterocycles from nitroarenes.

3.1.1. Synthesis of 5-membered heterocycles by cathodic nitro reduction

A variety of nitrogen-containing heterocycles such as benzisoxazolones, indazoles and 2-amino indoles can be synthesized from the electrochemically generated nitroso arenes even though a direct nitro-to-nitroso conversion is challenging due to the easier reduction of nitroso over nitro group. Moinet and co-workers were able to electrochemically generate nitroso arene **3.9** from nitrobenzoic acid **3.8** for the *ex-cell* synthesis of sulfonyl-2,1-benzisoxazolones **3.11** (Figure 3.2A).[11] The authors employed the "redox-flow" method where porous carbon cathode and porous carbon anode were separated by a porous insulator. The reaction solution flowed through two back-to-back electrodes: a cathode followed by an anode. Four-electron reduction of a nitro compound **3.8** to hydroxylamine **3.12** occurred at the porous cathode. As soon as it was formed, hydroxylamine **3.12** underwent two-electron oxidation into nitroso intermediate **3.9** (Figure 3.2B). Once the electrolysis was completed, the sodium salt of sulphinic acid **3.10** and HCl were added to the resulting solution. Sulfonyl-2,1-benzisoxazolones **3.11** were formed after stirring the reaction for two hours at elevated temperature (Figure 3.2A and B).

Similarly, 2-substituted indazoles **3.13** were synthesized from *o*-nitrobenzylamines **3.12** in the "redox-flow" cell (Figure 3.2C and D).[12] The electrophilic character of the nitroso group in intermediate **3.16** facilitated intramolecular cyclization and N–N bond formation, whereas acidic media of the electrolysis solution facilitated elimination of water in **3.17** and the *in-cell* formation of indazoles **3.13** (Figure 3.2D). Indazoles **3.13** can be further electrochemically reduced in the acetate buffer at a mercury cathode, as was demonstrated by the synthesis of 2-substituted tetrahydro-1*H*-indazole **3.14**. Finally, the "redox-flow" approach was also efficient for the synthesis of 2-amino indoles **3.19** from 2-(*o*-nitrophenyl)ethylamines **3.18** in basic media (Figure 3.2E).[13]

The electrochemical generation of nitroso arene intermediates and their electrophilic character were also employed in the synthesis of benzotriazoles. In 2000, Kim and co-workers attempted electrochemical synthesis of benzotriazoles **3.22** from the corresponding diazenes **3.20** (Figure 3.3A).[14] In the constant potential electrolysis with Pt electrodes in $LiClO_4$ solution of CH_2Cl_2/MeOH, nitro diazenes **3.20** underwent cathodic reduction and cyclization. However, benzotriazole-1-oxide **3.21** was formed instead of triazoles **3.22** (Figure 3.3A). This was circumvented by applying more negative potentials that allowed for both nitrodiazene **3.20** reduction and the cathodic reduction of the *N*-oxides **3.21** to benzotriazoles **3.22**. Moreover, the addition of NaOH facilitated the electroreduction of nitrodiazenes **3.20**, probably by improving the conductivity of the reaction media. Benzotriazoles **3.22** and their *N*-oxides **3.21** were obtained in moderate to excellent yields albeit a high amount of passed charge was required (Figure 3.3A).

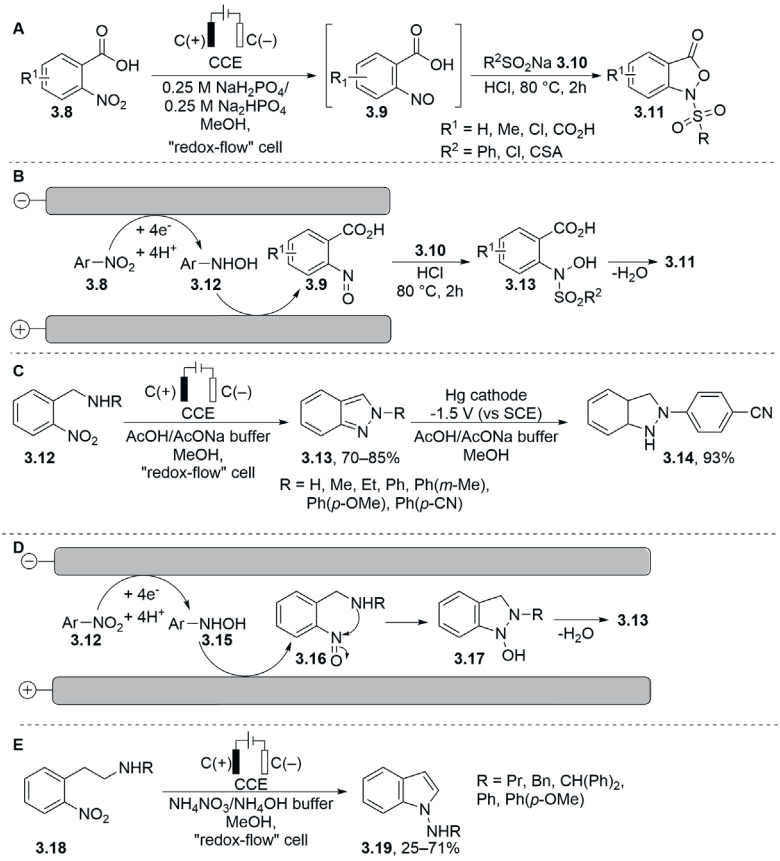

Figure 3.2. **Electrochemical synthesis of *N*-heterocycles using "redox-flow" approach**

Waldvogel group achieved galvanostatic electrosynthesis of both 2*H*-2(aryl) benzo[*d*]-1,2,3-triazoles **3.25** and their *N*-oxides **3.24** from nitro azabenzenes **3.23** (Figure 3.3B).[15] The electrolysis was performed in an undivided cell in the presence of a base (NaOH or Et_3N) in methanol solution, and leaded bronze was use as the cathode. Triazoles **3.25** or their *N*-oxides **3.24** could be obtained depending on applied current density. Lower current density (2.4 mA/cm^2) afforded triazole *N*-oxides **3.24**, whereas higher current densities (4.1 mA/cm^2) provided triazoles **3.25**. The authors showed that the use of tetrabutylammonium salt can be omitted since NaOH solution provides sufficient conductivity for successful electroreductive cyclization. The authors also proposed a mechanism, where nitro arene **3.23** is reduced to the corresponding nitroso intermediate **3.27** either via two-electron reduction or via four-electron reduction, followed by reversible two-electron oxidation (Figure 3.3C). Nitroso intermediate **3.27** undergoes 5-atom 6π-electrocyclization to generate triazole *N*-oxide **3.24**. Ultimately, two-electron reduction of triazole *N*-oxide **3.24** at higher current densities produces benzotriazole **3.25**. The paired anodic process was the oxidation of methanol to sodium formate.[15]

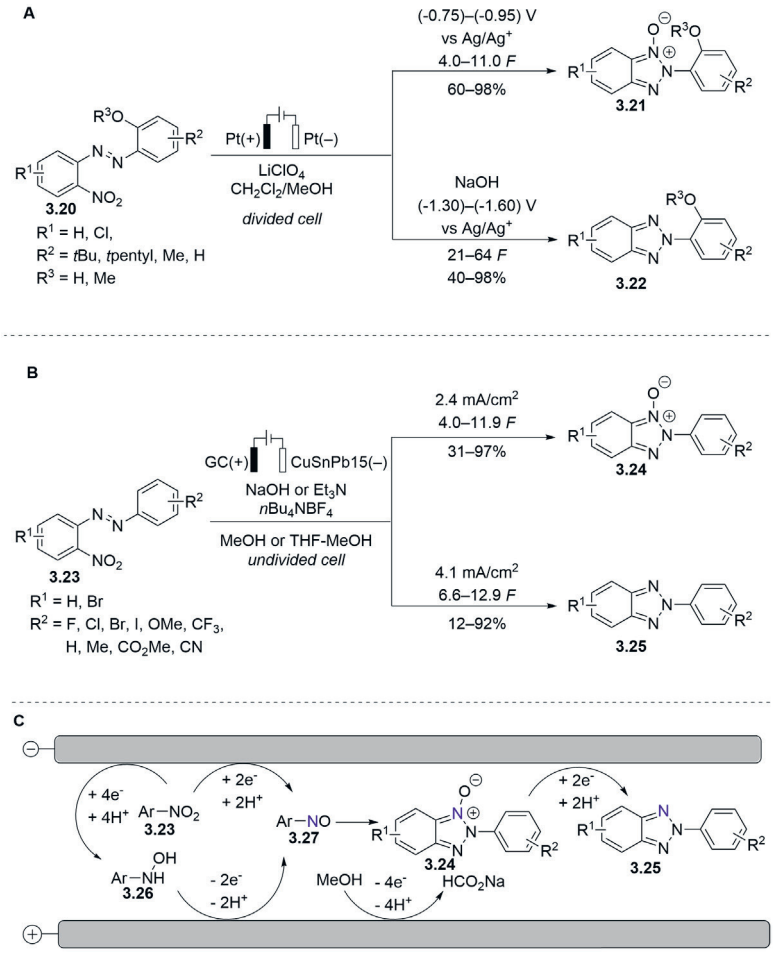

Figure 3.3. **Electroreductive synthesis of benzotriazoles and their *N*-oxides**

In 1998, Kim and co-workers described electrochemical synthesis of 2,1-benzisoxazoles **3.28** by electrochemical reduction of substituted 2-nitrobenzaldehyde or 2'-nitroacetophenone **3.27** under constant potential. The electrolysis was performed in methanol solution in the presence of $LiClO_4$ as a supporting electrolyte. Good yields of the heterocycles **3.28** were achieved when either Pt or sacrificial Pb cathode was used (Figure 3.4A).[16]

Recently, Peters and co-workers showed that 2,1-benzisoxazoles **3.28** also can be obtained under constant potential using RVC electrodes (Figure 3.4B).[17] The authors have also performed mechanistic studies. Accordingly, CV analyses of 2-nitrobenzaldehyde **3.27a** exhibited three cathodic peaks. The first one corresponded to the reversible one-electron reduction of a nitro group to radical anion **3.27a-I** (Figure 3.4C). When the electrolysis was performed at the potential of -0.2 V (vs Cd/Hg amalgam), the starting aldehyde **3.27a** was completely recovered. The second cathodic peak in the

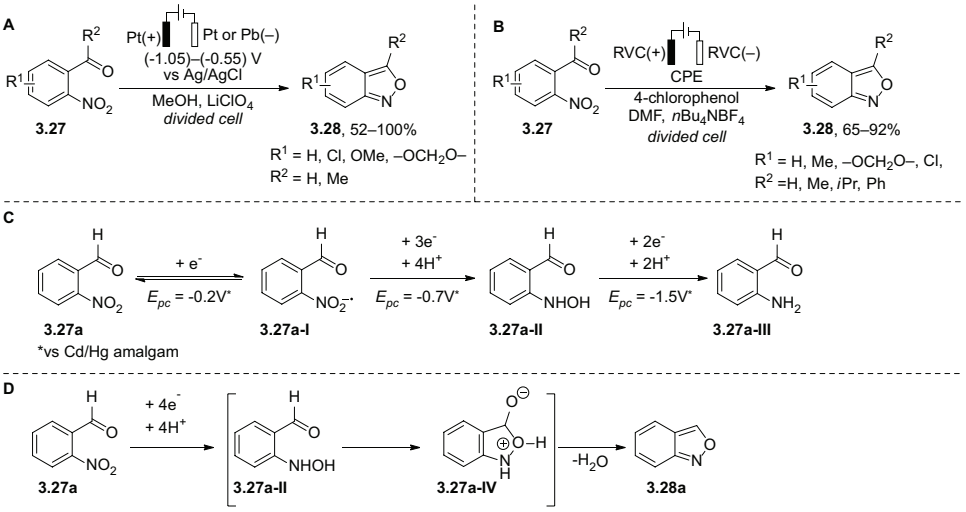

Figure 3.4. **Electroreductive synthesis of 2,1-benzisoxazoles 3.28**

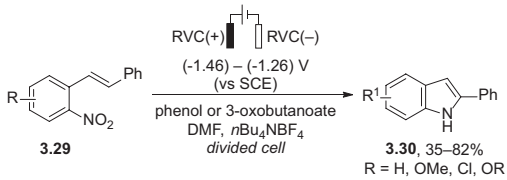

Figure 3.5. **Electroreductive synthesis of 2*H*-indoles 3.30**

CV measurements of aldehyde **3.27a** corresponded to the three-electron reduction and the generation of a hydroxylamine **3.27a-II**. The electrolysis at this potential (-0.7 V vs Cd/Hg amalgam) afforded the heterocyclic product **3.28a** in 78% yield. Finally, the third cathodic peak in the CV analysis represented two-electron reduction of hydroxylamine **3.27a-II** to aniline **3.27a-III**. When the electrolysis was performed at -1.4 V (vs Cd/Hg amalgam), nitrobenzaldehyde **3.27a** was converted to aminobenzaldehyde **3.27a-III** (Figure 3.4C). The authors have also demonstrated that a proton source must be present in the reaction mixture for a successful electroreduction of the nitro group, and the progress of the reaction strongly depends on the strength of the proton donor additive. 4-Chlorophenol (pKa 16.8 in DMF) was found to be the most suitable as the additive for the electrochemical synthesis of 2,1-benzisoxazoles **3.28** under the developed conditions (Figure 3.4B).[17] Mechanistically, four-electron reduction in the presence of a proton source generated hydroxylamine **3.27a-II** that underwent cyclization to intermediate **3.27a-IV**. Eventually, the elimination of water resulted in the formation of heterocycle **3.28** (Figure 3.4D).

The developed conditions (Figure 3.4B) were also suitable for the synthesis of substituted 2*H*-indoles **3.30** from *o*-nitrostyrenes **3.29** (Figure 3.5).[18] The potentials for the direct electroreduction of nitrostyrenes **3.29** were determined from the CV analysis

data. In the presence of a proton donor, there was only one broad cathodic wave in the cyclic voltammogram, which corresponds to the four-electron reduction of the nitro group and formation of a hydroxylamine intermediate.

Waldvogel and co-workers have also published on the electroreductive synthesis of 2,1-benzisoxazoles **3.28** (Figure 3.6).[19] In contrast to the previously described methods, their approach did not require any protic additives, and involved the electrochemical nitro reduction/cyclization in an undivided cell under constant current. Boron-doped diamond (BDD) was employed as a cathode, and the electrolysis was performed in the presence of nBu$_4$NBF$_4$ in the HFIP/H$_2$O mixture. The method was compatible with electron-withdrawing substituents such as CO$_2$Me, CF$_3$, and CN (Figure 3.6).[19]

Trazza and co-workers studied electrochemical properties of nitroanilides by polarography and described the electrochemical synthesis of two benzimidazoles **3.32** in a divided cell under constant current using mercury pool cathode (Figure 3.7).[20] This method represents the only approach toward benzimidazoles, which proceeds via electroreduction of a nitro group.

Gultyai and co-workers employed electrochemical reduction of (nitrophenyl) pyridinium salts **3.33** for the synthesis of pyrido[1,2-a]benzimodazoles **3.34** (Figure 3.8A).[21,22] Notably, the electroreduction could be performed using lead cathode and platinum anode in both undivided and divided cell (Figure 3.8A, method A).[21] In a follow-up study, the authors demonstrated that heterocycles **3.34** can be synthesized from pyridinium salts **3.33** through indirect electrolysis using a catalytic amount of SnCl$_2$.[22] Compared to the direct cathodic reduction of pyridinium salts **3.33**, the indirect electrolysis was conducted at higher current density (4 mA/cm^2 vs 14 mA/cm^2), which shortened the electrolysis time from 44 minutes to 13 minutes. Tin dichloride effected the reduction of nitroarene **3.33** to hydroxylamine **3.35-I**, which underwent intramolecular cyclization into intermediate **3.35-II** that was followed by elimination of water to furnish heterocycle **3.34** (Figure 3.8B). The concomitantly formed tin(IV) chloride was reduced at the cathode back to SnCl$_2$ that re-entered the catalytic cycle. The counter process at the anode was water oxidation.

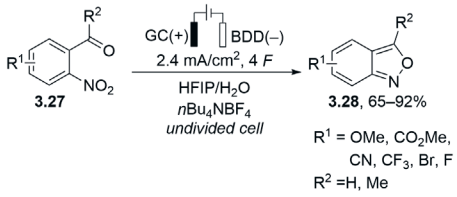

Figure 3.6. **Electroreductive synthesis of 2,1-benzisoxazoles 3.28**

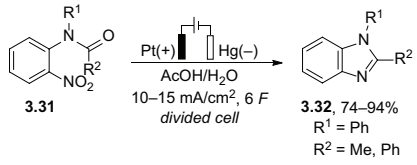

Figure 3.7. **Electroreductive synthesis of benzimidazoles 3.32**

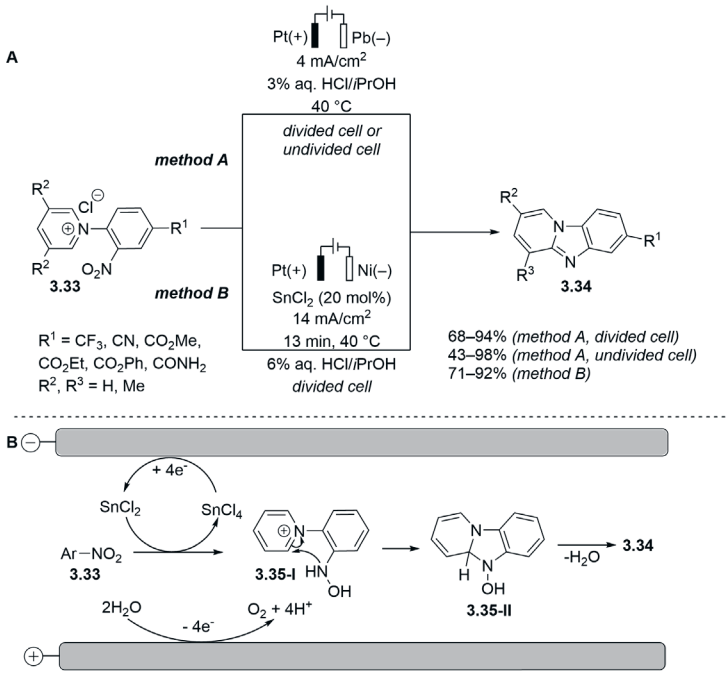

Figure 3.8. **Electroreductive synthesis of pyridobenzimidazoles 3.34**

3.1.2. 6-Membered heterocycles via the cathodic reduction of a nitro group

Tallec group investigated the electrochemical reduction of *o*-nitrophenylthioacetic acid derivatives **3.36** (Figure 3.9).[23,24] They discovered that the potentiostatic reduction of nitro arene **3.36** in a mixture of aqueous 0.5 M sulfuric acid and ethanol (1:4 v/v) in a divided cell using a mercury pool cathode resulted in benzothiazinone **3.37** formation (80% yield), along with 20% of heterocycle **3.38**.[23] Mechanistic studies pointed at the direct cathodic reduction of nitro arene **3.36** to hydroxylamine **3.39** that underwent cyclization to heterocycle **3.37**. In a competing process, hydroxylamine **3.39** reacts with EtOH to form intermediate **3.40** in a Bamberger-type reaction. Intramolecular cyclization of the intermediate **3.40** provides the byproduct **3.38**. The substitution of 0.5 M sulfuric acid with ammonium buffer solution led to the quantitative yield of benzothiazinone **3.37**.[24]

Electroreductive synthesis of quinoline *N*-oxides was first explored by Lund and Feoktistov already in 1969.[25] A substrate scope of the potentiostatic reaction was limited, and employment of a hazardous mercury electrode was required. In 2019, Waldvogel and co-workers reported the electroreductive synthesis of quinoline *N*-oxides from **3.42** substituted 2-nitrocinnamaldehydes **3.41** (Figure 3.10A) under conditions used for the synthesis of 2,1-benzisoxazoles **3.28** (cf. Figure 3.6).[19] The method was compatible with electron-withdrawing groups such as CO_2Me, CN, and CF_3. Recently, the same group showed that quinoline *N*-oxides **3.44** and **3.46** can be obtained by

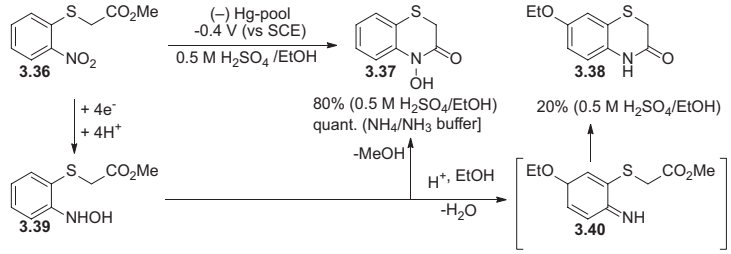

Figure 3.9. **Electrochemical reduction of *o*-nitrophenylthioacetic acid derivatives**

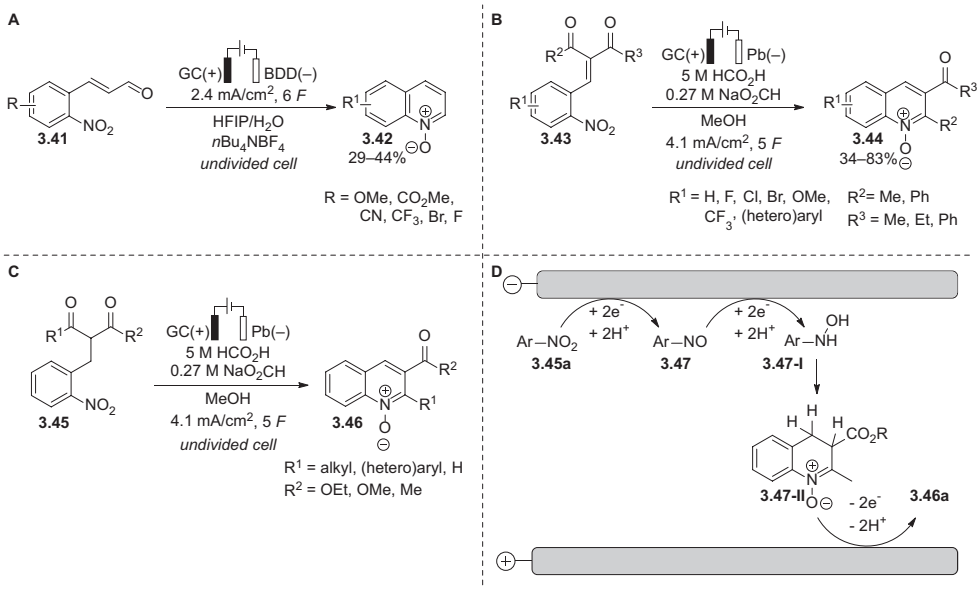

Figure 3.10. **Electroreductive synthesis of quinoline *N*-oxides 3.42, 3.44, and 3.46**

electroreduction of the corresponding nitro arenes **3.43** and **3.45** in an undivided cell using sodium formate buffer as the supporting electrolyte and methanol as the solvent (Figure 3.10B and C, respectively).[26] Interestingly, electrolysis of nitro compound **3.45** in a divided cell led to drop in yields, thus emphasizing the importance of the counter-reaction on the anode. To clarify the importance of the anodic counter-reaction and to understand the reaction mechanism, the authors performed CV studies of the nitro arene **3.45a** (R^1 = Me, R^2 = CO_2Et, Figure 3.10D). The first reductive wave at -1.13 V (vs Fc/Fc^+) corresponded to two-electron reduction of the nitro group to nitroso intermediate **3.47**. The second cathodic wave at -1.50 V (vs Fc/Fc^+) corresponded to the further reduction of nitroso arene **3.47** to hydroxylamine **3.47-I**. Subsequent intramolecular condensation of hydroxylamine **3.47-I** delivered cyclic intermediate **3.47-II** that oxidized at the anode to the desired *N*-oxide **3.46a**. The oxidation of intermediate **3.47-II** was also confirmed by the appearance of the anodic wave at +0.46 V (vs Fc/Fc^+) during CV analysis.

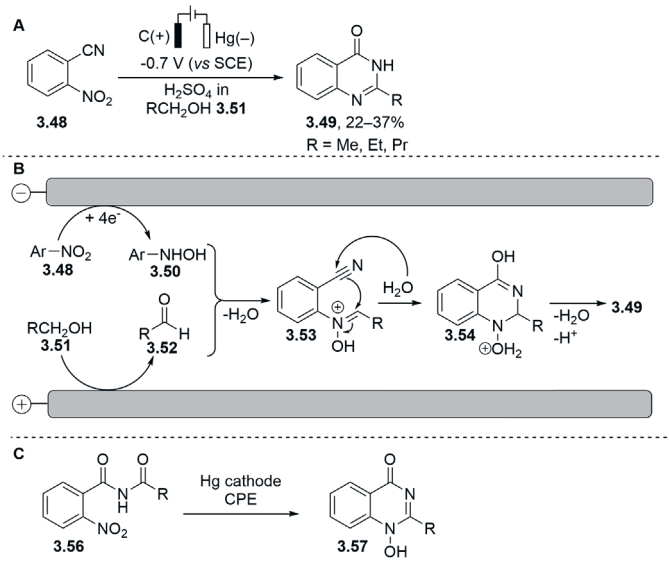

Figure 3.11. **Electroreductive synthesis of quinazolinones 3.49 and 3.57**

Rieker and Estrada reported the paired electrosynthesis of quinazolinones **3.49** from 2-nitrobenzonitriles **3.48** using a mercury pool cathode and a carbon anode in an undivided cell under potentiostatic control (Figure 3.11A).[27] The electrolysis was performed in the alcoholic solvent **3.51** which was oxidized to aldehyde **3.52** at the anode (Figure 3.11B). The anodically generated aldehyde **3.52** reacts with a cathodically generated hydroxylamine intermediate **3.50** to form imine oxide **3.53** that underwent cyclization/dehydration to quinazolinones **3.49**.[27]Additionally, the authors demonstrated that *N*-hydroxy-quinazolinones **3.57** could be also obtained from nitrobenzamides **3.56** (Figure 3.11C). It should be noted however that both methods necessitated the use of highly toxic mercury electrodes and a potentiostatic reaction setup. Furthermore, the scope of cathodic synthesis of quinazolinones was not explored.[27,28]

To sum up, the electroreductive cyclization of aryl nitro compounds mainly proceeds via $4e^-/4H^+$ reduction of a nitro group to hydroxylamine intermediates. The following intramolecular cyclization involving the hydroxylamine moiety provides a variety of *N*-containing heterocyclic compounds. Overall, cathodic reductions of nitroarenes in the early reports often were performed under the potentiostatic control and required the employment of a mercury pool cathode. The substrate scope of these reactions was not rigorously explored, or it was limited to the alkyl- or methoxy-substituted heterocycles. In recent publications, less hazardous electrodes such as leaded bronze, nickel or carbon-based cathodes (BDD, RVC) were successfully employed in the galvanostatic cathodic reduction of nitro group and the synthesis of a of *N*-containing heterocycles. Surprisingly, this approach has not been employed for the electroreductive synthesis of such pharmaceutically relevant heterocycles as *N*-hydroxy quinazolinone. Electroreductive synthesis *N*-hydroxy quinazolinone is represented by only one example of potentiostatic electrolysis using mercury cathode.

We envisioned development of the electroreductive method to synthesize *N*-hydroxy quinazolinones from corresponding nitrobenzamides using a convenient galvanostatic approach and environmentally benign conditions.

3.2. Results and discussion

This section is based on the published article (*Chem. Sci.* 2023, *14*, 2669–2675).[29]

Quinazolin-4-one is one particular example of the *N*-heterocycles that is present in a variety of drugs and bioactive compounds.[30] Thus, methaqualone (**3.58**) (Figure 3.12) is a hypnotic sedative that enhances GABA A receptor activity.[31] However, due to its potential for psychological addiction, and widespread abuse, the drug was removed from the U.S. market in 1985.[32] The medication idelalisib (**3.59**) (Figure 3.12) is employed in the treatment of specific types of blood cancer and functions as a phosphoinositide 3-kinase inhibitor.[33] The naturally occurring plant alkaloid tryptanthrine (**3.60**) displays a range of biological and pharmaceutical activities, including antimicrobial, antiviral, anticancer, and antiparasitic properties.[34] Additionally, the anti-metabolite and cytotoxic drug raltitrexed (**3.61**), developed by AstraZeneca, is utilized in chemotherapy treatments. This folic acid analogue acts as a selective inhibitor of thymidylate synthase.[35] It is worth noting that *N*-oxides and *N*-hydroxy derivatives of these pharmaceuticals have been identified as metabolites.[36,37] However, the therapeutic potential of endocyclic *N*-hydroxy and *N*-oxy compounds has not been investigated to the same extent. Given their metabolic stability and the distinctive attributes of the N–O bond, this category of novel compounds is currently a subject of pharmaceutical research.[38]

The literature contains limited examples of the syntheses of *N*-oxides and *N*-hydroxy derivatives of quinazolin-4-ones, and the few reported cases come with various challenges. Conventional syntheses of *N*-hydroxy[39] and *N*-oxides[40] quinazolin-4-one derivatives suffer from multiple-step synthesis, employment of harsh conditions,

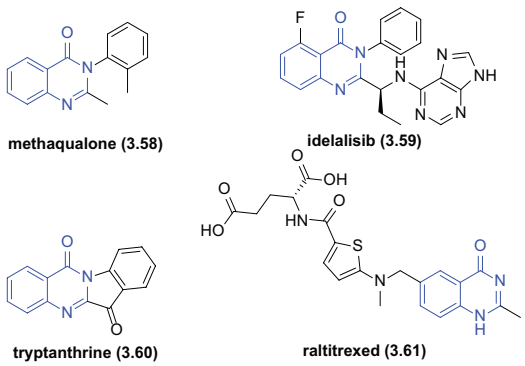

Figure 3.12. **Examples of quinazolin-4-one fragment-containing biologically active compounds**

and hazardous and toxic reagents. Reductive cyclization of nitro precursors is also known. However, it is often achieved through hydrogenation using costly palladium catalysts.[41] Electroreductive approaches are not broadly explored, and they require to use the highly toxic mercury electrodes (Section 3.1.2, Figure 3.11).[27,28] Based on our interest in the electrochemical synthesis of heterocyclic compounds and the demand for new approaches in the synthesis of 1*H*-1-hydroxy-quinazolin-4-ones, we envisioned to develop an electroreductive cyclization of nitro benzamides to obtain *N*-hydroxy quinazolin-4-one derivatives.

3.2.1. Optimization of the reaction conditions

Benzamide **3.56a** was selected as a test substrate for the cathodic reduction of a nitro group. It was easily synthesized in a single step from commercially available 2-nitrobenzamide (**3.62**) (Figure 3.13).[p] This synthesis was accomplished with acetic anhydride in a microwave-assisted acylation reaction or in a pressured vessel approach, both in high yields.[42,43]

The initial electrochemical conditions for the nitro reduction were established based on earlier work from the Waldvogel lab (Table 1, entry 1).[19,26,44] These conditions employed a water-methanol mixture (1:1 (v/v)) as an environmentally benign solvent capable to dissolve the nitro compound **3.56a**. Based on prior investigations into the concentration effect of the acidic component on the electrochemical reduction,[28,45] a moderate concentration of sulfuric acid (0.5 M) was chosen as the supporting electrolyte. Additionally, we anticipated that sulfuric acid might have a dual role in the reaction, as an acidic medium is expected to be advantageous for the intramolecular cyclization that follows the nitro group reduction. Considering this, we conducted constant-current electrolysis (3.7 mA/cm^2) of benzamide **3.56a** in an undivided cell containing a water-methanol medium using a glassy carbon anode and a boron-doped diamond (BDD) cathode. To add, the BDD is a carbon-based material that possesses distinctive reactivity for the electrochemical conversion of various substrates and can be produced sustainably by utilizing methane as a carbon source.[46] To our delight, we successfully isolated the desired 1-hydroxyquinazolinone **3.57a** in a 91% yield. Additionally, we applied the theoretically calculated amount of charge required for this process (4 *F*), and the obtained high yield indicates a high Faradaic efficiency (Table 1, entry 1). The molecular structure of heterocycle **3.56** was

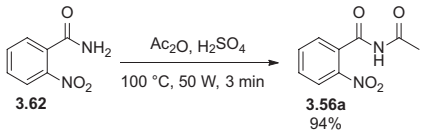

Figure 3.13. **Microwave-assisted acylation of 2-nitrobenzamide 3.62**

[p] For the detailed description of the synthesis of substituted nitro benzamides **3.56a–aa**, see Supporting information of Chem. Sci. featured article published in 2023.[29]

confirmed by X-ray analysis of a suitable single crystal.[q] Deviations from the initial electrolysis conditions resulted in reduced yields. Both lower and higher current densities led to a diminished yield of 1-hydroxyquinazolinone **3.57a**, achieving only 65–78% (Table 1, entries 2, 3, and 4). Substituting methanol with alternative solvents such as ethanol or acetonitrile (Table 1, entries 5 and 6) provided the desired heterocycle **3.57a**, albeit in slightly lower yields (84% and 71%, respectively). An acetate buffer (Table 1, entry 7) was employed as a milder and biologically derived substitute for sulfuric acid. However, this led to a decreased yield of product **3.57a** (66%).

The replacement of BDD with lead as the cathode material significantly reduced the yield of product **3.57a** to 27% (Table 1, entry 8). Additionally, this change led to cathodic corrosion, which resulted in the precipitation of lead salts. More stable alternatives to lead cathodes, such as leaded bronze[55] (Table 1, entry 9), proved entirely ineffective in the formation of **3.57a**. Platinum was similarly unsuccessful as a cathode

Table 3.1. **Optimization of electrolysis parameters for the synthesis of quinazolinone 3.57a**

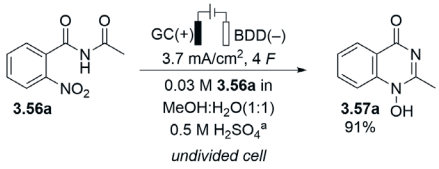

Entry	Deviation from standard conditions	Yield 3.57a, %[b]
1	None	91 (91)[c]
2	1.7 mA/cm^2	65
3	2.7 mA/cm^2	78
4	5.7 mA/cm^2	78
5	EtOH instead of MeOH	84
6	MeCN instead of MeOH	71
7	0.5 M acetate buffer[d]	66
8	Pb cathode	27
9	CuSn7Pb15 cathode	0
10	Pt cathode	0
11	Graphite cathode	84
12	GC cathode	90
13	0.06 M **3.56a**	85
14	0.10 M **3.56a**	73

[a] Concentration of H_2SO_4 in the electrolyte, obtained by using methanol and 1 M aqueous H_2SO_4 (1:1 (v/v)). [b] Yield of **3.57a** was determined by ^{1}H NMR spectroscopy using 2,2-dimethylmalonic acid as internal standard. [c] Isolated yield. [d] 0.5 M AcOH/AcONa was prepared with 90 mmol AcOH and 10 mmol NaOAc in 100 mL of distilled water and 100 mL MeOH.

[q] X-Ray analysis and structural elucidation was performed by D. Schollmeyer (JGU Mainz). For details see, Supporting information of Chem. Sci. featured article published in 2023.[29]

material (Table 1, entry 10), likely due to its low overpotential for the side reaction of hydrogen evolution. Aside from BDD, other carbon-based cathode materials like graphite and glassy carbon yielded product **3.57a** in comparable yields of 84% and 90% (Table 1, entries 11 and 12). Nonetheless we decided to continue with BDD cathode due to its sustainability and chemical resilience. Electrolysis at higher concentrations of benzamide **3.57a** resulted in diminished yields (Table 1, entries 13 and 14). Higher concentrations of the starting material probably led to the formation of high molecular weight byproducts, which were observed as a brownish residue after the electrolysis.

3.2.2. Scope of the reductive cyclization

The effectiveness of the optimized reaction conditions was demonstrated across a diverse range of substrates (Figure 3.14). Initially, we explored the impact of substitution patterns at the C-2 position of quinazolin-4-ones **3.57b–i** (Figure 3.14A). This involved studying the influence of primary, secondary, and tertiary alkyl substitutions in the synthesis of heterocycles **3.57a–c**, yielding the products in very good yields (78–91%). Notably, the *tert*-butyl derivative **3.57c**, featuring a sterically demanding substituent, exhibited the lowest yield (78%). Additionally, the hydrophobic chain-containing quinazolin-4-one (**3.57d**) was obtained in a moderate yield (52%). Both the 2-unsubstituted quinazolin-4-one **3.57e** and its 2-phenyl analogue **3.57h** were obtained in 65% and 79% yield, respectively. The alkene and benzylic moieties, susceptible to anodic oxidation, demonstrated good compatibility in the electrochemical reduction process. This allowed for successful synthesis of the desired heterocycles **3.57g** and **3.57i** in 67% and 81% yields, respectively. Notably, the 2-chloromethyl substituted product **3.57f** was isolated in 24% yield, likely due to its inherent instability.

Subsequently, a variety of functional groups in the aromatic component of 1-hydroxyquinazolin-4-ones **3.57j–r** were examined (Figure 3.14B). In all cases, the products **3.57j–r** were obtained in good yields (50–92%), irrespective of the electronic nature of the substituent. Benzamides featuring an electron-donating methoxy group and an electron-withdrawing ester moiety produced the corresponding heterocycles **3.57q** and **3.57r** in similar yields (77% and 85%, respectively). Similarly, the trifluoromethyl derivative **3.57n** and the methyl-substituted quinazolin-4-ones **3.57o**,**p** were obtained in 73–92% yields. Notably, the 6-methyl derivative **3.57o** represents an *N*-hydroxy analog of a precursor to raltitrexed (**3.61**), adding industrial significance to this transformation. Halides serve as redox-active groups in electrochemical reactions. We were pleased to find that fluoro-, chloro-, and bromo-substituted quinazolin-4-ones **3.57j–l** were obtained in 76–85% yields. Additionally, the developed electrochemical method successfully provided the iodo-substituted product **3.57m**, albeit in a moderate yield (50%), which is likely attributed to its susceptibility to oxidation. It is worth noting that heteroaromatic amides derived from pyridines and imidazoles are compatible with the developed conditions (Figure 3.14C). The pyrido-pyrimidinone **3.57s** was obtained in 82% yield, and the presence of the bromo substituent allows for various post-functionalization reactions. *N*-Hydroxy purine **3.57t** was also obtained in a favorable yield (57%).

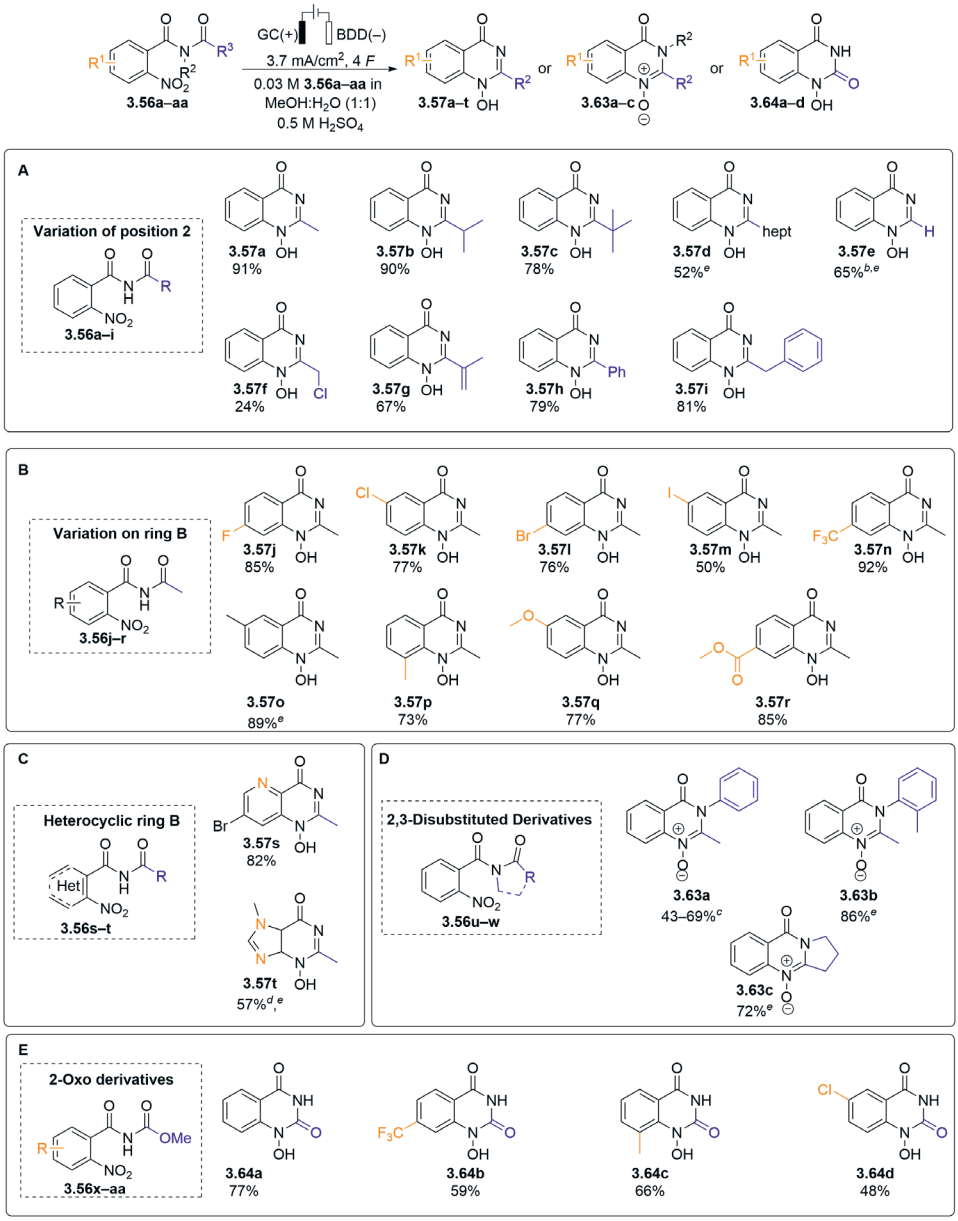

[a] Concentration of H_2SO_4 in the electrolyte, obtained by using 12.5 mL MeOH and 12.5 mL 1 M aqueous H_2SO_4 acid (1:1 (v:v)), undivided 25 mL beaker-type glass cell; [b] isolated yield as formate adduct; [c] variation in yield with repeated electrolysis; [d] isolated yield as acetate adduct; [e] obtained by T. Prenzel and J. Winter (JGU Mainz).

Figure 3.14. **Scope of the electrochemical reductive cyclization and isolated yields**

Furthermore, *N*-acetyl-*N*-aryl benzamides **3.56u**,**v** were transformed into the corresponding *N*-oxy-quinazolin-4-ones **3.63a**,**b** in good yields (Figure 3.14D). Notably, compound **3.63b** has been documented as a metabolite of methaqualone (**3.58**). Additionally, tertiary amides serve as viable substrates, as demonstrated in the synthesis of pyrrolidone-based *N*-oxy-quinazolin-4-one **3.63c** (72% yield). Lastly, the developed methodology has also been successfully applied in the synthesis of 1-hydroxy-quinazoline-2,4-diones **3.64a–d** through the electrochemical reduction of methyl-(2-nitrobenzoyl)carbamates (Figure 3.14E). In this context, the unsubstituted derivative **3.64a** exhibited the highest yield (77%). The electron-withdrawing trifluoromethyl- and chloro-substituted products **3.64b**,**d** were isolated in 59% and 48% yield, respectively. The methyl-substituted derivative **3.64c** was obtained in a moderate yield of 66%.

To demonstrate the synthetic utility and scalability of the developed method, the synthesis of 1*H*-1-hydroxy-2-methyl-quinazolin-4-one (**3.57a**) was successfully scaled up to 15 mmol in a single electrolysis batch (Table 3.2).[r] The 5-fold scale-up was performed with BDD and GC cathodes to demonstrate the robustness and applicability of the described method (entries 2 and 3, Table 3.2). Encouragingly, 20-fold scale-up (3.00 mmol) in a 100 mL electrolysis cell afforded the desired product **3.57a** without loss in yield or Faradaic efficiency (entry 4). Gram-scale electrolysis was also performed at 7.5 mmol and 15.0 mmol loading in a 250 mL electrolysis cell, affording 1.13 g and 2.19 g of the desired 1-hydroxy-quinazolin- 2-one **3.57a**, respectively (entries 5 and 6). The trend of decreased yield at higher concentrations was also observed in the optimization results (Table 3.1, entries 13 and 14).

Table 3.2. **Scale-up electroreduction of nitrobenzamide 3.56a**

Entry	Scale/mmol	Current (electrolysis time)	Yield 3.57a
1[b]	0.15	5.6 mA (2.9 h)	24 mg (91%)
2[c]	0.75	22.2 mA (3.6 h)	120 mg (91%)
3[c, e]	0.75	22.2 mA (3.6 h)	118 mg (89%)
4[c]	3.00	22.2 mA (14.5 h)	481 mg (91%)
5[d]	7.50	109.9 mA (7.3 h)	1.13 g (86%)
6[d, f]	15.0	109.9 mA (14.6 h)	2.16 g (83%)

[a] Constant current condition. [b] Surface area of the electrodes 1.5 cm^2; [c] Surface area of the electrodes 6.0 cm^2; [d] Surface area of the electrodes 29.7 cm^2; [e] GC cathode; [f] 0.06 M **3.56a**.

[r] The scale-up experiments were performed by T. Prenzel and J. Winter (JGU Mainz).

3.2.3. Mechanistic studies

A plausible mechanism for the electrochemical cyclization sequence is proposed based on the earlier studies on nitro reduction and cyclic voltammetry[s] measurements of benzamide **3.56a** (Figure 3.15).[26,28,44,45] The process starts with the reduction of the nitro group on the BDD cathode, which is evidenced by a single broad, irreversible wave (-0.94 V vs. Fc/Fc^+) corresponding to the $4e^-/4H^+$ reduction to the hydroxylamine **3.66**. It has been previously suggested that the reaction proceeds through two $2e^-$ steps via nitroso intermediate **3.65** and hydroxyl amine **3.66**. However, since only one broad wave was observed rather than two distinct or overlapping waves during CV analysis, this indicates that one reduction event takes place, directly converting nitro compound **3.56a** into intermediate **3.66**. The irreversible reduction to hydroxylamine **3.66** points to a rapid cyclization step to the product **3.57a**, as no corresponding oxidative wave was detected.

Furthermore, it is important to consider the impact of the counter reaction on the electrochemical conversion. The oxidation of water at the glassy carbon anode is potentially the primary counter reaction.[56] There was no evidence of glassy carbon anode corrosion after the electrolysis. Additionally, there were no indications of methanol oxidation – a phenomenon observed only under harsh basic conditions in previous studies.[56] Overall, the high performance of the reported method was enabled by the electrochemical stability of the product, the selective reduction to the hydroxylamine, and the fast cyclization process.

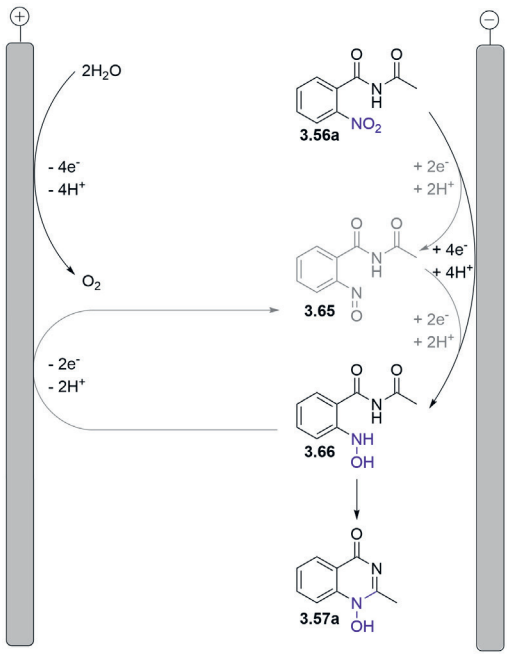

Figure 3.15. **Proposed mechanism for reductive cyclization of nitrobenzamide 3.56**

[s] The cyclic voltammetry measurements were performed by M. J. Gálvez-Vázquez and T. Prenzel.

3.2.4. Summary

In conclusion, this established method offers a straightforward and sustainable approach to access *N*-hydroxy- and *N*-oxyquinazolin-4-ones through a cathodic reduction sequence. The electrolytic conditions allow for a reproducible transformation in commercially available experimental setup. The most basic undivided cell setup was operated under constant current, employing easily accessible and sustainable carbon-based electrodes along with a water-methanol mixture as environmentally benign solvent. The sulphuric acid additive served as a supporting electrolyte and an acidic catalyst. The versatility of this method was demonstrated by 27 examples, with up to 92% isolated yields. The electrolysis exhibited tolerance towards various functional groups, including both electron-withdrawing and electron-donating substituents, as well as sterically demanding and redox-sensitive moieties like bromides and iodides. CV measurements confirmed that nitro reduction to the hydroxylamine was the key step in the mechanism. Furthermore, the scalability of this electrochemical protocol was demonstrated by multigram-scale electrolysis.

REFERENCES

(1) Sperry, J. B.; Wright, D. L. The Application of Cathodic Reductions and Anodic Oxidations in the Synthesis of Complex Molecules. *Chem. Soc. Rev.* **2006**, *35*, 605–621. DOI: 10.1039/b512308a.

(2) Francke, R.; Little, R. D. Redox Catalysis in Organic Electrosynthesis: Basic Principles and Recent Developments. *Chem. Soc. Rev.* **2014**, *43*, 2492–2521. DOI: 10.1039/c3cs60464k.

(3) Park, S. H.; Ju, M.; Ressler, A. J.; Shim, J.; Kim, H.; Lin, S. Reductive Electrosynthesis: A New Dawn. *Aldrichimica Acta* **2021**, *54*, 17–27.

(4) Huang, B.; Sun, Z.; Sun, G. Recent Progress in Cathodic Reduction-Enabled Organic Electrosynthesis: Trends, Challenges, and Opportunities. *eScience* **2022**, *2*, 243–277. DOI: 10.1016/j.esci.2022.04.006.

(5) Wirtanen, T.; Rodrigo, E.; Waldvogel, S. R. Recent Advances in the Electrochemical Reduction of Substrates Involving N–O Bonds. *Adv Synth Catal* **2020**, *362*, 2088–2101. DOI: 10.1002/adsc.202000349.

(6) Sadatnabi, A.; Mohamadighader, N.; Nematollahi, D. Convergent Paired Electrochemical Synthesis of Azoxy and Azo Compounds: An Insight into the Reaction Mechanism. *Org. Lett.* **2021**, *23*, 6488–6493. DOI: 10.1021/acs.orglett.1c02304.

(7) Chang, L.; Li, J.; Wu, N.; Cheng, X. Chemoselective Electrochemical Reduction of Nitroarenes with Gaseous Ammonia. *Org. Biomol. Chem.* **2021**, *19*, 2468–2472. DOI: 10.1039/D1OB00077B.

(8) Cyr, A.; Huot, P.; Belot, G.; Lessard, J. The Efficient Electrochemical Reduction of Nitrobenzene and Azoxybenzene to Aniline in Neutral and Basic Aqueous Methanolic Solutions at Devarda Copper and Raney Nickel Electrodes: Electrocatalytic Hydrogenolysis of N–O and N–N Bonds. *Electrochimica Acta* **1990**, *35*, 147–152. DOI: 10.1016/0013-4686(90)85052-O.

(9) Vitaku, E.; Smith, D. T.; Njardarson, J. T. Analysis of the Structural Diversity, Substitution Patterns, and Frequency of Nitrogen Heterocycles among U.S. FDA Approved Pharmaceuticals: Miniperspective. *J. Med. Chem.* **2014**, *57*, 10257–10274. DOI: 10.1021/jm501100b.

(10) Kerru, N.; Gummidi, L.; Maddila, S.; Gangu, K. K.; Jonnalagadda, S. B. A Review on Recent Advances in Nitrogen-Containing Molecules and Their Biological Applications. *Molecules* **2020**, *25*, 1909. DOI: 10.3390/molecules25081909.

(11) Gault, C.; Moinet, C. Reaction of Electogenerated 2-Nitrosobenzic Acids with Sulphinic Acids. A Convenient Route to *N*-Sulfonylbenzisoxazolones. *Tetrahedron* **1989**, *45*, 3429–3436. DOI: 10.1016/S0040-4020(01)81021-8.

(12) Frontana-Uribe, B. A.; Moinet, C. 2-Substituted Indazoles from Electrogenerated Ortho-Nitrosobenzylamines. *Tetrahedron* **1998**, *54*, 3197–3206. DOI: 10.1016/S0040-4020(98)00058-1.

(13) Frontana-Uribe, B. A.; Moinet, C.; Toupet, L. *N*-Substituted 1-Aminoindoles from Electrogenerated *N*-Substituted 2-(*Ortho*-nitrosophenyl)ethylamines. *Eur. J. Org. Chem.* **1999**, *1999*, 419–430. DOI: 10.1002/(SICI)1099-0690(199902)1999:2<419::AID-EJOC419>3.0.CO;2-V.

(14) Hyo Kim, B.; Byung Lee, D.; Ho Kim, D.; Han, R.; Moo Jun, Y.; Baik, W. Electrochemical Synthesis of 2-Aryl-2H-Benzotriazoles and Their *N*-Oxides by Controlled Potential Cathodic Electrolysis. *Heterocycles* **2000**, *53*, 841–850. DOI: 10.3987/COM-99-8824.

(15) Wirtanen, T.; Rodrigo, E.; Waldvogel, S. R. Selective and Scalable Electrosynthesis of 2*H*-2-(Aryl)-benzo[*d*]-1,2,3-triazoles and Their *N*-Oxides by Using Leaded Bronze Cathodes. *Chem.- Eur. J.* **2020**, *26*, 5592–5597. DOI: 10.1002/chem.201905874.

(16) Hyo Kim, B.; Moo Jun, Y.; Rack Choi, Y.; Byung Lee, D.; Baik, W. Electrochemical Synthesis of 2,1-Benzisoxazoles by Controlled Potential Cathodic Electrolysis. *Heterocycles* **1998**, *48*, 749–754. DOI: 10.3987/COM-97-8077.

(17) Hosseini, S.; Bawel, S. A.; Mubarak, M. S.; Peters, D. G. Rapid and High-Yield Electrosynthesis of Benzisoxazole and Some Derivatives. *ChemElectroChem* **2019**, *6*, 4318–4324. DOI: 10.1002/celc.201801321.

(18) Du, P.; Brosmer, J. L.; Peters, D. G. Electrosynthesis of Substituted 1*H*-Indoles from *o*-Nitrostyrenes. *Org. Lett.* **2011**, *13*, 4072–4075. DOI: 10.1021/ol2006049.

(19) Rodrigo, E.; Baunis, H.; Suna, E.; Waldvogel, S. R. Simple and Scalable Electrochemical Synthesis of 2,1-Benzisoxazoles and Quinoline *N*-Oxides. *Chem. Commun.* **2019**, *55*, 12255–12258. DOI: 10.1039/C9CC06054E.

(20) Alberti, A.; Carloni, P.; Greci, L.; Stipa, P.; Andruzzi, R.; Marrosu, G.; Trazza, A. Chemical and Electrochemical Reduction of Ortho-Nitroanilides. A Combined Chemical, Polarographic and EPR Study. *J. Chem. Soc., Perkin Trans. 2* **1991**, *7*, 1019–1023. DOI: 10.1039/p29910001019.

(21) Sokolov, A. A.; Syroeshkin, M. A.; Solkan, V. N.; Shebunina, T. V.; Begunov, R. S.; Mikhal'chenko, L. V.; Leonova, M. Yu.; Gultyai, V. P. Efficient Electrochemical Synthesis of Pyrido[1,2-a]benzimidazoles. *Russ. Chem. Bull.* **2014**, *63*, 372–380. DOI: 10.1007/s11172-014-0440-y.

(22) Sokolov, A. A.; Begunov, R. S.; Syroeshkin, M. A.; Mikhal'chenko, L. V.; Leonova, M. Yu.; Gul'tyai, V. P. Electrochemical Reduction of *N*-(2-Nitro-4*R*-phenyl)pyridinium Salts Using Redox-Mediators. *Russ. Chem. Bull.* **2016**, *65*, 209–214. DOI: 10.1007/s11172-016-1286-2.

(23) Sicker, D.; Hartenstein, H.; Hazard, R.; Tallec, A. Syntheses for 2-Hydroxy-2 *H* -1,4-Benzothiazin-3(4*H*)-one Derivatives as Thio Analogues of Natural Hemiacetals. *J. Heterocycl. Chem.* **1994**, *31*, 809–812. DOI: 10.1002/jhet.5570310420.

(24) Sicker, D.; Hartenstein, H.; Mouats, C.; Hazard, R.; Tallec, A. Electrochemical Reduction of O-Nitrophenylthioacetic Derivatives. Production of 2*H*-1,4-Benzothiazines. *Electrochimica Acta* **1995**, *40*, 1669–1674. DOI: 10.1016/0013-4686(95)00083-Q.

(25) Lund, H.; Feoktistov, L. G. *Acta Chem. Scand.* **1969**, *23*, 3482–3492.

(26) Winter, J.; Prenzel, T.; Wirtanen, T.; Schollmeyer, D.; Waldvogel, S. R. Direct Electrochemical Synthesis of 2,3-Disubstituted Quinoline *N*-Oxides by Cathodic Reduction of Nitro Arenes. *Chem.-Eur. J.* **2023**, *29*, e202203319. DOI: 10.1002/chem.202203319.

(27) Estrada, E.; Rieker, A. Electrosynthesis of 2-Alkyl-4(3*H*)-quinazolinones. *Naturforsch. B* **1994**, *49*, 1566–1568. DOI 10.1515/znb-1994-1119.

(28) Chibani, A.; Hazard, R.; Tallec, A. *Bull. Soc. Chim. Fr.* **1991**, *6*, 814.

(29) Koleda, O.; Prenzel, T.; Winter, J.; Hirohata, T.; De Jesús Gálvez-Vázquez, M.; Schollmeyer, D.; Inagi, S.; Suna, E.; Waldvogel, S. R. Simple and Scalable Electrosynthesis of 1 *H*-1-Hydroxy-quinazolin-4-ones. *Chem. Sci.* **2023**, *14*, 2669–2675. DOI: 10.1039/D3SC00266G.

(30) Masri, A.; Anwar, A.; Khan, N. A.; Shahbaz, M. S.; Khan, K. M.; Shahabuddin, S.; Siddiqui, R. Antibacterial Effects of Quinazolin-4(3*H*)-one Functionalized-Conjugated Silver Nanoparticles. *Antibiotics* **2019**, *8*, 179. DOI: 10.3390/antibiotics8040179.

(31) Wang, P.-F.; Jensen, A. A.; Bunch, L. From Methaqualone and Beyond: Structure–Activity Relationship of 6-, 7-, and 8-Substituted 2,3-Diphenyl-quinazolin-4(3*H*)-ones and in Silico Prediction of Putative Binding Modes of Quinazolin-4(3*H*)-ones as Positive Allosteric Modulators of GABA A Receptors. *ACS Chem. Neurosci.* **2020**, *11*, 4362–4375. DOI: 10.1021/acschemneuro.0c00600.

(32) Romanek, K.; Fels, H.; Dame, T.; Skopp, G.; Musshoff, F.; Eiglmeier, H.; Eyer, F. Return of the Quaaludes? Prolonged Agitated Delirium after Intentional Ingestion of the Methaqualone Analog SL-164 – a Case Report. *Substance Abuse* **2021**, *42*, 503–505. DOI: 10.1080/08897077.2021.1903648.

(33) Somoza, J. R.; Koditek, D.; Villaseñor, A. G.; Novikov, N.; Wong, M. H.; Liclican, A.; Xing, W.; Lagpacan, L.; Wang, R.; Schultz, B. E.; Papalia, G. A.; Samuel, D.; Lad, L.; McGrath, M. E. Structural, Biochemical, and Biophysical Characterization of Idelalisib Binding to Phosphoinositide 3-Kinase *δ*. *J. Biol. Chem.* **2015**, *290*, 8439–8446. DOI: 10.1074/jbc.M114.634683.

(34) Tucker, A. M.; Grundt, P. The Chemistry of Tryptanthrin and Its Derivatives. *Arkivoc* **2012**, *2012*, 546–569. DOI: 10.3998/ark.5550190.0013.113.

(35) Gunasekara, N. S.; Faulds, D. Raltitrexed: A Review of Its Pharmacological Properties and Clinical Efficacy in the Management of Advanced Colorectal Cancer. *Drugs* **1998**, *55*, 423–435. DOI: 10.2165/00003495-199855030-00012.

(36) Reynolds, C. N.; Wilson, K.; Burnett, D. Urinary Excretion of Methaqualone-*N*-Oxide in Man. *Xenobiotica* **1976**, *6*, 113–124. DOI: 10.3109/00498257609151620.

(37) Bickel, M. H. *N* -Oxide Formation and Related Reactions in Drug Metabolism. *Xenobiotica* **1971**, *1*, 313–319. DOI: 10.3109/00498257109041493.

(38) Rani, R.; Granchi, C. Bioactive Heterocycles Containing Endocyclic *N*-Hydroxy Groups. *Eur. J. Med. Chem.* **2015**, *97*, 505–524. DOI: 10.1016/j.ejmech.2014.11.031.

(39) Yamanaka, H. Reaction of 4-Alkoxyquinazolines with Organic Peracid. *Chem. Pharm. Bull.* **1959**, *7*, 152–158. DOI: 10.1248/cpb.7.152.

(40) Spence, T. W. M.; Tennant, G. The Chemistry of Nitro-Compounds. Part II. The Scope and Mechanism of the Base-Catalysed Transformations of some *N*,*N*-Disubstituted *o*-Nitrobenzamides. *J. Chem. Soc., Perkin Trans.* **1972**, 1, 97–102. DOI: 10.1039/p19720000097.

(41) Fielden, R.; oMeth-Cohn, O.; Suschitzky, H. Syntheses of Heterocyclic Compounds. Part XXVI. Photo-Rearrangements of Benzimidazole *N*-Oxides and Related Systems. *J. Chem. Soc., Perkin Trans.* **1973**, *1*, 702–704. DOI: 10.1039/p19730000702.

(42) Lee, J.; Hong, M.; Jung, Y.; Cho, E. J.; Rhee, H. Synthesis of 1,3,5-Trisubstituted-1,2,4-Triazoles by Microwave-Assisted *N*-Acylation of Amide Derivatives and the Consecutive Reaction with Hydrazine Hydrochlorides. *Tetrahedron* **2012**, *68*, 2045–2051. DOI: 10.1016/j.tet.2012.01.003.

(43) Yang, X.-G.; Zheng, K.; Zhang, C. Electrophilic Hypervalent Trifluoromethylthio-Iodine(III) Reagent. *Org. Lett.* **2020**, *22*, 2026–2031. DOI: 10.1021/acs.orglett.0c00405.

(44) Rodrigo, E.; Waldvogel, S. R. A Very Simple One-Pot Electrosynthesis of Nitrones Starting from Nitro and Aldehyde Components. *Green Chem.* **2018**, *20*, 2013–2017. DOI: 10.1039/C8GC00474A.

(45) Hazard, R.; Jubault, M.; Mouats, C.; Tallec, A. Preparation electrochimique de derives de la quinoleine I. Electroreduction de composes o-nitrobenzoyles monofonctionnalises. *Electrochimica Acta* **1986**, *31*, 489–497. DOI: 10.1016/0013-4686(86)80114-1.

(46) Lips, S.; Waldvogel, S. R. Use of Boron-Doped Diamond Electrodes in Electro-Organic Synthesis. *ChemElectroChem* **2019**, *6*, 1649–1660. DOI: 10.1002/celc.201801620.

CONCLUSIONS

1. The electrochemically generated dialkoxy-λ^3-iodane mediates the oxidative cyclization of *ortho*-imino phenols to benzoxazoles. The formation of the heterocyclic product proceeds through a concerted process that involves the oxidation of 2,3-dihydrobenzoxazole intermediate and the reduction of the electrochemically generated λ^3-iodane.

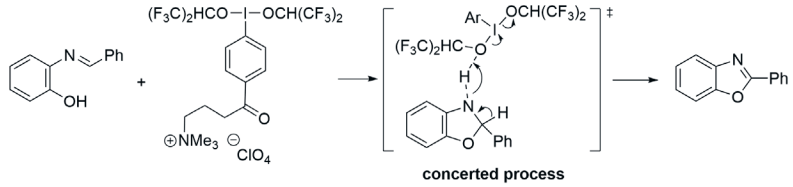

2. Electrochemically generated dialkoxy-λ^3-iodane is virtually impossible to isolate as it undergoes facile reductive elimination in the presence of anionic species.

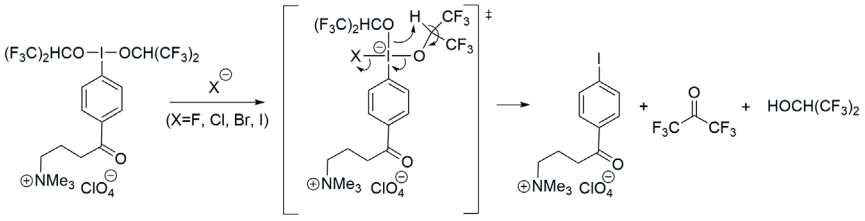

3. Mechanistic studies have confirmed that anodic decarboxylation/etherification of *N*-substituted 2-amino malonate monoesters proceeds via two-electron transfer.

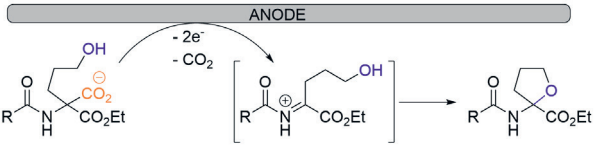

4. A stereogenic center in the *N*-acyl substituent of amino malonate does not influence the diastereoselectivity of the intramolecular Hofer-Moest cyclization. In contrast, a stereogenic center on the nucleophilic tethered alcohol controls diastereoselectivity with up to 73:27 dr.

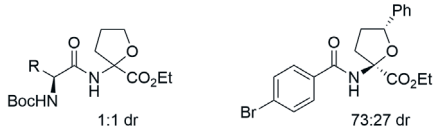

5. The synthesized THP and THF-containing amino acid derivatives are relatively stable under ester hydrolysis conditions (LiOH in THF/water).

6. The conditions of the developed intramolecular Hofer-Moest reaction are compatible with relatively easy-to-oxidize 3-furanoyl and 4-anisoyl moieties as well as with cyano and bromo substituents in the aryl ring.

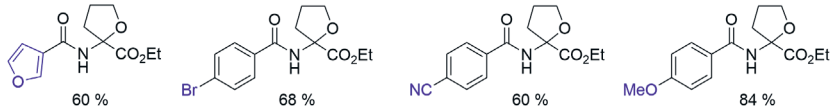

7. THP-amino acid fragment serves as a bioisoster for the 1-aminocyclohexane-1-carboxamide moiety in balicatib allowing for the reduction of lipophilicity (Log*P*), while retaining low nanomolar cathepsin K inhibitory potency.

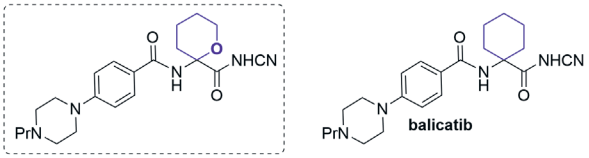

IC_{50} (nM)	0.34 ±0.11	0.46 ±0.08
Log *P*	0.95	1.60

8. Any carbon-based cathode such as BDD, GC, and C is suitable for the cathodic reduction of nitrobenzamides and a subsequent formation of substituted 1*H*-1-hydroxy-quinazolin-4-ones and quinazolin-4-one-*N*-oxides in good yields.

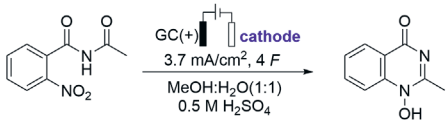

cathode	yield, %
BDD	91
GC	90
C	84

9. The electronic nature of a substituent in the aromatic ring of nitrobenzamide does not influence the developed electroreductive cyclization reaction.

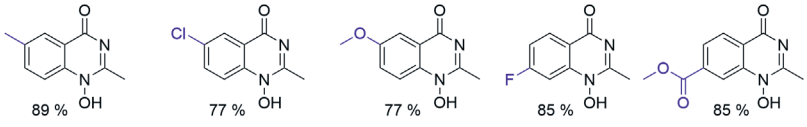

APPENDICES

Appendix I – "Synthesis of Benzoxazoles Using Electrochemically Generated Hypervalent Iodine"

Koleda, O.; Broese, T.; Noetzel, J.; Roemelt, M.; Suna, E.; Francke, R.

J. Org. Chem. **2017**, *82*, 11669–11681.

JOC The Journal of Organic Chemistry

Cite This: J. Org. Chem. 2017, 82, 11669-11681

Featured Article

pubs.acs.org/joc

Synthesis of Benzoxazoles Using Electrochemically Generated Hypervalent Iodine

Olesja Koleda,[†] Timo Broese,[‡] Jan Noetzel,[§] Michael Roemelt,*[,§,∥] Edgars Suna,*[,†] and Robert Francke*[,‡]

[†]Latvian Institute of Organic Synthesis, Aizkraukles 21, LV-1006 Riga, Latvia

[‡]Institute of Chemistry, Rostock University, Albert-Einstein-Str. 3a, 18059 Rostock, Germany

[§]Lehrstuhl für Theoretische Chemie, Ruhr-University Bochum, 44780 Bochum, Germany

[∥]Max-Planck Institut für Kohlenforschung, Kaiser-Wilhelm Platz 1, 45470 Mülheim an der Ruhr, Germany

Supporting Information

ABSTRACT: The indirect ("ex-cell") electrochemical synthesis of benzoxazoles from imines using a redox mediator based on the iodine(I)/iodine(III) redox couple is reported. Tethering the redox-active iodophenyl subunit to a tetraalkylammonium moiety allowed for anodic oxidation to be performed without supporting electrolyte. The mediator salt can be easily recovered and reused. Our "ex-cell" approach toward the electrosynthesis of benzoxazoles is compatible with a range of redox-sensitive functional groups. An unprecedented concerted reductive elimination mechanism for benzoxazole formation is proposed on the basis of control experiments and DFT calculations.

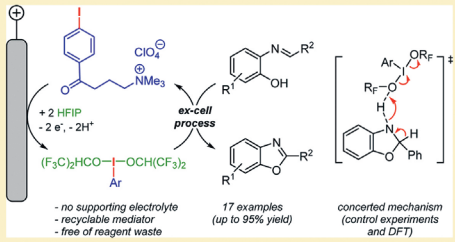

INTRODUCTION

Aryliodonium species constitute a versatile and efficient class of reagents with numerous applications in carbon−carbon and carbon−heteroatom cross-coupling reactions,[1] in oxidative rearrangements,[2] and as terminal oxidants in metal-catalyzed syntheses.[3] Stoichiometric amounts of preformed aryliodonium reagents are routinely employed in these oxidative transformations, resulting in coproduction of aryl iodide byproduct together with the target molecule. Synthetic approaches relying on the in situ generation of aryliodonium catalysts from substoichiometric amounts of iodoarenes and terminal oxidants such as *m*-CPBA and Oxone have been recently developed to minimize the aryl iodide byproduct and to reduce loadings of relatively expensive iodine(III) reagents.[4,5] Although the overall cost may be reduced by the catalytic process, terminal oxidants still remain the source of stoichiometric waste. Electrochemical synthesis provides an attractive solution to the waste reduction and the increase of atom economy and cost-efficiency because inexpensive electric current is employed as the terminal oxidant for the generation of I(III) reagents from iodoarenes.[6,7] Further improvement of atom economy can be accomplished by recovery and electrochemical reoxidation of the iodoarene species. Surprisingly, there are only few examples of separation and multiple reuse of the redox-active iodoarene reagents. This has been achieved by covalent attachment of iodoarene subunits to task specific ionic liquids[8] or to a polymer support.[9] In addition, Francke and Broese have recently demonstrated that merging of the redox-active iodoarene subunit with a tetraalkylammonium moiety not only facilitated efficient separation and reuse of the iodoarene reagent but also allowed for efficient electrochemical generation of I(III) reagent without added external supporting electrolyte.[10] Hence, the ionically tagged phenyl iodide served both as redox mediator and supporting electrolyte in direct oxidative C−N and C−C bond-forming reactions.[10] As a part of our ongoing research on electrochemical synthesis of heterocycles,[11] we report herein an application of the recyclable I(III) mediator−electrolyte system for electrosynthesis of 2-substituted benzoxazoles.

Benzoxazole is frequently encountered in biologically active natural products[12] and pharmaceuticals.[13] Several marketed drugs such as benoxaprofen, caboxamycin, flunoxaprofen, tafamidis, and pseudopteroxazole possess the benzoxazole subunit. Among a plethora of methods for synthesis of benzoxazoles,[14] electrochemical synthesis is one of the most appealing as it provides excellent atom economy and sustainability. For instance, benzoxazoles have been recently prepared by direct electrosynthesis of anilides under galvanostatic conditions (eq 1).[15] The developed approach is operationally simple; however, the method has been only demonstrated for substrates possessing specific substituents (F, Cl, or MeO) *para* to aniline nitrogen. Anodic oxidation of 2-phenoxypyrimidines followed by chemical reaction of cyclized

Special Issue: Hypervalent Iodine Reagents

Received: July 5, 2017
Published: August 11, 2017

DOI: 10.1021/acs.joc.7b01686
J. Org. Chem. 2017, 82, 11669−11681

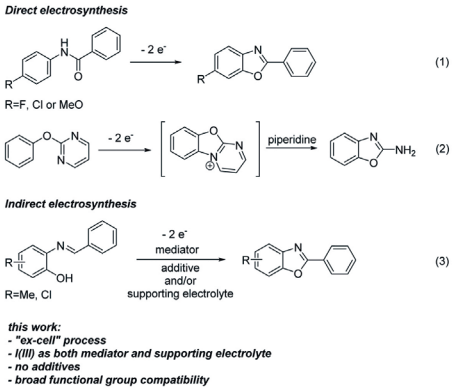

cationic intermediate with piperidine provided an access to 2-aminobenzoxazoles (eq 2).[16] Unfortunately, this approach features decreased atom economy due to the need for a postelectrochemical functionalization step. Direct electrochemical oxidation of imines is also possible (eq 3); however, it required addition of LiOMe to facilitate the formation of benzoxazoles.[17] The presence of the strongly basic methoxide decreases the functional group compatibility. Indirect electrosynthesis using redox mediators such as DDQ[18] or sodium iodide[19] allows for electrochemical generation of benzoxazole under considerably milder conditions (eq 3). However, stoichiometric additives such as carbonate buffer (in NaI-mediated reaction) or 2,6-lutidine and supporting electrolyte (in DDQ-mediated process) were necessary to accomplish the indirect electrosynthesis. Furthermore, relatively electron-rich imines were only used in the oxidative cyclization (R = Me, Cl; see eq 3), and nitro-substituted imines were unreactive. Herein, we report an alternative approach which is based on the electrochemical generation of I(III) mediator prior to the addition of imine ("ex-cell" process). Furthermore, the redox-active I(III) mediator possesses a quaternary ammonium moiety, which serves as supporting electrolyte and facilitates separation and reuse of the redox-active salt. The developed "ex-cell" approach does not require any additives; the oxidative formation of benzoxazoles proceeds under very mild conditions (room temperature), and the method is compatible with a broad range of functional groups as will be demonstrated below.[20]

RESULTS AND DISCUSSION

Mediator Properties. For the electrochemical generation of **2** from iodoarene **1**, previously reported optimized electrolysis parameters were applied (j = 15 mA cm^{-2}, Q = 1 F per mole **1**, [**1**] = 0.2 M, rt).[10] Due to its excellent anodic stability and its ability to stabilize iodine(III) species, the choice of 1,1,1,3,3,3-hexafluoroisopropanol (HFIP) as a solvent for electrolysis turned out to be the key to a successful oxidation of iodoarene **1** to **2** (Figure 1).[10] Unfortunately, the exact structure of the electrochemically prepared I(III) reagent **2** could not be determined because it undergoes decomposition as soon as HFIP is removed, and all attempts to isolate **2** in a pure form were not successful. The ^{1}H NMR spectrum of HFIP solution of **2** (acquired immediately after electrolysis with added 50 vol % CH_2Cl_2-d_2) shows signals corresponding to parent aryl iodide **1** (δ 7.95 and 7.67 ppm) together with a downfield-shifted *para*-substituted aromatic spin system (δ 8.28 and 8.13 ppm; see Figure 1). The downfield signals were assigned to the aromatic subunit of I(III) reagent **2** based on the similarity between ^{1}H and ^{13}C chemical shift values with those of hypervalent iodonium species **3** and **4**, prepared by chemical methods (Figure 1). Additional indirect support for the electrochemical formation of the I(III) reagent was obtained in a control experiment, where electrochemically prepared HFIP solution of I(III) reagent **2** effected clean oxidation of hydroquinone to 1,4-benzoquinone within 15 min at room temperature. Importantly, I(III) reagent **2** resulting from anodic oxidation of **1** is stable in HFIP *solution* at room temperature for several days (entry 1, Table 1). The observed stability of **2** is unusual because hypervalent I(III) species have been reported to oxidize secondary alcohols to the corresponding ketones.[21] In fact, relatively fast reduction of I(III) reagent **3** to aryl iodide **5** (ca. 40% after 15 min and ca. 65% after 20 h) with concomitant oxidation of HFIP to hexafluoroacetone (as evidenced by the appearance of a signal at −82.9 ppm in ^{19}F spectrum) was observed at room temperature (eq 1, Figure 1).

Several control experiments were performed to gain a better understanding of the unusual stability of the electrochemically generated I(III) species **2** and the observed facile decomposition

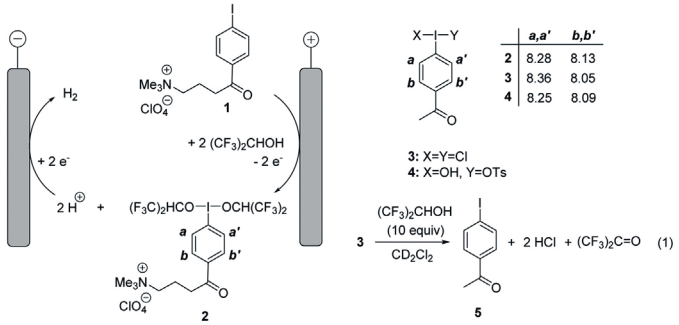

Figure 1. Indirect anodic oxidation of **1** to **2** in HFIP (15 mA cm^{-2}; WE, glassy carbon; CE, Pt sheet).

DOI: 10.1021/acs.joc.7b01686
J. Org. Chem. 2017, 82, 11669−11681

Table 1. Stability of Electrochemically Generated I(III) Species 2

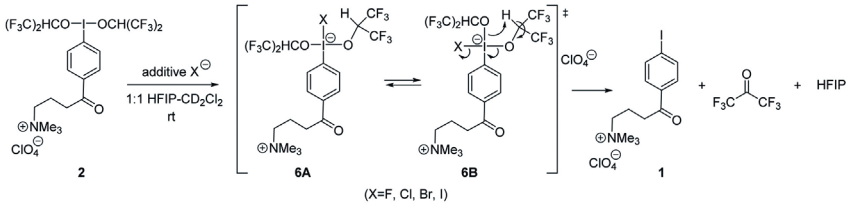

entry	additive (equiv)	time	**1**, %[a]	conv **2**, %[a]
1	none	10 days	12[b]	12
2	anhydrous HCl (1.4)	5 min	20[c]	76[c,d]
3	H_2SO_4 (1.4)	60 min	12[c]	12[c]
4	Bu_4NCl (10)	10 min	15	36[d]
5	Bu_4NF (10)	10 min	61	61
6	Bu_4NBr (10)	10 min	76	76
7	Bu_4NI (10)	10 min	86	86
8	1:1 Bu_4NI/TEMPO (1)	10 min	44	44
9	Bu_4NHSO_4 (10)	24 h	12	12
10	DIPEA (1)	24 h	6	6

[a]Determined by ^{1}H NMR using 1-methyl-1*H*-pyrrole-2,5-dione as internal standard. [b]Electrochemically generated solution of **2** was stored at +4 °C. [c]CH_2Cl_2 was employed as the internal standard. [d]Inseparable mixture of unidentified side products was also formed.

of structurally related λ^3-iodane **3** in HFIP solution (eq 1, Figure 1). We reasoned that formation of HCl in the ligand exchange between **3** and HFIP could facilitate reductive elimination of **3** to iodoarene **5** and hexafluoroacetone (Figure 1, eq 1). Indeed, addition of anhydrous HCl to electrochemically generated **2** resulted in rapid formation of aryl iodide **1** (entry 2, Table 1). The nature of the anion in the acid is more important than the acidity of the proton, as evidenced by considerably slower conversion of **2** to **1** in the presence of sulfuric acid (entry 3). Furthermore, addition of excess Bu_4NCl (10 equiv) as a chloride source triggered the reductive elimination of **2** to **1** under essentially neutral conditions (entry 4). Importantly, other halide anions were much more efficient (entries 5−7), with iodide effecting the most rapid decomposition of **2** (entry 7).[22] Addition of stoichiometric amounts of TEMPO did not affect the iodide-mediated conversion of **2** to **1** (entry 8), ruling out the reductive decomposition of **2** via a radical chain process. Finally, stability of the electrochemically generated **2** in the presence of added tertiary amine base (entry 10) as well as in the presence of a non-nucleophilic hydrogen sulfate additive (entry 9) led us to propose that nucleophilic reactivity of added halides is responsible for conversion of **2** to **1**. Hence, a plausible mechanism for halide anion-facilitated reductive decomposition of **2** is proposed involving addition of halide anion X to **2** to form equilibrating isomers of tetracoordinated [12-I-4] iodate **6** (scheme in Table 1).[23] Subsequent *intramolecular* β-elimination results in the oxidation of HFIP and concomitant reduction of I(III) species to iodoarene **1**.[24] The stability of electrochemically generated iodonium (III) species **2** apparently is attributed to the lack of nucleophiles in the electrolyte. Hence, electrosynthesis opens the door for preparation of new hypervalent I(III) species that are difficult to access using chemical methods such as oxidation or ligand exchange.[25]

Benzoxazole Synthesis. Next, the electrochemically generated I(III) reagent **2** was employed for oxidative cyclization of 2-(benzylideneamino)phenol **7** to benzoxazole **8**. The redox couple **1**/**2** has a higher oxidation potential (E_p(**1**) = 2.2 V vs Ag/$AgNO_3$) compared to that of imine **7** ((E_p(**7b**) = 0.8 V vs Ag/$AgNO_3$).[26] Therefore, electrochemical generation of redox mediator **2** in the presence of **7** (an "in-cell" process) is not possible because in this scenario the phenolic substrate **7** would be oxidized before iodoarene **1**. Consequently, imine **7** has to be added to the electrolyte after completion of anodic conversion of **1** to **2** (an "ex-cell" process). Indeed, addition of imine **7a** to electrochemically generated stoichiometric amounts of I(III) mediator **2** afforded 2-phenyl benzoxazole **8a** (Figure 2) in 87% yield (3.3 F mol^{-1} of passed charge with regard to the substrate **7a**). The I(III)-mediated, "ex-cell" electrochemical cyclization is compatible with a broad range of functional groups such as alkene moiety (**7f,g,i**), bromine (**7b,o,q**), nitro group (**7c,m,o,p**),[27a] ether moiety (**7e,f,p**), ester (**7n**), and even carboxylic acid (**7q**). A variety of imines derived from non-enolizable aldehydes such as electron-rich (**7d−g,p**) and electron-deficient (**7c**) aromatic aldehydes, pyridyl-2-aldehyde (**7h**), cinnamaldehyde (**7i**), and pivalic aldehyde (**7j**) are suitable for the I(III)-mediated cyclization (Figure 2). The formation of benzoxazoles is not sensitive to steric hindrance in the imine moiety because *ortho*-substituted imines (**7c,d,f,g**) undergo facile oxidative cyclization (Figure 2).[27b] It should be noted that simple ester hydrolysis in benzoxazole **8n** leads to the formation of the FDA-approved drug Tafamidis.[28] Benzoxazoles **8** can be also synthesized in a one-pot sequential two-step process from *ortho*-aminophenol and non-enolizable aldehyde without isolation of intermediate imine **7**. Accordingly, addition of I(III) mediator **2** to the in situ formed imine **7b,j** furnished the corresponding benzoxazoles in high yields (Figure 2). Finally, both HFIP and **1** can be recovered after completion of the cyclization. After HFIP removal by distillation, the redox-active iodoarene **1** possessing the tetra-alkylammonium moiety can be recovered and purified by dissolving the solid residue in acetone followed by precipitation upon addition of diethyl ether (typical recovery yield is 92−94%).

Mechanistic Studies. A series of control experiments have been carried out to elucidate the mechanism of benzoxazole

DOI: 10.1021/acs.joc.7b01686
J. Org. Chem. 2017, 82, 11669−11681

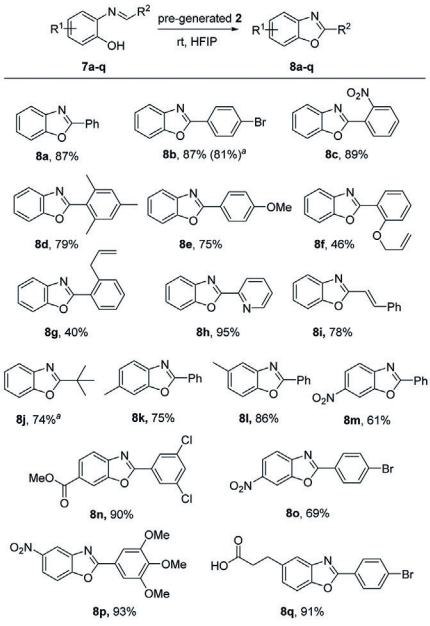

Figure 2. Scope of substrates. [a]Yield of sequential one-pot two-step synthesis.

formation. First, a single-electron transfer (SET) from relatively electron-rich arene **7a-A** to λ^3-iodane **2** was considered as a possible mechanistic scenario (pathway A, Figure 3).[29] The formed radical cation intermediates **IIa,b** would undergo another SET to form nitrenium-type species **IVb**, affording benzoxazole **8a** upon loss of a proton (Figure 3). A radical inhibition test was performed to examine the possibility of benzoxazole formation via the SET pathway. Accordingly, the reaction of **7a-A** with **2** was performed in the presence of added radical scavengers such as TEMPO[30] (1 equiv) or *N-tert*-butyl-α-phenylnitrone[5b] (1 equiv). However, neither of the additives influenced the yield of benzoxazole **8a** (87% yield in both cases; see Figure 2).

Next, imine **7g** containing an *ortho*-allyl moiety as a radical clock probe was employed to test for the intermediacy of radical cation species such as **II** in the synthesis of benzoxazoles (Figure 4). Based on the analogy with a previous study on the cyclization of 2-allylbenzyl radicals, where a rapid 5-*exo*-*trig* cyclization was reported (rate constant $k = 3 \times 10^2\ s^{-1}$),[31] one would expect the formation of 2-methyl-2,3-dihydro-1*H*-indene **VI** after abstraction of a hydrogen atom from the medium (eq 1, Figure 4). However, in our hands, benzoxazole **8g** was obtained as the major product, and no detectable amounts of the cyclization product **VI** were observed (eq 2, Figure 4). These data provide evidence that the I(III)-mediated benzoxazole formation occurs without involvement of benzyl radicals such as **IIb** (pathway A, Figure 3).

In an alternative possibility, pathway B involves reaction of nucleophilic phenolic oxygen with **2** in a ligand exchange process to form aryloxy-λ^3-iodane **III**. Decomposition of **III** via oxidation of the phenol followed by cyclization would afford intermediate **IV**, which is transformed into benzoxazole **8a** upon loss of a proton (Figure 3). To verify the intermediacy of aryloxy-λ^3-iodane **III** in the benzoxazole formation, substrates **7q** and **9** that contain a propionic acid moiety *para* to the phenolic oxygen were synthesized (eqs 3 and 4, Figure 4). It is

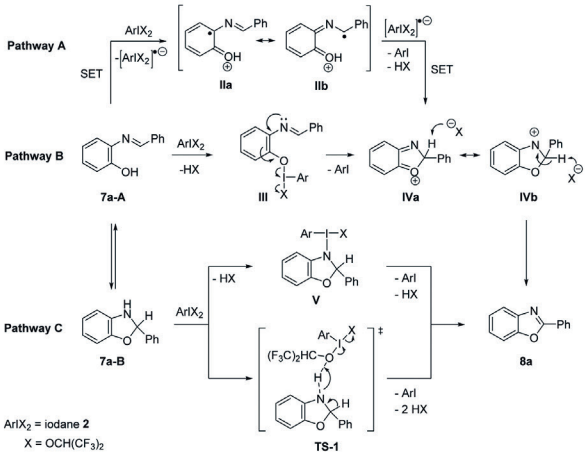

Figure 3. Plausible pathways for benzoxazole formation.

DOI: 10.1021/acs.joc.7b01686
J. Org. Chem. 2017, 82, 11669−11681

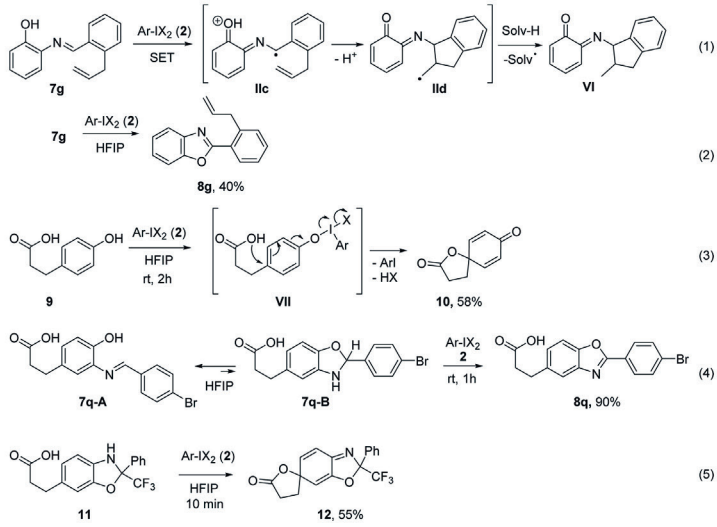

Figure 4. Control experiments.

well-known that the tethered carboxylic acid is suitable as a nucleophile for intramolecular trapping of phenol oxidation products, derived from fragmentation of transient aryloxy-λ^3-iodanes.[32] Indeed, electrochemically generated I(III) reagent **2** reacted with phenol **9** to form spirocycle **10** within 2 h at rt (eq 3, Figure 4). In sharp contrast, structurally related **7q** was converted to benzoxazole **8q** under similar conditions (1 h, rt, 90% yield), and none of the spirocyclization products could be observed in the reaction mixture (eq 4, Figure 4). Hence, the involvement of aryloxy-λ^3-iodane **III** in the formation of benzoxazoles can be questioned.

As a third option, pathway C involves equilibrium formation of cyclic hemiaminal **7a-B** from imine **7a-A**. Cyclic tautomer **7a-B** reacts with I(III) species **2** to form a new hypervalent iodine(III) intermediate **V**,[33] which undergoes reductive elimination of Ar–I to form **8a**. Alternatively, benzoxazole **8a** can be formed directly from cyclic hemiaminal **7a-B** by a concerted reductive elimination via transition state **TS-1** (Figure 3). Although cyclic hemiaminal **7a-B** has not been observed by NMR methods in a 1:1 HFIP/CD_2Cl_2 solution of imine **7a-B** (only signals at δ = 8.67 (^{1}H–C═N) and δ = 159.1 (^{13}C═N) could be seen), its equilibrium formation cannot be excluded. Furthermore, the cyclic tautomer **7a-B** may react with I(III) reagent **2** considerably faster than does imine **7a-A** (Curtin-Hammett conditions). In fact, such a scenario is in agreement with the observed distinct reactivity of phenols **7q-A** and **9** with I(III) reagent **2** (eqs 3 and 4, Figure 4). To verify the involvement of the cyclic tautomer **7a-B** in the benzoxazole formation, structurally related ketimine **11** with tethered carboxylic acid was synthesized. As anticipated, NMR spectra of ketimine **11** in 1:1 HFIP/CD_2Cl_2 solution only showed the presence of the cyclic hemiaminal tautomer (evidenced by ^{13}C signal at δ = 98.7, J = 32.2 Hz). Notably, clean transformation of ketimine **11** to spirocycle **12** (as a 1:1 mixture of diastereomers) was observed upon addition of I(III) reagent **2** under standard conditions (HFIP, rt, 10 min, 55% yield; see eq 5, Figure 4). Facile formation of spirocycle **12** from the cyclic ketimine **11** and the absence of spirocyclization products for the noncyclic aldimine **7q-A** renders the pathway C (Figure 3) as the most plausible mechanism of benzoxazole formation. Further support for pathway C as the most viable mechanistic scenario as well as evidence in favor of the concerted reductive elimination (via transition state **TS-1**) as opposed to intermediate **V** in the pathway C was obtained by theoretical investigations as shown below.

Computational Studies. The proposed reaction pathways B and C (Figure 3) have been probed by quantum chemical calculations on a model comprising substrate **7a**, iodine reagent **13**,[34] and an additional solvent molecule (Figure 5). Technical details together with a description of the chosen theoretical approach are provided in the Experimental Section and the Supporting Information. Computed reaction pathway B involved transfer of a phenolic proton of **7a-A** to the HFIP ligand of mediator **13** to induce a ligand substitution at the I(III) center and formation of intermediate **III** (Figure 6). The substitution is computed to be exothermic by 5.6 kcal mol^{-1}.

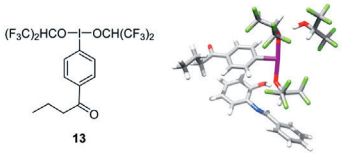

Figure 5. Model system containing iodine(III) species **13**, imine **7a**, and an additional HFIP molecule.

DOI: 10.1021/acs.joc.7b01686
J. Org. Chem. 2017, 82, 11669–11681

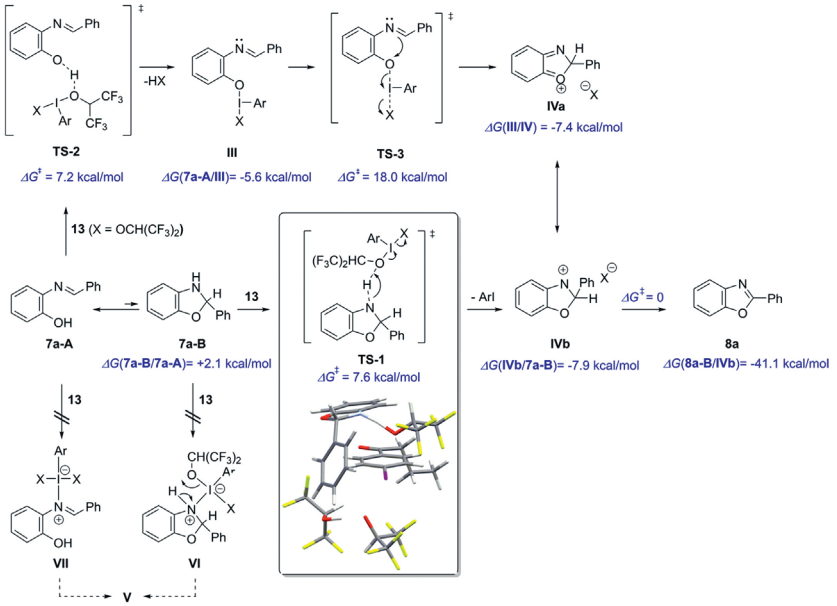

Figure 6. Summary of the computational results on the proposed pathways B and C (cf. Figure 3). The structure of transition state **TS-1** is inserted as sticks model (with iodine displayed violet, hydrogen white, carbon gray, oxygen red, nitrogen blue, and fluorine green). The black arrows indicate the corresponding reaction coordinate which is dominated by the proton transfer from the substrate to its adjacent HFIP anion.

Furthermore, the corresponding transition state **TS-2** could be identified. It is associated with a reaction barrier of 7.2 kcal mol^{-1}, and its reaction coordinate is dominated by the proton transfer from the substrate to the HFIP ligand. After the substrate is bound to the I(III) center, a reductive elimination from the iodine center triggers the ring closure to give intermediates **IVa,b**. The total reaction enthalpy for this step is $\Delta G = -7.4$ kcal mol^{-1} and is thus thermodynamically feasible. Unfortunately, despite intense efforts, the optimization of the corresponding transition state did not meet the convergence criteria. Nevertheless, our thorough search of the potential energy surface yielded a configuration with a single imaginary harmonic frequency that is associated with a symmetric mode of the iodine−oxygen bonds. Since such a motion eventually leads to the desired minima (as we have verified by separate relaxed surface scans), we strongly believe that the obtained structure resembles the true transition state. Thus, the obtained value of $\Delta G^{\ddagger}$ = 18.0 kcal mol^{-1} corresponding to **TS-3** is a reasonable approximation for the reaction barrier.

At this point, it should be noted that in order to obtain realistic reaction enthalpies for the reductive elimination, it is of great importance to explicitly include an additional solvent molecule (see Figure 5) that acts to stabilize the generated HFIP anion through formation of a strong hydrogen bond. Another important aspect of the explicit inclusion of a HFIP molecule is that it is required as structural aid during the ring closure. Without any solvent molecule in the vicinity of the imine group, no ring closure is observed. After the solvent-induced ring annulation, the formed nitrenium cation **IV** is stabilized by the adjacent alkoxide ion (X^-). However, this ion pair **IVa,b** is metastable. When the HFIP anion is manually placed in the vicinity of the proton in α-position to the nitrenium ion, the proton is abstracted without a barrier, resulting in the final product and a gain of $\Delta G = -41.1$ kcal mol^{-1}. This manual procedure simulates a solvent-mediated motion of the HFIP anion which we anticipate to readily occur at room temperature.[35] Alternatively, provided the concentration of mediator and substrate is sufficiently high, a HFIP anion from a neighboring reaction center could act as the required base. In both cases, the final product is formed under considerable heat production.

Next, theoretical investigations of the two alternative reaction coordinates (**TS-1** vs intermediate **V**) in pathway C were performed (cf. Figure 3). Intermediate **V** can be formed from imine **7a-A** and **13** through tetracoordinated [12-I-4] iodate **VII**.[20a] However, stationary points on a potential energy surface corresponding to intermediate **VII** could not be found (Figure 6). Alternatively, I(III) reagent **13** may react with cyclic hemiaminal **7a-B** to form iodate **VI**, which loses a HFIP molecule to afford intermediate **V** (cf. Figure 3). The latter pathway involves cyclic hemiaminal **7a-B**, a species that could not be observed by ^{1}H NMR methods (vide supra). Notably, our calculations indicate that the tautomerization of imine **7a-A** to hemiaminal **7a-B** in the presence of I(III) species **13** is favored by 5.7 kcal mol^{-1} (see Figure 6). As the relative stability is reversed when the Gibbs free energies of **7a-A** and **7a-B** are calculated without **13** and an additional HFIP molecule (ΔG(**7a-A**/**7a-B**) = 2.1 kcal mol^{-1}), this suggests a possible

DOI: 10.1021/acs.joc.7b01686
J. Org. Chem. 2017, 82, 11669−11681

stabilization of the cyclic hemiaminal tautomer by I(III) species **13**. In the meantime, calculations did not lead to stationary points on the potential energy surface corresponding to intermediate **VI**. Furthermore, intermediate **V** spontaneously undergoes reductive elimination when optimized with a solvent molecule in the vicinity of its hemiaminal part. Hence, lack of evidence for the formation of parent species **VI** and **VII** and its own instability puts in question the involvement of the key intermediate **V** in the pathway C for benzoxazole formation. Instead, we have found that precoordination through hydrogen bonding of N–H in **7a-B** with Lewis basic oxygen of the HFIP ligand in **13** triggers a concerted reductive elimination via **TS-1** to form iodoarene and ion pair comprising nitrenium cations **IVa,b** and a HFIP anion. The concerted reaction is exergonic with $\Delta G = -7.9$ kcal mol^{-1}, and it has a relatively low reaction barrier of $\Delta G^{\ddagger} = 7.6$ kcal mol^{-1} (**TS-1**). Transition state **TS-1** exhibits elongated I–O bonds (2.69 and 2.72 Å), whereas the N–H and O–H bond lengths are 1.18 and 1.31 Å, respectively. Hence, it appears that at this point the reductive elimination is almost completed while the hydride transfer has yet to take place. Accordingly, the corresponding reaction coordinate is mainly composed of the hydride transfer movement accompanied by only a minor stretching of the I–O bonds (see stick model for transition state **TS-1** in Figure 6).

The computed reaction barrier corresponding to transition state **TS-1** ($\Delta G^{\ddagger} = 7.6$ kcal mol^{-1}, pathway C) is considerably lower in energy compared to that for **TS-3** ($\Delta G^{\ddagger} = 18.0$ kcal mol^{-1}, pathway B). Hence, our computational results support the pathway C (Figure 3) as the most plausible mechanism for the observed oxidative cyclization as it involves only low kinetic barriers, and each step is thermodynamically favorable. Among the two possible scenarios within the pathway C, our results strongly favor the concerted reductive elimination via transition state **TS-1** as the most likely mechanism for benzoxazole formation.

■ CONCLUSIONS

Anodic oxidation of iodoarenes in HFIP as a solvent allows for convenient preparation of I(III) species under essentially neutral conditions and at room temperature. The electrochemically generated dialkoxy-λ^3-iodane is stable as a solution in HFIP for more than a week at +4 °C (12% decomposition after 10 days). In the presence of nucleophilic anions such as halides, facile reductive elimination of I(III) species to the corresponding aryl iodide, hexafluoroacetone, and HFIP takes place. Poor compatibility of dialkoxy-λ^3-iodanes with nucleophiles renders anodic oxidation a convenient alternative to the traditional approaches such as chemical oxidation or ligands exchange reaction for generation of HFIP-containing I(III) species. Addition of electrochemically generated I(III) species to *ortho*-iminophenols results in clean formation of benzoxazoles. The "ex-cell" electrochemical synthesis of benzoxazoles is compatible with a broad range of redox-sensitive functional groups, including alkene, bromine, and carboxylic acid. Benzoxazoles can also be synthesized in a one-pot sequential two-step process by addition of electrochemically generated I(III) oxidant to the in situ formed imines. Our combined experimental and theoretical approach suggests that oxidative cyclization of *ortho*-iminophenols to benzoxazoles proceeds through 2,3-dihydrobenzoxazole as the key intermediate. DFT studies of several conceivable pathways indicate that a sequence via a concerted reductive elimination represents the most plausible mechanistic scenario for the formation of benzoxazoles.

■ EXPERIMENTAL SECTION

General Information. Unless otherwise noted, all chemicals were used as received from commercial sources, and all reactions were performed under nitrogen or argon atmosphere. Anhydrous CH_2Cl_2 was obtained by passing the commercially available solvent through activated alumina columns. Analytical thin-layer chromatography (TLC) was performed on precoated silica gel F-254 plates. Nuclear magnetic resonance spectra were recorded on NMR spectrometers at the following frequencies: ^{1}H, 400 or 300 MHz; ^{13}C{^{1}H}, 100.6, 75, or 63 MHz; ^{19}F, 376.3 MHz. Chemical shifts are reported in parts per million (ppm) relative to TMS or with the residual solvent peak as an internal reference. High-resolution mass spectra (HRMS) were recorded on a mass spectrometer with a time-of-flight (TOF) mass analyzer using the ESI technique. Electrolysis was performed under galvanostatic control in an undivided cell. Glassy carbon (SIGRADUR G-plate, 10 × 50 × 5 mm) served as a working electrode; a Pt sheet (10 × 50 × 0.1 mm) served as a counter electrode.

Cyclic Voltammetry. The experiments were carried out in a three-electrode cell using a glassy carbon disc (diameter: 3 mm) as a working electrode and a platinum wire as a counter electrode. The glassy carbon disc was polished using polishing alumina (0.05 μm) prior to each experiment. An Ag/$AgNO_3$ electrode (silver wire in 0.1 M NBu_4ClO_4/CH_3CN solution; $c(AgNO_3) = 0.01$ M) was used as a reference, and this compartment was separated from the rest of the cell with a Vycor frit. A 0.1 M solution of NBu_4ClO_4 (electrochemical grade) in HFIP was used as electrolyte. The electrolyte was purged with argon for at least 5 min prior to recording the CVs.

***N*-[4-(4-Iodophenyl)-4-oxobutyl]-*N*,*N*,*N*-trimethylammonium perchlorate (1)** was synthesized in three steps from iodobenzene and 4-chlorobutanoyl chloride according to the procedure reported in the literature.[10] ^{1}H NMR data are identical to those reported in the literature: ^{1}H NMR (400 MHz, DMSO, ppm) δ 7.96–7.94 (m, 2H), 7.75–7.72 (m, 2H), 3.33–3.29 (m, 2H), 3.12 (t, J = 6.8 Hz, 2H), 3.08 (s, 9H), 2.08–1.99 (m, 2H); ^{13}C{^{1}H} NMR (100.6 MHz, $CDCl_3$, ppm) δ 198.0, 137.7, 135.6, 129.6, 102.0, 64.7, 52.2, 34.4, 16.8. Anal. Calcd for $C_{13}H_{19}ClINO_5$: C, 36.17; H, 4.44; N, 3.24. Found: C, 36.25; H, 4.38; N, 3.21.

Procedure for the Electrochemical Generation of I(III) Reagent 2. The electrolysis in an undivided cell was performed following the procedure reported in literature.[10] A glassy carbon piece (immersed surface area: A = 1 cm^2) served as a working electrode and a platinum sheet as a counter electrode. The experiment was carried out as follows: aryl iodide **1** (864 mg, 2 mmol) was dissolved in 1,1,1,3,3,3-hexafluoroisopropanol (HFIP, 10 mL), and molecular sieves (4 Å, 2.0 g) were added. After the cell was purged with argon, the clear solution was electrolyzed with a current density of 15 mA/cm^2 until a charge 1 F per mole of **1** was passed. Upon completion of the electrolysis, an aliquot (0.3 mL) from the light-yellow electrolysis solution was diluted with CD_2Cl_2 (0.3 mL). ^{1}H NMR analysis of the aliquot helped to determine the Faraday efficiency of 67% for the electrolysis. Accordingly, the concentration of the electrolysis solution was 0.67 M in **2**: ^{1}H NMR (400 MHz, CD_2Cl_2, ppm) δ 8.32–8.29 (m, 2H), 8.16–8.13 (m, 2H), 4.39 (septet, J = 5.9 Hz, 2H), 3.40–3.32 (m, 2H, the signal overlaps with those of **1**), 3.29 (t, J = 6.4 Hz, 2H), 3.17 (s, 9H), 2.31–2.19 (m, 2H, the signal overlaps with those of **1**); ^{13}C{^{1}H} NMR (100.6 MHz, CD_2Cl_2, ppm) δ 200.4, 140.0, 153.3, 132.0, 104.0 (the signal overlaps with those of **1**), 67.9, 54.7 (the signal overlaps with those of **1**), 35.5, 18.2. ^{19}F NMR (376.3 MHz, CD_2Cl_2) δ −75.07 (d, J = 5.8 Hz).

1-(4-(Dichloro-λ^3-iodanyl)phenyl)ethan-1-one (3) was synthesized according to the literature procedure.[36] Thus, 4′-iodoacetophenone (492 mg, 1 mmol) was dissolved in MeCN (4 mL), and aqueous 5.84% NaOCl solution (12 mL) was added, followed by the slow addition of aqueous concentrated HCl (4 mL). A light yellow precipitate was formed. After 20 min at room temperature, the precipitate was filtered off and washed with H_2O and hexanes. Drying at room temperature

DOI: 10.1021/acs.joc.7b01686
J. Org. Chem. 2017, 82, 11669–11681

overnight in the dark afforded the title compound **3** as a light yellow solid (620 mg, 98% yield). Pure material was obtained by recrystallization from hexanes/CH_2Cl_2, mp 76.5−75.5 °C (decomp.): ^{1}H NMR (400 MHz, CD_2Cl_2, ppm) δ 8.33−8.30 (m, 2H), 8.03−7.99 (m, 2H), 2.63 (s, 3H); $^{13}C\{^1H\}$ NMR (100.6 MHz, CD_2Cl_2, ppm) δ 196.7, 140.2, 134.6, 131.5. 129.5, 27.2; HRMS (ESI-TOF) m/z $[M]^+$ calcd for $C_8H_7ClIO^+$ 280.9230; found 280.9234.

(4-Acetylphenyl)(hydroxy)-λ^3-iodanyl 4-Methylbenzenesulfonate (4). To a stirred solution of 4′-iodoacetophenone (49 mg, 0.2 mmol) in 1:1 CH_2Cl_2/TFE (2 mL) was added *m*CPBA (49 mg, 0.2 mmol), followed with TsOH·H_2O (38 mg, 0.2 mmol). The resulting yellow solution was stirred at room temperature for 1 h and then concentrated under a stream of air. Et_2O (4 mL) was added to the remaining residue, and the resulting precipitate was filtered off to afford iodane **4** as an off-white solid (62 mg, 71%). Pure material was obtained after precipitation from a mixture of MeOH/CH_2Cl_2/hexanes: ^{1}H NMR (400 MHz, DMSO-d_6, ppm) δ 8.32- 8.29 (m, 2H), 8.11−8.09 (m, 2H), 7.49−7.47 (m, 2H), 7.13−7.11 (m, 2H), 2.63 (s, 3H), 2.28 (s, 3H); $^{13}C\{^1H\}$ NMR (100.6 MHz, DMSO-d_6, ppm) δ 197.5, 145.4, 139.2, 137.9, 134.4, 130.5, 128.2, 127.7, 125.6, 27.1, 20.9. Anal. Calcd for $C_{15}H_{15}IO_5S$: C, 41.49; H, 3.48. Found: C, 41.54; H, 3.49.

General Procedure A for the Synthesis of Imines 7a−q.[37] Benzaldehyde (2 mmol, 1.0 equiv) was added to a mixture of *ortho*-aminophenol (2 mmol, 1.0 equiv), anhydrous Na_2SO_4 (3 equiv), and anhydrous CH_2Cl_2 (5 mL) under argon atmosphere. The suspension was stirred at room temperature for 16 h, whereupon Na_2SO_4 was removed by filtration. The filtrate was concentrated under reduced pressure, and the crude solid residue was recrystallized from EtOH to afford the corresponding imine.

General Procedure B for the Synthesis of Imines 7a−q.[37] A mixture of *ortho*-aminophenol (2 mmol, 1.0 equiv) and aldehyde (2 mmol, 1.0 equiv) was stirred under reflux in anhydrous EtOH (4 mL) for 4 h. After being cooled to room temperature and concentration under reduced pressure, the crude solid residue was recrystallized from EtOH to afford the corresponding imine.

General Procedure C for the Synthesis of Imines 7a−q.[38] A mixture of *ortho*-aminophenol (2 mmol, 1.0 equiv) and aldehyde (2.4 mmol, 1.2 equiv) was stirred at 70 °C in anhydrous MeOH (4 mL) in the presence of molecular sieves 4 Å (1.5 g) for 20 h. After being cooled to ambient temperature, the reaction mixture was filtered to remove the molecular sieves, and the filtrate was concentrated under reduced pressure. The crude product was recrystallized from MeOH, EtOH, or a mixture of MeOH/CH_2Cl_2/hexanes to yield the corresponding imine.

(*E*)-2-(Benzylideneamino)phenol (7a) was obtained as a light yellow amorphous solid (319 mg, 81%) according to general procedure A. ^{1}H NMR spectral data are identical to those reported in the literature:[39] ^{1}H NMR (300 MHz, $CDCl_3$, ppm) δ 8.71 (s, 1H), 7.97−7.92 (m, 2H), 7.54−7.49 (m, 3H), 7.33 (dd, J = 7.9, 1.5 Hz, 1H), 7.29 (br s, 1H), 7.25−7.20 (m, 1H), 7.05 (dd, J = 8.1, 1.1 Hz, 1H), 6.96−6.91 (m, 1H); $^{13}C\{^1H\}$ NMR (75 MHz, $CDCl_3$, ppm) δ 157.1, 152.3, 135.8, 135.5, 131.7, 128.9, 128.8, 128.7, 120.1, 115.82, 115.0.

(*E*)-2-(4-Bromobenzylideneamino)phenol (7b) was obtained as a yellow solid (447 mg, 81%) according to general procedure A. Pure material was obtained by recrystallization from EtOH, mp 127−128 °C: IR (film, cm^{-1}) 3312 (O−H), 1626 (C═N); ^{1}H NMR (400 MHz, CD_2Cl_2, ppm) δ 8.68 (s, 1H), 7.85−7.801 (m, 2H), 7.67−7.62 (m, 2H), 7.34 (dd, J = 8.0, 1.4 Hz, 1H), 7.26−7.15 (m, 2H), 6.99 (dd, J = 8.1, 1.4 Hz, 1H), 6.92 (td, J = 7.7, 1.4 Hz, 1H); $^{13}C\{^1H\}$ NMR (100.6 MHz, $CDCl_3$, ppm) δ 155.7, 152.5, 135.2, 134.9, 132.3, 130.2, 129.4, 126.4, 120.3, 115.9, 115.3; HRMS (ESI-TOF) m/z $[M + H]^+$ calcd for $C_{13}H_{11}BrNO$ 276.0024; found 276.0032.

(*E*)-2-(2-Nitrobenzylideneamino)phenol (7c) was obtained as a yellow solid (391 mg, 54%) according to general procedure B from *ortho*-aminophenol (3 mmol) and 2-nitrobenzaldehyde (3 mmol). ^{1}H NMR spectral data are identical to those reported in the literature:[40] ^{1}H NMR (300 MHz, $CDCl_3$, ppm) δ 9.18 (s, 1H), 8.28 (dd, J = 7.7, 1.5 Hz, 1H), 8.08 (dd, J = 8.2, 1.2 Hz, 1H), 7.79−7.74 (m, 1H), 7.68−7.62 (m, 1H), 7.37 (dd, J = 7.9, 1.5 Hz, 1H), 7.30−7.24 (m, 1H), 7.15 (s, 1H), 7.05 (dd, J = 8.1, 1.3 Hz, 1H), 6.97−6.92 (m, 1H); $^{13}C\{^1H\}$ NMR (63 MHz, $CDCl_3$, ppm) δ 152.8, 152.0, 149.4, 134.7, 133.4, 131.4, 130.5, 130.2, 129.5, 124.7, 120.4, 116.4, 115.5.

(*E*)-2-((2,4,6-Trimethylbenzylidene)amino)phenol (7d) was obtained as a brown amorphous solid (84 mg, 70%) according to general procedure C from *ortho*-aminophenol (0.5 mmol) and 2,4,6-trimethylbenzaldehyde (0.5 mmol). ^{1}H NMR spectral data are identical to those reported in the literature:[38] ^{1}H NMR (400 MHz, $CDCl_3$, ppm) δ 9.09 (s, 1H), 7.28−7.26 (m, 1H), 7.23−7.19 (m, 1H), 7.05−7.03 (m, 1H), 6.97 (s, 2H), 6.97−6.92 (m, 1H), 2.58 (s, 6H), 2.35 (s, 3H); $^{13}C\{^1H\}$ NMR (100.6 MHz, $CDCl_3$, ppm) δ 157.9, 152.2, 140.6, 139.2, 137.0, 130.3, 130.1, 128.7, 120.2, 115.6, 114.9, 21.7, 21.4.

(*E*)-2-(4-Methoxybenzylideneamino)phenol (7e) was obtained as a yellow amorphous solid (186 mg, 41%) according to general procedure A. ^{1}H NMR spectral data are identical to those reported in the literature:[41] ^{1}H NMR (300 MHz, $CDCl_3$, ppm) δ 8.63 (s, 1H), 7.91−7.86 (m, 2H), 7.30−7.27 (m, 1H), 7.21−7.15 (m, 1H), 7.03−6.99 (m, 3H), 6.94−6.88 (m, 1H), 3.90 (s, 3H); $^{13}C\{^1H\}$ NMR (63 MHz, $CDCl_3$, ppm) δ 162.5, 156.6, 152.0, 135.9, 130.6, 128.9, 128.3, 120.0, 115.7, 114.8, 114.3, 44.5.

(*E*)-2-((2-(Allyloxy)benzylidene)amino)phenol (7f) was obtained as a dark brown oil (493 mg, 99% yield) according to general procedure C: IR (film, cm^{-1}) 3412 (O−H), 1594 (C═N); ^{1}H NMR (400 MHz, $CDCl_3$, ppm) δ 9.22 (s, 1H), 8.17 (dd, J = 7.7, 1.8 Hz, 1H), 7.44 (m, 1H), 7.32 (dd, J = 7.9, 1.5 Hz, 1H), 7.14 (td, J = 7.8, 1.5 Hz, 1H), 7.06 (t, J = 7.5 Hz, 1H), 7.02 (dd, J = 8.1, 1.4 Hz, 1H), 6.96 (d, J = 8.4 Hz, 1H), 6.91 (td, J = 7.7, 1.4 Hz, 1H), 6.16−6.06 (m, 1H), 5.46 (dd, J = 17.2, 1.6 Hz, 1H), 5.35 (dd, J = 10.5, 1.5 Hz, 1H), 4.66 (d, J = 5.2 Hz, 2H); $^{13}C\{^1H\}$ NMR (100.6 MHz, $CDCl_3$, ppm) δ 158.8, 153.3, 152.4, 136.4, 133.0, 132.9, 128.7, 127.6, 124.8, 121.2, 120.2, 118.1, 116.2, 114.9, 112.7, 69.4; HRMS (ESI-TOF) m/z $[M + H]^+$ calcd for $C_{16}H_{16}NO_2$ 254.1181; found 254.1180.

(*E*)-2-((2-Allylbenzylidene)amino)phenol (7g) was obtained as a brown oil (260 mg, 90%) according to general procedure C from *ortho*-aminophenol (1.5 mmol) and 2-allylbenzaldehyde[42] (1.2 mmol): IR (film, cm^{-1}) 3412 (O−H), 1587 (C═N); ^{1}H NMR (400 MHz, $CDCl_3$, ppm) δ 8.96 (s, 1H), 8.12 (dd, J = 7.7, 1.5 Hz, 1H), 7.44 (td, J = 7.4, 1.5 Hz, 1H), 7.39−7.35 (m, 1H), 7.29−7.23 (m, 2H), 7.22−7.18 (m, 1H), 7.02 (dd, J = 8.1, 1.3 Hz, 1H), 6.93−6.89 (m, 1H), 6.08 (ddt, J = 17.1, 10.2, 5.8 Hz, 1H), 5.17−5.11 (m, 1H), 5.02−4.94 (m, 1H), 3.75 (d, J = 5.8 Hz, 2H); $^{13}C\{^1H\}$ NMR (100.6 MHz, $CDCl_3$, ppm) δ 156.0, 152.5, 140.4, 137.3, 136.3, 133.9, 131.6, 131.0, 129.0, 128.5, 127.1, 120.2, 116.6, 116.0, 115.1, 37.4; HRMS (ESI-TOF) m/z $[M + H]^+$ calcd for $C_{16}H_{16}NO$ 238.1232; found 238.1236.

(*E*)-2-((Pyridin-2-yl)methyleneamino)phenol (7h) was obtained as a green solid (282 mg, 47%) according to general procedure B from 2-pyridinecarboxaldehyde (3 mmol) and *ortho*-aminophenol (3 mmol). Pure material was obtained by recrystallization from hexanes/CH_2Cl_2, mp 104−105 °C: IR (film, cm^{-1}) 3362 (O−H), 1588 (HC═N); ^{1}H NMR (300 MHz, acetone-d_6, ppm) δ 8.82 (s, 1H), 8.70 (dd, J = 4.8, 0.8 Hz, 1H), 8.43 (d, J = 8.0 Hz, 1H), 7.91 (td, J = 7.5, 1.2 Hz, 1H), 7.49−7.45 (m, 2H), 7.28−7.4 (m, 1H), 6.98−6.89 (m, 2H); $^{13}C\{^1H\}$ NMR (100.6 MHz, acetone-d_6, ppm) δ 159.3, 155.7, 153.7, 150.5, 137.4, 136.6, 130.1, 126.1, 122.4, 120.8, 118.2, 116.6; HRMS (ESI-TOF) m/z $[M + H]^+$ calcd for $C_{12}H_{11}N_2O$ 198.0788; found 198.0782.

(2*E*)-2-((*E*)-3-Phenylallylideneamino)phenol (7i) was obtained as a light yellow solid (112 mg, 25%) according to general procedure A. ^{1}H NMR spectral data are identical to those reported in the literature:[43] ^{1}H NMR (300 MHz, $CDCl_3$, ppm) δ 8.51 (d, J = 7.7 Hz, 1H), 7.59−7.55 (m, 2H), 7.47−7.38 (m, 3H), 7.27−7.16 (m, 4H), 7.01 (dd, J = 8.1, 1.1 Hz, 1H), 6.92−6.87 (m, 1H); $^{13}C\{^1H\}$ NMR (63 MHz, $CDCl_3$, ppm) δ 158.2, 152.3, 144.2, 135.6, 135.5, 129.8, 129.0, 128.9, 128.5, 127.6, 120.0, 115.5, 115.0.

(*E*)-2-(Benzylideneamino)-5-methylphenol (7k) was obtained as a yellow solid (413 mg, 98%) according to general procedure B. Pure material was obtained by recrystallization from EtOH, mp 94−96 °C: IR (film, cm^{-1}) 3332 (O−H), 1580 (C═N); ^{1}H NMR (300 MHz, $CDCl_3$, ppm) δ 8.70 (s, 1H), 7.94−7.90 (m, 2H), 7.52−7.47 (m, 3H), 7.28 (br s, 1H), 7.24 (d, J = 8.1 Hz, 1H), 6.86 (m, 1H), 6.75−6.72 (m, 1H), 2.35 (s, 3H); $^{13}C\{^1H\}$ NMR (75 MHz, $CDCl_3$, ppm) δ 155.7, 152.3, 139.4, 136.0, 132.9, 131.4, 128.8, 128.6, 120.8, 115.5, 115.4, 21.5;

DOI: 10.1021/acs.joc.7b01686
J. Org. Chem. 2017, 82, 11669−11681

HRMS (ESI-TOF) m/z $[M]^+$ calcd for $C_{14}H_{13}NO$ 211.0992; found 211.0984.

(*E*)-2-(Benzylideneamino)-4-methylphenol (7l) was obtained as a light yellow amorphous solid (17 mg, 4%) according to general procedure B. ^{1}H NMR spectral data are identical to those reported in the literature:[44] ^{1}H NMR (300 MHz, $CDCl_3$, ppm) δ 8.70 (s, 1H), 7.95−7.91 (m, 2H), 7.53−7.48 (m, 3H), 7.14−7.13 (m, 1H), 7.09 (br s, 1H), 7.05−7.01 (m, 1H), 6.94−6.91 (m, 1H), 2.34 (s, 3H); ^{13}C{^{1}H} NMR (63 MHz, $CDCl_3$, ppm) δ 156.7, 150.1, 135.9, 135.1, 131.6, 129.5, 128.8, 128.7, 116.3, 114.6, 20.8.

(*E*)-2-(Benzylideneamino)-5-nitrophenol (7m) was obtained as a yellow amorphous solid (353 mg, 55%) according to general procedure C. The pure product was obtained after precipitating from a mixture of MeOH/DCM/hexanes: ^{1}H NMR (400 MHz, acetone-d_6, ppm) δ 8.88 (s, 1H), 8.11−8.08 (m, 2H), 7.80 (dd, J = 8.7, 2.5 Hz, 1H), 7.75 (d, J = 2.5 Hz, 1H), 7.62−7.53 (m, 3H), 7.49 (d, J = 8.6 Hz, 1H); ^{13}C{^{1}H} NMR (100.6 MHz, acetone-d_6, ppm) δ 163.9, 152.9, 147.7, 144.8, 136.8, 133.2, 130.5, 129.7, 119.5, 116.2, 111.3; HRMS (ESI-TOF) m/z $[M + H]^+$ calcd for $C_{13}H_{11}N_2O_3$ 243.0770; found 243.0765.

(*E*)-Methyl 4-(3,5-dichlorobenzylideneamino)-3-hydroxybenzoate (7n) was obtained as a yellow solid (486 mg, 75%) according to general procedure A. Pure material was obtained by recrystallization from EtOH, mp 207−208 °C: IR (film, cm^{-1}) 3394 (O−H), 1714 (C═O), 1562 (C═N); ^{1}H NMR (300 MHz, DMSO, ppm) δ 8.73 (s, 1H), 8.09 (d, J = 2.1 Hz, 2H), 7.79 (t, J = 2.0 Hz, 1H), 7.47 (s, 1H), 7.46 (dd, J = 6.0, 1.9 Hz, 1H), 7.29−7.26 (m, 1H), 3.83 (s, 3H); ^{13}C{^{1}H} NMR (63 MHz, DMSO, ppm) δ 165.9, 158.9, 151.0, 141.5, 139.3, 134.6, 130.7, 128.7, 127.4, 120.6, 119.7, 116.8, 52.1; HRMS (ESI-TOF) m/z $[M + H]^+$ calcd for $C_{15}H_{12}Cl_2NO_3$ 324.0194; found 324.0190.

(*E*)-2-((4-Bromobenzylidene)amino)-4-nitrophenol (7o) was obtained as a yellow amorphous solid (238 mg, 37%) according to general procedure C. Pure product was obtained after precipitating from a mixture of MeOH/DCM: ^{1}H NMR (400 MHz, $CDCl_3$, ppm) δ 8.69 (s, 1H), 7.86−7.81 (m, 4H), 7.67 (d, J = 8.4 Hz, 2H), 7.34 (d, J = 8.7 Hz, 1H), 7.17 (s, 1H); ^{13}C{^{1}H} NMR (100.6 MHz, $CDCl_3$, ppm) δ 160.4, 152.2, 147.7, 141.2, 134.0, 132.6, 130.8, 128.0, 116.6, 116.1, 110.8; HRMS (ESI-TOF) m/z $[M + H]^+$ calcd for $C_{13}H_{10}BrN_2O_3$ 320.9875; found 320.9867.

(*E*)-4-Nitro-2-((3,4,5-trimethoxybenzylidene)amino)phenol (7p) was obtained as a yellow solid (215 mg, 72%) according to general procedure C from 2-amino-4-nitrophenol (0.9 mmol) and 3,4,5-trimethoxybenzaldehyde (0.9 mmol). Pure material was obtained by recrystallization from CH_2Cl_2, mp 187−188 °C: IR (film, cm^{-1}) 3349 (O−H), 1581 (C═N), 1462 (NO_2); ^{1}H NMR (400 MHz, $CDCl_3$, ppm) δ 8.70 (s, 1H), 8.22 (d, J = 2.6 Hz, 1H), 8.14 (dd, J = 9.0, 2.6 Hz, 1H), 7.19 (s, 2H), 7.10 (d, J = 8.9 Hz, 1H), 3.97 (s, 6H), 3.96 (s, 3H); ^{13}C{^{1}H} NMR (100.6 MHz, $CDCl_3$, ppm) δ 160.4, 157.7, 153.8, 142.5, 141.4, 135.9, 130.3, 124.5, 115.1, 112.3, 106.6, 61.2, 56.5; HRMS (ESI-TOF) m/z $[M + H]^+$ calcd for $C_{16}H_{17}N_2O_6$ 333.1087; found 333.1091.

3-(3-Amino-4-hydroxyphenyl)propanoic acid (14). To a solution of 3-(4-hydroxy-3-nitrophenyl)propanoic acid (815 mg, 3.86 mmol) in absolute EtOH (50 mL) was added 10% Pd−C (402 mg, 10 mol %), and H_2 gas was passed through the resulting suspension at room temperature for 2 h. The progress of the hydrogenation was followed by UPLC-MS analysis. Once the reaction was completed, it was filtered through a plug of Celite. The filtrate was concentrated to obtain the product as pale green foam (636 mg, 91%) that was used in the next step without additional purification: IR (film, cm^{-1}) 3370, 3335 (N−H), 2934 (O−H); ^{1}H NMR (400 MHz, CD_3OD, ppm) δ 6.64 (d, J = 2.2 Hz, 1H), 6.61 (d, J = 8.0 Hz, 1H), 6.47 (dd, J = 8.0, 2.2 Hz, 1H), 2.74 (t, J = 7.8 Hz, 2H), 2.50 (t, J = 7.8 Hz, 1H); ^{13}C{^{1}H} NMR (100.6 MHz, CD_3OD, ppm) δ 177.6, 145.0, 135.4, 133.8, 120.2, 117.7, 115.6, 37.6, 31.7; HRMS (ESI-TOF) m/z $[M + H]^+$ calcd for $C_9H_{12}NO_3$ 182.0817; found 182.0817.

(*E*)-3-(3-((4-Bromobenzylidene)amino)-4-hydroxyphenyl)-propanoic acid (7q) was obtained as a brown amorphous solid (106 mg, 25%) according to general procedure C from 3-(3-amino-4-hydroxyphenyl)propanoic acid (**14**; see above) (1.2 mmol) and 4-bromobenzaldehyde (1.5 mmol); product **7q** was used in the next step without additional purification because of its instability: IR (film, cm^{-1}) 3409 (O−H), 1699 (C═O), 1586 (C═N); ^{1}H NMR (300 MHz, CD_3OD, ppm) δ 8.67 (s, 1H), 7.92−7.89 (m, 2H), 7.65−7.63 (m, 2H), 7.13 (d, J = 2.1 Hz, 1H), 7.01 (dd, J = 8.2, 1.9 Hz, 1H), 6.81 (d, J = 8.2 Hz, 1H), 2.86 (t, J = 7.7 Hz, 2H), 2.52 (t, J = 7.7 Hz, 2H); ^{13}C{^{1}H} NMR (100.6 MHz, CD_3OD, ppm) δ 176.9, 159.2, 151.2, 138.3, 136.9, 133.9, 133.0, 131.5, 129.1, 126.6, 119.1, 116.7, 37.1, 31.4; HRMS (ESI-TOF) m/z $[M + H]^+$ calcd for $C_{16}H_{15}BrNO_3$ 348.0235; found 348.0237

General Procedure D for the Synthesis of Substituted Benzoxazoles from Imines. A solution of electrochemically prepared I(III) oxidant **2** (67 mM in HFIP) was added under argon to a solution of imine (0.3 mmol) in HFIP (0.5 mL). The resulting solution was stirred at room temperature until complete conversion of **7** (usually 10 min), and the progress of the reaction was monitored by GC-MS and ^{1}H NMR. Diethyl ether (50 mL) was then added, and the resulting suspension was kept at +4 °C for 15 min. The formed precipitate (iodoarene **1**) was removed by filtration and washed with Et_2O. Drying under air allowed for 92−94% recovery of mediator **1**. The combined filtrates were concentrated under reduced pressure, and the residue was purified by column chromatography on silica gel to yield the corresponding substituted benzoxazole.

General Procedure E for a One-Pot Two-Step Synthesis of Substituted Benzoxazoles from the Aldehyde and Aniline. A light brown solution of *ortho*-aminophenol (0.4 mmol, 1 equiv) and aldehyde (0.48 mmol, 1.2 equiv) in $CHCl_3$ (2 mL; for benzoxazole **8j**) or in HFIP (2 mL; for benzoxazole **8b**) was stirred at room temperature for 6 h. Then freshly prepared I(III) reagent **2** (67 mM solution in HFIP) was added under argon atmosphere, and stirring at room temperature was continued for 30 min. Addition of diethyl ether (50 mL) afforded a suspension that was cooled at +4 °C for 15 min. The formed sand-colored precipitate (iodoarene **1**) was removed by filtration. The filter cake was washed with Et_2O and dried under air. The filtrate was concentrated, and the residue was purified by column chromatography on silica gel to yield the corresponding benzoxazole.

2-Phenylbenzo[*d*]oxazole (8a) was obtained as a white solid (51 mg, 87%) according to general procedure D. The crude product was purified by column chromatography on silica gel using gradient elution from 0% EtOAc in heptane to 9% EtOAc in heptane. Analytical TLC on silica gel, 1:9 EtOAc/heptane, R_f = 0.4. Pure material was obtained by recrystallization from heptane, mp 105.5−106.5 °C. ^{1}H NMR spectral data are identical to those reported in the literature:[37] ^{1}H NMR (300 MHz, $CDCl_3$, ppm) δ 8.31−8.25 (m, 2H), 7.82−7.77 (m, 1H), 7.62−7.58 (m, 1H), 7.57−7.52 (m, 3H), 7.40−7.34 (m, 2H); ^{13}C{^{1}H} NMR (75 MHz, $CDCl_3$, ppm) δ 163.0, 150.7, 142.1, 131.5, 128.9, 127.6, 127.1, 125.1, 124.5, 120.0, 110.5; GC-MS (EI) m/z $[M]^+$ found for $C_{13}H_9NO$ 195.38.

2-(4-Bromophenyl)benzo[*d*]oxazole (8b) was obtained as a white solid (71 mg, 87%) according to general procedure D. The crude product was purified by column chromatography on silica gel using gradient elution from 0% EtOAc in heptane to 9% EtOAc in heptane. Analytical TLC on silica gel, 1:9 EtOAc/heptane, R_f = 0.45. Pure material was obtained by recrystallization from heptane, mp 158.5−159.5 °C. ^{1}H NMR spectral data are identical to those reported in literature:[37] ^{1}H NMR (300 MHz, $CDCl_3$, ppm) δ 8.14−8.10 (m, 2H), 7.80−7.74 (m, 1H), 7.69−7.64 (m, 2H), 7.61−7.55 (m, 1H), 7.40−7.34 (m, 2H); ^{13}C{^{1}H} NMR (63 MHz, $CDCl_3$, ppm) δ 162.1, 150.7, 142.0, 132.2, 129.0, 126.2, 126.1, 125.4, 124.8, 120.1, 110.6; GC-MS (EI) m/z $[M]^+$ found for $C_{13}H_8BrNO$ 273.44.

Use of general procedure E afforded benzoxazole **8b** in 81% yield (66 mg).

2-(2-Nitrophenyl)benzo[*d*]oxazole (8c) was obtained as pale yellow solid (64 mg, 89%) according to general procedure D. The crude product was purified by column chromatography on silica gel using gradient elution from 0% EtOAc in heptane to 33% EtOAc in heptane. Analytical TLC on silica gel, 1:9 EtOAc/heptane, R_f = 0.1. Pure material was obtained by recrystallization from heptane, mp 104.5−105.5 °C. ^{1}H NMR spectral data are identical to those reported in literature:[45] ^{1}H NMR (300 MHz, $CDCl_3$, ppm) δ 8.17−8.14 (m, 1H), 7.92−7.89 (dd, J = 7.9, 1.5 Hz, 1H), 7.85−7.79 (m, 1H), 7.78−7.67 (m, 2H), 7.62−7.55

DOI: 10.1021/acs.joc.7b01686
J. Org. Chem. 2017, 82, 11669−11681

(m, 1H), 7.45−7.37 (m, 2H); $^{13}C\{^1H\}$ NMR (75 MHz, $CDCl_3$, ppm) δ 158.8, 151.0, 141.5, 132.3, 131.8, 131.4, 126.0, 124.9, 124.2, 121.5, 120.7, 110.9; GC-MS (EI) m/z $[M]^+$ found for $C_{13}H_8N_2O_3$ 240.38.

2-Mesitylbenzo[*d*]oxazole (8d) was obtained as a yellow thick oil (56 mg, 79%) according to general procedure D. The crude product was purified by column chromatography on silica gel using gradient elution from 3% EtOAc in hexanes to 15% EtOAC in hexanes. Analytical TLC on silica gel, 1:10 EtOAc/hexanes, R_f = 0.48. ^1H NMR spectral data are identical to those reported in literature:[37] ^1H NMR (400 MHz, $CDCl_3$, ppm) δ 7.86−7.79 (m, 1H), 7.62−7.56 (m, 1H), 7.41−7.35 (m, 2H), 6.98 (s, 2H), 2.36 (s, 3H), 2.29 (s, 6H); $^{13}C\{^1H\}$ NMR (100.6 MHz, $CDCl_3$, ppm) δ 163.4, 150.8, 141.7, 140.4, 138.6, 128.8, 125.1, 125.0, 124.3, 120.3, 110.7, 21.4, 20.5; UPLC-MS (ESI) m/z $[M + H]^+$ found for $C_{16}H_{16}NO$ 238.29.

2-(4-Methoxyphenyl)benzo[*d*]oxazole (8e) was obtained as light brown solid (51 mg, 75%) according to general procedure D. The crude product was purified by column chromatography on silica gel using gradient elution from 0% EtOAc in heptane to 33% EtOAc in heptane. Analytical TLC on silica gel, 1:9 EtOAc/heptane, R_f = 0.2. Pure material was obtained by recrystallization from heptane, mp 99−100 °C. ^1H NMR spectral data are identical to those reported in literature:[37] ^1H NMR (300 MHz, $CDCl_3$, ppm) δ 8.23−8.18 (m, 2H), 7.78−7.72 (m, 1H), 7.59−7.53 (m, 1H), 7.37−7.29 (m, 2H), 7.06−7.01 (m, 2H), 3.90 (s, 3H); $^{13}C\{^1H\}$ NMR (63 MHz, $CDCl_3$, ppm) δ 163.2, 162.3, 150.7, 142.3, 129.4, 124.6, 124.4, 119.7, 119.6, 114.3, 110.4, 55.4; GC-MS (EI) m/z $[M]^+$ found for $C_{14}H_{11}NO_2$ 225.44.

2-(2-(Allyloxy)phenyl)benzo[*d*]oxazole (8f) was obtained as a light orange amorphous solid (33 mg, 46%) according to general procedure D. The crude product was purified by column chromatography on silica gel using gradient elution from 3% EtOAc in hexanes to 10% EtOAc in hexanes. Analytical TLC on silica gel, 1:4 EtOAc/hexanes, R_f = 0.55: ^1H NMR (400 MHz, $CDCl_3$, ppm) δ 8.15 (dd, J = 7.7, 1.8 Hz, 1H), 7.83−7.79 (m, 1H), 7.61−7.57 (m, 1H), 7.48−7.44 (m,1H), 7.40−7.30 (m, 2H), 7.11−7.03 (m, 2H), 6.15−6.06 (m, 1H), 5.64 (dq, J = 17.3, 1.8 Hz, 1H), 5.33 (dq, J = 10.7, 1.6 Hz, 1H), 4.75 (dt, J = 4.7, 1.8 Hz, 2H); $^{13}C\{^1H\}$ NMR (100.6 MHz, $CDCl_3$, ppm) δ 162.1, 157.6, 150.7, 142.1, 132.9, 132.7, 131.6, 125.0, 124.4, 121.1, 120.2, 117.4, 116.9, 113.8, 110.6, 69.7; HRMS (ESI-TOF) m/z $[M + H]^+$ calcd for $C_{16}H_{14}NO_2$ 252.1025; found 252.1029.

2-(2-Allylphenyl)benzo[*d*]oxazole (8g) was obtained as a light yellow oil (28 mg, 40%) according to general procedure D. The crude product was purified by column chromatography on silica gel using isocratic elution with 2% EtOAc in hexanes. Analytical TLC on silica gel, 1:10 EtOAc/hexanes, R_f = 0.58: ^1H NMR (400 MHz, $CDCl_3$, ppm) δ 8.18−8.15 (m, 1H), 7.83−7.79 (m, 1H), 7.62−7.58 (m, 1H), 7.49−7.45 (m, 1H), 7.41−7.35 (m, 4H), 6.14−6.04 (m, 1H), 5.11−5.04 (m, 2H), 4.05 (d, J = 6.6 Hz, 1H); $^{13}C\{^1H\}$ NMR (100.6 MHz, $CDCl_3$, ppm) δ 163.1, 150.5, 142.2, 140.8, 137.3, 131.2, 131.1, 130.4, 126.6, 126.2, 125.2, 124.5, 120.3, 116.0, 110.6, 38.6; HRMS (ESI-TOF) m/z $[M + H]^+$ calcd for $C_{16}H_{14}NO$ 236.1075; found 236.1074.

2-(Pyridin-2-yl)benzo[*d*]oxazole (8h) was obtained as an off-white solid (56 mg, 95%) according to general procedure D. The crude product was purified by column chromatography on silica gel using gradient elution from 0% EtOAc in heptane to 33% EtOAc in heptane. Analytical TLC on silica gel, 1:4 EtOAc/heptane, R_f = 0.15. Pure material was obtained by recrystallization from heptane, mp 100.5−101.5 °C. ^1H NMR spectral data are identical to those reported in the literature:[46] ^1H NMR (300 MHz, $CDCl_3$, ppm) δ 9.41 (br s, 1H), 8.71 (d, J = 4.3 Hz, 1H), 8.54−8.51 (m, 1H), 7.80−7.77 (m, 1H), 7.61−7.56 (m, 1H), 7.48 (dd, J = 7.8, 5.0 Hz, 1H), 7.42−7.35 (m, 2H); $^{13}C\{^1H\}$ NMR (63 MHz, $CDCl_3$, ppm) δ 160.3, 151.2, 150.7, 147.9, 141.5, 135.3, 125.8, 125.0, 123.9, 123.8, 120.3, 110.8; GC-MS (EI) m/z $[M]^+$ found for $C_{12}H_8N_2O$ 196.41.

(*E*)-2-Styrylbenzo[*d*]oxazole (8i) was obtained as a pale yellow solid (52 mg, 78%) according to general procedure D. The crude product was purified by column chromatography on silica gel using gradient elution from 0% EtOAc in heptane to 9% EtOAc in heptane. Analytical TLC on silica gel, 1:9 EtOAc/heptane, R_f = 0.23. Pure material was obtained by recrystallization from heptane, mp 83.5−84.5 °C. ^1H NMR spectral data are identical to those reported in the literature:[47] ^1H NMR (300 MHz, $CDCl_3$, ppm) δ 7.81 (d, J = 16.4 Hz, 1H), 7.76−7.71 (m, 1H), 7.63−7.59 (m, 2H), 7.57−7.51 (m, 1H), 7.47−7.39 (m, 3H), 7.38−7.32 (m, 2H), 7.10 (d, J = 16.4 Hz, 1H); $^{13}C\{^1H\}$ NMR (75 MHz, $CDCl_3$, ppm) δ 162.8, 150.4, 142.2, 139.5, 135.1, 129.8, 129.0, 127.6, 125.2, 124.5, 119.9, 113.9, 110.3; GC-MS (EI) m/z $[M]^+$ found for $C_{15}H_{11}NO$ 221.45.

2-*tert*-Butylbenzo[*d*]oxazole (8j) was obtained as an off-white amorphous solid (52 mg, 74%) according to general procedure E. The crude product was purified by column chromatography on silica gel using gradient elution from 0% EtOAc in heptane to 33% EtOAc in heptane. Analytical TLC on silica gel, 1:9 EtOAc/heptane, R_f = 0.33. ^1H NMR spectral data are identical to those reported in the literature:[39] ^1H NMR (300 MHz, $CDCl_3$, ppm) δ 7.73−7.68 (m, 1H), 7.50−7.46 (m, 1H), 7.32−7.26 (m, 2H), 1.50 (s, 9H); $^{13}C\{^1H\}$ NMR (63 MHz, $CDCl_3$, ppm) δ 173.5, 150.8, 141.2, 124.3, 123.9, 119.7, 110.3, 34.1, 28.4; GC-MS (EI) m/z $[M]^+$ found for $C_{11}H_{13}NO$ 175.32.

6-Methyl-2-phenylbenzo[*d*]oxazole (8k) was obtained as an off-white solid (47 mg, 75%) according to general procedure D. The crude product was purified by column chromatography on silica gel using gradient elution from 0% EtOAc in heptane to 10% EtOAc in heptane. Analytical TLC on silica gel, 1:9 EtOAc/heptane, R_f = 0.35. Pure material was obtained by recrystallization from heptane, mp 92−93 °C. ^1H NMR spectral data are identical to those reported in the literature:[48] ^1H NMR (300 MHz, $CDCl_3$, ppm) δ 8.27−8.23 (m, 2H), 7.65 (d, J = 8.1 Hz, 1H), 7.55−7.50 (m, 3H), 7.39 (dt, J = 1.6, 0.6 Hz, 1H), 7.19−7.16 (m, 1H), 2.52 (s, 3H); $^{13}C\{^1H\}$ NMR (75 MHz, $CDCl_3$, ppm) δ 162.5, 151.0, 139.9, 135.5, 131.2, 128.8, 127.4, 127.3, 125.8, 119.3, 110.7, 21.8; GC-MS (EI) m/z $[M]^+$ found for $C_{14}H_{11}NO$ 209.43.

5-Methyl-2-phenylbenzo[*d*]oxazole (8l) was obtained as an off-white amorphous solid (54 mg, 86%) according to general procedure D. The crude product was purified by column chromatography on silica gel using gradient elution from 0% EtOAc in heptane to 10% EtOAc in heptane. Analytical TLC on silica gel, 1:9 EtOAc/heptane, R_f = 0.36. ^1H NMR spectral data are identical to those reported in the literature:[37] ^1H NMR (300 MHz, $CDCl_3$, ppm) δ 8.29−8.24 (m, 2H), 7.57(dt, J = 1.7, 0.8 Hz, 1H), 7.56−7.51 (m, 3H), 7.48−7.45 (d, J = 7.9 Hz, 1H), 7.19−7.15 (m, 1H), 2.50 (s, 3H); $^{13}C\{^1H\}$ NMR (75 MHz, $CDCl_3$, ppm) δ 163.1, 149.0, 142.3, 134.4, 131.4, 128.9, 127.5, 127.33, 126.2, 119.9, 109.9, 21.5; GC-MS (EI) m/z $[M]^+$ found for $C_{14}H_{11}NO$ 209.44.

6-Nitro-2-phenylbenzo[*d*]oxazole (8m) was obtained as a light yellow amorphous solid (44 mg, 61%) according to general procedure D. The crude product was purified by column chromatography on silica gel using gradient elution from 0% EtOAc in heptane to 33% EtOAc in heptane; analytical TLC on silica gel, 1:9 EtOAc/heptane, R_f = 0.19. ^1H NMR spectral data are identical to those reported in literature:[48] ^1H NMR (300 MHz, $(CD_3)_2O$, ppm) δ 8.62 (dd, J = 2.2, 0.5 Hz, 1H), 8.37 (dd, J = 8.8, 2.2 Hz, 1H), 8.34−8.31 (m, 2H), 7.98 (dd, J = 8.8, 0.5 Hz, 1H), 7.72−7.64 (m, 3H); $^{13}C\{^1H\}$ NMR (63 MHz, $CDCl_3$, ppm) δ 167.4, 149.9, 147.4, 145.1, 132.9, 129.2, 128.3, 126.0, 120.9, 119.8, 107.2; GC-MS (EI) m/z $[M]^+$ found for $C_{13}H_8N_2O$ 240.43.

Methyl 2-(3,5-dichlorophenyl)benzo[*d*]oxazole-6-carboxylate (8n) was obtained as a white solid (87 mg, 90%) according to general procedure D. The crude product was purified by column chromatography on silica gel using gradient elution from 0% EtOAc in heptane to 10% EtOAc in heptane. Analytical TLC on silica gel, 1:9 EtOAc/heptane, R_f = 0.35. Pure material was obtained by recrystallization from heptane, mp 171.5−172.5 °C: IR (film, cm^{-1}) 1725 (C═O); ^1H NMR (250 MHz, $CDCl_3$, ppm) δ 8.27 (dd, J = 1.6, 0.6 Hz, 1H), 8.15 (d, J = 1.9 Hz, 2H), 8.12 (dd, J = 8.4, 1.6 Hz, 1H), 7.80 (dd, J = 8.5, 9.6 Hz, 1H), 7.54 (t, J = 1.9 Hz, 1H), 3.98 (s, 3H); $^{13}C\{^1H\}$ NMR (75 MHz, $CDCl_3$, ppm) δ 166.4, 162.8, 150.5, 145.5, 135.9, 131.9, 129.3, 127.9, 126.7, 126.1, 120.0, 113.5, 52.5; HRMS (ESI-TOF) m/z $[M + H]^+$ calcd for $C_{15}H_{10}Cl_2NO_3$ 322.0037; found 322.0035.

2-(4-Bromophenyl)-5-nitrobenzo[*d*]oxazole (8o) was obtained as a sand-colored solid (62 mg, 69%) according to general procedure D. The crude product was purified by column chromatography on silica gel using gradient elution from 3% EtOAc in hexanes to 10% EtOAc in hexanes. Analytical TLC on silica gel, 1:10 EtOAc/hexanes, R_f = 0.44. Pure material was obtained by recrystallization from hexanes/CH_2Cl_2, mp 176−177 °C. ^1H NMR spectral data are identical to those reported

DOI: 10.1021/acs.joc.7b01686
J. Org. Chem. 2017, 82, 11669−11681

in the literature:[49] ^{1}H NMR (400 MHz, $CDCl_3$, ppm) δ 8.48 (dd, J = 2.2, 0.5 Hz, 1H), 8.32 (dd, J = 8.7, 2.2 Hz, 1H), 8.15−8.12 (m, 2H), 7.84 (dd, J = 8.7, 0.5 Hz, 1H), 7.72−7.69 (m, 2H); $^{13}C\{^1H\}$ NMR (100.6 MHz, $CDCl_3$, ppm) δ 166.6, 150.1, 147.4, 145.4, 132.7, 129.7, 128.0, 125.0, 121.1, 120.1, 107.4; HRMS (ESI-TOF) m/z $[M + H]^+$ calcd for $C_{13}H_8BrN_2O_3$ 318.9718; found 318.9715.

5-Nitro-2-(3,4,5-trimethoxyphenyl)benzo[*d*]oxazole (8p) was obtained as a pale yellow solid (78 mg, 93%) according to general procedure D from (*E*)-4-nitro-2-((3,4,5-trimethoxybenzylidene)-amino)phenol (**7p**) (84 mg, 0.25 mmol). Crude **8p** was purified by column chromatography on silica gel using gradient elution from 9% EtOAc in hexanes to 20% EtOAc in hexanes. Analytical TLC on silica gel, 1:4 EtOAc/hexanes, R_f = 0.28. Pure material was obtained by recrystallization for hexanes/CH_2Cl_2, mp 187−188 °C: IR (film, cm^{-1}) 1498 (NO_2); ^{1}H NMR (400 MHz, $CDCl_3$, ppm) δ 8.62 (d, J = 2.3 Hz, 1H), 8.32 (dd, J = 8.9, 2.4 Hz, 1H), 7.67 (d, J = 8.9 Hz, 1H), 7.51 (s, 2H), 4.00 (s, 6H), 3.96 (s, 3H); $^{13}C\{^1H\}$ NMR (100.6 MHz, $CDCl_3$, ppm) δ 166.0, 154.4, 153.8, 145.6, 142.8, 142.2, 121.2, 121.0, 116.2, 110.7, 105.4, 61.2, 56.6; HRMS (ESI-TOF) m/z $[M + H]^+$ calcd for $C_{16}H_{15}N_2O_6$ 331.0930; found 331.0937.

3-(2-(4-Bromophenyl)benzo[*d*]oxazol-5-yl)propanoic acid (8q) was obtained as an amorphous sand-colored solid (37 mg, 91%) according to general procedure D from (*E*)-3-(3-((4-bromobenzylidene)amino)-4-hydroxyphenyl)propanoic acid (**7q**) (90 mg, 0.1 mmol). Crude **8q** was purified by column chromatography on silica gel using gradient elution from 3% MeOH in CH_2Cl_2 to 15% MeOH in CH_2Cl_2. Analytical TLC on silica gel, 1:40 MeOH/CH_2Cl_2, R_f = 0.26: IR (film, cm^{-1}) 3410 (O−H), 1700 (C═O); ^{1}H NMR (400 MHz, CD_3OD, ppm) δ 8.14−8.11 (m, 2H), 7.77−7.74 (m, 2H), 7.62 (d, J = 1.6 Hz, 1H), 7.58 (d, J = 8.5 Hz,1H), 7.33 (dd, J = 8.4, 1.7 Hz, 1H), 3.07 (t, J = 7.5 Hz, 2H), 2.66 (t, J = 7.6 Hz, 1H); $^{13}C\{^1H\}$ NMR (100.6 MHz, CD_3OD, ppm) δ 163.9, 150.7, 143.0, 139.7, 133.5, 130.1, 127.5, 127.4, 127.2, 120.2, 111.5, 111.4, 32.0, 29.5; HRMS (ESI-TOF) m/z $[M + H]^+$ calcd for $C_{16}H_{13}BrNO_3$ 346.0079; found 346.0087.

1-Oxaspiro[4.5]deca-6,9-diene-2,8-dione (10) was obtained as light yellow amorphous solid (37 mg, 58%) according to general procedure D from 3-(4-hydroxyphenyl)propanoic acid (65 mg, 0.35 mmol). Crude **10** was purified by column chromatography on silica gel using gradient elution from 20% EtOAc in hexanes to 33% EtOAc in hexanes. ^{1}H NMR spectral data are identical to those reported in the literature:[50] ^{1}H NMR (400 MHz, $CDCl_3$, ppm) δ 6.87−6.83 (m, 2H), 6.29−6.25 (m, 2H), 2.77 (t, J = 8.3 Hz, 2H), 2.37 (t, J = 8.3 Hz, 2H); $^{13}C\{^1H\}$ NMR (100.6 MHz, $CDCl_3$, ppm) δ 184.2, 175.2, 145.7, 129.3, 78.5, 32.4, 28.1.

6-Bromo-2-phenyl-2-(trifluoromethyl)-2,3-dihydrobenzo[*d*]-oxazole (15). A mixture of 2-amino-5-bromophenol (950 mg, 5 mmol) and neat trifluoroacetophenone (1.54 mL, 11 mmol, 2 equiv) was stirred at 140 °C for 18 h under argon atmosphere. The dark brown reaction solution was cooled to room temperature, whereupon a dark solid was formed. The crude reaction mixture was dissolved in CH_2Cl_2 and purified by column chromatography on silica gel using isocratic elution with 4% EtOAc in hexanes as a mobile phase. The fractions containing product were combined and concentrated. The residue was repeatedly purified by reverse-phase chromatography using gradient elution from 10% MeCN in water to 100% MeCN to afford **15** as a sand-colored amorphous solid (1.29 g, 68%); analytical TLC on silica gel, 1:10 EtOAc/hexanes, R_f = 0.26: IR (film, cm^{-1}) 3356 (N−H); ^{1}H NMR (400 MHz, $CDCl_3$, ppm) δ 7.68−7.68 (m, 2H), 7.51−7.47 (m, 3H), 7.08 (d, J = 1.8 Hz, 1H), 6.99 (dd, J = 8.1, 1.8 Hz, 1H), 6.70 (d, J = 8.1 Hz, 1H), 4.38 (s, 1H); $^{13}C\{^1H\}$ NMR (100.6 MHz, $CDCl_3$, ppm) δ 151.4, 135.2, 134.7, 130.4, 129.1, 125.8, 125.0, 122.83 (q, J = 287.7 Hz), 114.7, 113.5, 112.5, 98.8 (q, J = 32.6 Hz). ^{19}F NMR (376.3 MHz, $CDCl_3$) δ −83.87; HRMS (ESI-TOF) m/z $[M + H]^+$ calcd for $C_{14}H_{10}BrF_3NO$ 343.9898; found 343.9886.

Benzyl (*E*)-3-(2-Phenyl-2-(trifluoromethyl)-2,3-dihydro-benzo[*d*]oxazol-6-yl)acrylate (16). A vial (5 mL) was flushed with argon and charged with 6-bromo-2-phenyl-2-(trifluoromethyl)-2,3-dihydrobenzo[*d*]oxazole (**15**) (200 mg, 0.58 mg), $Pd(OAc)_2$ (13 mg, 10 mol %), and DMF (0.87 mL). Then, benzyl acrylate (178 μL, 1.16 mmol) was added, followed by triethylamine (122 μL, 0.87 mmol). The vial was sealed, and the dark brown solution was heated at 100 °C for 6 h, whereupon the reaction was cooled to room temperature, diluted with CH_2Cl_2 (20 mL), and washed with water (2 × 20 mL) and brine (20 mL). The organic layer was dried over Na_2SO_4, filtered, and concentrated under reduced pressure. The crude product was purified by column chromatography on silica gel using gradient elution from 20% CH_2Cl_2 in hexanes to 97% CH_2Cl_2 in hexanes. Product **16** was obtained as yellow thick oil (247 mg, 91%); analytical TLC on silica gel, 1:4 EtOAc/hexanes, R_f = 0.39: IR (film, cm^{-1}) 3309 (N−H), 1696 (C═O); ^{1}H NMR (400 MHz, $CDCl_3$, ppm) δ 7.67−7.62 (m, 2H), 7.49−7.45 (m, 3H), 7.43−7.35 (m, 4H), 7.12 (d, J = 1.5 Hz, 1H), 7.00 (dd, J = 7.8, 1.6 Hz, 1H), 6.77 (d, J = 7.9 Hz, 1H), 6.33 (d, J = 15.9 Hz, 1H), 5.25 (s, 2H), 4.81 (s, 1H); $^{13}C\{^1H\}$ NMR (100.6 MHz, $CDCl_3$, ppm) δ 167.2, 150.7, 145.1, 138.3, 136.3, 134.7, 130.3, 129.2, 128.7, 128.34, 128.33, 125.75, 125.73, 125.0, 122.8 (q, J = 288.0 Hz), 115.7, 111.3, 106.6, 98.3 (q, J = 32.4 Hz), 66.4; ^{19}F NMR (376.3 MHz, $CDCl_3$, ppm) δ −83.69; HRMS (ESI-TOF) m/z $[M + H]^+$ calcd for $C_{24}H_{19}F_3NO_3$ 426.1317; found 426.1327.

3-(2-Phenyl-2-(trifluoromethyl)-2,3-dihydrobenzo[*d*]oxazol-6-yl)propanoic acid (11). To a yellow solution of benzyl (*E*)-3-(2-phenyl-2-(trifluoromethyl)-2,3-dihydrobenzo[*d*]oxazol-6-yl)acrylate (**15**) (379 mg, 0.89 mmol) in absolute EtOH (13 mL) was added 10% Pd−C (379 mg, 40 mol %), and H_2 gas was passed through the resulting suspension at room temperature for 2 h. The progress of the hydrogenation was followed by UPLC-MS analysis. Once the reaction was completed, it was filtered through a plug of Celite. The filtrate was concentrated under reduced pressure to obtain the product that was used in the next step without additional purification: ^{1}H NMR (400 MHz, CD_3CN, ppm) δ 7.68−7.65 (m, 2H), 7.52−7.49 (m, 3H), 6.819−6.818 (m 1H), 6.75−6.70 (m, 2H), 5.53 (s, 1H), 2.81 (t, J = 7.6 Hz, 2H), 2.55 (s, J = 7.7 Hz, 2H); $^{13}C\{^1H\}$ NMR (100.6 MHz, CD_3CN, ppm) δ 174.4, 150.9, 136.2, 135.6, 135.4, 131.1, 129.8, 126.87, 126.86, 124.2, (q, J = 287.4 Hz), 122.8, 112.7, 109.3, 99.1 (q, J = 31.9 Hz), 36.0, 31.2; ^{19}F NMR (376.3 MHz, CD_3CN, ppm) δ −84.56; HRMS (ESI-TOF) m/z $[M + H]^+$ calcd for $C_{17}H_{15}F_3NO_3$ 338.1004; found 338.1008.

2-Phenyl-2-(trifluoromethyl)-3′,4′-dihydro-2*H*,5′*H*-spiro[benzo-[*d*]oxazole-6,2′-furan]-5′-one (12) was obtained according to general procedure D from 3-(2-phenyl-2-(trifluoromethyl)-2,3-dihydrobenzo-[*d*]oxazol-6-yl)propanoic acid (**11**). Purification by silica gel column chromatography using gradient elution from 9% EtOAc in hexanes to 33% EtOAc in hexanes afforded **12** as a 1:1 mixture of diastereomers (55 mg of red oil, 55%); analytical TLC on silica gel, 1:4 EtOAc/hexanes, R_f = 0.16. IR (film, cm^{-1}) 1784 (C═O), 1639 (C = N); HRMS (ESI-TOF) m/z $[M + H]^+$ calcd for $C_{17}H_{13}F_3NO_3$ 336.0848; found 336.0848.

Individual pure diastereomers were obtained by preparative HPLC using isocratic elution with 20% EtOAc in hexanes as a mobile phase.

*Diastereomer **12a**:* ^{1}H NMR (400 MHz, $CDCl_3$, ppm) δ 7.74−7.72 (m, 2H), 7.46−7.42 (m, 3H), 6.77 (d, J = 9.9 Hz, 1H), 6.62 (dd, J = 9.9, 2.2 Hz, 1H), 5.54 (d, J = 2.1 Hz, 1H), 2.74 (td, J = 8.3, 1.6 Hz, 2H), 2.34−2.29 (m, 2H); $^{13}C\{^1H\}$ NMR (100.6 MHz, $CDCl_3$, ppm) δ 175.2, 159.7, 153.2, 145.3, 132.6, 130.3, 128.6, 127.6, 122.2 (q, J = 286.1 Hz), 120.4, 111.4 (q, J = 30.9 Hz), 100.7, 83.4, 34.5, 28.5; ^{19}F NMR (376.3 MHz, $CDCl_3$) δ −80.13.

*Diastereomer **12b**:* ^{1}H NMR (400 MHz, $CDCl_3$, ppm) δ 7.73−7.70 (m, 2H), 7.46−7.42 (m, 3H), 6.77 (d, J = 9.8 Hz, 1H), 6.62 (dd, J = 9.8, 2.1 Hz, 1H), 5.54 (d, J = 2.1 Hz, m, 1H), 2.76 (td, J = 8.4, 2.3 Hz, 1H), 2.43−2.39 (m, 2H); $^{13}C\{^1H\}$ NMR (100.6 MHz, $CDCl_3$, ppm) δ 175.2, 159.8, 153.0, 145.4, 133.3, 130.3, 128.6, 127.6, 122.1 (q, J = 286.2 Hz), 120.7, 111.5 (q, J = 31.2 Hz), 100.9, 83.3, 34.4, 28.5; ^{19}F NMR (376.3 MHz, $CDCl_3$) δ −80.23.

Computational Methods. The presented theoretical considerations of the electrochemical cyclization of phenolic imines are predicated on calculations of a model system that comprises one substrate molecule with R^1 = H and R^2 = Ph (**7a**), one model iodine(III) molecule **13** (see also ref 34), and one additional solvent (HFIP) molecule as depicted in Figure 5. The application of the model system shown in Figure 1 serves the dual purpose of retaining a constant number of nuclei and electrons throughout the entire reaction

DOI: 10.1021/acs.joc.7b01686
J. Org. Chem. 2017, 82, 11669−11681

and stabilizing transitory charges by the extra solvent molecule. Moreover, as discussed above, the presence of at least one explicit solvent molecule is required as impetus for critical structural rearrangements. Nevertheless, it should be noted that the benefit of having a constant number of nuclei and electrons comes at the cost of underestimating the translation contributions to the enthalpy and entropy. In reality, each generated molecule, such as the released HFIP from **2**, gives rise to three translational degrees of freedom, whereas in the quantum chemical description of the applied model system, the number of translational degrees of freedom is constantly three. While the effect of this underestimation is small for all reaction steps that leave the number of independent molecules constant, it is more pronounced during the reduction of iodine where the number of molecules in the model is increased by two. In this regard, we just note in passing that the effect will act to stabilize the product side of the reaction.

All quantum chemical calculations presented in this work have been conducted with the ORCA program package in its version 3.0 and employed the TPSS functional.[51] The considerable scalar relativistic effects arising from the presence of iodine are taken into account by the zeroth order regular approximation (ZORA).[52] Accordingly, the scalar relativistically recontracted form of the def2-TZVP basis set was used.[53] Solvent effects that are not covered by the explicitly incorporated solvent molecule are modeled by the conductor-like screening model (COSMO) with a dielectric constant of $\varepsilon = 17.8$.[54] The generation of Coulomb integrals was accelerated by the well-established resolution of identity scheme together with the auxiliary basis set introduced by Weigend in 2006 (def2/J).[55] Dispersion effects were described using the semiempirical pairwise correction scheme by Grimme in its formulation of 2010 with Becke–Johnson damping (D3BJ).[56] Efficient numerical integration was ensured by using a dense integration grid (ORCA Grid 4). Harmonic vibrational frequencies were calculated numerically to verify the nature of the stationary points. Minimum energy points correspond to exclusively positive eigenvalues of the Hessian matrix, whereas transition states feature one negative eigenvalue. Thermochemical contributions were calculated using the ideal gas, rigid rotor, and harmonic oscillator approximations at a temperature of 298.15 K.

■ ASSOCIATED CONTENT

Supporting Information

The Supporting Information is available free of charge on the ACS Publications website at DOI: 10.1021/acs.joc.7b01686.

Photograph of the electrochemical cell, Cartesian coordinates, and NMR spectra (PDF)

■ AUTHOR INFORMATION

Corresponding Authors

*E-mail: michael.roemelt@theochem.ruhr-uni-bochum.de.
*E-mail: edgars@osi.lv.
*E-mail: robert.francke@uni-rostock.de.

ORCID

Edgars Suna: 0000-0002-3078-0576
Robert Francke: 0000-0002-4998-1829

Notes

The authors declare no competing financial interest.

■ ACKNOWLEDGMENTS

The work was in part funded by the German Research Foundation (DFG, Grant No. FR 3848/1-1) and by Latvian Science Council (Grant 274/2012). O.K. thanks INNOVA-BALT project for funding. R.F. is particularly grateful for a Liebig Fellowship (Fonds der Chemischen Industrie). M.R. gratefully acknowledges funding from the Otto-Hahn award program of the Max-Planck society.

■ REFERENCES

(1) (a) Zhdankin, V. V.; Stang, P. J. *Chem. Rev.* **2008**, *108*, 5299–5358. (b) Zhdankin, V. V. *ARKIVOC* **2009**, 1–62. (c) Yoshimura, A.; Zhdankin, V. V. *Chem. Rev.* **2016**, *116*, 3328–3435. (d) Sun, C.-L.; Shi, Z.-J. *Chem. Rev.* **2014**, *114*, 9219–9280.

(2) (a) Singh, F.; Wirth, T. *Synthesis* **2013**, *45*, 2499–2511. (b) Brown, M.; Kumar, R.; Rehbein, J.; Wirth, T. *Chem. - Eur. J.* **2016**, *22*, 4030–4035.

(3) (a) Martínez, C.; Wu, Y.; Weinstein, A. B.; Stahl, S. S.; Liu, G.; Muñiz, K. *J. Org. Chem.* **2013**, *78*, 6309–6315. (b) Liu, G.; Stahl, S. S. *J. Am. Chem. Soc.* **2006**, *128*, 7179–7181.

(4) For selected reviews on I(III)-catalyzed transformations, see: (a) Richardson, R. D.; Wirth, T. *Angew. Chem., Int. Ed.* **2006**, *45*, 4402–4404. (b) Ochiai, M.; Miyamoto, K. *Eur. J. Org. Chem.* **2008**, *2008*, 4229–4239. (c) Dohi, T.; Kita, Y. *Chem. Commun.* **2009**, 2073–2085. (d) Dohi, T. *Chem. Pharm. Bull.* **2010**, *58*, 135–142. (e) Singh, F. V.; Wirth, T. *Chem. - Asian J.* **2014**, *9*, 950–971. (f) Liu, D.; Lei, A. *Chem. - Asian J.* **2015**, *10*, 806–823.

(5) For selected recent examples, see: (a) Dohi, T.; Maruyama, A.; Minamitsuji, Y.; Takenaga, N.; Kita, Y. *Chem. Commun.* **2007**, 1224–1226. (b) Antonchick, A. P.; Samanta, R.; Kulikov, K.; Lategahn, J. *Angew. Chem., Int. Ed.* **2011**, *50*, 8605–8608. (c) Morimoto, K.; Sakamoto, K.; Ohshika, T.; Dohi, T.; Kita, Y. *Angew. Chem., Int. Ed.* **2016**, *55*, 3652–3656. (d) Reitti, M.; Villo, P.; Olofsson, B. *Angew. Chem., Int. Ed.* **2016**, *55*, 8928–8932. (e) Muñiz, K.; Barreiro, L.; Romero, R. M.; Martínez, C. *J. Am. Chem. Soc.* **2017**, *139*, 4354–4357.

(6) For a review on indirect electrosynthesis, see: (a) Francke, R.; Little, R. D. *Chem. Soc. Rev.* **2014**, *43*, 2492–2521. For recent outstanding applications of redox mediators in electrosynthesis, see: (b) Qian, X.-Y.; Li, S.-Q.; Song, J.; Xu, H.-C. *ACS Catal.* **2017**, *7*, 2730–2734. (c) Hou, Z.-W.; Mao, Z.-Y.; Zhao, H.-B.; Melcamu, Y. Y.; Lu, X.; Song, J.; Xu, H.-C. *Angew. Chem., Int. Ed.* **2016**, *55*, 9168–9172. (d) Röse, P.; Emge, S.; König, C. A.; Hilt, G. *Adv. Synth. Catal.* **2017**, *359*, 1359–1372. (e) Jiang, Y.-Y.; Wang, Q.-Q.; Liang, S.; Hu, L.-M.; Little, R. D.; Zeng, C.-C. *J. Org. Chem.* **2016**, *81*, 4713–4719. (f) Kang, L.-S.; Luo, M.-H.; Lam, C. M.; Hu, L.; Little, R. D.; Zeng, C.-C. *Green Chem.* **2016**, *18*, 3767–3774. (g) Qian, P.; Su, J.-H.; Wang, Y.; Bi, M.; Zha, Z.; Wang, Z. *J. Org. Chem.* **2017**, *82*, 6434–6440. (h) Li, Y.; Gao, H.; Zhang, Z.; Qian, P.; Bi, M.; Zha, Z.; Wang, Z. *Chem. Commun.* **2016**, *52*, 8600–8603.

(7) For selected synthetic applications of electrogenerated I(III) reagents, see: (a) Fuchigami, T.; Fujita, T. *J. Org. Chem.* **1994**, *59*, 7190–7192. (b) Fujita, T.; Fuchigami, T. *Tetrahedron Lett.* **1996**, *37*, 4725–4728. (c) Inoue, K.; Ishikawa, Y.; Nishiyama, S. *Org. Lett.* **2010**, *12*, 436–439. (d) Kajiyama, D.; Inoue, K.; Ishikawa, Y.; Nishiyama, S. *Tetrahedron* **2010**, *66*, 9779–9784. Watts, K.; Gattrell, W.; Wirth, T. *Beilstein J. Org. Chem.* **2011**, *7*, 1108–1114.

(8) Sawamura, T.; Kuribayashi, S.; Inagi, S.; Fuchigami, T. *Org. Lett.* **2010**, *12*, 644–646.

(9) Sawamura, T.; Kuribayashi, S.; Inagi, S.; Fuchigami, T. *Adv. Synth. Catal.* **2010**, *352*, 2757–2760.

(10) Broese, T.; Francke, R. *Org. Lett.* **2016**, *18*, 5896–5899.

(11) Francke, R. *Beilstein J. Org. Chem.* **2014**, *10*, 2858–2873.

(12) (a) Ovenden, S. P. B.; Nielson, J. L.; Liptrot, C. H.; Willis, R. H.; Tapiolas, D. M.; Wright, A. D.; Motti, C. A. *J. Nat. Prod.* **2011**, *74*, 65–68. (b) Yang, M.; Yang, X.; Sun, H.; Li, A. *Angew. Chem., Int. Ed.* **2016**, *55*, 2851–2855.

(13) Demmer, C. S.; Bunch, L. *Eur. J. Med. Chem.* **2015**, *97*, 778–785.

(14) (a) Rajasekhar, S.; Maiti, B.; Chanda, K. *Synlett* **2017**, *28*, 521–541. (b) Yu, C.; Guo, X.; Xi, Z.; Muzzio, M.; Yin, Z.; Shen, B.; Li, J.; Seto, C. T.; Sun, S. *J. Am. Chem. Soc.* **2017**, *139*, 5712–5715. (c) Nguyen, T. B.; Retailleau, P. *Org. Lett.* **2017**, *19*, 3887–3890.

(15) Gieshoff, T.; Kehl, A.; Schollmeyer, D.; Moeller, K. D.; Waldvogel, S. R. *Chem. Commun.* **2017**, *53*, 2974–2977.

(16) Morofuji, T.; Shimizu, A.; Yoshida, J. *Chem. - Eur. J.* **2015**, *21*, 3211–3214.

(17) (a) Shih, Y.; Ke, C.; Pan, C.; Huang, Y. *RSC Adv.* **2013**, *3*, 7330–7336. (b) There is a single example for electrochemical synthesis of benzoxazole (40% yield) from benzylic alcohol and *ortho*-aminophenol

DOI: 10.1021/acs.joc.7b01686
J. Org. Chem. 2017, 82, 11669–11681

in the presence of Co(II) salts: Lai, Y.-L.; Ye, J.-S.; Huang, J.-M. *Chem. - Eur. J.* **2016**, *22*, 5425−5429.
(18) Kang, L.-S.; Xiao, H.; Zeng, C.-C.; Hu, L.-M.; Little, R. D. *J. Electroanal. Chem.* **2016**, *767*, 13−17.
(19) Li, W.-C.; Zeng, C.-C.; Hu, L.-M.; Tian, H.-Y.; Little, R. D. *Adv. Synth. Catal.* **2013**, *355*, 2884−2890.
(20) Stoichiometric amounts of I(III) reagents have been employed for the oxidative cyclization of *ortho*-iminophenols to benzoxazoles: (a) Varma, R. S.; Saini, R. K.; Prakash, O. *Tetrahedron Lett.* **1997**, *38*, 2621−2622. (b) Zhang, J.-Z.; Zhu, Q.; Huang, X. *Synth. Commun.* **2002**, *32*, 2175−2179. (c) Naganaboina, R. T.; Peddinti, R. K. *Tetrahedron* **2015**, *71*, 6245−6253.
(21) (a) Tohma, H.; Takizawa, S.; Maegawa, T.; Kita, Y. *Angew. Chem., Int. Ed.* **2000**, *39*, 1306−1308. (b) Tohma, H.; Maegawa, T.; Takizawa, S.; Kita, Y. *Adv. Synth. Catal.* **2002**, *344*, 328−337. (c) Dohi, T.; Maruyama, A.; Yoshimura, M.; Morimoto, K.; Tohma, H.; Shiro, M.; Kita, Y. *Chem. Commun.* **2005**, 2205−2207.
(22) The published oxidation of *sec*-alcohols to ketones by I(III) reagents required the use of KBr as an additive. See ref 21.
(23) Ochiai, M. Reactivities, Properties and Structures. Modern Developments in Organic Synthesis. In *Topics in Current Chemistry*; Wirth, T., Ed.; Springer: Berlin, 2003; Vol. *224*, pp 5−68.
(24) Intermolecular β-elimination is a less likely mechanistic scenario as it requires dissociation of highly basic HFIP-derived alkoxide from the tetracoordinated iodate **6**.
(25) Attempts to prepare **2** using various oxidizing agents were not successful. Thus, treatment of **1** with excess sodium peroxysulfate or excess H_2O_2 (30% aqueous solution) in HFIP did not lead to any conversion, whereas the use of MCPBA (2 equiv) afforded **2** together with substantial amounts of an unidentified side product.
(26) As both species are oxidized irreversibly, peak potentials E_p are reported instead of the equilibrium potentials E_0.
(27) (a) Nitro-substituted imines were not suitable as substrates in DDQ and NaI-mediated electrocyclizations. See refs 18 and 19. (b) Preliminary experiments evidence that the electrochemically generated I(III) reagent **2** is also suitable for the cyclization of 2-(benzylideneamino)thiophenols to benzothiazoles.
(28) Said, G.; Grippon, S.; Kirkpatrick, P. *Nat. Rev. Drug Discovery* **2012**, *11*, 185−186.
(29) (a) Dohi, T.; Yamaoka, N.; Kita, Y. *Tetrahedron* **2010**, *66*, 5775−5785. (b) Dohi, T.; Ito, M.; Yamaoka, N.; Morimoto, K.; Fujioka, H.; Kita, Y. *Angew. Chem., Int. Ed.* **2010**, *49*, 3334−3337.
(30) Sokolovs, I.; Lubriks, D.; Suna, E. *J. Am. Chem. Soc.* **2014**, *136*, 6920−6928.
(31) Franz, J. A.; Barrows, R. D.; Camaioni, D. M. *J. Am. Chem. Soc.* **1984**, *106*, 3964−3967.
(32) Dohi, T.; Uchiyama, T.; Yamashita, D.; Washimi, N.; Kita, Y. *Tetrahedron Lett.* **2011**, *52*, 2212−2215.
(33) The formation of **V** is also possible directly from imine **7a-A** and **2** without involvement of cyclic tautomer **7a-B**. Accordingly, an interaction of Lewis basic imine nitrogen in **7a-A** with Lewis acidic I(III) center facilitates cyclization to **V** with concomitant formation of HFIP (see ref 20a).
(34) It was assumed that the presence of an ammonium group and its ClO_4^- counterion in the aliphatic chain of the mediator **2** have no influence on the cyclization reaction. Therefore, the charged moiety has been omitted in the model to reduce the computational costs (see structure **13**, Figure 5).
(35) Of course, the applied computational model is unfit to yield any reasonable estimates of the rates at which such a movement occurs or its associated barriers. An adequate description of this event would require a full molecular dynamics simulation that explicitly includes many shells of solvent molecules. Such a molecular dynamics simulation is out of scope of this work and from our perspective not worthwhile regarding the limited relevance of this step for the overall reaction mechanism. We believe it is safe to assume that, at room temperature, the anion itself or at least its negative charge is sufficiently mobile in the HFIP solution to readily undergo the required motion at sufficiently high rates.
(36) Zhao, X.-F.; Zhang, C. *Synthesis* **2007**, *2007*, 551−557.
(37) Wang, L.; Ma, Z.-G.; Wei, X.-J.; Meng, Q.-Y.; Yang, D.-T; Du, S.-F.; Chen, Z.-F.; Wu, L.-Z.; Liu, Q. *Green Chem.* **2014**, *16*, 3752−3757.
(38) Chen, C.-L.; Liu, Y.-H.; Peng, S.-M.; Liu, S.-T. *J. Organomet. Chem.* **2004**, *689*, 1806−1815.
(39) Cho, Y. H.; Lee, C.-Y.; Ha, D.-C.; Cheon, C.-H. *Adv. Synth. Catal.* **2012**, *354*, 2992−2996.
(40) Mas-Montoya, M.; Usea, L.; Espinosa Ferao, A.; Montenegro, M. F.; Ramírez de Arellano, C.; Tarraga, A.; Rodríguez-Lopez, J. N.; Curiel, D. *J. Org. Chem.* **2016**, *81*, 3296−3302.
(41) Bae, S. J.; Ha, Y. M.; Park, Y. J.; Park, J. Y.; Song, Y. M.; Ha, T. K.; Chun, P.; Moon, H. R.; Chung, H. Y. *Eur. J. Med. Chem.* **2012**, *57*, 383−390.
(42) Peacock, L. R.; Chapman, R. S. L.; Sedgwick, A. C.; Mahon, M. F.; Amans, D.; Bull, S. D. *Org. Lett.* **2015**, *17*, 994−997.
(43) Park, H. J.; Park, M. S.; Lee, T. H.; Park, K. H. *J. Heterocycl. Chem.* **2013**, *50*, 663−667.
(44) Cho, Y.-H.; Lee, C.-Y.; Cheon, C.-H. *Tetrahedron* **2013**, *69*, 6565−6573.
(45) Yang, K.; Wang, P.; Zhang, C.; Kadi, A. A.; Fun, H.-K.; Zhang, Y.; Lu, H. *Eur. J. Org. Chem.* **2014**, *2014*, 7586−7589.
(46) Zhu, F.; Wang, Z.-X. *Org. Lett.* **2015**, *17*, 1601−1604.
(47) Meng, L.; Kamada, Y.; Muto, K.; Yamaguchi, J.; Itami, K. *Angew. Chem., Int. Ed.* **2013**, *52*, 10048−10051.
(48) Liu, S.; Chen, R.; Guo, X.; Yang, H.; Deng, G.; Li, C.-J. *Green Chem.* **2012**, *14*, 1577−1580.
(49) Tan, H.; Pan, C.-X; Xu, Y.-L.; Wang, H.-S.; Pan, Y.-M. *J. Chem. Res.* **2012**, *36*, 370−373.
(50) Ohkata, K.; Tamura, Y.; Shetuni, B. B.; Takagi, R.; Miyanaga, W.; Kojima, S.; Paquette, L. A. *J. Am. Chem. Soc.* **2004**, *126*, 16783−16792.
(51) (a) Neese, F. *WIREs Comput. Mol. Sci.* **2012**, *2*, 73−78. (b) Tao, J.; Perdew, J. P.; Staroverov, V. N.; Scuseria, G. E. *Phys. Rev. Lett.* **2003**, *91*, 146401.
(52) (a) Lenthe, E. v.; Baerends, E. J.; Snijders, J. G. *J. Chem. Phys.* **1993**, *99*, 4597−4610. (b) van Wüllen, C. *J. Chem. Phys.* **1998**, *109*, 392−399.
(53) (a) Weigend, F.; Ahlrichs, R. *Phys. Chem. Chem. Phys.* **2005**, *7*, 3297−3305. (b) Pantazis, D.; Chen, X.; Landis, C.; Neese, F. *J. Chem. Theory Comput.* **2008**, *4*, 908−919.
(54) (a) Klamt, A.; Schüürmann, G. *J. Chem. Soc., Perkin Trans. 2* **1993**, *2*, 799−805. (b) Hong, D.-P.; Hoshino, M.; Kuboi, R.; Goto, Y. *J. Am. Chem. Soc.* **1999**, *121*, 8427−8433.
(55) (a) Whitten, J. L. *J. Chem. Phys.* **1973**, *58*, 4496−4501. (b) Dunlap, B. I.; Connolly, J. W. D.; Sabin, J. R. *J. Chem. Phys.* **1979**, *71*, 3396−3402. (c) Vahtras, O.; Almlöf, J.; Feyereisen, M. W. *Chem. Phys. Lett.* **1993**, *213*, 514−518. (d) Neese, F. *J. Comput. Chem.* **2003**, *24*, 1740−1747. (e) Weigend, F. *Phys. Chem. Chem. Phys.* **2006**, *8*, 1057−1065.
(56) (a) Grimme, S.; Antony, J.; Ehrlich, S.; Krieg, H. *J. Chem. Phys.* **2010**, *132*, 154104−1−154104−19. (b) Grimme, S.; Ehrlich, S.; Goerigk, L. *J. Comput. Chem.* **2011**, *32*, 1456−1465.

DOI: 10.1021/acs.joc.7b01686
J. Org. Chem. 2017, 82, 11669−11681

Appendix II – "Electrochemical Synthesis of Unnatural Amino Acids via Anodic Decarboxylation of *N*-Acetylamino Malonic Acid Derivatives"

Koleda, O.; Prane, K.; Suna, E.

Org. Lett. **2023**, *25*, 7958–7962. https://doi.org/10.1021/acs.orglett.3c02687.

OL | Organic Letters

pubs.acs.org/OrgLett

Letter

Electrochemical Synthesis of Unnatural Amino Acids via Anodic Decarboxylation of *N*-Acetylamino Malonic Acid Derivatives

Olesja Koleda, Katrina Prane, and Edgars Suna*

Cite This: https://doi.org/10.1021/acs.orglett.3c02687

Read Online

ACCESS | Metrics & More | Article Recommendations | Supporting Information

ABSTRACT: Broad application of α,α-disubstituted cyclic amino acid derivatives in medicinal chemistry urges for analogue design with improved pharmacokinetic properties. Herein, we disclose an electrochemical approach toward unnatural THF- and THP-containing amino acid derivatives that relies on anodic decarboxylation-intramolecular etherification of inexpensive and readily available *N*-acetylamino malonic acid monoesters under Hofer–Moest reaction conditions. The decarboxylative cyclization proceeds under constant current conditions in an undivided cell in an aqueous medium without any added base. A successful bioisosteric replacement of the 1-aminocyclohexane-1-carboxylic acid subunit by the THP-containing amino acid scaffold in cathepsin K inhibitor balicatib helped to reduce lipophilicity while retaining low nanomolar enzyme inhibitory potency and comparable microsomal stability.

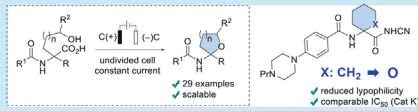

Unnatural (non-proteinogenic) amino acids (AAs) are widely employed structural fragments in the design of small molecule drugs and peptidomimetics.[1] Among them, α,α-disubstituted cyclic AAs have been incorporated into clinically used anesthetics carfentanil **1** and remifentanil **2**, anticancer drug candidate AZD5363 (**3**),[2] FDA-approved antipruritic medication difelikefalin **4** and antipruritic drug candidate **5**,[3] development candidate balicatib **6**,[4] and cathepsin C inhibitor **7** for treatment of COPD[5] (Figure 1A). α,α-Disubstituted cyclic AAs are also commonly used to introduce constraints into a peptide backbone and improve stability, permeability, and bioavailability of peptidomimetics.[6] Wide application and valuable properties of α,α-disubstituted cyclic AAs justify the design of new congeners and also urge the development of efficient synthetic methods to access these medicinally relevant structural fragments. Herein we disclose an electrochemical synthesis of previously unreported THP- and THF-containing AA derivatives[7] (Figure 1A) and demonstrate their bioisosteric relationship with the corresponding α,α-disubstituted carbocyclic AAs.

We envisioned that both THP-AA and THF-AA could be accessed from readily available *N*-acetylamino malonic acid monoester by electrochemical decarboxylation/oxidation to a transient *N*-acyliminium intermediate, followed by etherification with a tethered *O*-nucleophile (Figure 1B, eq 3). The electrochemical oxidative decarboxylation under Hofer–Moest (HM) conditions[8] has recently become increasingly popular to generate transient *N*-acetyliminium[9] and oxocarbenium[10] species as well as stabilized benzylic and tertiary carbocations[11] for inter- and intramolecular C–O bond formation. A wide variety of α-amino, α-alkoxyoxy, α-aryloxy, and tertiary carboxylic acids have found application in the HM reaction. However, only a handful of reports exist on electrochemical decarboxylation of malonic acid derivatives (Figure 1B). Thus, Markò and Ma et al. disclosed electrochemical oxidative decarboxylation of disubstituted malonic acids under constant current electrolysis in methanol as a solvent to furnish dimethyl ketals (Figure 1B, eq 1).[12] Anodic decarboxylation of *N*-acylamino malonic acid monoesters in alcoholic solvents to afford α-alkoxy α-amino acid derivatives was also reported by Iwasaki and Matsumoto et al. in the late 1970s (eq 2).[13] The above-mentioned electrolyses proceeded in alcoholic media and required the addition of an external base. We realized that the anodic decarboxylation of *N*-acetylamino malonates does not require the added base if performed in aqueous media because paired cathodic reduction of water would generate hydroxide anions. Combined with low costs of malonic acid derivatives and rich malonate functionalization chemistry, the developed decarboxylation approach features operational simplicity and high cost efficiency.

N-Acetylamino malonate **8a** was selected as a model substrate for the development of intramolecular etherification under HM conditions. The acid **8a** was easily prepared in two steps from commercially available diethyl 2-acetamidomalonate by an alkylation/hydrolysis sequence (see the Supporting Information). The selection of starting conditions for the anodic decarboxylation of **8a** was based on a literature survey. Accordingly, graphite is the most frequently employed anode material for HM reaction,[14] whereas Pt is routinely used as a

Received: August 21, 2023

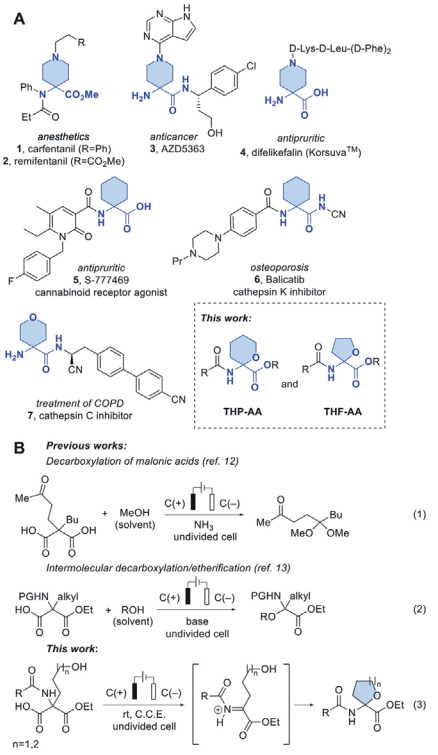

Figure 1. (A) α,α-Disubstituted unnatural AA in drug design. (B) Electrochemical decarboxylation of malonic acid derivatives.

cathode to favor proton reduction.[9b,13a] HM reaction also benefits from low current densities and polar aprotic solvents.[14b] Hence, the initial electrolysis of **8a** was carried out in an undivided cell under constant current conditions (j = 10 mA/cm^2) in aqueous MeCN and without any added base or supporting electrolyte. Pleasingly, the desired **9a** was formed in 44% yield after passing 1.3 F charge (Table 1, entry 1). Unfortunately, incomplete conversion of **8a** was observed, and the decarboxylation stalled because of low conductivity (>30 V cell potential was reached during the electrolysis). The addition of Li_2CO_3 (0.5 equiv with respect to **8a**) as a supporting electrolyte helped to improve conductivity and increased the yield of **9a** to 55% (entry 2). Further increase in the yield of **9a** to 62% was accomplished by replacement of Pt for considerably less expensive Ni as a cathode material (entry 3). Screening of various salts (entries 4–9) helped to identify NaOAc, $LiClO_4$, and NaTFA as the preferred supporting electrolytes for the decarboxylative cyclization (74–77% yield of **9a**; entries 4, 6, and 9, respectively). Comparable efficiency of a non-basic $LiClO_4$ and a relatively basic NaOAc as supporting electrolytes indicated that the anodic decarboxylation does not require an external base. A brief survey of anode materials using NaOAc as the supporting electrolyte

Table 1. Optimization of Decarboxylative Etherification

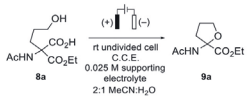

Entry	Cathode	Supporting electrolyte[a]	j, mA/cm^2	Yield, %[b]
1[c]	Pt		10	44
2[d]	Pt	Li_2CO_3	10	55
3[d]	Ni	Li_2CO_3	10	62
4[e]	Ni	NaOAc	10	74[g]
5[e]	Ni	LiOAc	10	69
6[f]	Ni	NaTFA	10	74
7[d]	Ni	NaO*t*Bu	10	60
8[e]	Ni	NH_4OAc	10	69
9[e]	Ni	$LiClO_4$	10	77
10[e]	C	$LiClO_4$	10	83
11[e]	**C**	**$LiClO_4$**	**12**	**82 (80)**[h]

[a]0.5 equiv with respect to **8a**. [b]Yields were determined by ^{1}H NMR post-electrolysis using CH_2Br_2 as an internal standard. Performed on a 0.15 mmol scale. [c]1.3 F. [d]4 F. [e]3 F. [f]2 F. [g]Average yield of two runs. [h]Isolated yield in parentheses.

confirmed the superiority of graphite over glassy carbon (GC), reticulated vitreous carbon (RVC), and boron-doped diamond (BDD; see the Supporting Information). However, **9a** was formed in higher yield when graphite was used instead of Ni as the cathode material with both NaOAc (see the Supporting Information) and $LiClO_4$ as the supporting electrolytes (83%, entry 10). Hence, graphite was chosen as both anode and cathode material, and $LiClO_4$ was selected as the non-basic and non-nucleophilic supporting electrolyte for all subsequent experiments. Current density increase from to 12 mA/cm^2 did not affect the yield of **9a** (82%, entry 13); however, larger deviations lead to inferior results (see the Supporting Information, page S3).

With the optimized conditions in hand (entry 11, Table 1), the scope of the developed method was investigated (Figure 2). *N*-Acetyl, *N*-Cbz, and *N*-Boc protected aminotetrahydrofuran-2-carboxylates **9a–c** were readily obtained in 51–80% yield. The decarboxylative anodic oxidation is compatible with relatively easy-to-oxidize 3-furanoyl and 4-anisoyl substituents (heterocycles **9e**, **9k**) as well as with the presence of cyano, mesyl, and trifluoromethyl groups in the aryl moiety of cyclic ethers **9j,h,l** (Figure 2A).

Noteworthy is the compatibility with bromo substituent that allows for further transformations of **9i,o**, e.g., in Buchwald–Hartwig amination as shown below. The electrochemical decarboxylation of pyridine-containing substrate **8f** was slow and afforded the desired **9f** in only 7% yield together with multiple side-products. Six-membered heterocycles **9m–o** (Figure 2B) are also accessible under the developed conditions albeit in slightly lower yields (56–64%) as compared to the corresponding 5-membered analogues **9a,b,i** (68–80%). The reduced yield of tetrahydropyranes **9m–o** can be possibly attributed to the slower formation of a 6-membered ring[15] from *N*-acyl iminium intermediates and the competing formation of an open-chain hemiaminal in the reaction with water. Indeed, hemiaminal **10** was the major product in the attempted decarboxylative cyclization of **8z** (Figure 2E) that afforded only trace amounts of the desired 7-membered

https://doi.org/10.1021/acs.orglett.3c02687
Org. Lett. XXXX, XXX, XXX–XXX

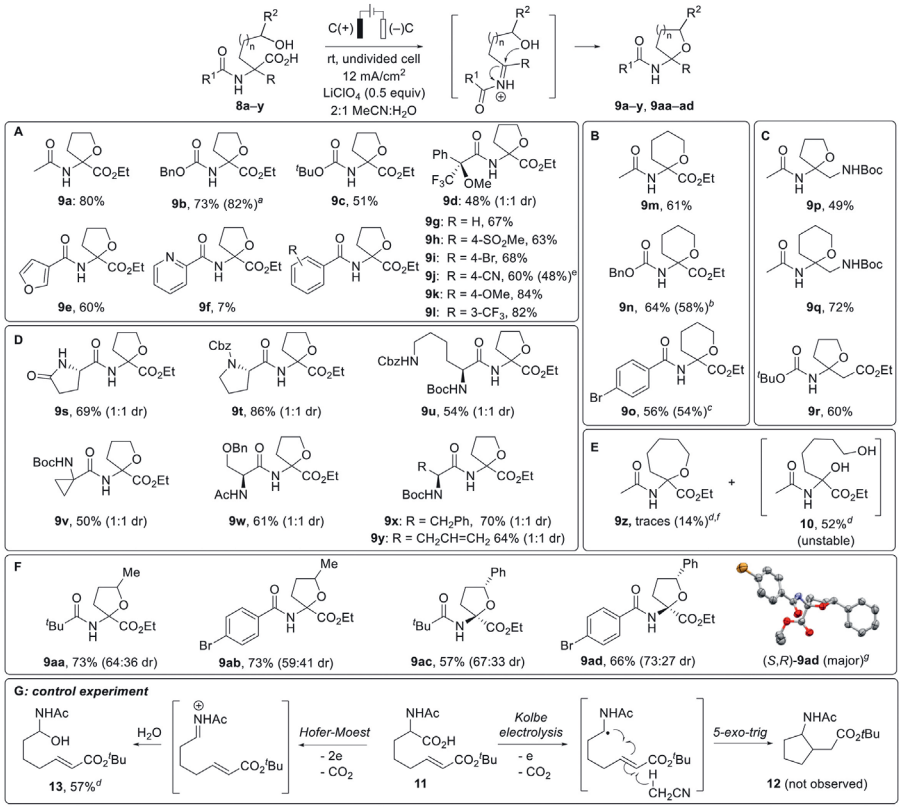

Figure 2. Scope of the decarboxylation/cyclization reaction. [a]Performed at the 1.17 g scale. [b]At 1.00 g scale. [c]At 2.0 g scale. [d]NMR yield. [e]Obtained according to the procedure from ref 11b. [f]Obtained according to the procedure from ref 11a. [g]Ellipsoids are shown at 50% probability, with hydrogen atoms omitted for clarity.

heterocycle **9z** as evidenced by LC-MS assay of the crude reaction mixture.

The developed anodic decarboxylation/cyclization is applicable also to AA derivatives such as protected 2,3-diamino propionic acid derivatives **8p,q** and aspartic acid ester **8r** (Figure 2C). Wide application of unnatural AA in the design of peptidomimetics prompted us to examine the suitability of the developed conditions for dipeptide synthesis. Gratifyingly, cyclization of AA-containing substrates **8s−y** afforded dipeptides **9s−y** in 50−86% yield (Figure 2D). Notably, the decarboxylative cyclization is compatible with the alkene moiety and cyclopropyl subunit (**9y** and **9v**, respectively). All dipeptides **9s−y** were obtained as a 1:1 mixture of diastereomers, and the absence of diastereoselectivity in the cyclization was also observed for Mosher amide **9d**.[16] In contrast, moderate diastereoselectivity could be achieved in the cyclization of chiral secondary alcohols (Figure 2F) with the highest 73:27 dr observed for the formation of **9ad** from the parent (*R*)-benzyl alcohol. Configuration of the quaternary stereogenic center in the major diastereomer (*S*,*R*)-**9ad** was established by X-ray crystallography. Finally, to demonstrate the synthetic utility and scalability of the developed method, the synthesis of five-membered heterocycle **9b** was successfully scaled up from 0.9 to 3.5 mmol to afford 0.83 g of the heterocycle in a single electrolysis batch. An upscale from 0.9 to 2.8 mmol was also successful for six-membered products **9n,o**.

A brief mechanistic study was performed to gain experimental evidence for the two-electron anodic oxidation to *N*-acyliminium ion (HM reaction) vs one-electron oxidation (Kolbe electrolysis) as a mechanistic scenario for the developed cyclization. Accordingly, cyclic voltammetry (CV) studies for acid **8a** showed a single irreversible feature at a scan rate of 100 mV/s (E_p = 1.77 V vs Ag/Ag$^+$) that corresponds to carboxylate oxidation (for details, see p S69 of the Supporting Information). Notably, **8a** exhibited two anodic peaks at a higher scan rate (600 mV/s) suggesting the formation of an unstable intermediate after the first irreversible oxidation step

https://doi.org/10.1021/acs.orglett.3c02687
Org. Lett. XXXX, XXX, XXX−XXX

(E_{P1} = 1.98 V vs Ag/Ag^+) that undergoes chemical transformation followed by a second oxidation step (E_{P1} = 2.24 V vs Ag/Ag^+). Hence, CV data point to the ECE pathway for the decarboxylative cyclization that involves anodic oxidation of **8a**, followed by decarboxylation and the second oxidation of the carbon-centered radical to *N*-acyliminium ion, a scenario that is characteristic for the HM reaction.

Additional evidence favoring the ionic pathway for the cyclization was obtained by exposing unsaturated acid **11** to the developed anodic decarboxylation conditions. 5-Hexenyl acids that are structurally closely related to **11** have been reported to undergo facile radical 5-exo-trig cyclization under Kolbe electrolysis conditions.[17] Radical 5-exo-trig cyclizations proceed with extremely high rate constants (e.g., 1.6×10^8 s^{-1} for 6-cyano-5-hexenyl radical),[18] and therefore, they have found applications as radical clock reactions. Notably, the formation of 5-exo-trig cyclization product **12** from **11** was not observed (Figure 2G). Instead, unstable hemiaminal **13** was formed as the major product (57% NMR yield) together with unreacted **11** (18%). Taken together, a mechanistic study provides strong evidence for the two-electron anodic decarboxylation to the *N*-acyliminium ion as the most plausible mechanism for the electrosynthesis of AA derivatives **9a–y,aa–ad**.

Next, we briefly explored the reactivity of the THF- and THP-AA derivatives. THF-AA is stable under basic conditions as evidenced by aqueous LiOH hydrolysis of ester **9b** to acid **14** in 78% yield (Figure 3A).[19] An additional proof of the

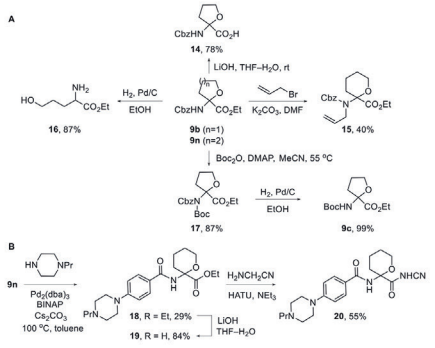

Figure 3. Synthetic modifications of THF-AA and THP-AA.

THF-AA stability under basic conditions was obtained by successful *N*-alkylation of ester **9n** to afford amide **15** (40%). Pd-catalyzed hydrogenolysis of *N*-Cbz in **9b** afforded ring-opening product **16** (87%), suggesting the instability of *N*-unprotected hemiaminal that obviously undergoes the reduction of the open chain imine tautomer. In the meantime, *N*-Cbz protection can be swapped for *N*-Boc in a two-step sequence comprising *N*-acylation of carbamate **9b** with Boc_2O and catalytic DMAP, followed by Pd-catalyzed hydrogenolysis (86% over two steps; Figure 3A).

Finally, THP-AA derivative **20** was synthesized to examine its bioisosteric relationship with balicatib **6** (Figure 3B). Thus, Pd-catalyzed amination of **9n** with piperazine followed by ester hydrolysis and amide bond formation furnished **20**. As anticipated, the THP-AA derivative **20** features reduced lipophilicity (Log *P* = 0.95) as compared to that of balicatib **6** (Log *P* = 1.60), while possessing similar enzymatic activity (0.34 nM vs 0.46 nM, respectively) as well as comparable metabolic stability and plasma protein binding (see the Supporting Information, Table S3, page S76). Hence, THF- and THP-containing AA are suitable as bioisosters of the corresponding α,α-disubstituted carbocyclic AA, offering a reduction in lipophilicity (Log *P*).

In summary, electrochemical decarboxylation-intramolecular etherification of inexpensive and readily accessible *N*-acetyl malonic acid monoesters under HM conditions provides a route to previously unreported THP- and THF-containing AA derivatives. The decarboxylative cyclization under constant current conditions in an undivided cell proceeds in aqueous media without any added base. When incorporated into dipeptides and peptidomimetics, THP- and THF-containing AAs may serve as bioisosters of α,α-disubstituted cyclic AAs. A successful bioisosteric replacement of the 1-aminocyclohexane-1-carboxamide subunit in balicatib by a THP-AA moiety was demonstrated, allowing for the reduction of lipophilicity (Log *P*), while retaining low nanomolar cathepsin K inhibitory potency and comparable microsomal stability to that of balicatib. Given the broad use of α,α-disubstituted cyclic AA in organic and medicinal chemistry, we believe that oxygen-containing unnatural AA scaffolds described in this work have great potential for application in drug discovery campaigns.

■ ASSOCIATED CONTENT

Data Availability Statement

The data underlying this study are available in the published article and its Supporting Information

Supporting Information

The Supporting Information is available free of charge at https://pubs.acs.org/doi/10.1021/acs.orglett.3c02687.

Experimental procedures, analytical and spectroscopic data for new compounds, and copies of NMR spectra (PDF)

Accession Codes

CCDC 2287549–2287550 contain the supplementary crystallographic data for this paper. These data can be obtained free of charge via www.ccdc.cam.ac.uk/data_request/cif, or by emailing data_request@ccdc.cam.ac.uk, or by contacting The Cambridge Crystallographic Data Centre, 12 Union Road, Cambridge CB2 1EZ, UK; fax: +44 1223 336033.

■ AUTHOR INFORMATION

Corresponding Author

Edgars Suna – *Latvian Institute of Organic Synthesis, LV-1006 Riga, Latvia; University of Latvia, Department of Chemistry, LV-1004 Riga, Latvia;* orcid.org/0000-0002-3078-0576; Email: edgars@osi.lv

Authors

Olesja Koleda – *Latvian Institute of Organic Synthesis, LV-1006 Riga, Latvia; University of Latvia, Department of Chemistry, LV-1004 Riga, Latvia*

Katrina Prane – *Latvian Institute of Organic Synthesis, LV-1006 Riga, Latvia*

Complete contact information is available at:

https://doi.org/10.1021/acs.orglett.3c02687
Org. Lett. XXXX, XXX, XXX–XXX

https://pubs.acs.org/10.1021/acs.orglett.3c02687

Notes

The authors declare no competing financial interest.

■ ACKNOWLEDGMENTS

The authors thank Dr. S. Belyakov for X-ray crystallographic analysis, Dr. I. Kanepe for inhibitory potency measurements, Dr. H. Kazoka for Log*P* determination, and B. Gukalova for measuring plasma protein binding and metabolic stability.

■ REFERENCES

(1) (a) Blaskovich, M. A. T. Unusual Amino Acids in Medicinal Chemistry. *J. Med. Chem.* **2016**, *59*, 10807−10836. (b) Han, J.; Konno, H.; Sato, T.; Soloshonok, V. A.; Izawa, K. Tailor-Made Amino Acids in the Design of Small-Molecule Blockbuster Drugs. *Eur. J. Med. Chem.* **2021**, *220*, 113448. (c) Hickey, J. L.; Sindhikara, D.; Zultanski, S. L.; Schultz, D. M. Beyond 20 in the 21st Century: Prospects and Challenges of Non-Canonical Amino Acids in Peptide Drug Discovery. *ACS Med. Chem. Lett.* **2023**, *14*, 557−565.

(2) Addie, M.; Ballard, P.; Buttar, D.; Crafter, C.; Currie, G.; Davies, B. R.; Debreczeni, J.; Dry, H.; Dudley, P.; Greenwood, R.; Johnson, P. D.; Kettle, J. G.; Lane, C.; Lamont, G.; Leach, A.; Luke, R. W. A.; Morris, J.; Ogilvie, D.; Page, K.; Pass, M.; Pearson, S.; Ruston, L. Discovery of 4-Amino-*N*-[(1*S*)-1-(4-chlorophenyl)-3-hydroxypropyl]-1-(7*H*-pyrrolo[2,3-*d*]pyrimidin-4-yl)piperidine-4-carboxamide (AZD5363), an Orally Bioavailable, Potent Inhibitor of Akt Kinases. *J. Med. Chem.* **2013**, *56*, 2059−2073.

(3) Odan, M.; Ishizuka, N.; Hiramatsu, Y.; Inagaki, M.; Hashizume, H.; Fujii, Y.; Mitsumori, S.; Morioka, Y.; Soga, M.; Deguchi, M.; Yasui, K.; Arimura, A. Discovery of S-777469: An Orally Available CB2 Agonist as an Antipruritic Agent. *Bioorg. Med. Chem. Lett.* **2012**, *22*, 2803−2806.

(4) Falgueyret, J.-P.; Desmarais, S.; Oballa, R.; Black, W. C.; Cromlish, W.; Khougaz, K.; Lamontagne, S.; Massé, F.; Riendeau, D.; Toulmond, S.; Percival, M. D. Lysosomotropism of Basic Cathepsin K Inhibitors Contributes to Increased Cellular Potencies against Off-Target Cathepsins and Reduced Functional Selectivity. *J. Med. Chem.* **2005**, *48*, 7535−7543.

(5) Furber, M.; Tiden, A.-K.; Gardiner, P.; Mete, A.; Ford, R.; Millichip, I.; Stein, L.; Mather, A.; Kinchin, E.; Luckhurst, C.; Barber, S.; Cage, P.; Sanganee, H.; Austin, R.; Chohan, K.; Beri, R.; Thong, B.; Wallace, A.; Oreffo, V.; Hutchinson, R.; Harper, S.; Debreczeni, J.; Breed, J.; Wissler, L.; Edman, K. Cathepsin C Inhibitors: Property Optimization and Identification of a Clinical Candidate. *J. Med. Chem.* **2014**, *57*, 2357−2367.

(6) (a) Ding, Y.; Ting, J. P.; Liu, J.; Al-Azzam, S.; Pandya, P.; Afshar, S. Impact of Non-Proteinogenic Amino Acids in the Discovery and Development of Peptide Therapeutics. *Amino Acids* **2020**, *52*, 1207−1226. (b) Tanaka, M. Design and Synthesis of Chiral α,α-Disubstituted Amino Acids and Conformational Study of Their Oligopeptides. *Chem. Pharm. Bull.* **2007**, *55*, 349−358.

(7) A single report exists on a photochemical synthesis of *N*-Ac- and *N*-Bz-substituted THF-AA methyl esters. See: Du, Y.; Wei, Z.; Wang, T. Visible-Light-Mediated Synthesis of Oxidized Amides via Organic Photoredox Catalysis. *Synthesis* **2018**, *50*, 3379−3386.

(8) For recent reviews, see: (a) Ramadoss, V.; Zheng, Y.; Shao, X.; Tian, L.; Wang, Y. Advances in Electrochemical Decarboxylative Transformation Reactions. *Chem. Eur. J.* **2021**, *27*, 3213−3228. (b) Zeng, Z.; Feceu, A.; Sivendran, N.; Gooßen, L. J. Decarboxylation-Initiated Intermolecular Carbon-Heteroatom Bond Formation. *Adv. Synth. Catal.* **2021**, *363*, 2678−2722.

(9) For representative recent examples, see: (a) Tajima, T.; Kurihara, H.; Fuchigami, T. Development of an Electrolytic System for Non-Kolbe Electrolysis Based on the Acid−Base Reaction between Carboxylic Acids as a Substrate and Solid-Supported Bases. *J. Am. Chem. Soc.* **2007**, *129*, 6680−6681. (b) Mazurkiewicz, R.; Adamek, J.; Październiok-Holewa, A.; Zielińska, K.; Simka, W.; Gajos, A.; Szymura, K. α-Amidoalkylating Agents from *N*-Acyl-α-Amino Acids: 1-(*N*-Acylamino) Alkyltriphenylphosphonium Salts. *J. Org. Chem.* **2012**, *77*, 1952−1960.

(10) For selected recent works, see: (a) Luo, X.; Ma, X.; Lebreux, F.; Markó, I. E.; Lam, K. Electrochemical Methoxymethylation of Alcohols − a New, Green and Safe Approach for the Preparation of MOM Ethers and Other Acetals. *Chem. Commun.* **2018**, *54*, 9969−9972. (b) de Kruijff, G. H. M.; Waldvogel, S. R. Electrochemical Synthesis of Aryl Methoxymethyl Ethers. *ChemElectroChem.* **2019**, *6*, 4180−4183. (c) Garcia, A. D.; Leech, M. C.; Petti, A.; Denis, C.; Goodall, I. C. A.; Dobbs, A. P.; Lam, K. Anodic Oxidation of Dithiane Carboxylic Acids: A Rapid and Mild Way to Access Functionalized Orthoesters. *Org. Lett.* **2020**, *22*, 4000−4005.

(11) For representative studies, see: (a) Xiang, J.; Shang, M.; Kawamata, Y.; Lundberg, H.; Reisberg, S. H.; Chen, M.; Mykhailiuk, P.; Beutner, G.; Collins, M. R.; Davies, A.; Del Bel, M.; Gallego, G. M.; Spangler, J. E.; Starr, J.; Yang, S.; Blackmond, D. G.; Baran, P. S. Hindered Dialkyl Ether Synthesis with Electrogenerated Carbocations. *Nature* **2019**, *573*, 398−402. (b) Yamada, R.; Sakata, K.; Yamada, T. Electrochemical Synthesis of Substituted Morpholines via a Decarboxylative Intramolecular Etherification. *Org. Lett.* **2022**, *24*, 1837−1841.

(12) (a) Ma, X.; Luo, X.; Dochain, S.; Mathot, C.; Markò, I. E. Electrochemical Oxidative Decarboxylation of Malonic Acid Derivatives: A Method for the Synthesis of Ketals and Ketones. *Org. Lett.* **2015**, *17*, 4690−4693. (b) Ma, X.; Dewez, D. F.; Du, L.; Luo, X.; Markó, I. E.; Lam, K. Synthesis of Diketones, Ketoesters, and Tetraketones by Electrochemical Oxidative Decarboxylation of Malonic Acid Derivatives: Application to the Synthesis of *Cis*-Jasmone. *J. Org. Chem.* **2018**, *83*, 12044−12055.

(13) (a) Horikawa, H.; Iwasaki, T.; Matsumoto, K.; Miyoshi, M. A New Synthesis of 2-Alkoxy-and 2-Acetoxy-2-Amino Acids by Anodic Oxidation. *Tetrahedron Lett.* **1976**, *17*, 191−194. (b) Iwasaki, T.; Horikawa, H.; Matsumoto, K.; Miyoshi, M. An Electrochemical Synthesis of 2-Acetoxy-2-Amino Acid and 3-Acetoxy-3-Amino Acid Derivatives. *J. Org. Chem.* **1977**, *42*, 2419−2423.

(14) (a) Heard, D. M.; Lennox, A. J. J. Electrode Materials in Modern Organic Electrochemistry. *Angew. Chem., Int. Ed.* **2020**, *59*, 18866−18884. (b) Schäfer, H.-J. Recent Contributions of Kolbe Electrolysis to Organic Synthesis. In *Electrochemistry IV*; Steckhan, E., Ed.; Topics in Current Chemistry; Springer-Verlag: Berlin/Heidelberg, 1990; Vol. *152*, pp 91−151.

(15) Di Martino, A.; Galli, C.; Gargano, P.; Mandolini, L. Ring-Closure Reactions. Part 23. Kinetics of Formation of Three- to Seven-Membered-Ring *N*-Tosylazacycloalkanes. The Role of Ring Strain in Small- and Common-Sized-Ring Formation. *J. Chem. Soc., Perkin Trans.* 2 **1985**, 1345.

(16) The newly formed stereogenic center is configurationally stable as evidenced by the lack of epimerization for diastereomerically and enantiomerically pure (*S*,*S*)-**9x** under the cyclization conditions.

(17) Lebreux, F.; Buzzo, F.; Markó, I. Synthesis of Five- and Six-Membered-Ring Compounds by Environmentally Friendly Radical Cyclizations Using Kolbe Electrolysis. *Synlett* **2008**, *2008*, 2815−2820.

(18) Newcomb, M.; Varick, T. R.; Ha, C.; Manek, M. B.; Yue, X. Picosecond Radical Kinetics. Rate Constants for Reaction of Benzeneselenol with Primary Alkyl Radicals and Calibration of the 6-Cyano-5-Hexenyl Radical Cyclization. *J. Am. Chem. Soc.* **1992**, *114*, 8158−8163.

(19) Acid **14** is stable at pH 4 (phosphate buffer) for at least 48 h.

Appendix III – "Simple and Scalable Electrosynthesis of 1 *H* -1-Hydroxy-Quinazolin-4-Ones"

Koleda, O.; Prenzel, T.; Winter, J.; Hirohata, T.; De Jesús Gálvez-Vázquez, M.; Schollmeyer, D.; Inagi, S.; Suna, E.; Waldvogel, S. R.

Chem. Sci. **2023**, *14*, 2669–2675.

Chemical Science

ROYAL SOCIETY OF CHEMISTRY

EDGE ARTICLE

View Article Online
View Journal | View Issue

Cite this: *Chem. Sci.*, 2023, **14**, 2669

All publication charges for this article have been paid for by the Royal Society of Chemistry

Received 15th January 2023
Accepted 13th February 2023

DOI: 10.1039/d3sc00266g

rsc.li/chemical-science

Simple and scalable electrosynthesis of 1*H*-1-hydroxy-quinazolin-4-ones†

Olesja Koleda, ‡[ac] Tobias Prenzel, ‡[a] Johannes Winter, ‡[a] Tomoki Hirohata,[ad] María de Jesús Gálvez-Vázquez,[a] Dieter Schollmeyer,[a] Shinsuke Inagi,[d] Edgars Suna [c] and Siegfried R. Waldvogel *[ab]

Cathodic synthesis provides sustainable access to 1-hydroxy- and 1-oxy-quinazolin-4-ones from easily accessible nitro starting materials. Mild reaction conditions, inexpensive and reusable carbon-based electrode materials, an undivided electrochemical setup, and constant current conditions characterise this method. Sulphuric acid is used as a simple supporting electrolyte as well as a catalyst for cyclisation. The broad applicability of this protocol is demonstrated in 27 differently substituted derivatives in high yields of up to 92%. Moreover, mechanistic studies based on cyclic voltammetry measurements highlight a selective reduction of the nitro substrate to hydroxylamine as a key step. The relevance for preparative applications is demonstrated by a 100-fold scale-up for gram-scale electrolysis.

Introduction

Nitrogen containing heterocycles are ubiquitous in pharmaceuticals[1] and biomolecules as core motifs.[2] One particular example is quinazolin-4-ones. Derivatives are present in a variety of drugs and biomolecules with anticancer, diuretic, anti-inflammatory, anticonvulsant, and antihypertensive properties.[3]

Methaqualone (**1**) (Chart 1), known by its brand name Quaalude, is a hypnotic sedative that increases $GABA_A$ receptor activity.[4] The drug was withdrawn from the U.S. market in 1985, primarily because of its psychologically addictive potential, widespread abuse, and illicit recreational use.[5] The medication idelalisib (**2**) (Chart 1) is used to treat certain types of blood cancer and acts as a phosphoinositide 3-kinase inhibitor.[6] This drug alone amounted to a $72 million annual revenue for Gilead Sciences, Inc.[7] The naturally occurring plant alkaloid tryptanthrine (**3**) exhibits a broad spectrum of biological and pharmaceutical activity including antimicrobial, antiviral, anticancer, and antiparasitic properties.[8] In addition, the AstraZeneca anti-metabolite and cytotoxic drug raltitrexed (**4**) is used in chemotherapy treatments. The folic acid analogue acts as a selective inhibitor of thymidylate synthase.[9] Notably, *N*-oxides and *N*-hydroxy derivatives of these pharmaceuticals were found to be metabolites of these drugs.[10,11] However, the therapeutic effects of endocyclic *N*-hydroxy and *N*-oxy compounds have not been researched to the same degree. Considering their metabolic stability and the unique features of the N–O bond, this class of novel compounds are the subject of current pharmaceutical research.[12]

The synthesis of *N*-oxides and *N*-hydroxy derivatives of quinazolin-4-ones is scarce in the literature and the few published examples present various challenges. The synthesis of 1-oxy-2-alkylquinazolin-4-ones was described by Tennant starting from *N*-(1-cyano-alkyl)-2-nitro benzamides (Scheme 1, top).[13] Its base-catalysed cyclisation approach does not require additional

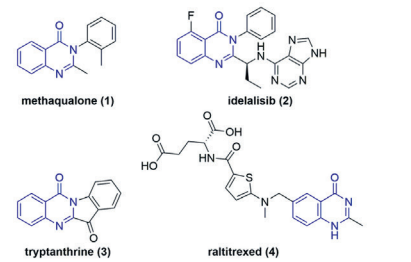

Chart 1 Important biologically active substances with quinazolin-4-one motif.

[a]*Department of Chemistry, Johannes Gutenberg University Mainz, Duesbergweg 10–14, 55128 Mainz, Germany. E-mail: waldvogel@uni-mainz.de; Web: https://www.aksw.uni-mainz.de/*

[b]*Institute of Biological and Chemical Systems –Functional Molecular Systems (IBCS-FMS) Hermann-von-Helmholtz-Platz 1 76344 Eggenstein-Leopoldshafen, Germany*

[c]*Latvian Institute of Organic Synthesis, Aizkraukles 21, LV-1006 Riga, Latvia*

[d]*Department of Chemical Science and Engineering, School of Materials and Chemical Technology, Tokyo Institute of Technology, 4259 Nagatsuta-cho, Midori-ku, Yokohama 226-8502, Japan*

† Electronic supplementary information (ESI) available. CCDC 2234739. For ESI and crystallographic data in CIF or other electronic format see DOI: https://doi.org/10.1039/d3sc00266g

‡ Contributed equally.

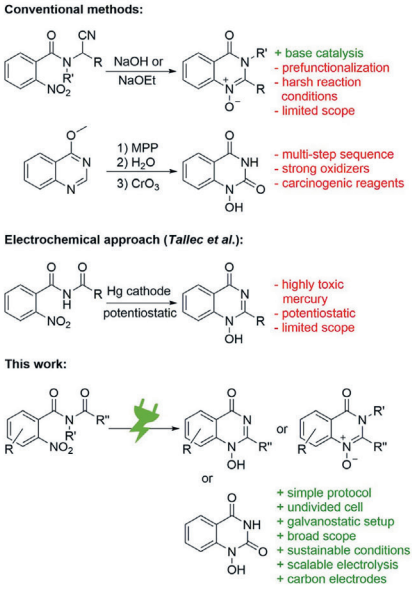

Scheme 1 Synthetic approaches to 1*H*-1-hydroxy-quinazolin-4-ones. MPP = monoperoxyphthalate.

reagents, but does use harsh reaction conditions.[13] The synthesis of 1-hydroxyquinazoline-2,4-diones by Yamanaka comprises a multi-step sequence from 4-methoxyquinazoles and involves two oxidizers: hazardous monoperoxyphthalate for the generation of the 1-oxide and highly toxic chromium(VI) oxide for the oxidation of the C-2 (Scheme 1, top).[14] Reductive cyclisation of nitro precursors is also known, typically *via* hydrogenation with expensive palladium catalysts.[15] In addition, Tallec described an electrochemical synthesis within polarographic studies (Scheme 1, middle). However, highly toxic mercury electrodes were required in a sophisticated potentiostatic reaction setup that was run on a small scale with a limited scope.[16]

Herein, a versatile, scalable, and high-yielding electrochemical reductive cyclisation of widely available, easy to prepare, and inexpensive nitro arenes[17] into 1-hydroxyquinazolin-4-ones is presented. The method uses a simple constant current setup and applies conditions that consider sustainable and environmental aspects (Scheme 1, bottom). In particular, this methodology can easily pay off for high value-added products.[18] The field of electrosynthesis is experiencing a renaissance as an alternative to conventional synthesis protocols[19–21] and is emerging as a key discipline for future synthetic applications.[22] The use of electric current as a reagent enables inherently safe processes by precise control of the reaction. Practically, turning off the electricity immediately stops the conversion and, unlike with traditional reagents, thermal runaway reactions are not possible. The absence of toxic and hazardous reagents and the use of sustainable electricity makes these methods almost waste- and pollutant-free, especially when solvents and supporting electrolytes are reused.[23,24] However, several parameters and counter reactions seem to play a crucial role for success.[25,26] Carbon-based electrode materials such as graphite, glassy carbon (GC), and boron-doped diamond (BDD) are sustainable and widely available.[27] In particular, these are superior in the synthesis of pharmaceuticals or APIs where trace metal impurities must be avoided.[22,28]

Results and discussion

Optimisation of the electrolysis conditions

Benzamide **5a** was chosen as a test substrate for cathodic reduction of a nitro group, and it was easily synthesised in a single step from commercially available 2-nitrobenzamide by treatment with acetic anhydride in a microwave-assisted acylation reaction or in a pressured vessel approach, both in high yields (see ESI† for detailed description).[29] Based on previous work by the Waldvogel lab, a foundation for the electrochemical conditions for nitro reduction were initially tested (Table 1, entry 1).[30–32]

The starting conditions used a water–methanol mixture (1 : 1 (v/v)) as a green solvent capable of dissolving the nitro compound **5a**. A moderate concentration of sulphuric acid (0.5

Table 1 Screening of electrolysis parameters for the optimisation of the synthesis of 1*H*-1-hydroxy-2-methyl-quinazolin-4-one (**6a**)

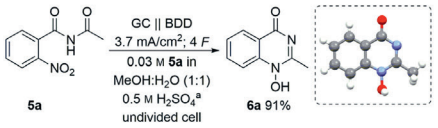

Entry	Deviation from standard conditions	Yield **6a**[b]/%
1	None	91% (91%)[c]
2	2.7 mA cm^{-2}	78%
3	5.7 mA cm^{-2}	78%
4	EtOH instead of MeOH	84%
5	MeCN instead of MeOH	71%
6	0.5 M acetate buffer[d]	66%
7	Pb cathode	27%
8	CuSn7Pb15 cathode	0%
9	Pt cathode	0%
10	Graphite cathode	84%
11	GC cathode	90%
12	0.06 M **5a**	85%
13	0.10 M **5a**	73%

[a] Concentration of sulphuric acid in the electrolyte, obtained by using methanol and 1 M aqueous sulphuric acid (1 : 1 (v/v)). [b] Yield of **6a** was determined by ^{1}H NMR spectroscopy using 2,2-dimethylmalonic acid as internal standard. [c] Isolated yield. [d] 0.5 M AcOH/AcONa was prepared with 90 mmol acetic acid and 10 mmol sodium acetate in 100 mL of distilled water and 100 mL methanol. BDD = boron-doped diamond; GC = glassy carbon.

M) was used as the supporting electrolyte based on previous investigations into the concentration effect of the acidic component on the electrochemical reduction.[16,33] Moreover, it was envisioned that sulphuric acid may play a dual role in the reaction since acidic media should be beneficial for cyclisation after a nitro group reduction. Taking this into account, we examined constant current electrolysis (3.7 mA cm^{-2} current density) of benzamide **5a** in an undivided cell in water–methanol media, using a glassy carbon anode and a boron-doped diamond (BDD) cathode. BDD as a carbon-based material offers unique reactivity towards electrochemical conversion of a multitude of substrates and can be manufactured in a sustainable manner by utilizing methane as carbon source.[34]

To our delight, the desired 1-hydroxyquinazolinone **6a** was isolated in 91% yield. Furthermore, the theoretical amount of charge required for this process (4 *F*) was applied and the high yield obtained shows that this process has a high current efficiency (Table 1, entry 1). The molecular structure of heterocycle **6a** was confirmed by X-ray analysis of a suitable single crystal.

Deviation from the starting electrolysis conditions obtained by electrosynthetic screening resulted in lower yields.[20,21,24,35] Both lower or higher current densities led to a decreased yield of 1-hydroxyquinazolinone **6a** to 78% (Table 1, entries 2 and 3). Replacement of methanol with other solvents such as ethanol and acetonitrile (Table 1, entries 4 and 5) afforded the desired heterocycle **6a** in slightly lower yields of 84% and 71%, respectively. Acetate buffer (Table 1, entry 6) was used as a weaker and biogenic alternative to sulphuric acid; however, the yield of **6a** decreased to 66%. Substitution of BDD as cathode material for lead significantly decreased the yield of **6a** to 27% (Table 1, entry 7). Furthermore, cathodic corrosion was observed resulting in the precipitation of lead salts.

More stable alternatives to lead cathodes such as leaded bronzes[36] (Table 1, entry 8) failed entirely in the formation of **6a**. Platinum was equally unsuccessful as cathode material (Table 1, entry 9), completely avoiding the desired reaction likely due its low overpotential for the hydrogen evolution side-reaction.[37]

Besides BDD, other carbon-based cathode materials such as graphite and glassy carbon provided product **6a** in comparable yields of 84% and 90% (Table 1, entries 10 and 11). Nevertheless, we decided to proceed with BDD due to its sustainability and chemical durability.[38] Electrolysis at higher benzamide **5a** concentrations resulted in lowered yields by up to nearly 20% (Table 1, entries 12 and 13). It is likely that higher concentrations of starting material result in the formation of high molecular weight side products which were observed as a brown plaque after the electrolysis was finished.

Scope of the reductive cyclisation

The broad applicability of the optimised reaction conditions was demonstrated on a versatile scope of substrates (Chart 2). First, we explored the effect of substitution pattern at the C-2 position of quinazolin-4-ones **6b–i** (Chart 2, top). The influence of primary, secondary, and tertiary alkyl substitutions was investigated in the synthesis of heterocycles **6a–c**, resulting in good yields of 78–91%. Here, the *tert*-butyl derivative **6c** with its sterically demanding substituent gave the lowest yield. Furthermore, 1*H*-2-heptyl-1-hydroxy-quinazolin-4-one (**6d**) with a hydrophobic chain was obtained in a moderate yield of 52%.

Both the 2-unsubstituted quinazolin-4-one **6e** and the 2-phenyl analogue **6h** were obtained in moderate to good yields (65% and 79%, respectively). Alkene as well as a benzylic moieties, usually prone to anodic oxidation, were well tolerated in the electrochemical reduction, and the desired heterocycles **6g** and **6i** were obtained in 67% and 81% yield. Interestingly, even the 2-chloromethyl substituted product **6f** was isolated in 24% yield despite its inherent instability.

Next, various functional groups in the aromatic subunit of 1-hydroxyquinazolin-4-ones **6j–r** were tested (Chart 2, middle). In all cases, the products were obtained in good to excellent yields regardless of the substituent's electronic nature. Benzamides with an electron-donating methoxy group and an electron-withdrawing ester moiety afforded the corresponding heterocycles **6q** and **6r** in comparable yields (77% and 85%, respectively). Likewise, the trifluoromethyl derivative **6n** and methyl quinazolin-4-ones **6o** and **6p** were obtained in 73–92% yield.

The 6-methyl derivative **6o** is an *N*-hydroxy analogue of a precursor to raltitrexed (**4**), thus its successful formation adds industrial relevance to this transformation.[39] Halides are redox-active groups in electrochemical reactions. To our delight, fluoro-, chloro- and bromo-substituted quinazolin-4-ones **6j–l** were obtained in 76–85% yield. Moreover, the developed electrochemical method also afforded the iodo-substituted product **6m**, albeit in moderate yield (50%) likely due to its susceptibility to oxidation.

It is noteworthy that heteroaromatic amides such as those derived from pyridines and imidazoles are applicable with the developed conditions (Chart 2, middle left). The pyrido pyrimidinone **6s** was obtained in 82% yield and the bromo substituent offers availability for a variety of post-functionalization reactions. Even the *N*-hydroxy purine **6t** was obtained in a good yield of 57%.

Furthermore, *N*-acetyl-*N*-aryl benzamides were converted into the corresponding *N*-oxy-quinazolin-4-ones **7a** and **7b** in moderate yields, likely due to their tendency to rearrangement reactions (Chart 2, middle right).[40] Interestingly, **7b** is a reported metabolite of methaqualone (**1**).[10] Furthermore, tertiary amides are also suitable as substrates as exemplified by the synthesis of pyrrolidone-based *N*-oxy-quinazolin-4-one **7c** (72%).

Finally, the presented methodology has also been applied to the synthesis of 1-hydroxy-quinazoline-2,4-diones **8a–d** by electrochemical reduction of methyl-(2-nitrobenzoyl)carbamates, which gave up to 77% yield (Chart 2, bottom). Here, the unsubstituted derivative **8a** had the best yield of 77%. The electron-withdrawing trifluoromethyl- and chloro-substituted products **8b** and **8d** were isolated in 59% and 48% yield. The methyl-substituted derivative **8c** was obtained in moderate yield of 66%.

Scale-up of electrolysis

To demonstrate the synthetic utility and scalability of the developed method, the synthesis of 1*H*-1-hydroxy-2-methyl-

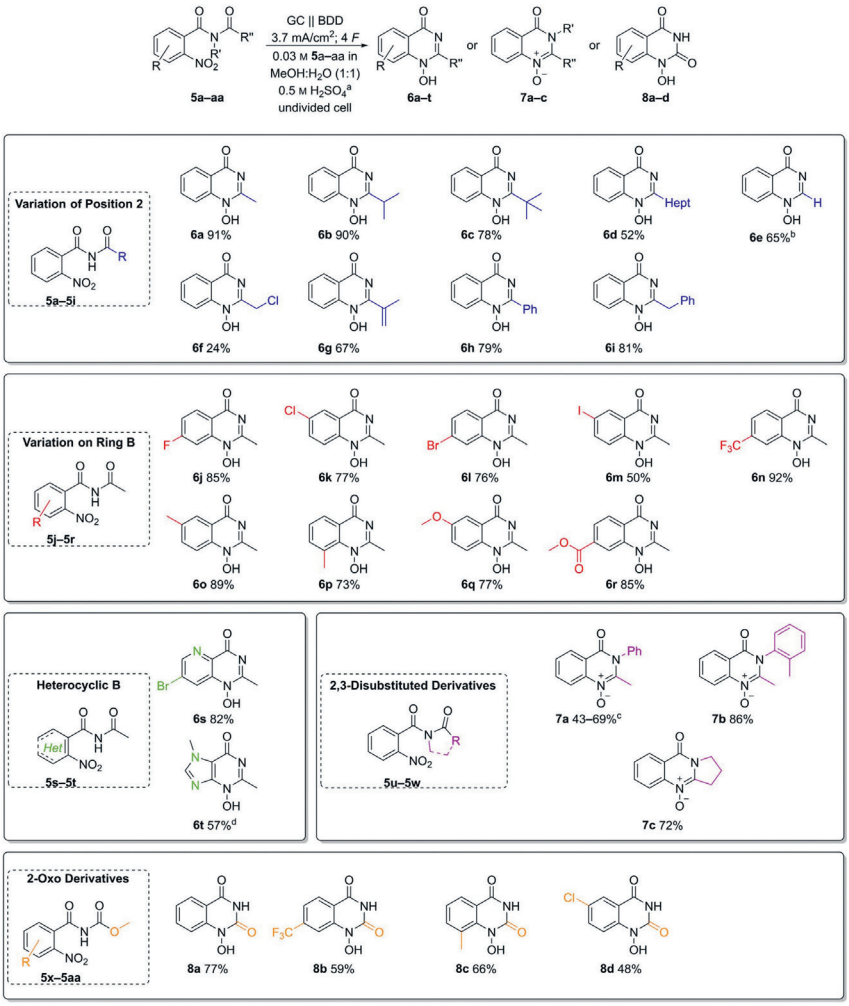

Chart 2 Scope of electrochemical reductive cyclisation and isolated yields. [a] Concentration of sulphuric acid in the electrolyte, obtained by using 12.5 mL methanol and 12.5 mL 1 M aqueous sulphuric acid (1 : 1 (v:v)), undivided 25 mL beaker-type glass cell; [b] isolated yield as formate adduct; [c] variation in yield with repeated electrolysis; [d] isolated yield as acetate adduct.

quinazolin-4-one (**6a**) was successfully scaled up to 15 mmol in a single electrolysis batch (Table 2). The 5-fold scale-up was performed with BDD and GC cathodes to demonstrate the robustness and applicability of the described method. Encouragingly, 20-fold scale-up (3.00 mmol) in a 100 mL electrolysis cell afforded the desired product **6a** without loss in yield or faradaic efficiency. Gram-scale electrolysis was also performed at 7.5 mmol and 15.0 mmol loading in a 250 mL electrolysis cell, affording 1.13 g and 2.19 g of the desired 1-hydroxy-quinazolin-2-one **6a**, respectively. The trend of decreased yield at higher

Table 2 Scale-up of the electroreduction of 1*H*-1-hydroxy-2-methyl-quinazolin-4-one (**6a**)[a]

Electrolysis cell	Scale/mmol	Current (electrolysis time)	Yield **6a**
	0.15	5.6 mA (2.9 h)	24 mg (91%)
	0.75 0.75[b]	22.2 mA (3.6 h)	120 mg (91%) 118 mg (89%)
	3.00	22.2 mA (14.5 h)	481 mg (91%)
	7.50 15.0[c]	109.9 mA (7.3 h) 109.9 mA (14.6 h)	1.13 g (86%) 2.19 g (83%)

[a] Constant current conditions; surface areas of the electrodes: 5 mL Teflon™ cell (1.5 cm^2), 25 mL and 100 mL glass cell (6.0 cm^2), 250 mL glass cell (29.7 cm^2). [b] GC cathode. [c] 0.06 M **5a**.

concentrations was also observed in the optimisation results (Table 1, entries 12 & 13).

Mechanistic studies

A plausible mechanism for the electrochemical cyclisation sequence is proposed based on earlier nitro reduction studies and cyclic voltammetry (CV) measurements of benzamide **5a** (Scheme 2; for detailed information see ESI†).[16,31–33] Accordingly, the reactions starts with the reduction of the nitro group on the BDD cathode which is evidenced by a single broad, irreversible wave (−0.94 V *vs.* FcH/FcH$^+$) corresponding to the 4e$^-$/4H$^+$ reduction to the hydroxylamine. It has been previously suggested that the reaction proceeds with two 2e$^-$ steps *via* intermediates **Int-I** and **Int-II**. However, because only one broad wave was observed rather than two distinct or overlapping waves, this suggests one reduction event occurs and that **5a** is reduced directly to **Int-II** The irreversible reduction to **Int-II** indicates a fast cyclisation step as no corresponding oxidative wave was observed. Further reduction of the *N*-hydroxy moiety was not observed for non-cyclised **Int-II** or the product **6a**. The impact of the counter reaction on the electrochemical conversion must also be considered; the oxidation of water at the glassy carbon anode is possibly the main counter reaction.[25] The corrosion of the glassy carbon anode was not observed after electrolysis. There was no indication of the oxidation of methanol, which was only observed under harsh basic conditions in previous studies.[41] Overall, the high performance of the reported method was enabled by the electrochemical stability of the product, the selective reduction to the hydroxylamine, and the fast cyclisation process.

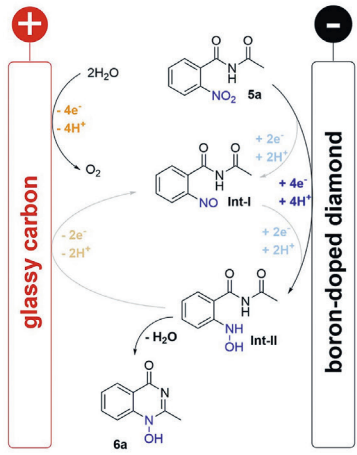

Scheme 2 Proposed mechanism for the reductive cyclisation.

Conclusions

In summary, the established method provides simple, direct, and sustainable electrochemical access to *N*-hydroxy- and *N*-oxyquinazolin-4-ones by a cathodic reduction sequence. The electrolytic conditions allow for a reproducible transformation in commercially available experimental setups. The simplest undivided cell was operated under constant current with widely available and sustainable carbon-based electrodes and a water–methanol mixture as an environmentally benign solvent. The sulphuric acid additive served a dual role as supporting electrolyte and acidic catalyst. The broad applicability of this method was demonstrated by 27 examples with up to 92% isolated yield. The electrolysis tolerates various functional groups, including electron-withdrawing and -donating, sterically demanding, and redox labile moieties such as bromides and iodides. The *N*-hydroxy analogue precursor of the cytotoxic drug raltitrexed was obtained in 89% yield. Selective nitro reduction to the hydroxylamine was confirmed by CV measurements to be a key step in the mechanism. The scalability of this electrochemical protocol was demonstrated by multigram-scale electrolysis.

Data availability

The ESI is available and contains experimental and analytical data.

Author contributions

O. K., T. P. and J. W. contributed equally. T. P. and S. W. conceived the idea of the research. O. K., T. P., J. W. and T. H. designed and carried out the batch electrolysis experiments and analysed the data. M. G. and T. P. designed and analysed the cyclic voltammetry measurements. D. S. performed the X-ray analysis and structural elucidation of the synthesised test substrate. T. P., O. K., J. W., and S. W. wrote the manuscript. S. W. supervised the project and E. S. and S. I. reviewed and edited the manuscript. All authors discussed the results and agreed to the manuscript.

Conflicts of interest

The authors declare no conflict of interest.

Acknowledgements

The authors acknowledge funding by the DFG (Wa1276/17-2 and Wa1276/26-1). Support by the profile area SusInnoScience (Forschungsinitiative Rheinland-Pfalz) is highly appreciated. This project was funded by Japan Science and Technology Agency's SPRING program under the grant agreement no. JPMJSP2106 (T. H.). We would like to thank Dr R. Hamill for her assistance with editing the manuscript.

References

1 E. Vitaku, D. T. Smith and J. T. Njardarson, *J. Med. Chem.*, 2014, **57**, 10257.
2 N. Kerru, L. Gummidi, S. Maddila, K. K. Gangu and S. B. Jonnalagadda, *Molecules*, 2020, **25**, 1909.
3 A. Masri, A. Anwar, N. A. Khan, M. S. Shahbaz, K. M. Khan, S. Shahabuddin and R. Siddiqui, *Antibiotics*, 2019, **8**, 179.
4 P.-F. Wang, A. A. Jensen and L. Bunch, *ACS Chem. Neurosci.*, 2020, **11**, 4362.
5 K. Romanek, H. Fels, T. Dame, G. Skopp, F. Musshoff, H. Eiglmeier and F. Eyer, *Subst. Abuse*, 2021, **42**, 503.
6 J. R. Somoza, D. Koditek, A. G. Villaseñor, N. Novikov, M. H. Wong, A. Liclican, W. Xing, L. Lagpacan, R. Wang, B. E. Schultz, G. A. Papalia, D. Samuel, L. Lad and M. E. McGrath, *J. Biol. Chem.*, 2015, **290**, 8439.
7 San. Franc. Bus. Times, **https://www.bizjournals.com/sanfrancisco/news/2022/01/21/blood-cancer-gilead-sciences-gild-zydelig-fl-sll.html**, accessed January 2023.
8 A. M. Tucker and P. Grundt, *Arkivoc*, 2012, 546.
9 N. S. Gunasekara and D. Faulds, *Drugs*, 1998, **55**, 423.
10 C. N. Reynolds, K. Wilson and D. Burnett, *Xenobiotica*, 1976, **6**, 113.
11 M. H. Bickel, *Xenobiotica*, 1971, **1**, 313.
12 R. Rani and C. Granchi, *Eur. J. Med. Chem.*, 2015, **97**, 505.
13 T. W. M. Spence and G. Tennant, *J. Chem. Soc., Perkin Trans. 1*, 1972, 97.
14 H. Yamanaka, *Chem. Pharm. Bull.*, 1959, **7**, 152.
15 R. Fielden, O. Meth-Cohn and H. Suschitzky, *J. Chem. Soc., Perkin Trans. 1*, 1973, 702.
16 A. Chibani, R. Hazard and A. Tallec, *Bull. Soc. Chim. Fr.*, 1991, **6**, 814.
17 A. Z. Halimehjani, I. N. N. Namboothiri and S. E. Hooshmand, *RSC Adv.*, 2014, **4**, 31261.
18 (*a*) J. Seidler, J. Strugatchi, T. Gärtner and S. R. Waldvogel, *MRS Energy Sustain.*, 2020, **7**, 42; (*b*) S. Möhle, M. Zirbes, E. Rodrigo, T. Gieshoff, A. Wiebe and S. R. Waldvogel, *Angew. Chem., Int. Ed.*, 2018, **57**, 6018.
19 (*a*) D. Cantillo, *Chem. Commun.*, 2022, **58**, 619; (*b*) A. Shatskiy, H. Lundberg and M. D. Kärkäs, *ChemElectroChem*, 2019, **6**, 4067; (*c*) S. R. Waldvogel and B. Janza, *Angew. Chem., Int. Ed.*, 2014, **53**, 7122.
20 C. Kingston, M. D. Palkowitz, Y. Takahira, J. C. Vantourout, B. K. Peters, Y. Kawamata and P. S. Baran, *Acc. Chem. Res.*, 2020, **53**, 72.
21 M. C. Leech and K. Lam, *Nat. Rev. Chem.*, 2022, **6**, 275.
22 D. Pollok and S. R. Waldvogel, *Chem. Sci.*, 2020, **11**, 12386.
23 (*a*) B. A. Frontana-Uribe, R. D. Little, J. G. Ibanez, A. Palma and R. Vasquez-Medrano, *Green Chem.*, 2010, **12**, 2099; (*b*) M. D. Kärkäs, *Chem. Soc. Rev.*, 2018, **47**, 5786; (*c*) R. D. Little and K. D. Moeller, *Chem. Rev.*, 2018, **118**, 4483; (*d*) J. L. Röckl, D. Pollok, R. Franke and S. R. Waldvogel, *Acc. Chem. Res.*, 2020, **53**, 45; (*e*) A. Wiebe, T. Gieshoff, S. Möhle, E. Rodrigo, M. Zirbes and S. R. Waldvogel, *Angew. Chem., Int. Ed.*, 2018, **57**, 5594; (*f*) S. R. Waldvogel, S. Lips, M. Selt, B. Riehl and C. J. Kampf, *Chem. Rev.*, 2018,

118, 6706; (*g*) T. Wirtanen, E. Rodrigo and S. R. Waldvogel, *Adv. Synth. Catal.*, 2020, **362**, 2088.
24 M. Yan, Y. Kawamata and P. S. Baran, *Chem. Rev.*, 2017, **117**, 13230.
25 M. Klein and S. R. Waldvogel, *Angew. Chem., Int. Ed.*, 2022, **61**, e202204140.
26 S. B. Beil, D. Pollok and S. R. Waldvogel, *Angew. Chem., Int. Ed.*, 2021, **60**, 14750.
27 D. M. Heard and A. J. J. Lennox, *Angew. Chem., Int. Ed.*, 2020, **59**, 18866.
28 T. Wirtanen, T. Prenzel, J.-P. Tessonnier and S. R. Waldvogel, *Chem. Rev.*, 2021, **121**, 10241.
29 (*a*) J. Lee, M. Hong, Y. Jung, E. J. Cho and H. Rhee, *Tetrahedron*, 2012, **68**, 2045; (*b*) X.-G. Yang, K. Zheng and C. Zhang, *Org. Lett.*, 2020, **22**, 2026.
30 E. Rodrigo, H. Baunis, E. Suna and S. R. Waldvogel, *Chem. Commun.*, 2019, **55**, 12255.
31 E. Rodrigo and S. R. Waldvogel, *Green Chem.*, 2018, **20**, 2013.
32 J. Winter, T. Prenzel, T. Wirtanen, D. Schollmeyer and S. R. Waldvogel, *Chem.–Eur. J.*, 2022, e202203319.
33 R. Hazard, M. Jubault, C. Mouats and A. Tallec, *Electrochim. Acta*, 1986, **31**, 489.
34 S. Lips and S. R. Waldvogel, *ChemElectroChem*, 2019, **6**, 1649.
35 (*a*) C. Zhu, N. W. J. Ang, T. H. Meyer, Y. Qiu and L. Ackermann, *ACS Cent. Sci.*, 2021, **7**, 415; (*b*) J. Rein, J. R. Annand, M. K. Wismer, J. Fu, J. C. Siu, A. Klapars, N. A. Strotman, D. Kalyani, D. Lehnherr and S. Lin, *ACS Cent. Sci.*, 2021, **7**, 1347; (*c*) G. Hilt, *ChemElectroChem*, 2020, **7**, 395; (*d*) M. Dörr, M. M. Hielscher, J. Proppe and S. R. Waldvogel, *ChemElectroChem*, 2021, **8**, 2621; (*e*) C. Gütz, B. Klöckner and S. R. Waldvogel, *Org. Process Res. Dev.*, 2016, **20**, 26; (*f*) P. Enders and R. Francke, in *Science of Synthesis*, ed. L. Ackermann, Georg Thieme Verlag KG, Stuttgart, New York, 2022, pp. 67–72.
36 C. Gütz, V. Grimaudo, M. Holtkamp, M. Hartmer, J. Werra, L. Frensemeier, A. Kehl, U. Karst, P. Broekmann and S. R. Waldvogel, *ChemElectroChem*, 2018, **5**, 247.
37 A. Hickling and F. W. Salt, *Trans. Faraday Soc.*, 1940, **36**, 1226.
38 (*a*) Y. Einaga, *Acc. Chem. Res.*, 2022, **55**, 3605; (*b*) S. R. Waldvogel, S. Mentizi and A. Kirste, *Top. Curr. Chem.*, 2012, **320**, 1.
39 (*a*) S.-L. Cao, Y.-P. Feng, Y.-Y. Jiang, S.-Y. Liu, G.-Y. Ding and R.-T. Li, *Bioorg. Med. Chem. Lett.*, 2005, **15**, 1915; (*b*) S.-L. Cao, R. Wan and Y.-P. Feng, *Synth. Commun.*, 2003, **33**, 3519.
40 F. P. Theil, H. Poehlmann, S. Pfeifer and P. Franke, *Pharmazie*, 1985, **40**, 328.
41 T. Wirtanen, E. Rodrigo and S. R. Waldvogel, *Chem.–Eur. J.*, 2020, **26**, 5592.

Appendix IV – Publications of abstracts

1. Koleda, O.; Prane, K.; Suna, E. Electrochemical decarboxylation of *N*-substituted 2-aminomalonic acid monoesters in intramolecular Hofer-Moest reaction. *Program & Abstracts*, Balticum Organicum Syntheticum, Vilnius, Lithuania, July 3–6, 2022, P057 p. 101 (**Best poster award**).

2. Koleda, O.; Prane, K.; Suna, E. Electrochemical decarboxylation of *N*-substituted 2-aminomalonic acid monoesters in intramolecular Hofer-Moest reaction. 23rdTetrahedron Symposium, Gothenburg, Sweden, June 27–30, 2023, P1.050.

Electrochemical decarboxylation of *N*-substituted 2-aminomalonic acid monoesters in intramolecular Hofer-Moest reaction

Olesja Koleda, Katrina Prane, Edgars Suna
Latvian Institute of Organic Synthesis, Riga, Latvia

Malonic acid is an inexpensive and readily available substrate that can be easily functionalized, e.g. by alkylation reactions. Highly functionalized substrates can be obtained even after decarboxylation of the malonate. Hence, malonic acid derivatives are well-suited for electrochemical decarboxylation. Herein we report a previously unreported intramolecular Hofer-Moest reaction of *N*-substituted 2-aminomalonic acid monoesters (Scheme 1). A stabilized cation **2** is formed after anodic decarboxylation of a malonic acid monoester **1**. Subsequent cyclization affords quaternary carbon-containing tetrahydrofurans and tetrahydropyrans in high yields.

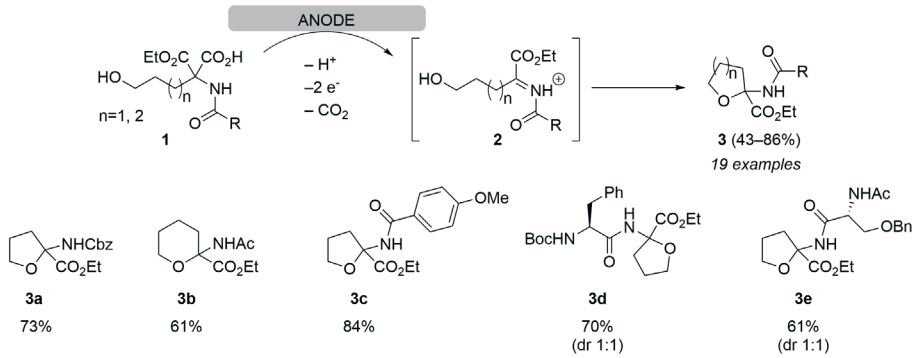

Scheme 1. **Intramolecular Hofer-Moest reaction of *N*-substituted 2-aminomalonic acid monoesters.**

Certificate

In order to support the generation of MSc, PhD and postdoctoral students, poster prizes are awarded by Thieme Chemistry both at in-person and virtual conferences and events.

For the best Latvian poster presentation at the

22nd Balticum Organicum Syntheticum (BOS)
July 3-6, 2022

Olesja Koleda

is awarded the

Thieme Chemistry Poster Prize

consisting of a one-year subscription to SYNFACTS.

Sponsored by Thieme Group Stuttgart • New York in collaboration with the editors of SYNFACTS

Stuttgart, July 6, 2022

Susanne Haak
Senior Director, Operations, Thieme Chemistry Journals

Thieme

Electrochemical decarboxylation of *N*-substituted 2-aminomalonic acid monoesters in intramolecular Hofer-Moest reaction

Olesja Koleda, Katrina Prane, Edgars Suna
Latvian Institute of Organic Synthesis, Aizkraukles 21, Riga, LV-1006
e-mail: olese@osi.lv

Kolbe reaction is one of the oldest electroorganic reactions, where an alkyl radical is generated upon anodic decarboxylation.[1] In contrast, in Hofer-Moest reaction a carbocation is generated after anodic decarboxylation followed by a reaction with a nucleophilic solvents, alcohols or amines.[2,3]

Malonic acid is an inexpensive and readily available substrate that can be easily functionalized, e.g. by alkylation reactions. Highly functionalized substrates can be obtained even after decarboxylation of the malonate. Hence, malonic acid derivatives are well-suited for electrochemical decarboxylation. Herein we report a previously unreported intramolecular Hofer-Moest reaction of *N*-substituted 2-aminomalonic acid monoesters (Scheme 1). A stabilized cation **2** is formed after anodic decarboxylation of a malonic acid monoester **1**. Subsequent cyclization affords quaternary carbon-containing tetrahydrofurans and tetrahydropyrans in high yields.

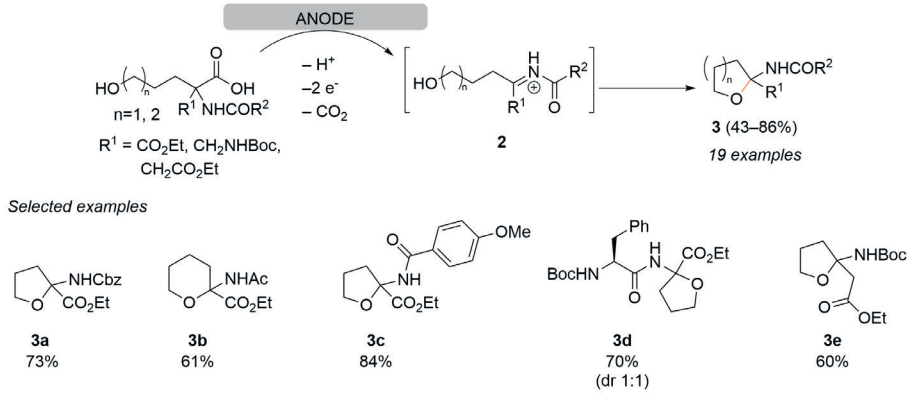

Scheme 1. **Intramolecular Hofer-Moest reaction of *N*-substituted 2-aminomalonic acid monoesters.**

References

1. Kolbe, H. *Ann. Chem. Pharm.* **1848**, *64*, 339.
2. Hofer, H.; Moest, M. *Justus Liebigs Ann. Chem.* **1902**, *323*, 284.
3. Ramadoss, V.; Zheng, Y.; Shao, X.; Tian, L.; Wang, Y. *Chem.–Eur. J.* **2021**, *27*, 3213.

I hereby declare and confirm with my signature that the doctoral thesis **"Electrochemical synthesis of biologically relevant heterocycles"** is exclusively the result of my own autonomous work based on my research and literature published, which is seen in the notes and bibliography used. I also declare that no part of the submitted doctoral thesis has been made in an inappropriate way, whether by plagiarizing or infringing on any third person's copyright. Finally, I declare that no part of the submitted doctoral thesis has been used for any other thesis in another higher education institution, research institution or educational institution.

Author: Olesja Koleda

Signature _____

Supervisor: Dr. chem., Prof. Edgars Suna

Signature _____

Supervisor: PhD, Prof. Siegfried R. Waldvogel

Signature _____

Thesis submitted in the Promotion Council in Chemistry of University of Latvia for the commencement of the degree of Doctor of Chemistry on _____.

Secretary of the Promotion Council: Vita Rudoviča _____

Thesis defended at the session of Promotion Council in Chemistry of University of Latvia for the commencement of the degree of Doctor of Chemistry on

_____, protocol No. _____

Secretary of the Promotion Council: Vita Rudoviča _____

Olesja was born in 1987 in Kraslava. She earned her Bachelor's Degree in Chemistry from the University of Latvia in 2010. Subsequently, she pursued her Master's studies at the University of Illinois at Chicago (USA), where she conducted research in Professor V. Gevorgyan's group. Upon completing her Master's studies, Olesja returned to Latvia and, in 2015, embarked on her Ph.D. studies at the University of Latvia. She conducted her research under the supervision of Professor E. Suna at the Latvian Institute of Organic Synthesis. During her Ph.D. studies, Olesja gained valuable experience in electrochemistry by visiting Prof. R. Franke's group at Rostock University (Germany) in 2016 and Prof. S. R. Waldvogel's group at Johannes Gutenberg University Mainz (Germany) in 2022. Her research interests include organic electrosynthesis, with a specific focus on developing new electrochemical methods for the synthesis of heterocycles.